GENE REGULATION DURING
STRESS RESPONSE TRANSCRIPTION IN *SACCHAROMYCES CEREVISIAE:*
DYNAMIC TRANSCRIPTOME ANALYSIS OF OSMOTIC STRESS
RESPONSE AND MEDIATOR PHOSPHORYLATION

Christian Miller

aus

Füssen, Deutschland

2013

Erklärung

Diese Dissertation wurde im Sinne von §7 der Promotionsordnung vom 28. November 2011 von Herrn Prof. Dr. Patrick Cramer betreut.

Eidesstattliche Versicherung
Diese Dissertation wurde eigenständig und ohne unerlaubte Hilfe erarbeitet.

München, am   29.01.2013

Christian Miller

Dissertation eingereicht am: 29.01.2013

1. Gutachter: Prof. Dr. Patrick Cramer
2. Gutachter: PD Dr. Dietmar Martin

Mündliche Prüfung am: 27.02.2013

ACKNOWLEDGEMENTS

I was growing up in front of the Bavarian alps, and I learned that it takes a few but essential things to reach the summit. First, you have to be part of a team that is strong and motivated enough to accept the challenge. Second, it's up to you to put in the efford of going upwards. Third, there is no perfect time for attacking the summit, but there are perfect opportunities.

In 2007, I became part of the Cramer-team. First of all I would like to thank my supervisor Prof. Dr. Patrick Cramer, the leader of the rope-team, for giving me the opportunity to join his group of young and extraordinary motivated scientists. Patrick, you gave me the freedom to improve my skills and to bring forward new ideas for my challenging projects. You provided uncomplicated help whenever it was required – no matter if it was about scientific work or during my two-year training program in major incident management.

Special thank goes to Jesper Olsen and Heidi Feldmann for being members of my PhD advisory board. You gave valuable feedback and supported my scientific work with helpful advices. I would like to thank Francesc Posas and Eulalia de Nadal for answering many questions about the HOG pathway. My trip to the Parc de Recerca Biomédica de Barcelona was one of the highlights.

I am also thankful to Matthias Mann for his collaboration and for his feedback to my work on Mediator phosphorylation. Special thank goes to Ivan Matic, who performed all mass spectrometry analysis of my Mediator project and for all the lively discussions.

Kerstin, thank you for being such a great collegue. Thank you for support and your extraordernary help throughout the experimental work on dynamic transcriptome analysis and the Mediator phosphorylation. I am also very thankful to Dietmar, for your earnest interest in my experimental ideas and for giving me valuable feedback. I would like to thank Achim (Tresch) and Björn (Schwalb) for taking their time for many discussions, feedbacks and the collaborative work that result in the development of DTA.

Since I was part of a strong and motivated rope-team, I would like to thank my teammates. Elmar, for working side by side throughout my lab time, for talking about attitudes, economics, politics, philosophy, all the stuff beyond science and for the many special moments inside and outside the lab as we had so much fun. Rieke, for sharing the deep passion for sports, for all the very welcome discussions during our coffee breaks and for illustrating the contrasts of urban- and country life, which nowhere else could be larger than between Essen and Kirchthal. Tobias for all the help with the Äkta systems, the discussions of cloning problems and nice moments at the barbecue and wine-tasting. Laurent, for your contagious enthusiasm on science issues and your open minded way of problem-solving. Martin for all the helpful discussions about transcription and the Mediator and for performing the in vitro transcription assay. Stefan (Benkert) and Claudia (Buchen) for managing the daily lab routine and for being a source of continuity. Stefan (Dengl) and Stefan (Jennebach) for talking about all the little but serious issues of lab-life. Jasmin for sharing the long days in the lab and for the work on the Pol II in vitro elongation assay. Andreas for all the discussions about high-throughput data and the nice moments during the Harvard young scientist´s forum (…hoping to meet you at Paulaner`s). Claudia (Blattner) for the very welcome interruptions of the daily routine and the varied topics during our coffee-breaks.

PUBLICATIONS

Parts of this work have been published:

2011 <u>Christian Miller*</u>, Björn Schwalb*, Kerstin Maier*, Daniel Schulz, Sebastian Dümcke, Benedikt Zacher, Andreas Mayer, Jasmin Sydow, Lisa Marcinowski, Lars Dölken, Dietmar E. Martin, Achim Tresch and Patrick Cramer
*contributed equally

Dynamic transcriptome analysis measures rates of mRNA synthesis and decay in yeast.[1,2]
Molecular Systems Biology, 7:458, doi:10.1038/msb.2010.112

Author contributions:
CM and KM conducted DTA experiments, BS, SD, BZ, and AT developed the statistical workflow and carried out computational analysis, DS and AM conducted ChIP experiments, JS conducted enzymatic assays, LM, LD, and DEM conducted initial experiments, LD and PC initiated the study, DEM supervised experimental work, and AT and PC supervised research and wrote the manuscript.

2012 <u>Christian Miller*</u>, Ivan Matic*, Kerstin C. Maier*, Susanne Roether, Björn Schwalb, Katja Sträßer, Achim Tresch, Matthias Mann, and Patrick Cramer
*contributed equally

Mediator phosphorylation prevents stress response transcription during non stress conditions.
Journal of biological chemistry, 2012, 287(53), 44017-26

Author contributions:
CM designed and conducted the SILAC & DTA experiments and final data analysis. CM and PC wrote the manuscript. IM conducted the phospho-proteomics data processing and analysis. KM performed the DTA experiments and cloned the D7P and D30P strains. SR and KS created the strain for phospho-proteomics. BS and AT carried out the computational analysis of DTA/cDTA data. MM and PC supervised the projects.

---

[1] The Molecular Systems Biology journal has published a top ten chart of the articles that have been downloaded most often over the previous 30 days. This article reached the top rank of the top ten charts within 13 days and reached the 6th rank of the of the top 10 most read research articles published in *Molecular Systems Biology* in 2011.

[2] Overview to this work has been published in Cell: Szewczak, L. & Plosky, B. (2011) Leading Edge Select, *Cell*, 144, 831-832;

SUMMARY

TOPIC I:

DYNAMIC TRANSCRIPTOME ANALYSIS MEASURES RATES OF MRNA SYNTHESIS AND DECAY IN YEAST

To obtain rates of mRNA synthesis and decay in yeast, we established dynamic transcriptome analysis (DTA). DTA combines non-perturbing metabolic RNA labeling with dynamic kinetic modeling. DTA reveals that most mRNA synthesis rates are around several transcripts per cell and cell cycle, and most mRNA half-lives range around a median of 11 min. DTA can monitor the cellular response to osmotic stress with higher sensitivity and temporal resolution than standard transcriptomics. In contrast to monotonically increasing total mRNA levels, DTA reveals three phases of the stress response. During the initial shock phase, mRNA synthesis and decay rates decrease globally, resulting in mRNA storage. During the subsequent induction phase, both rates increase for a subset of genes, resulting in production and rapid removal of stress-responsive mRNAs. During the recovery phase, decay rates are largely restored, whereas synthesis rates remain altered, apparently enabling growth at high salt concentration. Stress-induced changes in mRNA synthesis rates are predicted from gene occupancy with RNA polymerase II. Thus, DTA realistically monitors the dynamics in mRNA metabolism that underlie gene regulatory systems.

TOPIC II:

MEDIATOR PHOSPHORYLATION PREVENTS STRESS RESPONSE TRANSCRIPTION DURING NON STRESS CONDITIONS

The multiprotein complex Mediator is a coactivator of RNA polymerase (Pol) II transcription that is required for the regulated expression of protein-coding genes. Mediator serves as an endpoint of signaling pathways and regulates Pol II transcription, but the mechanisms it uses are not well understood. Here we used mass spectrometry and dynamic transcriptome analysis to investigate a functional role of Mediator phosphorylation in gene expression. Affinity purification and mass spectrometry revealed that Mediator from the yeast *S. cerevisiae* is phosphorylated at multiple sites a 17 out of its 25 subunits. Mediator phosphorylation levels change upon an external stimulus set by exposure of cells to high salt concentrations. Phosphorylated sites in the Mediator tail subunit Med15 are required for suppression of stress-induced changes in gene expression under non-stress conditions. Thus dynamic and differential Mediator phosphorylation contributes to gene regulation in eukaryotic cells.

TABLE OF CONTENTS

TABLE OF CONTENTS

CHAPTER I:
GENERAL INTRODUCTION

Regulation of Gene Expression in Eukaryotes

1. Regulation of gene expression in Eukaryotes

In 1958, Francis Crick postulated the fundamental model of how the flow of genetic information is directed through the cell. The central dogma of molecular biology describes the basic features involved in gene expression: DNA, which provides all information about evolution and functionalities of the organism. Messenger RNA as the activated and fleeting form of information, which serves as blueprint for proteins that execute cellular functions (Crick, 1958; Crick, 1970).

Many levels are involved in gene expression and each level is targeted for regulation. On the level of transcription (SECTION 1.1.1), activated transcription factors recognize DNA sequence elements and act as nucleation point for recruitment of coactivators and the Pol II machinery onto promoter regions (SECTION 1.1.2). Chromatin constitutes DNA topology and forms a structural barrier for transcription. Chromatin remodeling complexes adapt DNA topology to transcription by shifting nucleosome positions. Positioning and repositioning of nucleosomes as well as dynamic modification of histone tails are involved in regulation of every step of transcription (SECTION 1.1.3). Coactivators integrate the activation signal of transcription factors to the general Pol II machinery and coordinate the removal of nucleosomal barriers for proper transcription (SECTION 1.1.4). The chronology of regulatory events is modeled by the transcription cycle, which divides the transcriptional process into the main steps: initiation, elongation, termination and reinitiation. The transcritption cycle model integrates different steps to activate DNA encoded information by synthesis of RNA, as the activated and fleeting form of genetic information (SECTION 1.1.5 & 1.1.6). RNA molecules are processed on the post-transcriptional level before being transported to the cytoplasm to be subjected to the ribosome for translation. The major pathway for cytoplasmic messenger RNA degration is initiated by deadenylation (SECTION 1.2.1), followed by two alternative degradation pathways. The Exosome pathway degrades mRNA in 3'-5' direction, which requires the removal of 3'-poly(A) tail (SECTION 1.2.2 & 1.2.3). An alternative pathway requires decapped mRNA and degrades in 5'-3' direction, which includes cotranslational degradation of ribosome-bound mRNA (SECTION 1.2.4). A minority of mRNA is degraded deadenylation-independently, indicating an additional level of regulation for selected mRNA (SECTION 1.2.5). Messenger RNA can be stored in cytoplasmic P-bodies, which appear when excess of mRNA substrates overburdened the 5'-3'degradation system (SECTION 1.2.6).

Regulation of genetic information requires coordination of many levels, resulting in well defined temporal expression patterns that are characteristic for specific gene expresssion programs (Yosef, et al. 2011). Cell cycle, starvation, stress response and many other processes require a dynamic reorganisation between alternative gene expression programs that ensure cellular functionality under negative environmental changes. The high osmolarity glycerol

(HOG) pathway in *S. cerervisiae* is a paradigma for studying stress induced gene expression in eukaryotes (SECTION 2.1 & 2.2). Stress induced dynamics of gene expression require the exact quantitative and temporal coordination of individual transcript levels, which might result from an dynamic equilibrium of mRNA synthesis and decay.

1.1 Regulation of Transcription in *Saccharomyces cerevisiae*

The process of transcription is initiated by sequence specific transcription factors that recognize unique DNA sequence elements. The "ground state" of yeast promoters is inactive and activation can be achieved by single transcription activators or a combination of different activators binding to the upstream activation sequence (UAS) (Hahn & Young, 2011). Alternatively, transcription inactivation is achieved by repressors binding to upstream repression sequences (URS). The principle of combinatorial control of transcription has been shown for transcription of cell cycle genes, stress response (Bhoite, et al. 2001; Simon, et al. 2001; Horak, et al. 2002; Tan et al. 2008; Ni, et al. 2009) and glucose starvation (Young, et al. 2003; Tachibana, et al. 2005; Ratnakumar & Young 2010). DNA bound transcription factors serve as nucleation point for coregulators and general transcription factors to initiate the PIC assembly on the promoter.

1.1.1 Transcription factors

Transcription factors connect cellular regulation processes to transcription. Activated by several regulatory events, like phosphorylation, oxidation, cytoplamsic-nuclear shuttling, proteolysis or interaction with regulatory proteins, transcription factors are able to either initiate (activators) or repress (repressors) transcription. Transcription factors are one major determinant that connects cellular signaling to gene expression. There are several mechanisms of transcription factor activation. One of the best studied mechanisms is the activation of oxidative stress response (high H_2O_2 concentrations) by Yap1. Oxidative stress induces a conformational change of Yap1 by forming a disulfide bond between Cys598 and Cys303 that masks a C-terminal export signal (NES) leading to the accumulation of Yap1 in the nucleus (Delaunay, et al. 2000; Georgiou, 2002; Okazaki, et al. 2007). Yap1 activates transcription by recognition and binding to the SV40-AP1 recognition element ARE (TGACTAA), a specific DNA sequence which is recognized by an basic leucine zipper domain (Fernandes, et al. 1997; Landschulz, et al. 1998).

      The common functionalities of transcription factors are organized in functional modules. The DNA binding module, that recognizes specific DNA sequences, the transactivation module, that exhibits transcriptional activation potential and a multimerization module, that mediate homo- or heterologous interactions (Kadonagan, 2004). These functional modules can be either combined in one protein or shared between different proteins that act synergistically (Brivanlou, et al. 2002). A major mechanism of transcriptional activation is the recruitment of regulatory proteins onto the promoter region of specific genes (Brivanlou, et al. 2002). Many of these proteins are chromatin associated factors, e.g. chromatin remodelers, histone acetylases, histone methylases, HDACs, kinases, which modulate transcriptional activity (Orphanides, et al. 2002). For example, the activation domain of the human heat shock factor Hsf1 has been shown to recruit SWI/SNF to stress responsive genes (Sullivan, et al. 2001). In yeast, a number of acidic activators, e. g. Gcn4, Gal4 or Hap4 have been shown to interact with Tra1, a common subunit of SAGA and histone acetyl transferase NuA4 (Brown, et al. 2001; Narlikar, et al. 2002; Baker, et al. 2009; Bhaumik, et al. 2001).

Transcriptional repressors are involved in regulation of transcription by preventing the assembled general transcription machinery to initiate transcription. The Ssn6-Tup1complex, for example, is a conserved family of repressors, which has been found in yeast, flies, worms and mammals (Smith & Johnson, 2000). Ssn6-Tup1 is recruited to the promoter region of target genes by DNA binding proteins, like Mig1, Crt1 and Rox1 (Nehlin, et al. 1991; Balasubramanian, et al, 1993; Huang, et al. 1998), resulting in a decrease of respective transcript levels by up to 10^{-3} (Redd, et al. 1996). The majority of Ssn6-Tup1 repressed genes are involved in stress response and response to environmental changes. As an example, low glucose levels lead to phosphorylation of Mig1, which is exported from the nucleus and leads to derepression of glucose-repressed genes by removal of Ssn6-Tup1 from the promoter (De Vit, et al. 1997; Treitel, et al. 1998; Ostling & Ronne, 1998). Ssn6-Tup1 appears most likely to repress genes by preventing the promoter assembled general transcription machinery from transcription initiation. Evidence comes from the deletion of several Mediator proteins in yeast which all affect Ssn6-Tup1 repression (Carlson, M. 1997; Myer & Young, 1998), and the interaction of Tup1 with N-terminal tails of histones H3 and H4 (Edmondson, et al. 1998; Ducker & Simpson, 2000).

Expression of most eukaryotic genes is context dependent and might by modulated through combinatorial assembly of a set of gene specific regulators. There is striking evidence, that regulation of transcription is achieved by a set of factors which assemble in unique combinations of factors that result in a highly selective activation of transcription. The promoter regions contain many specific binding sites for multiple transcription factors to allow each gene to be regulated by multiple signaling pathways (Orphanides & Reinberg, 2002). In some cases, DNA binding proteins function as both, activator or repressor. For example, the yeast Mcm1 transcription factor combines both functions as activator or repressor. Mcm1 activates transcription when associated to Fkh2 or represses when bound to Yox1 (Darieva, et al. 2010; Leatherwood, et al. 2010). During osmotic stress the yeast transcription factor Sko1 is activated by phosphorylation and converts the repressor Ssn6-Tup1 into an activating state which recruits SAGA histone acetylase and SWI/SNF to osmotic stress inducible promoters (Proft & Struhl, 2002). However, the combinatorial assembly of regulatory proteins is modulated by several processes, like posttranslational modifications, nuclear localization, conformational changes, proteolysis, chromatin assembly and accessibility to DNA binding sites. The mechanisms of regulation of gene expression at the level of transcription factors and repressors are conserved from yeast to human and the fact, that 5% of the human genome is predicted to encode transcription factors underscores the importance to this level of regulation (Tupler, et al. 2001).

1.1.2 Core promoter architecture

The general transcription factors and Pol II assemble to the preinitiation complex (PIC) at specific sequence elements on the promoter. The minimal set of DNA elements required for basal transcription is defined as the core promoter (Smale & Kadonaga, 2003). The core promoter architecture consists of the TATA element, initiator (INR), downstream promoter element (DPE), motif 10 element (MTE) and TFIIB recognition element (BRE). These functional elements are recognized by basal transcription factors and serve as platform for PIC assembly.

TATA elements. The TATA element consists of a T/A rich sequence exhibiting a conserved TATWAWR motif, which is recognized by the TATA box binding protein (TBP) (Basehoar, et al. 2004). In *S. cerevisiae,* the TATA element is located within a window of 50-120 bp upstream of

transcription start site (TSS) (Hampsey, 1998; Zhang & Dietrich, 2005). TBP recognizes the TATA element by two quasi-symmetrical domains, which contact the DNA minor groove by hydrophobic interactions. TBP kinks the DNA at the 5' and 3' ends of the TATA element and partially unwinds the DNA helix (Smale & Kadonaga, 2003). DNA recognition by TBP serves as a nucleation point for PIC assembly (Koleske & Young, 1994; Ranish, et al. 1999). TBP has been identified as a subunit of the general transcription factor TFIID, but, however, TBP interacts also with the Spt-ADA-Gcn5-acetyltransferase complex (SAGA). Only 13 % of yeast promoters contain TATA elements and the majority of these promoters are SAGA dependent, highly regulated and generally stress responsive (Hahn & Young, 2011). TATA-less promoters, however, require TBP also for function, but bind the basal transcription factor TFIID, which indicates alternative pathways for PIC assembly (Seizl, et al. 2011; Cormack, et al. 1992; Burley, 1996; Pugh & Tijan 1991; Hahn, et al. 1989; Sikorsky & Buratowski, 2009; Smale, 1996).

Initiator (INR). The initiator sequence is located around the transcription start site (TSS) and can be weakly bound by Pol II itself or strongly when Pol II is accompanied by TFIIB, TFIID and TFIIF (Dikstein, 2011). The TFIID subunits Taf1 and Taf2 directly contact the INR element. The functionality of the INR can be either alone, in combination with the TATA element or in conjunction with the downstream promoter element (DPE) (Dikstein, 2011). TATA element and INR function synergistically when both are located within a window of 25-30 bp, but independently when separated by more than 30 bp (Smale & Kadonaga, 2003).

DPE and MTE. The downstream promoter element (DPE) and the motif-10 element (MTE) are two important sequence elements in higher eukaryotes. However, DPE and MTE do not appear to be present in *S. cerevisiae*, but belong to the class of sequence elements recognized by TFIID and function in combination either with the INR or in combination with TATA and INR (Juven-Gershon & Kadonaga, 2010).

BRE (BREu / Bred). TFIIB interacts with the major groove upstream and with the minor groove downstream of the TATA element (Nikolov, et al. 1995). The DNA sequence which promotes the interaction was named TFIIB recognition element (BRE) and the two contact sites were titled upstream BRE (BREu) and downstream BRE (BREd). Both sites function in conjunction with the TATA element and have been found to increase or decrease the levels of basal transcription (Juven-Gershon & Kadonaga, 2010).

All of these core promoter elements are degenerate, low specificity DNA sequences that vary in conservation among species. The variations and multiplicity of different core promoter element combinations contribute to the nature of combinatorial gene regulation (Hahn & Young, 2011; Smale & Kadonaga, 2003).

1.1.3 Chromatin and Chromatin remodeling

Nucleosomes are inhomogeneously distributed throughout the genome and form a defined DNA topology pattern. The region approximately 150-200 bp upstream of the TSS is kept free of nucleosomes and is called the nucleosome free region (NFR), which might ensure the accessibility for non-histone proteins and assemblation of the transcription machinery (Yuan, et al. 2005; Lee, et al. 2007; Jiang & Franklin, 2009). Nucleosomal DNA is wrapped around core histones (H3, H4, H2A, H2B), which are predominant globular proteins. Histones form an

unstructured N-terminal tail, which is dynamically modified with defined consequences for chromatin function and structure. Histone modifications show two functional characteristics: First, the change in the net charge of nucleosomes affects inter- or intranucleosomal DNA-histone interactions, which result in a closed, unaccessible topology (heterochromatin) or in an open, accessible topology (euchromatin) (Li, et al. 2007). Second, individual histone modifications are recognized by non-histone proteins, which coordinate adaption of the DNA topology to every step of transcription as well as to reestablish the correct chromatin state. Histone modifications are selectively recognized by specialized domains that can be found in many non-histone proteins. For example, the yeast methyltransferase Set1 has been shown to catalyze the di- and tri-methylation of H3K4 and stimulate the transcriptional activity of many genes, as shown for *pph3, ino1* and *met16* (Santos-Rosa, 2002; Briggs, et al. 2001). Tri-methylated H3K4 is present exclusively at active genes and peaks at transcription start sites (Santos-Rosa, et al. 2002; Pokholok, 2005). The SAGA subunit Chd1 recognizes di- and trimethylated of H3K4 by its chromodomain (Pray-Grant, et al. 2005; Daniel, et al. 2005; Flanagan, et al. 2005) and mediate the stabilization of SAGA onto chromatin (Bhaumik, S.R., 2011). Once SAGA is recruited to the promoter region, it may stimulate recruitment of TBP to SAGA dependent genes by an combined interaction with Spt3 and Spt8 to TBP (Bhaumik, et al. 2002; Larschan, et al. 2001; Laprade, et al. 2007).

Chromatin remodeling. Chromatin creates a structural barrier for each step of eukaryotic transcription (Narlikar, et al. 2002). DNA is wrapped 1.65 turns around the histone octamer and the resulting chromatin structure constitute DNA topology which leads to either accessible or buried DNA regions (Luger, et al. 1997). To ensure a proper activation of transcription, chromatin must be dynamically coordinated with all steps of transcription to ensure accessibility of all regulatory factors and general transcription machinery to DNA. By altering the nucleosome position, coactivator proteins enhance or regulate the accessibility of the general transcription machinery to the transcription start site. Chromatin remodeling complexes use ATP hydrolysis to slide, eject, insert or restructure histones to change nucleosomal topology (Mohrmann, et al. 2005; Saha, et al. 2006; van Vugt, et al. 2007). Histones exhibit 14 DNA contacts, which have to be broken and reconstructed by remodeling complexes during translocation of nucleosomes along the DNA. Approximately 4.2 kJ/mol are required for breaking one histone-DNA contact and approx. 59 kJ/mol to remove the histone completely (Luger, et al. 1997; Gottesfeld, et al. 2001). The different substrate specificity is provided by additional domains or associated factors, because all chromatin remodeling activities are part of a multiprotein complex (Narlikar, et al. 2002).

In yeast, there are five different subfamilies of the ATPase super-family 2 (SF2) of the DEAD/H-box nucleic acid stimulated ATPase (Eisen, et al. 1995). According to their additional specificity, the yeast chromatin remodeling complexes are classified by their protein motifs: SWI2/SNF2-types have bromodomains which recognize acetylated lysines (Winston, et al. 1999), ISWI-types contain SANT and SLIDE domains, that involve histone tail and linker DNA binding respectively (Grune, et al. 2003), CHD-types bear chromo-domains, that bind to methylated lysines (Bannister, et al. 2001), and INO80-type have DBINO domains that are predicted to bind DNA (Bakshi, et al. 2004). Nucleosome remodeling by SWI/SNF is stimulated by promoter bound SAGA, which acetylates histone H3 by its intrinsic HAT activity. SWI/SNF removes acetylated histone 3 from the *gal1*-promoter (Hassan, et al. 2002; Chandy, et al. 2006). Moreover, HAT complexes such NuA4 and SAGA increase RSC-stimulated transcription of Pol II

in vitro (Carey, et al. 2006). Therefore, the HAT activity of SAGA promotes SWI/SNF activity and the rapid removal of promoter nucleosomes and contribute to transcription initiation as it has been shown for *gal1* and *pho5* promoters (Reinke, et al. 2005; Weake & Workman, 2010).

ISWI proteins are involved in nucleosome repositioning at the promoter which may block transcription by potentially impeding the TBP binding to DNA (Mellor, et al. 2004; Stockdale, et al. 2006; Morillon, et al. 2003; Lindstrom, et al. 2006; van Vugt, et al. 2007). Upon transcription initiation, ISWI force the repositioning of nucleosomes on the coding region, which may shift Pol II into elongation (Mellor, et al. 2004; Morillon, et al. 2003).

1.1.4 Transcription Coactivators: Mediator, SAGA, TFIID and Tafs

The Mediator complex bridges gene specific regulatory factors to the general Pol II transcription machinery and stimulates high induction levels of activator-dependent transcription (see CHAPTER IV). The *S. cerevisiae* Mediator complex consists of 25 subunits which can be subdivided into four distinct modules:

The head module consists of seven individual subunits (Med6, Med8, Med11, Med17, Med18, Med20 and Med22). The Med8 subunit links two parts of the head module, the Med8(C), Med11/22 part which contacts the TBP and the Med8(N), Med6, -17, -22, -11 part which contacts the Rpb3/11 subunits of Pol II (Takagi, et al. 2006; Lariviere, et al, 2008; Cai, et al. 2010). The Mediator head binds weakly to a minimal PIC composed of Pol II, TFIIF, TFIIB, TBP and promoter DNA, suggesting a possible function in stabilizing the PIC.

The middle module appears as an elongated subcomplex composed of nine subunits (Med1, Med4, Med7, Med9, Med10, Med21, Med31, Med14 and Med19). The middle module is targeted by gene specific transcription factors. The flexibility of the elongated structure may allow for the conformational changes upon binding to Pol II (Koschubs, et al. 2010; Cai, et al. 2009).

The tail module interacts with a variety of transcription activators and consists of Med5, Med16 and the Med15, Med2 & Med3 submodule. Mutations in the tail module result in predominantly decreased gene expression (Hahn & Young, 2011), suggesting a function in integrating signaling pathways to activation of transcription.

The kinase module consists of four subunits (Med12, Med13, CDK8 and cycC), which are dissociable from the Mediator complex and have both, positive and negative effects on gene expression (Björklund & Gustafsson, 2005; van de Peppel, et al. 2005; Taatjes, et al. 2010). The kinase module provides the cyclin dependent kinase (CDK) activity of the Mediator. During transcription initiation, the S5 position of the C-terminal domain of Pol II (CDT) is phosphorylated by Kin28 subunit of TFIIH and CDK8, which promotes the dissociation of the Mediator complex from the CTD (Jasnovidova & Stefl, 2012).

In yeast, there are two distinct mechanisms, which are mediated either by SAGA (Spt-Ada-Gcn5-Acetyltransferase) or TFIID. Both complexes share TBP and are involved in PIC formation. The *S. cerevisiae* SAGA complex consists of fifteen non-essential and six essential subunits, which regulate gene expression through covalent modification of histones (Bhaumik, 2011). The Gcn5 and Ubp8 components possess histone acetyl transferase (HAT) and histone

deubiquitylase activity. In addition, SAGA is targeted by transcription activators, which promote the recruitment and histone covalent modifications and guide its stabilization with TBP on the promoter (Daniel, et al. 2007; Bhaumik, 2011). Approx. 90% of genes require TFIID for expression and this mechanism is SAGA independent. TFIID is composed of TBP and a conserved set of TBP associated factors (TAFs), which are arranged in a promoter dependent composition. The direct interaction of the TAFs and transcription activators suggest a flow of information from the activators to the PIC at TFIID dependent genes (Garbett, et al. 2007; Bhaumik, 2011).

Table 1: Complexes involved in Pol II preinitiation complex (PIC) assembly (adapted from Sikorski & Buratowski, 2009);

Pol II	12 Subunits; catalyzes transcription of all mRNAs and a subset of noncoding RNAs including snoRNAs and miRNAs
TFIIA	2–3 subunits; functions to counteract repressive effects of negative cofactors like NC2; acts as a coactivator by interacting with activators and components of the basal initiation machinery
TFIIB	Single subunit; stabilizes TFIID-promoter binding; aids in recruitment of TFIIF/Pol II to the promoter; directs accurate start site selection
TFIID	14 subunits including TBP and TBP Associated Factors (TAFs); nucleates PIC assembly either through TBP binding to TATA sequences or TAF binding to other promoter sequences; coactivator activity through direct interaction of TAFs and gene specific activators
TFIIE	Two subunits; helps recruit TFIIH to promoters; stimulates helicase and kinase activities of TFIIH; binds ssDNA and is essential for promoter melting
TFIIF	2–3 subunits; tightly associates with RNA Pol II; enhances affinity of RNA Pol II for TBP-TFIIB-promoter complex; necessary for recruitment of TFIIE/TFIIH to the PIC; aids in start site selection and promoter escape; enhances elongation efficiency
TFIIH	10 subunits; ATPase/helicase necessary for promoter opening and promoter clearance; helicase activity for transcription coupled DNA repair; kinase activity required for phosphorylation of RNA Pol II CTD; facilitates transition from initiation to elongation
Mediator	At least 24 subunits; bridges interaction between activators and basal factors; stimulates both activator dependent and basal transcription; required for transcription from most RNA Pol II dependent promoters
SAGA	20 subunits; interacts with activators, histone H3, and TBP; histone acetyltransferase activity; deubiquitinating activity
TFIIS	One subunit; stimulates intrinsic transcript cleavage activity of RNA Pol II allowing backtracking to resume RNA synthesis after transcription arrest; stimulates PIC assembly at some promoters
NC2	Two subunits; binds TBP/DNA complexes and blocks PIC assembly; can have both positive and negative effects on transcription
Mot1/bTAF1	Single subunit; induces dissociation of TBP/DNA complexes in ATP dependent manner; can have both positive and negative effects on transcription

1.1.5 RNA Polymerase II and Preinitiation Complex

Transcription initiation by RNA Polymerase II requires a set of general transcription factors, which assemble to the preinitiation complex (PIC) on the promoter region (Table 1). The general transcription factors mediate promoter recognition, recruitment of Pol II, connect gene-specific factors to the PIC, interact with histones and promote DNA unwinding (Sikorsky & Buratowski, 2009). Furthermore, regulation of Pol II activity depends on a plethora of additional factors that mediate the central steps in the transcription cycle.

RNA Polymerase II. Synthesis of mRNA in eukaryotes is carried out by the RNA dependent Polymerase II (Pol II). The structure is composed of 12 subunits, which consist of the 10-subunit catalytic core and the heterodimeric Rpb4/7 subcomplex (Cramer, et al. 2001; Armache, et al. 2005) (Figure 1). The largest subunit, Rpb1, exhibits an elongated C-terminal

domain (CTD), which consists of tandem repeats with the consensus sequence YSPTSPS. The number of YSPTSPS-repeats varies between *S. cerevisiae* (26 repeats) and *H. sapiens* (52 repeats), which appear to correlate with genomic complexity (Egloff, et al. 2012). Post-translational modifications of the Pol II CTD mediate a variety of functional processes. The dynamic modifications synchronize transcriptional and co-transcriptional steps with every step of the transcription cycle. The possibilities of CTD phsophorylation generate a wide range of distinct combinations, which led to the CTD-code model (Egloff, et al. 2012). The CTD is involved in assembly of the PIC, functionally interacting with the Mediator, coupling chromatin remodeling to transcription, synchronizing mRNA processing (capping, splicing, polyadenylation) and mediating mRNA export (Hahn & Young, 2011; Egloff, et al. 2012).
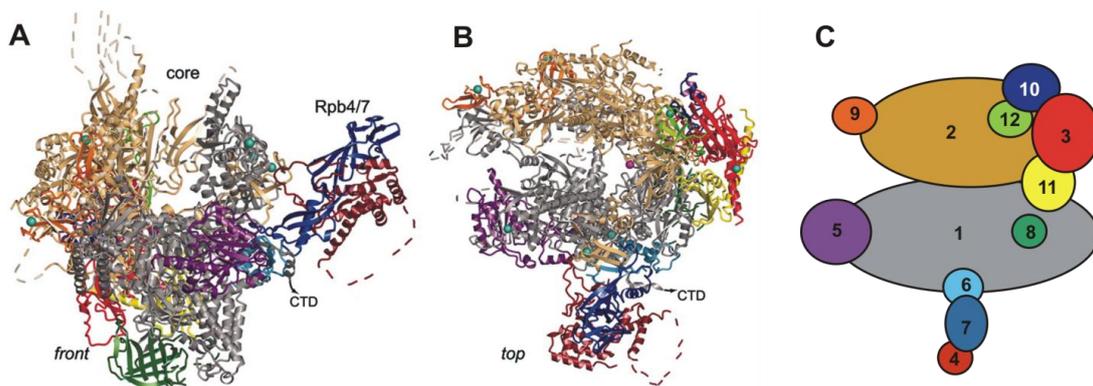
Figure 1: *Complete RNA Polymerase II structure.* (adapted from Armache, et al. 2005). **A)** & **B)** ribbon diagram showing RNA Polymerase II model from the front view (A) and top view (B). Dashed lines represent disordered loops. **C)** The diagram illustrate the relative positions of the subunits within the structure.

1.1.6 Polymerase II Transcription cycle

The process of mRNA synthesis can be functionally organized in the transcription cycle which is divided into the major steps: Transcription initiation, elongation, termination and reinitiation (Orphanides, et al. 1996; Roeder, 1996; Svejstrup, 2004).

Transcription initiation begins with the formation of the PIC at the promoter. Although a number of activation mechanisms have been proposed, the best-studied and apparently the major mechanism of transcription activation is described by the recruitment model (Hahn & Young, 2011; Ptashne and Gann, 2002; Chatterjee & Struhl, 1995). Gene specific activators recruit the co-activators (e.g. Mediator) and general transcription factors onto the promoter (Figure 2). The TBP (TFIID), TFIIA and TFIIB form a complex with promoter DNA for binding Pol II. Additionally, TFIIF is involved in stabilization of the PIC and contributes to setting the transcription start site (Hahn & Young, 2011). Transcription initiation begins with the formation of the closed promoter complex, which includes the 10 subunit Pol II, the subcomplex Rpb4/7, the promoter complex (TBP/TFIID; TFIIA, TFIIB, TFIIF), TFIIE, TFIIH and TFIIS (Sikorsky & Buratowski, 2009; Cheung & Cramer, 2012; Hahn & Young, 2011).

Transcription start site scanning in S. cerevisiae. There is evidence, that *S. cerevisiae* Pol II scans the DNA sequence for a suitable transcription start. Consistent with this, the *gal1* and *gal10* promoter regions are unwound from approx. 20 bp to 90 bp downstream from the TATA element and through the TSS (Giardina & Lis, 1993; Kuehner & Brow, 2006; Steinmetz, et al. 2006). The proposed mechanism requires DNA strand unwinding and DNA translocation which

is promoted by the TFIIH (Rad25/XBP) helicase under ATP hydrolysis (Hahn & Young, 2011). The mechanism of start site selection in *S. cerevisiae* is dependent on TFIIB, TFIIF and Pol II, as mutations in all of this factors reduce accuracy of start site selection significantly (Kostrewa, et al. 2009; Hahn & Young, 2011). Isomerisation from the closed to the open promoter complex involves a dramatic conformational change that requires the TFIIH helicase dependent separation of DNA strands around the TSS (DNA melting). The single stranded DNA is inserted into the active site of Pol II. The initially formed DNA/RNA hybrid is not sufficient to form a stable complex, which results in short RNAs during abortive initiation (Luse & Jacob, 1987; Shandilya & Roberts, 2012). When the RNA reaches a length of 6 nucleotides and more, initiation factors are released and a stable transcription elongation complex is formed (Cheung & Cramer, 2012).

Transcription elongation starts with the escape of Pol II from the promoter region and catalyzes template-directed formation of the RNA phosphodiester bond, which is stimulated by several transcription elongation factors (Brueckner, et al. 2009). At DNA lesions in the template strand or incorporation of noncomplementary nucleotides, Pol II moves backwards (backtracking) and can cause transcriptional arrest. Negative elongation factors can significantly slow elongation or induce a transient pause to allow promoter proximal regulation or overcoming the nucleosome barrier during elongation (Petesch & Lis, 2012; Palangat, et al. 2005). The reactivation of Pol II elongation requires additional factors, such as TFIIS, which stimulate RNA cleavage or Spt4/5, which increases transcriptional processivity (Martinez-Ruboco, et al. 2011; Werner, 2012; Sikorsky & Buratowski, 2009). The nascent mRNA is processed co-transcriptionally, to form the 5'-cap (m7G-PPP), splice introns, assemble mRNPs and form the poly(A)-tail when reaching the termination.

Termination of transcription involves dissociation of the template DNA at the termination site, which is located up to 1 kb downstream of the poly(A) site. This stage of transcription is critical, because mRNA is released from the DNA template and Pol II is prepared to re-initiate transcription. Additionally, accurate termination prevents active Pol II from perturbing nearby promoters. Such transcriptional interference has been observed in yeast where genes are closely spaced and commonly expressed (Greger & Proudfoot, 1998; Proudfoot, et al. 2002). There are two different models describing the termination mechanism. The "anti-terminator-model" postulates that 3'-processing factors induce a conformational change to enable recruitment of termination factors or to displace an anti-termination factor (Logan, et al. 1987). The "torpedo model" postulates that the 5'-end of the RNA, which is formed by poly(A) directed cleavage of the RNA, is used as substrate for a nuclease, such as Rat1 or nuclear Xrn1. The nuclease catches up with the elongating Pol II and dissociates the elongation complex from DNA (Proudfoot, 1989). The released pre-mRNA undergoes subsequent maturation and processing steps before it is exported to the cytoplasm and prepared for translation.

Re-initiation and gene looping. In yeast the transcription factor TFIIB has been shown to interact with termination specific complexes. From this observation, a model was proposed that assumes the formation of DNA loops which position the termination site in close proximity to the promoter. TFIIH has been shown to be involved in promoter-terminator contacts and recycling of Pol II by recruiting to the re-initiation scaffold, that have remained on the promoter after the previous round of transcription (Calvo, et al. 2003; Singh, et al. 2007; Shandilya & Roberts, 2012).
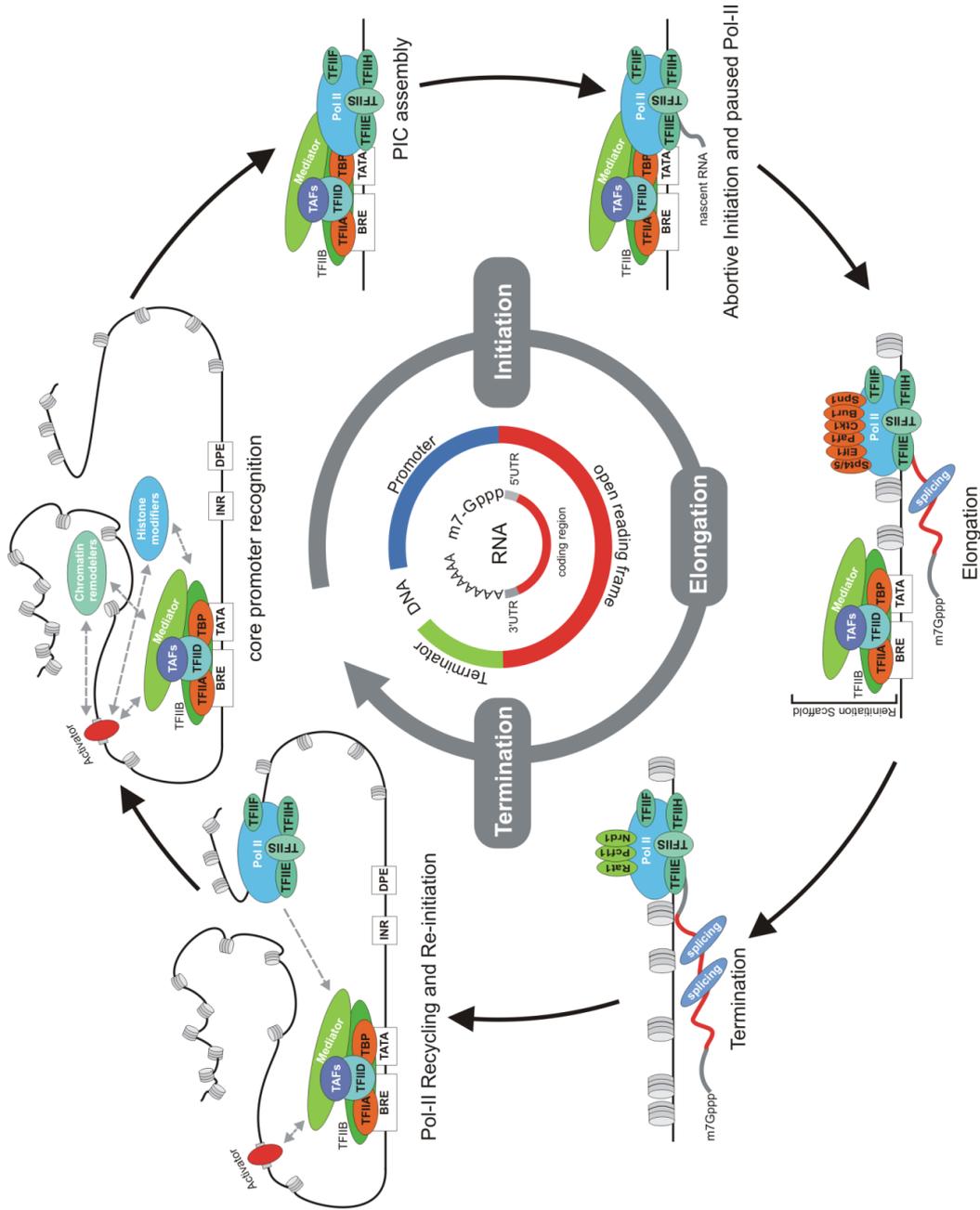
Figure 2: *Transcription cycle in eukaryotes.* Principle steps in RNA Polymerase II transcription: Initiation, Elongation and Termination and central features on the protein-, DNA- and RNA layer. The protein-layer (outer circle) illustrates the basic features and main proteins during transcription in *Saccharomyces cerevisiae*. The corresponding DNA features (inner circle) are illustrated as promoter, open reading frame and termination region. The corresponding RNA (center circle) features are illustrated within the center-circle as m7Gppp (mRNA-cap), 5'UTR, protein coding region, 3'UTR and poly(A)-tail. (own figure based on Lenhard, et al. 2012; Smale & Kadonaga, 2003; Shandilya & Roberts, 2012; Svejstrub, 2004; Hahn, 2004; Mayer, et al. 2010)

1.2 Post-transcriptional regulation of gene expression

The mRNA degradation network plays a crucial role in quality control, surveillance and mRNA metabolism. There are only two enzymatic functions, Xrn1 and the Exosome, which execute cytoplasmic degradation of bulk mRNA. In principle, mRNA itself carries intrinsic singals for guiding its own degradation encoded in sequence features like AU-rich elements, stabilizer elements (STE) and others cis-acting elements. The main stability determants, however, are 5'-cap and 3'-poly-A-tail, which act as safeguards to prevent mRNA from unspecific degradation (Figure 3).

1.2.1 Deadenylation dependent decay

Degradation of cytoplasmic bulk mRNA is initiated by shortening the 3'-poly(A)-tail. This deadenylation step is the only reversible step in the turnover-pathway and it allows - under specific circumstances - selected transcripts to get readenylated and return to polysomes (Gray, et al. 1998; Tucker, et al. 2001; Mitchell and Tollervey, 2001). In *S. cerevisiae*, two deadenylase complexes, namely Pan2-Pan3 and Ccr4-Not, have been identified. Current models suggest that the Pan2-Pan3 complex is involved in the early step of poly(A) metabolism, because it trims a poly(A)-tail of initially approx. 200 nucleotides to about 55-75 nucleotides in length (Brown, et al. 1998). The main deadenylase in yeast is Ccr4-Not, a large multisubunit complex which exists in two prominent forms of 1.2 MDa or 2 MDa and consits of 9 core subunits (Collart, 2003). The Ccr4 and Caf1 subunits provide the deadenylase activtiy and both are required for normal deadenylation within the cytoplasm. After removal of the poly(A)-tail, the transcript takes one of two irreversible routes for degradation. The unprotected mRNA 3'-end is substrate for the Exosome, which hydrolysis mRNA in 3'-5' direction (Exosome pathway). Transcripts taking the other route for degradation, must undergo an additional step which removes the 5'-cap from the mRNA body. This decapping step is followed by hydrolysis in 5'-3' direction accomplished by the exoribonuclease Xrn1. Interestingly, Hu et al. (Nature, 2010) could show, that Xrn1 hydrolysis even polysomal mRNA and therfore degrade transcripts cotranslationally. However, both the Xrn1 and the Exosome pathway are not mutually exclusive, because knock-out experiments on each pathways had only minimal effects on the transciptome. This observation implies a functional redundancy of the two pathways but the question of their relative contribution to bulk mRNA degradation is not fully understood. (Garneau, et al. 2007, Collard, 2003).

1.2.2 The 3'-5' exoribonucleolytic pathway: Exosome

The Exosome pathway degrades transcripts in 3'-5' direction after the initial polyadenylation step. The Exosome is a multiprotein complex which is present in protozoa, yeast and mammalian cells and exists as a nucleic and a cytoplasmic variant. The structural core of the eukaryotic Exosome is composed of nine subunits. Central structural element is a ring-like structure consisting of six PH-domain carrying RNase proteins (Ibrahim, et al, 2008) which are flanked by three proteins harbouring either S1- or KH domains, which are often found in RNA binding proteins (Bonneau, et al. 2009). This overall structural composition is conserved in other RNA-degrading protein complexes of simpler architecture in archeae and bacteria.

  Regulation of Exosome activity: There are in principle two mechanisms that block Exosome activity and provide a possible strategy for modulation between Exosome and Xrn1 dependent degradation. A well characterized example is the heptameric Lsm complex in yeast. The initial deadenylation step forms a short oligo(A)-fragment which provides an unprotected

3'-terminus which is a preferred substrate for Exosome degradation. The Lsm complex, recognizes and binds to the unprotected 3'-end to prevent the transcript from Exosome activity. Lsm bound transcripts are shifted to degradation by the alternative 5'-3' exonucleolytic pathway (decapping-pathway), where Lsm is required for efficient decapping (Tharun, et al. 2005). Another example is the PAPBD domain of the 3'-poly(A) binding protein Pap1 (PAPBC1) which has been described to prevent mRNA from 3'-5' degradation, when PAPBC1 is bound to the poly(A)-tail. Trans-acting factors may induce a conformational change in PAPBC1 and induce its dissociation from poly(A) sequence (Ibrahim, et al. 2009).

1.2.3 Scavenger enzymes and stress response

After mRNA degradation by the Exosome, a short oligonucleotide is released which carries the 5'-cap structure. An accumulation of capped oligonucleotides in the cytoplasm is problematic, because cap-binding proteins, like the translation initiation factor eIF4E, can be titrated and this might lead to inhibition of translation (Filman, et al. 2006). To ensure that capped oligonucleotides are rapidly removed, a specialized function is needed to recognize and immediatly degrade selectively those structures. This function is provided by scavenger decapping enzymes, like Dcp-S in humans and a heterodimer consisting of Dcp1 and Dcp2 in yeast. Scavenger enzymes are members of the HIT family of pyrophosphatases and use a histidine-triad for their enymatic activity (Coller, 2000). The substrates of both Dcp-S and Dcp1/Dcp2 are selectively short oligonucleotide. This selectivity is important to prevent scavenger enzymes from prematurely decapping mRNA which are not targeted for degradation (Coller, et al. 2004). Recent studies, however, demonstrated that the Dcs1/Dcs2 heterodimer is involved in regulation of mRNA turnover and stress response. Malys, et al. (2004) could show, that the transcription of Dcs1/Dcs2 heterodimer is induced by nutrient stress and disruption of Dcs1/Dcs2 heterodimer anticipate trehalose regulation, which is critical for cellular stress response (Malys, et al. 2004). Although the principle task of Dcs1/Dcs2 heterodimer is to dispose capped oligonucleotides resulting from Exosome mRNA degradation, the heterodimer plays also a role in stress response and modulation of mRNA stability by maintaining the 5'-3' decay pathway.

1.2.4 The 5'-3'-exoribonucleolytic pathway: Decapping and degradation by Xrn1

After deadenylation, cytoplasmic bulk mRNA can be exoribonucleolytically degraded in 5'-3' direction by the exonuclease Xrn1. Transformation of mature mRNA into Xrn1 substrate requires transcripts with a free 5'-monophosphate mRNA. This is achieved by hydrolysis of m^7Gpp-cap structure from 5'-end of mRNA (decapping). In *S. cerevisiae* decapping is performed by a heterodimeric enzyme complex which consists of Dcp1 and Dcp2. Several experiments revealed, that the heterodimer accepts execusivly a 7-methyl-group, bound to mRNA of at least 25 nucleotides in length (Coller, et al. 2000). The catalytic acitivity is intrinsic to Dcp2, which harbours a NUDIX motif that is often found in pyrophosphatases. Mutations in the Dcp2-NUDIX-motif inactivate the decapping activity of the Dcp1/Dcp2 heterodimer. This observation suggests a model that Dcp1 modulates the enzymatic activity of Dcp2.
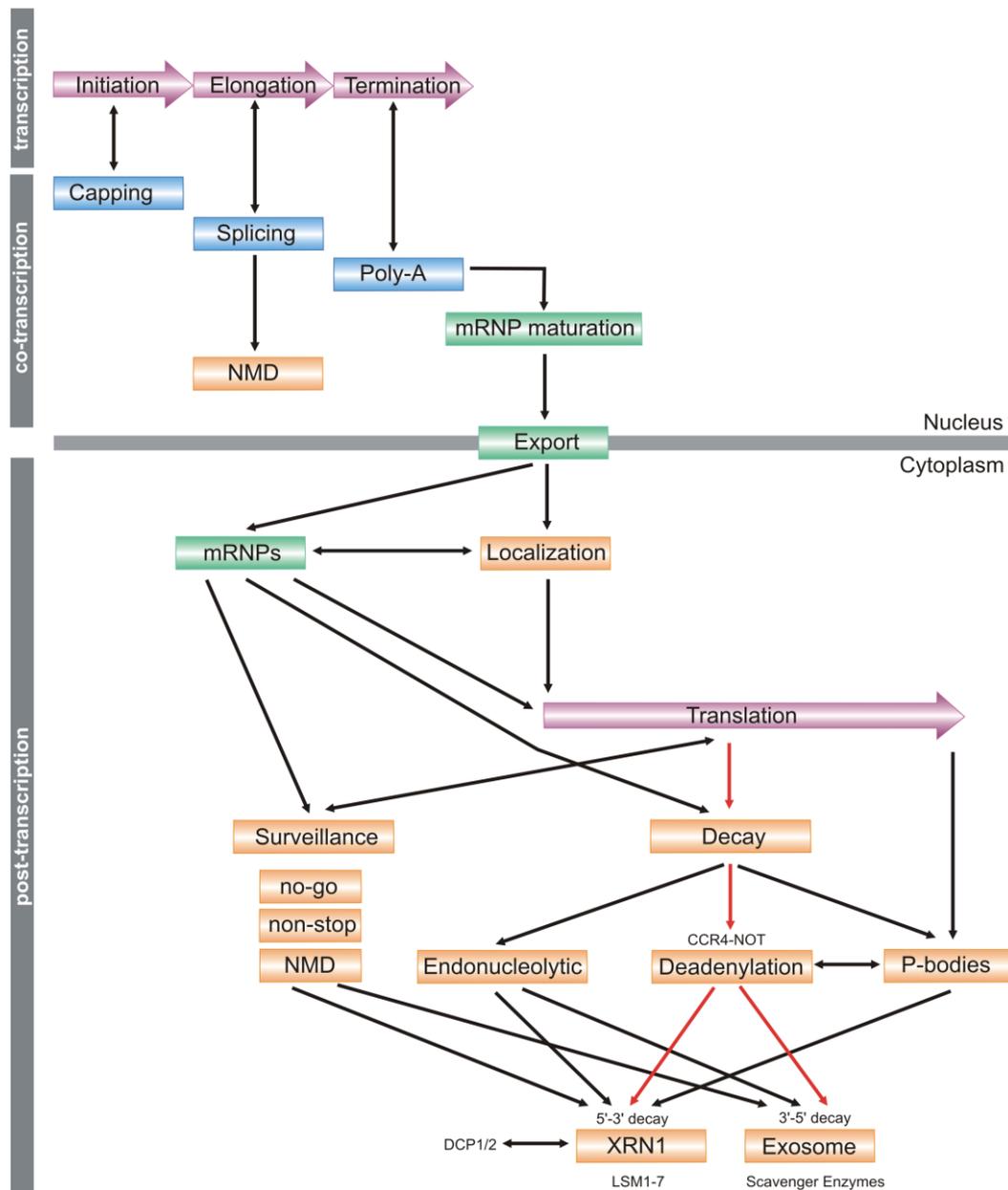
Figure 3: *Overview to key processes of mRNA life-cycle in Saccharomyces cerevisiae.* **Transcription:** Nascent RNA is generated by Pol II transcription, which is divided in three major steps: initiation, elongation and termination. **Co-transcriptional processes:** The major determinants of mRNA stability (5'-cap and 3'-poly(A)tail) are covalently added to the precursor mRNA. Cotranscriptionally, the 5'-end is covalently modified by addition of 7-methylguanylate cap (capping) and the 3'-end is polyadenylated. Most eukaryotic genes require the removal of introns from precursor mRNA to form mature mRNA (splicing). Transcripts containing an premature nonsense codon are recognized and subjected to the nonsense mediated decay (NMD) pathway, which is part of the general mRNA surveillance mechanism (Vasudevan, et al. 2003). Export factors assemble on the mature mRNA, form a messenger ribonuclecleoprotein complex (mRNP), which directs the transcript to the cytoplasm. **Post-transcriptional processes** localize the mRNPs to specific foci, where polysome assembly result in translation of genetic information into amino acid sequence and protein formation. Messenger RNA decay can occur after an initial deadenylation step, followed by degradation using one of two alternative degradation pathways. Degradation by the exonuclease Xrn1 degrades transcripts in 5'-3' direction after removal of the 5'-cap structure. Degradation by Xrn1 includes even polysomal mRNA and can occur co-translationally (Hu, et al., 2009). The alternative pathway degrades mRNA in 3'-5'direction by the Exosome. Selected transcripts carry intrinsic degradation singnals and undergo an specific degradation pathway, that cleaves mRNA endonucleolytically. The resulting fragments are subjected to Xrn1 or to the Exosome for comlete degradation. Messenger RNA can be stored in cytoplasmic P-bodies, which appear when the 5'-3'degradation system is seemingly overloaded. The surveillance mechanism ensure fidelity and quality of mRNPs and translation. The No-go mechanism degrades ribosomal transcripts, on which the ribosome have stalled during translation. The non-stop mediated decay detect and degrade transcripts, which lack a stop codon. Analogous to the nuclear NMD, the cytoplasmic nonsense-mediated decay degrades transcriptis containing an premature stop codon to prevent from production of truncated proteins. (own figure based on following references: Housley, et al 2009; Garneau, et al. 2007; Kultarni, et al., 2010; Parker & Song 2004; Atkinson, et al., 2008; Tomecki et al. 2010; Keene, 200; Rodriguez-Navarro, et al. 2011; Hu, et al., 2009; Harel-Sharvit, et al., 2010; Lotan, et al. 2005).

Regulation of decapping enzymes: Decapping is the critical step to initiate 5'-3' exoribonucleolytic decay by Xrn1. Several proteins have been identified which function either to accelarate or decelerate the decapping process. Inhibitors of decapping are among proteins involved in upstream processes, like deadenylation. For example, the poly(A)-binding protein Pab1 is able to inhibit decapping and might connect the upstream deadenylation step to decapping (Morrissey, et al. 1999). In addition, the cap-binding protein eIF-4E, required for initiation of translation, also impedes decapping (Coller et al. 2004). Proteins belonging to decapping enhancers can be separated in two groups. The first group contains proteins, that act as general enhancers and are not transcript specific. The predominant representative is the LSM-heptamer, that binds to the 3'-oligo(A)-tail after deadenylation (Tharun, et al. 2005). The LSM-complex might act as a switch to favor the decapping/Xrn1 pathway versus degradation by the Exosome. Further members are Dhh1, which is a DEAD-box containing helicase (Coller, et al. 2001) and Pat1 (alias: MRT1), a topoisomerase II associated factor, which has been shown to interact with the LSM complex and is functionally linked to poly(A)-binding protein Pab1 (Bonnerot, et al. 2000; Wang, et al. 1996). The second class of decapping enhancers act not globally but have an effect on selected transcripts. Other representatives are members of the Puf family, which bind to individual mRNAs and control decapping processivity with high specificity (Isken, et al. 2008). A connection to another decay-process, the nonsense-mediated-decay (NMD), is made by the mRNA-specific regulators Upf1/2/3 wich are required for recognition and rapid decapping induced by NMD (Isken, et al. 2008; Maquat, et al. 2001).

5'-3'-exoribonucleolytic activity: Xrn1

After decapping, transcripts provide a 5'-monophosphate which is a preferred substrate for the 5'-3' exoribonnuclease Xrn1 (alias: KEM1), a member of a large familiy of conserved exonucleases. Homologues of Xrn1 are found in all eukaryotes, including the human homologue *Hs*Xrn1 and pacman in *Drosophila melanogaster.* A nuclear variant of Xrn1 has been identified, the exonuclease Rat1 (alias: Xrn2), which is involved in RNA processing and poly(A)-dependend and –independent transcription termination. Rat1 and Xrn1 are closely related sharing a sequence identity of 39% (Kenna, et al. 1993) and suggesting a functional redundancy of both enzymes, which is provided in different cellular compartments (Johnson, et al. 1997). Xrn1 has been located in P-bodies and colocalizes with enzymes required for mRNA decapping (Sheth, et al. 2003).

1.2.5 Deadenylation independent decay

Unusual degradation pathways

Although deadenylation-dependent decay is the major route for bulk mRNA degradation in the cytoplasm, there is a minority of mRNAs which undergo unusual pathways for degradation. Recent studies on selected reporter transcripts revealed that selected mRNAs can bypass the regular deadenlyation step and are subjected to degradation by either Xrn1 or Exosome.

     Deadenylation-independent decapping. Selected transcripts bypass the initial deadenylation step and are degraded despite a poly(A)-tail on their 3'-end (deadenylation-independent decapping). The predominant representative for deadenylation-independent decapping is an mRNA encoding for Edc1, a protein which has been identified as enhancer of decapping. Analysis of the 3'-UTR revealed a poly(U)-track that is required for both protection from deadenylation and deadenylation-independent degradation. Muhlrad & Parker (2005)

hypothesized that this mechanism is essential for a feedback-loop regulation that might compensate a decrease of decapping activity. Surprisingly, the decapping of Edc1-mRNA is slowed in the absence of Not2, Not4 and Not5. All three proteins interact with Ccr4/Pop2 deadenylase complex and might be a possible link between mRNA deadenylation and decapping (Muhlrad & Parker, 2005). A second example of deadenylation-independent decay is given by the mRNA of yeast ribosomal protein Rps28b, member of the small 40S subuint. The Rps28b protein is able to bind a specific stem-loop structure in the 3'-UTR of its own transcript and recruits thereby Edc3, an enhancer of decapping. Badis, et al. (2004) could show, that this autoregulatory mechanism is strongly dependent of Edc3 and binding of Rps28b to its own transcript might recruit the decapping machinery via Edc3. In summary, these two examples illustrate that deadenylation-independent decapping – in contrast to degradation of bulk cytoplasmic RNAs – provides a possible regulatory mechanism for selected subsets of transcripts.

mRNA decay fast-track: Endoribonucleolytic pathway
In *S. cerevisiae*, the RNase multiprotein-complex Mrp cleaves the 5'-UTR (as shown for the *clb2* transcript) at several points and creates fragments with accessible substrates for both Xrn1 and Exosome (Gill, et al. 2004). The resulting fragments are degraded in both directions at once. Mrp is restricted to the nucleus and mitochondria, with exeption at the end of mitosis, when it is transported to special foci called TAM- a special type of P-bodies, the place where degradation of transcripts takes place. This strategy is a fast-track for degradation of mRNA and perhaps the most efficient and it provides a novel way to regulate the cell-cycle via regulated degradation of selected transcripts encoding regulatory proteins.

1.2.6 P-bodies

In *S. cerevisiae*, proteins involved in translation-initiation, deadenylation, decapping and 5'-3' exonucleolytic pathway, nonsense-mediated decay and components of the Exosome form granular cytoplasmic foci, which are called P-bodies and appear when the 5'-3' decay system is overloaded with mRNA (Garneau, et al. 2007). P-bodies decrease in number and size or disappear completely, when the amount of mRNA to be decayed is reduced. Current models suggest, that P-bodies are cellular sites of mRNA decay, but all proteins involved are not exclusively located inside P-bodies but also in the cytoplasm. It is most likely that P-bodies are formed when the interplay between translation and mRNA decay has to be regulated, e.g. in response to cellular stress (Garneau, et al. 2007).

Upon severe osmotic stress, stabilized mRNAs are observed to be moved into a nontranslating pool in P-bodies which coincides with an inhibition of translation (Uesono, et la., 2002). A decrease in translation rates correlates with an increase in P-bodies, where mRNA decay factors are concentrated and mRNA decay can occur (Teixeira, et al, 2005; Parker and Sheth, 2007; Halbeisen, et al. 2009). Simultaneous repression of translation and deadenylation allows cells to selectively translate mRNA required for stress response, while retaining the majority of the cytoplasmic pool of mRNAs for later reuse and recovery from stress (Hilgers, et al. 2006). Inhibition of mRNA deadenylation and degradation after hyperosmotic stress was also observed in human cells (Gowrinshankar, et al. 2006). In a *hog1* mutant, the P-bodies remain assembled for hours and Hog1 affects the kinetics of P-body disassembly and the return of mRNA to translation (Romero-Santacreu, et al. 2009).

2. HOG pathway in Yeast

2.1 HOG-pathway as model for stress induced gene expression

In all eukaryotes, response to environmental changes are mediated via stress activated protein kinases (SAPKs), which lead to a complex reorganization of cellular functions and extensive reorganisaiton of gene expression (Hohmann, S., 2002; De Nadal, et al. 2010). The network which coordinates stress induced gene expression is highly dynamic, efficient and responds remarkably flexible to different stress types and intensities by constant reconfiguration with tight temporal coherence (Yosef, et al. 2011; de Nadal and Posas, 2010; Lopez-Maury, et al. 2008). To analyze the characteristics of stress induced gene expression, the response of *S. cerevisiae* to osmotic stress is commonly used as a model, because many of the components have highly conserved homologues in humans. Individual kinases of the yeast high osmolarity – glycerol (HOG) pathway can be replaced by the corresponding human enzymes, as it has been shown for Hog1, Pbs2 and Ssk2 when replaced by their mammalian counterparts, p38 alpha, Mkk3, Mtk1 respectively (de Nadal & Posas, 2010).

2.1.1 Human Hog1 homologue p38 and associated diseases

The human Hog1-homologue p38 is involved in neuronal cell death and has been shown to be activated in Parkinson's disease models (Kim et al. 2010). p38 is implicated in cytoskeletal abnormalities of spinal motor neurons, a feature of familial and sporadic ALS, through aberrant phosphorylation and consequent aggregation of neurofilaments (Kim, et al. 2010). P38 activation results in downstream activation of p53 and treatment with p38-inhibitor (SB239063) protected primary dopaminergic neurons from cell death and prevented the downstream phosphorylation of p53 and its translocation into the nucleus in vivo in the ventral midbrain (Karunakaran, et al. 2008).

2.2 HOG pathway in *S. cerevisiae*

Environmental changes such as high salt concentrations create a hyperosmotic force that causes water efflux and reduction of intracellular pressure (Hohmann, 2002; Melamed, et al. 2008). The altered membrane potential change the activity of transmembrane proteins (Norbeck & Blomberg, 1998), and disrupts ion homeostasis and pH equilibrium, which causes protein misfolding and generation of reactive oxygen species (ROS) (Mendoza et al. 1994; Lahav et al. 2004; Koziol et al. 2005; Mortensen et al. 2006). Cells respond to high salinity by activation of several processes which monitor osmotic pressure, control water content, turgor, cellular shape and result in activation of gene expression program to antagonizes osmotic stress (Klipp, et al.

2005; Hohmann, 2002). In yeast, high salt concentrations are sensed by two transmembrane osmosensor systems, Sln1 and Sho1. Both activate the HOG phosphorylation cascade, that activates the mitogen activated kinase Pbs2 (Hao, et al. 2007; Tatebayashi, et al. 2006; O'Rourke, et al. 2002). Pbs2 phosphorylates the cytoplasmic kinase Hog1 which translocates into the nucleus within minutes (Westfall, et al. 2008; Ferrigno, 1998), induces cell cycle arrest (Escote, et al. 2004), dissociation of chromatin bound proteins (Proft & Struhl, 2004), and translation inhibition (Uesono & Toh, 2002). Activated Hog1 induces reorganization of transcription by phosphorylation of several specific transcription factors and interaction with the Pol II transcription machinery (Hohmann, 2002). The stress response results in intracellular production of glycerol and trehalose which function as osmolytes to reduce osmotic pressure and enable cells to reenter the cell cycle (Hohmann, et al. 2002; Macia, et al. 2009). Glycerol accumulation is enhanced by the rapid closing of aquaglyceroporin Fps1 (osmolarity-regulated glycerol channel) (Klipp, et al. 2005; Mollapour, et al. MCB, 2007).

2.2.1 Activation of transcription

Hog1 is activated by Pbs2 via phosphorylation and regulates activity of several transcription factors involved in activation of stress responsive genes. Hot1, Smp1, Msn2 and Msn4 activate transcription of different subsets of genes and ensure a coordinated expression of genes with similar functions (coregulation). Msn2 and Msn4, for example, are required for transcription of genes belonging to the environmental stress response (ESR) (Gasch, et al. 2000). ESR genes are induced by several stresses, such as DNA damage, heat shock, osmo- and oxidative stress; In *S. cerevisiae*, the induction of ESR genes is not governed by a single regulatory system but rather by many pathways and transcription factors. Another type of coregulation is carried out by Sko1, which functions as activator or repressor of different subgroups of stress inducible and Hog1 dependent genes (Rep, et al. 2000; Proft, et al. 2001). Phosphorylation by Hog1 modifies the association of Sko1 with Tup1-Ssn6 and allows the recruitment of chromatin remodeling complexes, such as SAGA and SWI/SNF to promoters (Proft & Struhl, 2002; Zapater, et al. 2007; Proft & Struhl, 2004; Guha, et al. 2007; Kobayashi, et al. 2008).

Hog1 regulate not only the function and activity of several transcription factors, Hog1 itself is recruited to target promoter and indicate a role in regulation of transcription (De Nadal & Posas, 2010; Alepuz, et al. 2001; Chellappan, 2001; Proft & Struhl, 2002). The binding of Hog1 is only restricted to osmotic stress inducible genes (Pascual-Ahuir, et al. 2006; Pokholok, et al. 2006; Proft, et al, 2006). Hog1 interacts tightly to the largest Pol II subunit Rpb1 (phosphorylated on Ser5 and Ser7 of the C-terminal domain) and play a role in elongation (Alepuz, et al. 2003). Hog1 interacts with elongating Pol II and recruits Rpd3 histone deacetylase complex to stress-specific promoters which leads to a reduced accessibility of Pol II and deficient gene expression (deNadal and Posas, 2010; deNadal, et al. 2004).

CHAPTER II
MATERIALS AND METHODS

1. Materials

1.1 Bacterial strains

Bacterial strains which were used in this work are listed in table 2. For cloning, *E. coli* XL-1 Blue strains were used. Protein expression was performed with *E. coli* BL21-CodonPlus (DE3)RIL cells.

Table 2: *Echerischia coli* strains

Strain	Description	Source
XL-1Blue	rec1A; endA1; gyrA96; thi-1; hsdR17; supE44; relA1; lac[F' proAB lacIqZΔM15Tn10(Tetr)]	Stratagene
BL21-CodonPlus(DE3)RIL	B; F-; ompT; hsdS(rB, mB); dcm+; Tetr; gal (DE3); endA; Hte [argU, ileY, leuW, Camr]	Stratagene

1.2 Yeast strains

Yeast strains which were used within the experimental work for this study are listed in table 3. The strains were generated by Susanne Röther (lab of Katja Strässer, Gene Center, Ludwig-Maximilians University, Munich), by Stephan Jellbauer (lab of Ralf-Peter Jansen, Gene Center, Ludwig-Maximilians Unviersity, Munich) or by own preparation. Selected strains were purchased from European *Saccharomyces cerevisiae* Archive for Funktional Analysis (Euroscarf; Institute of Molecular Biosciences, Johann Wolfgang Goethe-University, Frankfurt).

Table: 3: *Saccharomyces cerevisiae* strains

Strain	Genotype	Source
RS453 TAP-Srb4	MATa; Ade2-1; His3-11,15; Ura3-52; Leu2-3,112; Trp1-1; Can1-100;Gal+;	Susanne Röther
RS453 TAP-Srb4Lys1::KanMX	MATa; Ade2-1; His3-11,15; Ura3-52; Leu2-3,112; Trp1-1; Can1-100; Gal+;Lys1::KanMX	Susanne Röther
BY4742	MATα,*his2Δ1*,leu2Δ0,met15Δ0,ura3Δ0	Euroscarf
BY4742 Med15/ YOL051w::KanMX	MATα,*his2Δ1*,leu2Δ0,met15Δ0,ura3Δ0,YOL051w::KanMX	Euroscarf
BY4742 Hog1/YLR113w::KanMX	MATα; *his2Δ1*; leu2Δ0; met15Δ0; ura3Δ0; YLR113w::KanMX	Euroscarf
TAP-Med19	W303; *MATa* or *MATα*; *leu2*D3; 112 *trp1*D1;*can1*D100; *ura3*D1; *ade2*D1; *his3*D11-15; TAP-Rox3	Stephan Jellbauer
W303 Med19/YBL093c::clonNAT	W303; *MATa* or *MATα*; *leu2*D3; 112 *trp1*D1;*can1*D100; *ura3*D1; *ade2*D1; *his3*D11-15; *YBL093C::ClonNAT*	Stephan Jellbauer

YBL093cΔ181–220::clonNAT	MATa,*his2Δ1*,leu2Δ0,met15Δ0,ura3Δ0,YBL093CΔ181–220::clon NAT	Stephan Jellbauer
BY4742 Med15phospho-mutant (D30P)	MATα,*his2Δ1*,leu2Δ0,met15Δ0,ura3Δ0, Med15T728A Med15S729A Med15S730A Med15S746A Med15T750A Med15S752A Med15S767A Med15T769A Med15S783A Med15S785A Med15S789A Med15T793A Med15S796A Med15S798A Med15T800A Med15S803A Med15T804A Med15S810A Med15T820A Med15T828A Med15TS831A Med15S978A Med15S983A Med15S984A Med15S985A Med15S987A Med15S1003A Med15S1008A Med15S1018A Med15S1034A	This work
BY4742 Med15phospho-mutant (D7P)	MATα,*his2Δ1*,leu2Δ0,met15Δ0,ura3Δ0, Med15T746A Med15T750A Med15T796A Med15T798A Med15T769A Med15T767A Med15T800A	This work

1.3 Oligonucleotides

Oligonucleotides were used for classical cloning. The oligonucleotides were purchased from Thermo (Thermo Fisher Scientific Inc.) in RP-HPLC quality. The oligonucleotides were named in the following order: name of the gene – organism – restriction site – occasionally: N-termanl/C-terminal tag for affinity purification; seq = sequencing primer; UTR = untranslated region; rt_pcr = quantitative real time PCR; – foreward/reverse primer.

Table: 4: Oligonucleotides

ID	Name	Sequence
CM-18	Rox3-Sc-NdeI-N-Strep-TEV-For	GGGCCCGGGCATATGGCTTCTAGAGTGGACGAAACTACAGTCCCC T
CM-19	Rox3-Sc-HindIII-Rev	GGGCCCGGGAAGCTTTTACTACTCCAGCCTCCTTCTTTTCATATCCCTTCA
CM-54	Rox3-Sc-pET-NdeI-TEV-Strep-8-For	GGGCCCGGGCATATGGAAAACCTGTATTTTCAGGGATGGAGCCACCCGCAGTTCGAAA AAACTACAGTCCCCTCATACTACTATTACGTGGAT

CM-38	Rox3-Sc-Rev-HindIII-Cterm-Strep-TEV	GGGCCCGGGAAGCTTTTATTTTTCGAACTGCGGGTGGCTCCA TCCCTGAAAA TACAGGTTTTCCTACTCCAGCCTCCTTCTTTTCATATCCTC
CM-54	Rox3-Sc-pET-NdeI-TEV-Strep-8-For	GGGCCCGGGCATATGGAA AACCTGTATTTTCAGGGATGGAGCCACCCGCAG TTCGAAAAA ACTACAGTCCCCTCATACTACTATTACGTGGAT
CM-55	Rox3-Sc-pET-NdeI-TEV-Strep-30-For	GGGCCCGGGCATATGGAAAACCTGTATTTTCAGGGATGGAGCCACCCGCAGTTCGAAA AACTACAGGACTTGATATCGGTGTATGGCTTGGATGACATCTCCAGGCAAGTG
CM-56	Rox3-Sc-pET-NdeI-TEV-Strep-102-For	GGGCCCGGGCATATGGAA AACCTGTATTTTCAGGGATGGAGCCACCCGCAG TTCGAAAAAGATACAACCACCTCAGCAGGGTCAAAACATGTCAGA
CM-57	Rox3-Sc-pET-NdeI-TEV-Strep-180-For	GGGCCCGGGCATATGGAAAACCTGTATTTTCAGGGATGGAGCCACCCGCAG TTCGAAAAAAAGCCAATCCGGCTCAAATTCAGGTAACAA
CM-58	Rox3-Sc-pET-HindIII-101-Rev	GGGCCCGGG AAGCTT TTACATGTCTGGGTTATTTTGGAAAAGAATATGTGCTAT
CM-60	Rox3-Sc-pET-HindIII-160-Rev	GGGCCCGGG AAGCTTTTATCCCCCTTGGTTCTGGTTTGCGAATCTGCTTGG ATA TGA
CM-61	Rox3-Sc-pET-HindIII-180-Rev	GGGCCCGGGAAGCTTTTAGCTTTTTCCTGTACCGTCTAGATCAAACGCCAAGTCGTCT ACATC
CM-77	Gal11-seq-001-for	ATGTCTGCTGCTCCTGTCCAAGACAAA
CM-78	Gal11-seq-001-rev	TGTTGTTGAGGAGTCAATTGACGCCTC
CM-79	Gal11-seq-002-for	ACAATTAGTGAACCAGATGAAAGTGGC
CM-80	Gal11-seq-002-rev	GCTTGACAGGTTCCGTCATCGTACTAC
CM-81	Gal11-seq-003-for	AAAGTTTTATTAGGAAATACATTAACC
CM-82	Gal11-seq-003-rev	TGGGTTAGGTTGTTGCTGAGCTTGTTG
CM-83	Gal11-seq-004-for	CTACATGGGTTGACACCTACTGCAAAG
CM-84	Gal11-seq-004-rev	TGCTGCATTTGCTGTAGTGACTGTTGC
CM-85	Gal11-seq-005-for	TTTACAGCAATTGAAAATGCAGCAGCA
CM-86	Gal11-seq-005-rev	CCATAGGAGACTGTACAGTCTTCATAT
CM-87	Gal11-seq-006-for	GTGCACAACCATCATATAATAGTGCCA
CM-88	Gal11-seq-006-rev	TCTTTTTCTTGGGTTGCCGACATCCAT
CM-89	Gal11-seq-007-for	AAAGCCAGCGTATTAGAAATAAGCCCG
CM-90	Gal11-seq-008-rev	TCAAGTAGCACTTGTCCAATTATTCCA
CM-101	Sc-Rox3-18-NdeI-Strep-TEV-F	GGGCCCGGGCATATGTGGAGCCACCCGCAGTTCGAAAAAGAAAACCTGTATTTTCAGG GACCGGAAACTACATATACGTACCAACAA
CM-106	Sc-Rox3-18-NdeI-His-TEV-F	GGGCCCGGGCAATGCACCATCACCATCACCATGAAAACCTGTATTTTCAG GGACCGGAAACTACATATACGTACCAACAA

CM-120	Sc-Rox3-39-NdeI-Strep-Throm-For	GGGCCCGGGCATATGTGGAGCCACCCGCAGTTCGAAAAACTGGTGCCAAGGGGCAGCGGCTTGGATGACATCTCCAGGCAAGTG
CM-130	Sc-Rox3-UTR-SmaI-for	GGGCCCGGGCCCGGGTCCAGACGGAAACCATACAATGCCTCC
CM-131	Sc-Rox3-UTR-SacI-rev	GGGCCCGGGGAGCTCAAGCATTGTGCTATTGTGGCTTCCCTT
CM-234	Sc-Gal11-NLS-974-EcoRI-for	GGGCCCGGGGAATTCTTTAAAGACTTGTCC
CM-235	Sc-Gal11-NLS-1044-XhoI-rev	GGGCCCGGGCTCGAGTCCTGATTTTGTCAT
CM-358	Ctt1-rt_pcr-for	TGGTCTTGTTCGTTTTTCCA
CM-359	Ctt1-rt_pcr-rev	TGGGTCTCTTGCAGTGTCTG
CM-360	Stl1-rt_pcr-for	CCGTGTCAATGCAAATCGT
CM-360	Stl1-rt_pcr-for	CGTGGCGATTCAGGTAGTTT
CM-362	Gpd1-rt_pcr-for	GGTCTAGGCTGGGGTAACAA
CM-363	Gpd1-rt_pcr-rev	GATCTCACCCAAACCGACTC
CM-377	Act1-rt_pcr-for	TCCGTCTGGATTGGTGGT
	Tub1-rt_pcr-for	AGGGAAGAGTTTCCTGATCGT
	Tub1-rt_pcr-rev	AAGTCTTCGGAGAGGGCAAG
	Kss1-rt_pcr-for	TGCTTCAATTCAATCCTGACA
	Kss1-rt_pcr-rev	TTGCCAGGTAAGGGTGTCTT
	Sfg1-rt_pcr-for	ACGAACCCTCTCACCGTCTA
	Sfg1-rt_pcr-rev	TTCAGAGATTTGGCTGGTACTG
	Rnd18-rt_pcr-for	AAACGGCTACCACATCCAAG
	Rnd18-rt_pcr-rev	TCCCTGAATTAGGATTGGGTAAT
CM-430	RT-PCR-Cpt1-for1	TGCGATATTGTGCAGCTTTT
CM-431	RT-PCR-Cpt1-rev1	GCTAGATAAAGTTTGTGGGTGTGA
CM-432	RT-PCR-Cpt1-for2	TCAAACCATCTGGCACACTAA
CM-433	RT-PCR-Cpt1-rev2	CGGTTTCAACATCAAACACAA

CM-434	RT-PCR-Gpi10-for1	TTGCATTTCTGGCATGTTTG
CM-435	RT-PCR-Gpi10-rev1	TGCTGGGAATTACCCAAATAA
CM-436	RT-PCR-Gpi10-for2	AATGATTTTAACTTCTATTGCCCTCT
CM-437	RT-PCR-Gpi10-rev2	TTTTATCATTTGTCCGCCTGT
CM-438	RT-PCR-Pac1-for1	CGTCCTGTTCCAGAGATCAAA
CM-439	RT-PCR-Pac1-rev1	TTCAACGACCAACCATTGTG
CM-440	RT-PCR-Pac1-for2	TCTGTTGCAAGAATCAGTGGA
CM-441	RT-PCR-Pac1-rev2	CCATACTTTCGTTACTGGTGTCA

1.4 Plasmids

Plasmids which were used in this study are listed in table 5. The plasmids were generated by classical cloning or by insertion of synthetic genes (purchased from GeneArt or Mr. Gene; both are now registered trademarks of Invitrogen) into the respective vector of interest. Some of the plasmids were ordered from Addgene (Cambrigde, MA, USA) or from Dana-Farber/Harvard Cancer Center (Boston, MA, USA).

Table: 5: Plasmids

code	Construct	aa	vector	sites	Affinity-Tag	Primer	Comment
CH-9	S.c.-Rox3 full lenth	1 – 222	pET-21b	NdeI / HindIII	Strep-tag@N-terminus	CM-18 CM-19	Classical cloning
CH-10	S.c.-Rox3 full length	1 - 222	pET-21b	NdeI / HindIII	Strep-tag@C-terminus	CM-18 CM-38	Classical cloning
CH-13	S.c.-Rox3-Δ7-Δ102	8-101	pET-21b	NdeI / HindIII	Strep-tag@N-terminus	CM-54 CM-58	Classical cloning
CH-14	S.c.-Rox3-Δ7-Δ161	8-160	pET-21b	NdeI / HindIII	Strep-tag @ N-terminus	CM-54 CM-60	Classical cloning
CH-15	S.c.-Rox3-Δ7-Δ181	8-180	pET-21b	NdeI / HindIII	Strep-tag@N-terminus	CM-54 CM-61	Classical cloning
CH-16	S.c.-Rox3-30-180	30-180	pET-21b	NdeI / HindIII	Strep-tag@N-terminus	CM-55 CM-61	Classical cloning
CH-17	S.c.-Rox3-Δ101-Δ181	102-180	pET-21b	NdeI / HindIII	Strep-tag@N-terminus	CM-56 CM-61	Classical cloning
CH-18	S.c.-Rox3-Δ180-220	181-220	pET-21b	NdeI / HindIII	Strep-tag@N-terminus	CM-57 CM-19	Classical cloning

CH-26	S.c.-Rox3-Δ7	8-222	pET-21b	NdeI / HindIII	Strep-tag@N-terminus	CM-54 CM-19	Classical cloning
CH-29	Sc-Rox3-Δ17Δ181	18-180	pET-21b	NdeI/HindIII	Strep-Tag@N-term	CM-101 CM-61	Classical cloning
CH-30	Sc-Rox3-Δ17Δ180 (163 aa+tag; 18430 Da+tag)	18-180	pET-21b	NdeI/HindIII	His-Tag@N-term	CM-106 CM-61	Classical cloning
CH-37	Sc-Rox3-Δ32Δ180	33-180	pET-21b	NdeI/HindIII	Strep-Tag@N-term; Thrombin	CM-101 CM-61	Classical cloning
CH-39	S.c.-Med15/Gal11-full length (+UTR) (Insert-length: 4445 bp)	5'-UTR (500bp) +Gal11ΔNLS 3'-UTR (300bp)	pRS-316	KpnI/XbaI	--------		Classical cloning
CH-40	S.c.-Med15/Gal11-fl	1-1081	pUC-36	EcoRI/XhoI	-----	CM-24 CM-25	Classical cloning
CH-44	Sc-Rox3-NLS	181-221	VCH2 mCherry-puc36	EcoRI/XhoI	--------	--------	Classical cloning
CH-45	Sc-Rox3-full length	1-220	VCH2 mCherry-puc36	EcoRI/XhoI	--------	--------	Classical cloning
CH-46	Sc-Rox3ΔNLS	1-180	VCH2 mCherry-puc36	EcoRI/XhoI	--------	--------	Classical cloning
CH-49	S.c.-Med15/Gal11-NLSonly	974-1044	VCH-2 (mCh-Puc36)	EcoRI/XhoI	-----	CM-234 CM-235	Classical cloning
CH-50	Sc-Rox3-UTR 500 up UTR 300 down UTR	Full length + UTR	Prs-316	SacI/SmaI		CM-130 CM-131	Classical cloning
CH-54	Sc-Rox3-Δ17Δ220	18-220	pET-21b	NdeI/HindIII	Strep-Tag@N-term; TEV	CM-101 CM-19	Classical cloning
CH-61	S.c.-Med15/Gal11-NLS only	974-1044	Prs-316	EcoRI/XhoI	-----	CM-234 CM-235	Classical cloning
CH-63	Sc-Rox3-UTR +500 up UTR +300 down UTR	Full length + UTR	Prs-314	SacI/SmaI		CM-130 CM-131	Classical cloning
CH-68	Sc-Rox3-UTR 500 up UTR 300 down UTR	Full length + UTR	Prs-315	SacI/SmaI		CM-130 CM-131	Classical cloning
CH-71	Gal11-full length +UTR		Yeplac181	SmaI (destroyed)	----------	----------	
CH-78	Sc-Rox3-Δ38Δ220	39-220	pET-21b	NdeI/HindIII	Strep-Tag@N-term; Thrombin	CM-120 CM-19	Classical cloning
CH-89	Gal11-C-terminus all phosphosites mutaed to alanine -Syntehic clone-	974-1044	pMA	BamHI/HindIII	----------	----------	Synthetic clone (MrGene) Oder-Nr.: 0910454 S983A S984A S985A S1003A S1008A S1018A S1034A

CH-90	Sc-Rox3-EWE6	1-192+ KKGRTNL EVRWLH QHIVTVM RI	pMK-RQ	---------	---------	Deletion of A577 causes a frameshift @ R193	Synthetic clone ordered from MrGENE; designed after EWE6 from David Gross
CH-91	Gal11-C-terminus all phosphosites mutated to alanine -Syntehic clone-	974-1044	VCH2 (pug36 with mCherry)	BamHI/ HindIII	---------	---------	Synthetic clone (MrGene) Oder-Nr.: 0910454 S983A S984A S985A S1003A S1008A S1018A S1034A
CH-92	Sc-Rox3-EWE6	1-192+ KKGRTNL EVRWLH QHIVTVM RI	VCH2	HindIII/ XhoI	CM-341 CM-342	Deletion of A577 causes a frameshift @ R193	Cloned from CH-90
CH-93	Gal11-full length with all phosphosites are mutated to alanine	Nucleo-tides: -583- Gal11- +624	pMK				Synthetic clone from GeneART;
CH-94	Gal11-full length with all phosphosites are mutated to alanine	Nucleo-tides: -583- Gal11- +624	Prs-315				Synthetic clone from GeneART;
CH-95	Sc-Med3 full length	1-397	Prs315	HindIII/ SacII		CM-346 CM-347	Templ@e: MSe-P016
CH-97	Sc-Med6+Point Mutations+UTR	1-296+UTR	Pmk	ApaI/ SacII	---------	---------	Sc-Med6 PMs: T206A T208A S209A T211A T216A S225A S228A S229A T233A T240A S243A T244A T245A T250A T253A T256A T260A T265A Ordered form MrGene: 0921300_Sc-Med6 +500bpup +300b_pmk

CH-98	Sc-Med6+Point Mutations+UTR	1-296+UTR	Prs315	ApaI/ SacII	---------	---------	Sc-Med6 PMs: T206A T208A S209A T211A T216A S225A S228A S229A T233A T240A S243A T244A T245A T250A T253A T256A T260A T265A Ordered form MrGene: 0921300_Sc-Med6 +500bpup +300b_pmk
VCH-2	pmCherry-puc36	mCherry-CDS	Puc36	XbaI/ EcoRI	---------	---------	EGFP-CDS was replaced by mCherry-CDS
PEN5	Promoter fusion construct: S.c.-STL1-promoter (-800/+3) Fused to LAC-Z coding sequence		Ylp358R	EcoRI/ PstI		---------	Eulalia de Nadal (Proft, et al. 2006) and Alepuz, et al. 2002
SB-131	Sc-Rox3 full length	1-220	pUC-36	EcoRI/ XhoI	---------	---------	Sonja Baumli; Lab-stock
SB-132	Sc-Rox3ΔNLS	1-180	pUC-36	EcoRI/ XhoI	---------	---------	Sonja Baumli; Lab-stock
SB-133	Sc-Rox3 full length	1-220	pET-24d	NcoI/ NotI	---------	---------	Sonja Baumli; Lab-stock
SB-134	Sc-Rox3ΔNLS	1-180	pET-24d	NcoI/ XhoI	---------	---------	Sonja Baumli; Lab-stock
SB-135	Rox3-NLS	181-221	pUC-36	EcoRI / XhoI	---------	---------	Sonja Baumli; Lab-stock
TEVnew	TEV protease		pET-24d		His-tag@N-terminus;	---------	Arie Gerlof; Michael Stattler Lab; Munich;

1.5 Chemicals and reagents

Chemicals which were used in this study were obtained from Roth (Karlsruhe, Germany), Serva Electrophoresis (Heidelberg, Germany), Sigma Aldrich (Seelze, Germany), Invitrogen (NY, USA), Merck (Darmstadt, Germany), Formedium (Hunstanton, Norfolk, GB). Chemicals and reagents from other sources are explicitly mentioned. Chemicals, reagents and enzymes for cloning were obtained from Roche (F. Hoffmann La-Roche; Germany), Fermentas (St. Leon Rot, Germany), New England Biolabs (Frankfurt am Main, Germany), Agilent/Stratagene (Waldbronn,

Germany). Commercial kits from Qiagen (Hilden, Germany) were used for DNA preparations during classical cloning.

Table 6: Growth media

Media	Application	Description
LB	E. coli culture	1% (w/v) tryptone; 0.5% (w/v) yeast extract; 0.5% (w/v) NaCl
SOB	E. coli culture	2% (w/v) tryptone; 0.5% (w/v) yeast extract; 8.55 mM NaCl; 2.5 mM KCl; 10 mM MgCl2
SILAC-media	Yeast culture	0.67% (w/v) Formedia yeast nitrogen base without amino acids,, 2% glucose, 200 mg/l adenine, 200 mg/l tyrosine, 10 mg/l histidine, 10 mg/l methionine, 60 mg/l phenylalanine, 40 mg/l tryptophan, 20 mg/l uracil, 20 mg/l arginine For stable isotope labeling, SILAC media contained 30 mg/l $^{13}C_6$-, $^{15}N_2$-lysine (heavy lysine, Cambridge Isotopes) or 30 mg/ml $^{12}C_6$, $^{14}N_2$-lysine (light lysine, Sigma Aldrich)
YPD	Yeast culture	2% (w/v) peptone; 2% (w/v) glucose; 1.5% (w/v) yeast extract
Synthetic complete media (SC)	Yeast culture	0.69% (w/v) nitrogen base; 0.6% (w/v) CSM amino acid drop out mix; 2% (w/v) glucose; pH 5.6-6.0
YPD solid media	Yeast culture	2% (w/v) peptone; 2% (w/v) glucose; 1.5% (w/v) yeast extract; 1.5% (w/v) agar
SC drop out solid media	Yeast culture	0.69% (w/v) nitrogen base; 0.6% (w/v) CSM amino acid drop out mix; 2% (w/v) glucose; pH 5.6-6.0; 1.5% (w/v) agar
5'FOA-solid media	Yeast culture	SC (-ura) + 0.01% (w/v) uracil; 0.2% (w/v) 5-FOA
Synthetic defined media (SD)	Yeast culture	Nitrogen and carbon sources, vitamins, trace elements, minerals according to manufacturer`s information (ForMedium) with specific drop outs; only essential amino acids; pH 5.6-6.0

Table 7: Media additives for *E. coli* and *S. cerevisiae*

Media	Description	Stock solution	Applied concentration
IPTG	Isopropyl-ß-D-thiogalactopyranosid	1 M in H20	0.5 mM for *E. coli* culture
Ampicillin	Antibiotic	100 mg/ml in H20	100 μg/ml for *E. coli* culture, 50 μg/ml for yeast culture
Kanamycin	Antibiotic	30 mg/ml in H20	30 μg/ml for *E.a coli* culture
Chloramphenicol	Antibiotic	50 mg/ml in EtOH	50 μg/ml for *E. coli* culture
Tetracyclin	Antibiotic	12.5 mg/ml in 70% EtOH	12.5 μg/ml for yeast culture
Nourseothricin (clonNAT)	Antibiotic	100 mg/ml in H20	100 μg/ml for yeast culture
Geneticin (G418)	Antibiotic	200 mg/ml in H20	200 μg/ml for yeast culture

1.6 Buffers and solutions

Buffers, dyes and solutions which were generally used for different experiments are listed in table 8. Buffers which were used for protein purification were filtered sterile or autoclaved. Buffers for HPLC systems were additionally degassed before usage.

Table 8: Buffers and solutions

Name	Description	Method
electrophoresis buffer	25 mM Tris; 0.1% (w/v) SDS; 250 mM glycine	SDS-PAGE
4x stacking gel buffer	0.5M Tris; 0.4% (w/v) SDS; pH 6.8 at 25°C	SDS-PAGE
4x separation gel buffer	3 M Tris; 0.4% (w/v) SDS; pH 8.9 at 25°C	SDS-PAGE
1x Bradford dye	1:5 dilution of Bradford concentrate (BioRad)	SDS-PAGE
MOPS electrophoresis buffer	10.46% (w/v) MOPS (3-(N-Morpholino)propanesulfonic acid); 6.06% (w/v)TRIS base; 1% (w/v) SDS; 0.3% EDTA	SDS-PAGE
MES electrophoresis buffer	1% (w/v) MES 2-(N-morpholino)ethanesulfonic acid 6.06% (w/v)TRIS base; 1% (w/v) SDS; 0.3% EDTA	SDS-PAGE
5x SDS sample buffer	250 mM Tris/HCl pH 7.0 at 25°C, 50% v/v glycerol, 0.5% (w/v) bromophenol blue, 7.5% (w/v) SDS, 12.5% (w/v) mercaptoethanol	SDS-PAGE
Gel staining solution	50% (v/v) ethanol; 7% (v/v) acetic acid; 0.125% (w/v) Coomassie Brilliant Blue R-250	Coomassie staining
Gel destaining solution	5% (v/v) ethanol; 7.5% (v/v) acetic acid	Coomassie staining
TBE	8.9 mM Tris; 8.9 mM boric acid; 2 mM EDTA (pH 8.0, 25°C)	Agarose gel Electrophoresis
TE	10 mM Tris pH 7.4; 1 mM EDTA	Nucleic acids; yeast transformation
10xTBS	500 mM Tris/HCl pH 7.5, 1.5 M NaCl	Agarose gel Electrophoresis
1 x PBS	2 mM KH2PO4; 4 mM Na2HPO4; 140 mM NaCl 3 mM KCl, pH 7.4 @ 25°C	Diverse applications
6x Loading dye (Fermentas)	1.5 g/l bromophenol blue; 1.5 g/l xylene cyanol; 50% (v/v) glycerol	Agarose gel Electrophoresis
100x PI	0.028 mg/ml Leupeptin; 0.137 mg/ml Pepstatin A; 0,017 mg/ml PMSF; 0.33 mg/ml benzamidine in 100% EtOH p.a.	Protease inhibitor mix
TFB-1	30 mM KOAc, 50 mM MnCl2, 100 mM RbCl, 10 mM CaCl2, 15% (v/v) glycerol, pH 5.8 at 25°C	Chemically competent cells
TFB-2	10 mM MOPS pH 7.0 at 25°C, 10 mM RbCl, 75 mM CaCl2, 15% (v/v) glycerol	Chemically competent cells
Phosphatase-Inhibitor Mix	40 mM p-nitrophenylphosphate, 2 mM sodiumpyrophosphate, 2 mM sodium ortho-vanadate, 50 mM sodium fluoride	SILAC
TAP buffer A	250 mM sodium chloride, 50 mM TRIS/HCl pH 7.5, MgCl$_2$, 0.15% m/w NP-40, 1 mM DTT	Tandem affinity purification
TAP buffer B	100 mM sodium chloride 50 mM TRIS/HCl pH 7.5, MgCl$_2$, 1 mM DTT	Tandem affinity purification
Calmodulin-buffer	100 mM sodium chloride 50 mM TRIS/HCl pH 7.5, MgCl$_2$, 2 mM CaCl2; 1 mM DTT	Tandem affinity purification

TAP elution buffer	10 mM Tris pH 8.0, 20 mM EGTA	Tandem affinity purification
Avidin	50 µmol/l avidin; 50% (w/v) glycerin; 20 mM Tris pH 8.0; 150 mM NaCl; 10 mM ß-mercaptoethanol	Strep-tagII
50x d-Desthiobiotin	125 mM d-desthiobiotin; in 500 mM Tris pH 8.0	Strep-tagII
Rox3-buffer A	500 mM sodium chloride, 20 mM TRIS pH 8.0, 10 mM ß-mercaptoethanol	Protein purification
Rox3-buffer B	150 mM sodium chloride, 20 mM TRIS pH 8.0, 10 mM ß-mercaptoethanol	Protein purification
MonoQ-buffer A	50 mM NaCl, 20 mM Tris pH 8.5@4°C, 10 mM ß-mercaptoethanol	Protein purification
MonoQ-buffer B	2 M NaCl, 20 mM Tris pH 8.5 @ 4°C, 10 mM ß-mercaptoethanol	Protein purification
50% (w/v) PEG 3,350	50% (w/v) PEG 3,350, sterile	Yeast transformation
1 M lithium acetate	1 M lithium acetate, pH 7.5	Yeast transformation
Salmon sperm DNA	2 mg/ml Salmon sperm DNA in water (dd)	Yeast transformation
YTFB	0.2 M lithium acetate, 40% (w/v) PEG 3,350, 100 mM DTT	Yeast transformation
TCA-buffer A	10% Trichloracetic acid (TCA) in water (dd)	Protein precipitation

1.7 Buffers and solutions for DTA

Buffers and solution used for dynamic transcriptome anaylsis (DTA) are listed in table 9. Additional buffers and solutions were used as part of commercial kits. RNA extraction for DTA was perfomed with RiboPure-Yeast Kit (Ambion/Applied Biosystems), µMACS Streptavidin Kit (Miltenyi Biotec, Bergisch Gladbach, Germany) and RNeasy MinElute Cleanup Kit (Qiagen, Hilden, Germany).

Table 9: Buffers and solutions for dynamic transciptome analysis (DTA)

Name	Description	Method
10x Biotinylation buffer	100 mM Tris pH7.5; 10 mM EDTA; H_2O (RNAse free)	DTA
RNA washing buffer	100 mM Tris, pH7.5; 10 mM EDTA; 1M NaCl; 0.1%Tween; H_2O (RNAse free)	DTA
Biotin-HPDP-stock	1 mg/ml biotin-HPDP dissolved in dimethylformamide	DTA
RNA-Wash-solution1	100 mM TRIS pH 7.5; 10 mM EDTA; 1 M sodium chloride, 0.1 % (w/v) TWEEN 20; RNAse-free water;	DTA
RNA-Elution buffer	100 mM DTT in RNAse free water	DTA

2. Methods

2.1 General Methods

2.1.1 Preparation of chemically competent *E. coli* cells

A 200 ml LB medium was inocculated from an over night grown preculture to an OD_{600} of 0.05. The culture was incubated for several hours at 37°C to a final OD_{600} of 0.5, chilled on ice for 10 min before the cells were centrifuged at 3200 g for 10 min. The cells were washed with 50 ml TFB-1 buffer (Table 8) and resuspended in 4 ml TFB-2 buffer (Table 8). The resulting cell suspension was divided into 50 µl aliqotes, flash-frozen in liqid nitrogen and stored at -80°C.

2.1.2 Transformation of *E. coli* cells

To a 50 µl aliquot of the chemically competent E. coli cells (MATERIAL & METHODS, 2.1.1), 100 ng of plasmid DNA or 3-5 µl of the ligation reaction (Material & Methods 2.1.3) were added and incubated on ice for 20 min. The transformation mix was heat shocked for 15 sec at 45°C and immediatly cooled down on ice for at least 1 min, before 250 ml of room temperature LB medium was added. Cells were incubated for 1 hour at 37°C under constant shaking at 1400 rpm using the Thermomixer (Eppendorf). The transformation mix was plated on selective LB plates and incubated at 37°C over night.

2.1.3 Molecular cloning

Primer design: Primer used in PCR were designed with the following properties: First, a 9 nucleotide GC-rich sequence was added at the 5'-end, followed by a restriction site and optional sequence encoding (in-frame) for hexahistidine- or streptavidin-tag (strep-tag II). Second, the complementary sequence was designed between 18 and 25 nucleotides to reach a theoretical melting temperature (calculated with BioEdit (Hall, 1999)) of approx. 55°C. The complementary sequence ended with either a G or C nucleotide. Third, complementary sequences between the primerpairs were avoided. An overview to all primer which were used in this study is given in table 4 in this section.

Polymerase chain reaction (PCR): The polymerase chain reaction was carried out with Pwo polymerase (Invitrogen), Taq polymerase (Fermentas), Herculase or Herculase II polymerase (Agilent), Phusion (Finnzymes) and Pfu polymerase (Fermentas). The respective conditions and requirements are adapted according to the manufactorer's manual and recommendations. Typically, the reaction was performed in 50 µl scale, which contained 1-30 ng of plasmid DNA or 100-200 ng of genomic DNA template, polymerase specific buffer, 0.2 mM dNTP-mix, 0.5 µM forward and reverse primer each, optionally $MgCl_2$ or DMSO, and variable amounts of polymerase (0.5 to 5 U). For test purposes, the PCR mix was scaled down to 25 µl.

Thermocycling programs (Biometra T3000 thermocycler) were optimized for each PCR in particular by variation of specific primer annealing temperature (gradient PCR cycler; Biometra TProfessional) and elongation time. PCR products were visualized by 1% agarose gel electrophoresis (MATERIAL & METHODS, 2.2.1) and purified with QIAquick gel extraction kit following the manufacturer's protocol (Qiagen).

Enzymatic restriction cleavage and ligation: PCR products and plasmids were cleaved by restriction endonucleases (New England Biolabs and Fermentas) as recommended by the manufacturer's protocol. The enzymes were thermally inactivated and digested vectors were dephosphorylated by addition of 2.0 U CIAP (Fermentas), incubated at 37°C for 30 min and inactivated by heating at 85°C for 15 min. Vectors were visualized by 1% agarose gel electrophoresis (MATERIAL & METHODS, 2.2.1) in 1 x TBE buffer, and visualized by ethidiumbromide (Invitrogen) or SYBR safe DNA staining (1:10.000, Invitrogen). Plasmids were purified by QIAquick gel extraction kit following the manufacturer's protocol (Qiagen). Cleaved PCR products were purified using QIAquick PCR purification kit (Quiagen). PCR fragments and linearized vectors were ligated in a 20 µl scale using T4 DNA Ligase (5 U, Fermentas) following the manufacturer's recommendations. Concentrations of vectors and PCR fragments were adjusted dependent on the different reactions. The ligation mix was incubated at 16°C overnight and transformed into chemically competent *E. coli XL1 blue* cells (Table 2) as described in this section (2.1.2). Transformed cells were plated on selective LB plates and incubated at 37°C overnight. Single colonies were picked to inoculate a 5 ml LB media containing the respective selectivity marker and the cells were cultured at 37°C overnight. Plasmids were isolated by QIAquick Miniprep kit (Qiagen) and verified by 1% agarose gel electrophoresis after endonucleolytic cleavage and DNA sequencing (MWG and GATC-biotech).

2.1.4 Protein expression in E. coli

Typically, recombinant proteins were expressed in *E. coli* BL21- Codon plus (DE3)RIL cells (Stratagene). The cells were transformed with the expression vector carrying the desired protein coding sequence as described above (MATERIAL & METHODS 2.2). The expression culture of the disired volume containing LB-medium and the required antibiotics was inoculated from an overnight grown preculture of the transformed cells in a 1:100 dilution. Cells were grown at 37°C up to an OD$_{600}$ between 0.5 to 0.8 and then cooled on ice for 30 min. Protein expression was induced by the addition of IPTG to a final concentration of 0.5 mM. The expression cultures were incubated at 18°C for 12 hours. All subsequent steps were performed on ice or in the cold room at 4°C. The cells were pelleted by centrifugation at 4400 g for 20 min (Sorvail, SLC-6000 rotor) and washed with the lysis buffer. The cell pellet was flash-frozen in liquid nitrogen and stored at -80°C.

2.1.5 Lysis of *E. coli* cells

Cell pellets were resuspended in 50 ml of the protein specific lysis buffer (MATERIAL & METHODS, Table 8) and sonicated for 20 min using a flat 0.5'' working tip with 20% duty time and 40% output on a Branson sonifier system. For larger volumes of expression culture, cell lysis was performed using the cell homogenizer (Emulsiflex, Avestin). The completeness of cell lysis was checked by microscopy. The resulting cell extract was centrifuged two times at 24000 g (Sorvail, SS-34 rotor) for 20 min each and the clearified lysate was applied to the subsequent protein

purification procedure. For analysis, a sample from the remaining pellet was resuspended with SDS containing buffer (SDS loading buffer, see Table 8), incubated 5 min at 92°C and analysed by SDS-PAGE (MATERIAL & METHODS 2.2.4).

2.1.6 Measurement of protein concentration

Protein concentrations were measured usually with Bradford assay (Bradford, 1976) by addition of 1 μl to 5 μl of protein solution to 1 ml of the Bradford reagent solution (Bio-Rad). The protein concentration was measured by absorbtion at 595 nm and corrected relative to a reference curve which was prepared for each batch of the Bradford reagent solution using bovine serum albumin (Fraktion V, Roth) as a standard. Alternatively, protein concentrations were measured by absorption at 280 nm spectrophotometer (ND-1000, NanoDrop) and calculated by molar absorption coefficient obtained from the protein sequence using the ProtParam program (Gasteiger, et al. 2005).

2.1.7 Limited proteolysis

Limited proteolysis time course in combination with Edman sequencing was used to localize relative positions of ordered protein regions. The purified protein (100 μl; 1 mg/ml) was mixed with 1 μg of either Trypsin or Chymotrypsin. The protein digestion was performed as time course starting upon addition of the protease followed by incubation at 37°C. Samples were taken after 30 sec and 1, 3, 8, 15 and 30 min. The reactions were inhibited by addition of 5 x SDS sample buffer (Table 8) and incubation at 92°C for 5 min. The samples were analyzed by SDS-PAGE and the N-terminal sequence of the separated protein fragments were analyzed by Edman sequencing (Niall, 1973).

2.2 Electrophoresis

2.2.1 Electrophoretic separation of DNA

Electrophoretic separation of DNA was performed by horizontal agarosegel electrophoresis using PerfectBlue Gelsystems electrophoresis chambers (Peqlab). The agarose concentrations varied between 1% to 3% in 1 x TBE buffer, depending on the length of DNA. To visualize DNA samples, either ethidiumbromide (0.7 μg/ml, Invitrogen) or SYBR safe DNA staining (1:10.000; Invitrogen) was added. Samples were mixed with 6 x loading dye (Table 8) and DNA was visualized and documented using the UV-transiluminator at 366 nm (Royal-INTAS Science Imaging Instruments).

2.2.2 Electrophoretic separation of RNA

For electrophoretic separation and analysis of RNA the E-Gel agarose gel electrophoresis system (E-Gel Power Base; Invitrogen) was typically used. The RNA sample (250 ng to 2 μg) was mixed with sterile distilled and RNase free water (Invitrogen) to a final volume of 20 μl and loaded onto the agarose E-gel (1%). If needed, RNA was denatured by incubating the samples for 5 min at 65°C, before the samples were loaded onto the E-gel (1%).

2.2.3 Spectrophotometric analysis of RNA

For quality control prior to microarray analysis, RNA samples during the preparation were analyzed by the automated spectrophotometric system Experion (BioRad). RNA samples (5 ng/µl to 500 ng/µl) were denatured by incubation for 2 min at 70°C, followed by immediately cooling down on ice. The preparation of the RNA samples for analysis were performed as described in the manufacter's manual using the Experion RNA StdSens Starter Kit (2008). All chemicals and reagents are original consumables from BioRad, with exception of RNase free water, which was provided from Invitrogen.

2.2.4 Electrophoretic separation of proteins – SDS-PAGE

Proteins were separated by SDS-polyacrylamid gel electrophorsis (SDS-PAGE) using the electrophoresis system of Biorad. Typically, proteins were separated in 15% acrylamide (Roth) and 0.4% bisacrylamide (Roth) gels in SDS electrophoresis buffer (Table 8) (Laemmli, 1970). To separate protein from protein complexes which require separation of a broad range of molecular weights, 4-12% gradient gels were used (Bis-Tris Nupage; Invitrogen). Dependent on the range of molecular weights of the proteins, either MOPS or MES buffer (Table 8) was used in combination with X-cell Sure Lock Mini Cell electrophoresis system (Invitrogen) following the manufacturer's instructions.

2.3 Edman sequencing

Edman sequencing allows for identification of the amino-acid sequence at the N-terminus of proteins or protein fragments. The protein fragments of interest were carefully excised from SDS-gel after separation by SDS-PAGE and staining with Coomassie blue (Table 8). The proteins were transferred to a PVDF membrane (Roth) by Western blotting or passive adsorption. The Western blotting was performed in PABS buffer (Table 8) at 100 V for 2 h or 20 V overnight at 4°C. The passive adsorption was performed in several steps: First, the excised band from SDS-PAGE, containing the protein of interest, was dried in a speed-vac and rehydrated in 20 µl of swelling buffer at room temperature. Second, 100 µl of sterile destilled water was added to the previous mix. Third, a piece of PVDV membrane, previously soaked in absolute ethanol, was added to the mix. After the mix turned blue, 10 µl of methanol was added and the mix was incubated for 4 days at room temperature until the transfer was complete. This is inidicated by the migration of the coomassie blue from the solution onto the PVDF membrane. The membrane was washed five times with 10% methanol and vortexing for 30 sec. The PVDV membrane was dried by evaporation of the remaining methanol and applied to PROCISE 491 sequencer (Applied Biosystems). For identification of the N-terminal amino acid sequence, 5 cycles were performed based on the automated Edman degradation (Niall, 1973).

2.4 Standard mass spectromety

To identify proteins copurified in endogenous preparations, mass spectrometry analysis was used (MALDI) after separation of the proteins with SDS-PAGE and in-gel digestion of the proteins of interest. The analysis was performed at the central lab for protein analytics (ZfP, Axel Imhof, University of Munich).

2.5 Bioinformatic tools

Gene and protein sequences were retrieved from NCBI database (www.ncbi.nlm.nih.gov), from UniProt (www.uniprot.org) or from the Saccharomyces Genome database (SGD; http://www.yeastgenome.org).

Primer design and DNA sequence analysis was displayed and edited by Bioedit sequence alignment editor (Hall, 1999; http://www.mbio.ncsu.edu/bioedit/ bioedit.html).

Bioinformatic analysis were performed by ProtParam (http://web.expasy.org/ protparam/) and the Bioinformatic Toolkit (Biegert, et al. 2006).

Multiple sequence alignments were performed with ClustalW2 (http://www.ebi.ac.uk/Tools/msa/clustalw2/) or T-Coffee (http://www. ebi.ac.uk/Tools/msa/tcoffee/) and multiple sequence alignments were displayed with ESPript (Gouet, et al. 1999; http://espript.ibcp.fr/ESPript/ESPript/).

Protein secondary structure prediction were predicted by I-Tasser (Zhang, 2008; Roy, et al. 2010) (http://zhanglab.ccmb.med.umich.edu/I-TASSER/), HHPred (Soeding, et al. 2005) (http://toolkit.lmb.uni-muenchen.de/), Jpred (http:// www.compbio.dundee.ac.uk/www-jpred/) (Cole, et al. 2008) and PsiPred (http://bioinf.cs.ucl.ac.uk/psipred/) (Bryson, et al. 2005; Jones, 1999).

The *primer design for quantitative real-time PCR* was supported by ProbeFinder version 2.45 for Yeast (http://qpcr.probefinder.com/ organism.jsp).

Nuclear localization sequences were analysed with NLSdb database system (Nair, et al. 2003) (http://rostlab.org/services/nlsdb/submit.php). Transcription factor analysis was performed with Yeastract database (Teixeira, et al. 2006) (http://www.yeastract.com/).

Analysis of *protein interaction* were performed with support of the STRING database (Jensen, et al. 2009) (http://string-db.org/) and BioGrid database (Breitkreuz, et al. 2008) (http://thebiogrid.org/). The interaction data were visualized by Cytoscape softwar package (Melissa, et al. 2007) (http://www.cytoscape.org/). Microarray data were visualized by the Mev software package (Saeed, et al. 2003) (http://www.tm4.org/mev/).

Gene ontology search was performed with GO Gene Ontology Slim mapper (http://www.yeastgenome.org/cgi-bin/GO/goSlimMapper.pl).

Bioinformatics for dynamic transcriptome analysis was performed by Achim Tresch and Björn Schwalb under usage of the R-package Bioconductor (Gentleman, et al. 2004; Smyth, 2004) and LSD (http://www.lmb.uni-muenchen.de/tresch/LSD.html).

2.6 Yeast genetics and methods

2.6.1 Isolation of genomic DNA from yeast

(modified protocol from the Lab of Steven Hahn; (Hoskins, 1997))

Cells taken from a single yeast colony were cultured in a 10 ml YPD over night. From this preculture, 30 ml YPD were inocculated and grown over night to a final OD of 2×10^8 cells/ml. Cells were pelleted at 3000 rpm/5 min/4°C and washed with 10 ml sterile distilled (SD) water. Cell pellet was resuspended in 3 ml of buffer 1 (0.9 M sorbitol, 0.1 M EDTA, 50 mM DTT, pH 7.5) and incubated with Zymoylase (0.25 mg dissolved in 0.9 M sorbitol) with occasional shaking at 37°C for 15-120 min until 80-90% of the cells were converted to spheroblasts. The spheroblasts were centrifuged at 3000 rpm/5 min/4°C and resuspended in 3 ml of buffer 2 (50 mM Tris-HCl, 50 mM EDTA, pH 8.0) followed by addition of 0.3 ml of 10% SDS and incubation at 65°C for 30 min. After addition of 1 ml of KOAc, the spheroblast suspension was set on ice for 60 min. The supernatant was transferred to a new 50 ml centrifuge tube and centrifuged at 15.000 rpm/30 min/4°C (Sorval, SS34). The supernatant was transferred into a new centrifuge tube and 4 ml of ice-cold absolute ethanol was added to the precipitated nucleic acids. After centrifugation, the supernatant was removed and the pellet was washed with 4 ml 70% ethanol. The pellet was resuspended with 300 µl TE-buffer (pH 7.5) and 15 µl RNase (10 mg/ml, DNase-free) was added and incubated at 37°C for 30 min. The resulting DNA was extracted with 300 µl phenol/cholorform soultion (1:1) and washed with 15 µl isopropanol containing buffer (3 M NaOAc, 900 µl isopropanol). The resulting pellet was washed with 80% ethanol. The obtained DNA pellet was dried on air, resuspended in 100-300 µl TE (pH 7.5).For extraction of yeast genomic DNA for test purposes, the DNeasy blood & tissue kit (Quiagen) was used in combination with the QIAcube robot (Quiagen). The extraction was carried out as described in the manufacturer's manual (May 2008).

2.6.2 Yeast transformation

A 20 ml YPD culture was inocculated from a single colony and incubated over night at 30°C. An aliquot from the preculture was used to inoculate a 100 ml YPD culture to reach an initial OD_{600} of 0.25. The cells were cultured at 30°C für 5-6 hours to reach an OD_{600} of 1.0. Cells were pelleted (5 min, 2500 rpm, room temterature) and washed with 25 ml sterile destilled water, before resuspension in 1 ml Lithium Acetate (freshly diluted from a 1 M stock solution). After centrifugation for 15 sec at top speed (Eppendorf micro centrifuge), the pellet was resuspended with 400 µl L 100 mM LiAc. To this suspension, 240 µl polyethyleneglycol (50% w/v PEG 3350), 36 µl LiAc (1 M), 50 µl single stranded DNA (salmon-testis DNA, 2mg/ml; previously incubated at 95°C for 5 min and immediately kept on ice) and 34 µl PCR product or plasmid (susspended in sterile distilled water) was added in this order. The transformation mix was vortexed and incubated at 30°C for 30 min before the cells were heat shocked at 25°C for 30 min. The cells were centrifuged at for 15 sec. at 6000 rpm (Eppendorf micro centrifuge) and resuspended in 500 µl of 1 x TE (pH 7.5). For antibiotic resistance selection, cells were resuspended in 1 ml of room temperature YPD and incubated at 30°C for 3 hours. Finally, cells were plated on selectivity plates at 30°C over night.

2.6.3 Yeast cell lysis

Cell lysis was performed by adding one pelletvolume of lysisbuffer (250 mM NaCl; containing phosphatase- and protease Inhibitors) and two volumes of glassbeads (0.5 mm of diameter;

Soda lime/Roth) to the pellet. The mixuture was transferred to planetary mill (Pulverisette, Fritsch) and run 2 cycles of 500 rpm/4 min. The lysate was centrifuged at 4000 rpm for 5 min at 4°C (Eppendorf 5810 R; rotor: A-4-62). The supernatant was ultracentrifuged (Beckman L-70; SW-28 rotor) at 27000 rpm for 1 h at 4°C before the fatty top phase was removed with a water pump and the clarified supernatant was transferred into a 50 ml Falcon tube.

2.6.4 TAP integration

For tandem affinity purification of selected yeast proteins, the TAP-tag was integrated into the genomic locus by homologous recombination according to the original protocol (Puig, et al. 2001; Rigaut, et al. 1999). For homologous recombination for N- or C-terminal tagging, the respective PCR product carrying the the epitope and complementary sequence of the genetic locus, was generated as described previously (Baudin, et al. 1993). The protocol is described in detail in (Knop, et al. 1999).

2.6.5 Tandem affinity purification

To the clarified lysate resulting from a 2 l culture, 0.4 ml of lysisbuffer washed IgG beads were added and incubated for 1 h at 4°C (mixing by rotation) (Table 8). The mixture was centrifuged once (*Eppendorf* 5810 R; rotor: A-4-62) at 1800 rpm for 2 min at 4°C before the supernatant was removed. IgG-beads were transferred onto one 5 ml mobicol column and washed 3 times each with 10 ml 250 mM NaCl containing lysis buffer and subsequently with 5 ml 100 mM NaCl containing lysisbuffer before IgGbeads were equally divided into six 1.5 ml eppendorf tubes. For TEV-cleavage, 10 µl TEV was added to each of the tubes and incubated at 18°C for 90 min (mixing by rotation). The TEV-eluate was removed by centrifugation at 13000 rpm for 5 min (*Heraeus, Biofuge pico*; rotor: PP-1/99). The supernatant from each tube was transferred to a 2.0 ml eppendorf tube.

Binding to *Calmodulin Sepharose 4B beads* (GE Healthcare, Sweden) was performed by adding 2.5 ml Calmodulin-buffer (Table 8) to the IgG-TEV-eluate. According to the manufacturer's recommendations, the appropriate amount of Calmodulin beads were washed with Calmodulin-buffer and added to the proteinsolution, which was previously divided equally into several 2 ml gravity flow columns (Biorad). The mixture was incubated for 2 h at 4°C (mixing by rotation). After the supernatant was removed by gravity flow, each of the Calmodulin columns was washed twice with 10 ml of Calmodulin-buffer. Proteins were eluted by adding 600 µl TAPelution-buffer (Table 8) and incubated at 37°C for at least 1 h or overnight. Alternatively, the proteins were eluted by addition of 50 µl SDSsample buffer (Table 8) and incubated at 90°C for 10 min for a subsequent analysis by SDS-PAGE.

2.6.6 yeast microscopy

Preparation of slides: The slides were coated with 0.02% (w/v) poly-L-Lysine. The solution was dropped onto the slide (Roth, Germany) and incubated at room temperature for 5 min and washed three times with sterile and deionized water.

Preparation of cells: Yeast cells expressing GFP- or mCherry- (Shanner, et al. 2004) tagged proteins were grown over night in YPD medium, diluted to OD_{600} of 0.2 and incubated at 30°C to an OD_{600} of approx. 0.8. To reduce the autofluorescence of YPD medium, 1 ml of the cellsuspension was washed three times with SD-medium (Table 8). The cells were resuspended

in 200 µl of SDmedium and 5 µl of the suspension was spotted onto the poly-L-Lysine coated slides. After the cells were sitting down for 10 min, the slides were washed with 50 µl 1x PBS buffer (Table 8) with 1.0 ng/ml DAPI and incubated for another 10 min. After washing two times with 1x PBS-buffer, 5 µl of 1x PBS was added and the cells were covered with a cover-slip (Roth, Germany) and appropriately sealed. The cells were immediately analyzed by microscoy.

Microscopy: The cells were analyzed using a Leica AF6000 at 100x magnification and LAS AF Software. Exposure times and intensity were adjusted to an optimal contrast and ranged up to 200 ms for DIC images, up to 500 ms for DAPI and up to 2 s for the GFP or mCherry channel.

2.7 Dynamic Transciptome Analysis (DTA)

2.7.1 Cell growth and RNA labeling

The *S. cerevisiae* strain used was BY4741 *MAT*a, *his2Δ1*, leu2Δ0, met15Δ 0, ura3Δ 0 (Euroscarf). The strain was transformed with plasmid YEpEBI311 (2 micron, *LEU2*) carrying the human equilibrative nucleoside transporter hENT1 (S. Jellbauer and P. Milkereit, unpublished). Samples for establishing DTA method were grown in SD medium (Table 6) overnight, diluted to an OD_{600} of 0.1 the next day and grown to mid-log phase (final OD_{600} of 0.8, corresponding to 1.75×10^7 cells per ml). 4-thiouridine (Sigma) was added to the media to a final concentration of 500 µM and cells were harvested after different labeling times. Cells were centrifuged at 4,000 rpm for 1 min and cell pellets were immediately flash frozen in liquid nitrogen. Samples for quantitative qRT-PCR and for salt-stress experiments were grown in SILAC medium (Table 6) overnight, diluted to an OD_{600} of 0.1 the next day and grown to mid-log phase (final OD_{600} of 0.8 corresponding to 1.75×10^7 cells per ml). Cells were harvested 0, 6, 12, 18, 24, 30 and 36 min after addition of NaCl to a final concentration of 0.8 M. 6 min before each of the timepoints, 4-thiouridine was added to the cells.

2.7.2 RNA extraction

Total RNA was extracted with the RiboPure-Yeast Kit (Ambion/Applied Biosystems), following the manufacturer's protocol. Labeled RNA was chemically biotinylated and purified using strepatavidin coated magnetic beads as described (Doelken, et al. 2008).

2.7.3 Microarray analysis

Labeling of samples for array analysis was performed using the GeneChip 30IVT labeling assay (Affymetrix) with 100 ng input RNA. Samples were hybridized to GeneChip Yeast Genome 2.0 microarrays following the instructions from the supplier (Affymetrix). Quality control and array processing was done using GCRMA (Wu et al, 2004) for expression quantification and LIMMA (Smyth & Speed, 2003) for elementary array comparisons.

2.7.4 Extraction of mRNA synthesis and decay rates

Steady-state assumption: During the labelingtime, 4-thiouridine is integrated into transcribed mRNA and generates a pool of labeled mRNA. At time-point t=0, 4-thiouridine is added to the cells and the total mRNA amount at any time $t \neq 0$ consists of preexisting mRNA (unlabeled) and nascent mRNA (labeled). Without any disturbance of the cells, the total mRNA amount per cell is considered to be constant over time, because constant synthesis and decay rates basically

determine an equilibrium if averaged over a cell cycle period ("steady-state" assumption). This assumption is valid, because – although different sets of transcripts exhibit variations in synthesis and decay rates during cell cycle – we measure a large, unsynchronized ensemble of cells. The steady-state assumption also averages temporal fluctuations of transcript levels. Thus, for unsynchronized cells, DTA measures the average mRNA synthesis and decay rates.

Synthesis- and decayrates under steady state assumption: Synthesis and decay rates determine a mRNA equlibrium (steady state). Assuming that the total mRNA levels are constant over time, the amount of newly synthesized mRNA after normalization is equal to the amount of preexisting mRNA which is decayed within the same time. An increase of total mRNA abundance over all cells is proportional to an increase in cell number during labeling time. Since cells are labeled during mid-log phase an increase in cellnumber follows an exponential growth. Therefore we define a constant growthrate α. We assume that a specific mRNA (originating from the corresponding gene) decays with a constant decay rate Δ, if no other processes interfere, the unknown decay rate can be obtained by solving for *lg*. Once the decay rate is known, the corresponding half-life is given by $(ln\ 2)/lg$. The steady-state assumption implies that mRNA is decayed at the same rate as they are synthesized.

Model improvement: The basic assumptions derive a model that describes an idealized state which does not cover experimental limitations, e.g. mRNA labeling efficiencies, incomplete biotinylation and strepavidin purification, technical variance, etc.; Moreover the model does not account for unsystematic experimental variations. Therefore a set of parameters has to be defined which represents all significant discrepancies between the experimental conditions and the idealized model. Most parameters are not experimentally accessible and have to be iteratively converged. The parameter optimization were performed by Björn Schwalb and Achim Tresch and can be found in detail within the Supplementary Material to our publication (Miller, et al. 2011).

2.7.5 Dynamics of mRNA synthesis and decayrates

For conditions which might alter transcription globally, the steady state approach has to be extended. Under highly dynamic conditions, the total mRNA levels might not be assumed to be constant over time, because synthesis and decayrates are not necessarily in a dynamic equilibrium. Under those conditions, the total mRNA amount and any single mRNA population is dynamically growing with altered rates. This assumption was introduced into the static model described above by definition of an mRNA specific and time dependent "growth-rate" which describes the temporal variations of individual transcript levels. Due to the short labelingtime, we modeled the local dynamic behavior of the total mRNA by an exponential function. The dynamic model was validated by complementary data for mRNA half-lives obtained by quantitative real-time PCR (MATERIALS & METHODS 2.7.6). The optimization of the dynamic model was performed by Björn Schwalb and Achim Tresch and description can be found in detail within the Supplementary Material to our published article (Miller, et al. 2011).

2.7.6 Quantitative Real-Time PCR

mRNA levels were determined for 8 genes: *act1* (YFL039C), *ctt1* (YGR088W), *gpd1* (YDL022W), *kss1* (YGR040W), *rdn1* (rRNA locus), *sfg1* (YOR315W), *stl1* (YDR536W), and *tub2* (YFL037W).

The experiment was performed in two similar steps: Step 1 was performed under normal growth conditions whereas step 2 was performed the identically after addition of 0.8 M NaCl. mRNA levels were analyzed at 0, 2.5, 6, 10, and 16 min after addition of 1,10-phenanthroline (100µg/ml final concentration) and 0, 12, 30, and 36 min. 4-thiouridine labeling time (500 µM final concentration) for all samples was 6 min. RNA was extracted using the RiboPure-Yeast Kit (Ambion/Applied Biosystems), following the manufacturer's protocol. cDNA synthesis was performed with 500 ng RNA originating from total, unlabeled and labeled mRNA using the iScript cDNA Synthesis Kit (BioRad). Primers were designed with the ProbeFinder software (Roche Applied Science) and individual primer-pair efficiency was tested and ranged between 95%-100%. PCR reactions contained 1 µl DNA template, 2 µl of 10 µM primer pairs and 12.5 µl SsoFast EvaGreen Supermix (BioRad). Quantitative PCR was performed on a Bio-Rad CFX96 Real-Time System (Bio-Rad Laboratories, Inc.) using a 3 min denaturing step at 95°C, followed by 49 cycles of 30 s at 95°C, 30 s at 61°C and 15 s at 72°C. Threshold cycle (Ct) values were determined by application of the corresponding Bio-Rad CFX Manager software version 1.1 using the Ct determination mode "Regression". Two biological and three technical replicates were used for each time point and technical variance was minimized using in-plate controls.

2.7.7 Estimation of mRNA labeling efficiency
The model is based on the incorporation of 4-thiouridine into newly synthesized transcripts. Therefore, the correction for incomplete 4-thiouridine labeling (labeling bias) is essential for data normalization. Because the biotinylation and purification efficiency was already corrected by introduction of a set of parameters (MATERIALS & METHODS 2.7.4), we assumed here that every biotinylated transcript contributes to the measured labeled mRNA fraction. Under the assumption that incorporation of uridine resp. 4-thiouridine at each position occurs stochastically and independently, the labeling bias can be described as the probability that a newly synthesized single mRNA does not accidently incorporate a 4-thiouridine at a uridine position. Based on this, the labeling bias is dependent on the number of uridines within a certain transcript. Therefore, the labeling bias results in a systematic, non-linear prolongation of mRNA half-life estimates, which might have a stronger impact on shorter transcripts. The introdution of the labeling bias into the model were performed by Björn Schwalb and Achim Tresch. The labeling-bias correction was extensively simulated and details can be found within the Supplementary Material to our published article (Miller, et al. 2011).

2.7.8 Genomic occupancy profiling
For genomic occupancy profiling by ChIP-chip we used *S. cerevisiae* strain BY4741 containing a C-terminal tandem affinity purification (TAP) tag on the Pol II subunit Rpb3 (Open Biosystems). We confirmed that the TAP tag was at the correct genomic position, that the tagged Rpb3 subunit was expressed, and that the strain grew normally at 30°C. Yeast cells were grown in YPD medium until exponential phase (OD$_{600}$ ~ 0.8) and then were stressed by the addition of 0.8 M NaCl. ChIP-chip was performed for biological replicates 0, 12, and 24 min after salt addition with high-resolution tiling microarrays and data were analyzed as described (Mayer, et al. 2010).

2.7.9 Rank gain analysis:
Rank gain analysis was introduced to the dynamic DTA formalism to replace the total least squares regression as the first step in steady-state estimation. To identify genes, which exhibit

induction or repression during osmotic stress, we considered the gain or loss of ranks relative to the initial timeframe 0-6 min. This procedure is considered to be more robust than the fold change approach, because of the assumption that most genes do not respond to the osmotic stress. To identify induced or repressed genes, synthesis rates were ranked for each time frame: 0-6, 6-12, 12-18, 18-24, 24-30 and 30-36 min. Genes demonstrating similar rankgains were categorized into 5 cluster: The up-cluster contains genes showing a rank gain of more than 2000, the up-even cluster between 1000 and 2000 and the even-cluster between 1000 and 1000. The down-even cluster contains genes which show a rank-gain between -1000 and -2000, the down cluster lower than -2000. With this approach, a set of 480 genes was identified, whose mRNA stability exhibit a rank gain below 500 during the osmotic stress response. Thus, as this set of genes exhibits no significant variation during osmotic stress, this set is considered as stable mRNA and used for linear normalization of the labeled datasets. The rank gain analysis was introduced by Björn Schwalb and Achim Tresch and details can be found within the Supplementary Material to our published article (Miller, et al. 2011).

2.8 Mediator Phosphorylation

2.8.1 Cell growth and SILAC

For purification of endogenous Mediator, we introduced a tandem affinity purification (TAP) tag at the N-terminus of Med17 in *S. cerevisiae* strain RS453 with mating type alpha (Puig, et al. 2001). For SILAC, we modified this strain by disruption of the *lys1* gene with KanMX6 to introduce lysine auxotrophy. Cells were grown in YPD or SILAC media (Table 6) at 30°C to late log-phase. For stable isotope labeling, SILAC media contained 30 mg/l $^{13}C_6$-, $^{15}N_2$-lysine (heavy lysine, Cambridge Isotopes) for the salt stress sample, or 30 mg/ml $^{12}C_6$-, $^{14}N_2$-lysine (light lysine, Sigma Aldrich) for the control. Salt stress was introduced by adding crystalline sodium chloride to the heavy lysine-containing media to a final concentration of 0.5 M. After incubation for 20 min, equal amounts the two populations were mixed.

2.8.2 Purification of endogenous Mediator proteins

Cells were lysed by beat-beating (500 rpm, 4 min, 2 cycles) using glassbeads (0.5 mm diameter). Purification of endogenous Mediator using ProteinA/IgG (GE healthcare) affinity precipitation was performed as described (Puig, et al. 2001), except that all buffers contained 1 mM dithiotreitol (DTT), protease inhibitors (Table 7), and phosphatase inhibitors (40 mM p-nitrophenylphosphate, 2 mM sodium-pyrophosphate, 2 mM sodium ortho-vanadate, 50 mM sodium fluoride). IgG-bound proteins were washed with high salt buffer (Table 8) and low-salt buffer (Table 8). Proteins were cleaved from IgG beads by tobacco edge virus (TEV) protease for 60 min at 18°C. Eluted proteins were precipitated by adding four volumes of methanol, one volume of chloroform, and three volumes of protease-free double-distilled water. After centrifugation, the pellet was washed with four volumes of methanol and centrifuged again. Remaining methanol was discarded and the proteinprecipitate was dried. A sample was analyzed by 4-12% SDS-PAGE (NUPAGE, Invitrogen).

2.8.3 Mass spectrometry

The protein pellet was dissolved and denatured in 8 M urea (Roth), reduced with 1 mM DTT for 45 min and alkylated with 5 mM iodoacetamide for 45 min. Proteins were digested in solution either with endoproteinase trypsin or Lys-C (Wako) overnight at room temperature.

Phosphopeptide enrichment was performed using titanium dioxide (TiO$_2$) beads (Larsen, et al. 2005). LC-MS/MS analysis was performed on an LTQ-Orbitrap instrument (Thermo Fisher) connected to a nanoflow HPLC system (Agilent 1100 or Proxeon EASY-nLC system) through a Proxeon nanoelectrospray ion source. Peptides were separated on an in-house packed 75 µm reversed-phase C18 column. Survey scans were acquired in the Orbitrap analyzer and the ten most intense precursor ions were subjected to collision-induced fragmentation and acquisition in the ion trap. The instrument was operated with the "lock mass option" (Olsen, et al. 2005) and multistage activation was enabled to improve phosphopeptide fragmentation. The MS raw data files were processed with MaxQuant (version: 1.1.1.18) (Cox, et al. 2008; Cox, et al. 2009). The MS/MS spectra were searched against the concatenated target decoy *S. cerevisiae* ORF protein database, concatenated with reversed versions of all sequences and combined with the most commonly observed contaminants. Enzyme specificity was set to Lys-C and up to three missed cleavages and three labeled lysine residues were allowed. Cysteine carbamidomethylation was considered as a fixed modification, and methionine oxidation, protein N-acetylation and phosphorylation on serine, threonine and tyrosine residues were set as variable modifications.

2.8.4 Generation of *med15* mutant strains

D7P and *D30P* mutant strains were generated in three steps. First, to replace selected phosphorylated serine and threonine residues in the Med15/YOL051w coding sequence by alanine (Chapter IV, Table 21 and Table 22), we synthesized (GeneART) a DNA construct containing the 5'-UTR (583 bp upstream). The modified coding sequence of Med15/YOL051w (*D30P* mutant-sequence), and the 3'UTR (624 bp downstream) were inserted in vector prs-315 (AMP/Leu) (Sikorsky, et al. 1989) under the control of the *cen6/arsh4* promoter with the use of NotI/SalI restriction sites. Second, a Med15/ YOL051w::URA3 strain was generated by integration of a Ura3 cassette harboring overlapping sequences to Med15/YOR051w 5'- and 3'- UTR regions into BY4741 strain (*MAT*a , *his3Δ1*, *leu2Δ0, met15Δ0, ura3Δ0*, Euroscarf) by homologous recombination. Med15/YOL051w::URA3 strain was selected twice on URA minus medium and confirmed by sequencing. Third, the Ura3 cassette was removed by *D7P* or *D30P* mutant sequence using homologous recombination and selected twice on 5'-fluorotic acid (5'-FOA) containing media. The exact genetic position and completeness of the genomic *D7P* or *D30P* mutant insertion were analyzed by sequencing. For mutant *D7P* all steps were as above except that we synthesized (Invitrogen) a DNA construct containing the Med15 positions (2114 bp and 3333 bp) with the modified coding sequence of Med15/YOL051w (*D7P* mutant-sequence), in vector prs-315 (AMP/Leu), and that we generated a Med15/YOL051w::URA3 strain by integration of a Ura3 cassette harboring overlapping sequences to Med15/YOR051w between the relative postions 2139 bp and 3243 bp into BY4741 strain (*MAT*a, *his3Δ1*, *leu2Δ0*, *met15Δ0*, *ura3Δ0*, Euroscarf).

2.8.5 DTA of *D7P, D30P* and *Δmed15*

For DTA, the *D30P, D7P* and *Δmed15* mutant and wild-type strains (BY4741, MATa, *his3Δ1, leu2Δ0, met15Δ0, ura3Δ0*, Euroscarf) were transformed with plasmid YEpEBI311 (2 micron, Leu2) carrying the human equilibrative nucleoside transporter hEnt1. Cells were grown in SILAC media without leucine. Cells were grown to mid-log-phase of 0.8 (corresponding to 1.75x10^7 cells). For control samples, 4-thiouridine (SIGMA) was added to the media and

adjusted to a final concentration of 500 μM. Cells were further incubated for 6 min (labeling time) and harvested by centrifugation at 4000 r.p.m. for 1 min. For stress samples, sodium chloride was added to the sample to a final concentration of 0.8 M. 4-thiouridine was added 18 min after salt addition and cells were harvested after 6 min labeling time as above. DTA was performed with Affymetrix arrays as described in this section.

2.8.6 Sensitivity screen

We tested the med15 mutant for sensitivity to high salt conditions and *Δmed15* deletion mutant for different stress conditions. Wild-type (BY4742, Euroscarf), med15 mutant, *Δmed15* deletion mutant cells (MATalpha, his2Δ1, leu2Δ0, met15Δ0, ura3Δ0; YOR051w::KanMX; (Euroscarf)) and *Δhog1* deletion mutant (MATalpha, his2Δ1, leu2Δ0, met15Δ0, ura3Δ0; YLR113w::KanMX; (Euroscarf)) were grown in liquid YPD media (1% yeast extract, 2% bacto-peptone, 2% glucose, 2% agar, 200 mg/liter adenine) to mid logarithmic phase. The cells were pelleted by centrifugation and washed twice with sterile, double distilled water. The first cell suspension was adjusted to an optical density at 600 nm to 1.0 and diluted in 1: 10 steps to 10-1, 10-2, 10-3, 10-4. The resulting cell suspensions were spotted on YPD/agar solid media and incubated either at 25ºC, 30ºC or 37ºC 3 days or 5 days. Sensitivity to high salt concentrations was tested by the same procedure except that YPD/agar solid media contained either 0, 0.4 M or 1.2 M sodium chloride (*Δmed15* deletion mutant) or 0, 1.2 M (*med15* mutant) and cells were incubated at 30ºC for 5 days.

2.8.7 Comparative DTA (cDTA)

For cDTA, we used the published protocol (Sun, et al., 2012), with the following exceptions. The *D7P* mutant strain, *Δmed15* and wild-type strain (BY4741, MATa, *his3Δ1*, *leu2Δ0*, *met15Δ0*, *ura3Δ0*, Euroscarf) were transformed with plasmid YEpEBI311 (2 micron, *Leu2*) carrying the human equilibrative nucleoside transporter hEnt1. Cells were grown in SILAC media without leucine to mid-log-phase of 0.8 (corresponding to 1.75×10^7 cells) and labeled with 4sU for 6 min. Cells were centrifuged at 2465 x g at 30ºC for 1 min and re-suspended in RNAlater solution (Ambion/Applied Biosystems). The cell concentration was determined by Cellometer N10 (Nexus) before flash-freezing in N_2 (liq). *Schizosaccaromyces pombe* (*Sp*) cells were grown in YES medium overnight, diluted to $OD_{600}=0.1$ and grown to $OD_{600}=0.8$. 4sU (SIGMA) was added to a final concentration of 500 μM and cells were incubated for 6 min. Cells were centrifuged at 2465 g at 30ºC for 1 min and re-suspended in RNAlater solution (Ambion/Applied Biosystems) before flash-freezing in liquid nitrogen. The *Sp* cells were taken from a general stock to eliminate errors by experimental variations. *Sp* cells were counted by Cellometer N10 (Nexus) and mixed with *Sc* cells in a 1:3 ratio, resulting in 4×10^8 cells in total. Control and stress samples were treated as described in this section. Total RNA extraction, labeled RNA purification, sample hybridization, and microarray scanning were as described in this section and (Sun, et al., 2012).

2.9 Mediator Subunit Rox3

2.9.1 Recombinant expression of *Saccharomyces cerevisiae* Rox3

Recombinant Rox3 protein variants were expressed with *E. coli* BL21- Codon plus (DE3)RIL cells (Stratagene) as described in MATERIALS & METHODS section 2.1. After centrifugation at 4400 g for 20 min at 4ºC (Sorvail, SLC-6000), the cells were resuspended in Rox3-buffer A with protease inhibitors (MATERIALS & METHODS section, Table 1.7). Cell lysis was performed as described

MATERIALS & METHODS section 2.1) with the following exceptions: Sonication was performed for 12 min with 25% duty cycle and 40% output on ice. The cell lysate was centrifuged two times at 16.000 rpm for 30 min at 4°C (Sorvail, SS34 rotor).

Purification by Ni-NTA: Corresponding to a 2 l expression culture volume, a 2 ml colomn of Ni-NTA (Qiagen) was prepared and equilibrated with Rox3-buffer A (Material & Method section, Table 1.7). The clearified lysate was loaded to the Ni-NTA colomn and the column was washed with 12 column volumes (CV) of Rox3-buffer A, 25 CV of Rox3-buffer A containing 20 mM imidazole and finally with 3 CV buffer B (Table 8). Proteins were eluted from the column with Rox3-buffer B containing 300 mM imidazole. Samples from the pellet, cell lysate, washing steps and elution were analyzed by SDS-PAGE (MATERIAL & METHOD 2.1). The proteins were purified by anion exchange chromatography using the MonoQ (5/50, GE Healthcare). The MonoQ column was preequilibrated with MonoQ-buffer A (Material & Method section, Table 1.7) and proteins were eluted with 10 CV gradient until 50% MonoQ-buffer B (Table 8). The elutionfractions were collected and analyzed by SDS-PAGE. After concentration (10 kDa cutoff) the sample was applied to size exclusion chromatography (Superose 12, GE Healthcare), and equilibrated with Rox3-buffer B (Table 8).

Purification by Streptavidin: Corresponding to a 2 l expression culture volume, Rox3 variants were purified with 1 ml Strep-Tactin MacropPrep (IBA) by gravity flow colums (BioRad) according to the manufacturer's instructions. The column was equilibrated with Rox3buffer A (Table 8), before the clarified lysate was loaded (note that the manufacturer recommends the addition of avidin to the cell lysate). The bound proteins were washed with 12 column volumes (CV) of Rox3buffer A, 5 CV of Rox3buffer B (Table 8). Proteins were eluted by addition of d-Desthiobiotion (IBA) and concentrated in a 10 kDa MWCO spin concentrator and applied to size exclusion chromatography (Superose 12, GE Healthcare), and equilibrated with Rox3buffer B.

2.9.2 *In vitro* transcription assays

An *in vitro* transcription assay was used to quantify the activity of various Rox3 protein variants to activate transcription of a model plasmid (the in vitro transcription assay was performed by Martin Seizl, Cramer lab, Gene Center, Munich). Nuclear extracts were prepared from 3 l of culture as described elsewhere (Hahn lab, www.fhcrc.org/labs/hahn) and plasmid transcription was performed essentially as described (Ranish and Hahn, 1991). Transcription reactions were carried out in a 25 ml volume. The reaction mixture contained 100 mg nuclear extract, 150 ng of pSH515 plasmid, 1_ transcription buffer (10 mM HEPES pH 7.6, 50 mM potassium acetate, 0.5 mM EDTA, and 2.5 mM magnesium acetate), 2.5 mM DTT, 192 mg of phosphocreatine, 0.2 mg of creatine phosphokinase, 10U of RNase inhibitor (GE Healthcare), and 100 mM nucleoside triphosphates. For activated transcription, 150 ng of Gal4–VP16 or 200 ng of Gal4–Gal4AH was added. The reaction was incubated at room temperature for 40 min and then stopped with 180 ml of 100mM sodium acetate, 10mM EDTA, 0.5% sodium dodecyl sulphate, and 17 mg of tRNA/ml. Samples were extracted with phenol–chloroform and precipitated with ethanol. Transcripts were analyzed by primer extension essentially as described (Ranish & Hahn, 1991). Instead of the ^{32}P-labelled lacI oligo, 0.125 pmol of a fluorescently labelled 50-FAM-oligo was used. Quantification was performed with a Typhoon 9400 and the ImageQuant Software (GE Healthcare).

2.10 Supporting Methods

2.10.1 Preparation of TEV protease

Tabacco egde virus protease was recombinantly expressed in *E. coli* as described in section (MATERIALS & METHODS 2.1). The coding sequence of N-terminally tagged His6-TEV protease was cloned into a pET-24d vector (plasmid was friendly supplied by Arie Geerlof). The cell pellet was resuspended in 30 ml lysis buffer (50 mM Tris HCl pH8.0, 200 mM NaCl, Protease Inhibitor mix, 40 µl DNaseI (1 mg/ml). The suspension was lysed by sonication for 20 min using a flat 0.5'' working tip with 20% duty time and 40% output on a Branson sonifier system. The resulting cell extract was centrifuged at 24000 g (Sorvail, SS-34 rotor) for 20 min followed by ultracentrifuging step for 30 min at 27.000 rpm (SW32 rotor, Beckman). Imidazole was added to the clarified lysate to a final concentration of 10 mM and applied to 5 ml Chelating Sepharose column (Pharmacia), charged with $NiCl_2$ and equilibrated with chelating buffer (50 mM Tris-HCl pH8.0, 300 mM NaCl, 1 mM ß-mercaptoethanol, 20% (w/v) glycerol) containing 10 mM imidiazole. The column was washed with 10 CV chelating buffer containing 30 mM imidazole before the protein was eluted with chelating buffer containing 300 mM imidazole. The protein solution was loaded onto a 50 ml HiTrap 26/10 desalting column (GE healthcare) and preequilibrated with desalting buffer (50 mM Tris-HCl pH 8.0, 150 mM NaCl, 1 mM DTT, 20% (w/v) glycerol). The fractions were pooled and glycerol was added to a final concentration of 50% (w/v) glycerol and stored at -80°C.
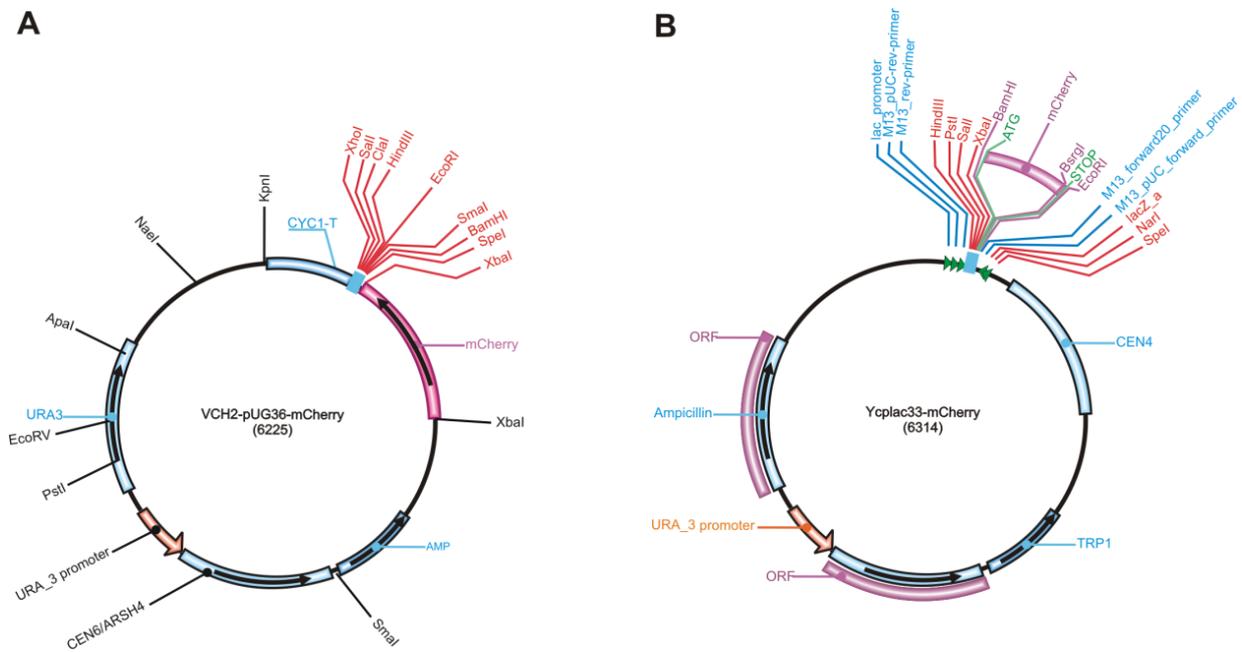
Figure 4: *Vectormap of mCherry vectors VCH2 and Ycplac33-mCherry.* **A** The VCH2 vector can be used in yeast for creation of N-terminal tagged proteins with mCherry. **B** The Ycplac33-mCherry vector allow for creating C-terminal tagged proteins with mCherry in yeast.

2.10.2 Generation of mCherry vectors for *S. cerevisiae*

VCH2-vector: The coding sequence mCherry coding sequence from the pRSET-B mCherry vector was amplified by PCR and cloned into the yeast puc36 vector to replace the GFP coding sequence. This construct allowed for N-terminal tagging of proteins with mCherry (MATERIALS & METHODS, classical cloning)

Ycplac33-mCherry-vector: The mCherry coding sequence from the pRSET-B mCherry vector was amplified by PCR and cloned into the yeast Ycplac33 into the multiple cloning site. This construct allowed for C-terminal tagging of proteins with monomeric fluorescence protein mCherry (Shanner, et al. 2004).

CHAPTER III:
DYNAMIC TRANSCRIPTOME ANALYSIS MEASURES RATES OF mRNA SYNTHESIS AND DECAY IN YEAST

Miller, et al. (2011) *Molecular Systems Biology,* 7:458

1. Introduction

1.1 Dynamic coordination of mRNA synthesis and decay

The flexibility of living organisms to adapt to environmental changes is a key competence for survival. This phenomenon is based on the ability of all living organisms to switch dynamically between alternative gene expression programs. The dynamic reprogramming adjusts homeostasis, governs differentiation in response to environmental signals and adaption to stress. Regulation of dynamic reorganization of gene expression requires a tightly coupled network that generates transcripts with optimal timing and efficiency, coordinates transcription, post-transcription and protein production, and combines robustness to flexibility of re-adaption (Keene, et al. 2007).

Most studies on gene expression regulation are focused on mechanistic details of transcription and the principles that control mRNA production. However, recent studies revealed that post-transcriptional mechanisms are involved in gene expression control, especially variation of mRNA stability during stress response (Petersen & Lindquist, 1988; Bönisch, et al. 2007; Romero-Santacreu, et al., 2009). To understand the principles and mechanisms that control gene expression, it is essential to monitor transcriptional and post-transcriptional events within a well defined context. The response to environmental changes induce extensive dynamic reorganisation of gene expression, which require regulation on both levels, mRNA synthesis and decay.

Changes in mRNA synthesis and decay rates must be measured without perturbation of the cellular system and the changes in mRNA synthesis and decay rates must be monitored globally and with high temporal resolution. However, this cannot be achieved by standard transcriptomics, which only measures mRNA abundance. Current methods for mRNA half-live determination use heat shock, chemical inhibitors or sarkosyl to achieve transcriptional inhibition. These methods measure mRNA abundance and either mRNA half-lives or synthesis rates. However, to study regulation of gene expression, the simultaneous measurement of mRNA synthesis and decay rates is essential to reveal transcriptional and post-transcriptional control principles.

Post-transcriptional mRNA processes are regulated by mRNA binding ribonucleoproteins (RNPs), which recognize specific mRNA features such as secondary structure elements or sequence motifs and direct mRNA to the decay machinery (Parker & Sheth, 2007; Halbeisen, et al. 2006; Halbeisen, et al. 2009). RNPs may control groups of functionally related genes, which are regulated by similar signatures. This kind of coregulation at the post-transcriptional level was denoted as "RNA operons" or "decay regulons" (Keene & Tenenbaum, 2002; Wang, et al. 2002) and has been shown to regulate gene expression in *S. cerevisiae, D. melanogaster* and *mammalian* cells (Keene, et al. (2007).

1.1.1 Variation of synthesis rates in response to environmental changes

Variation of synthesis rates in response to environmental changes reveal a general discrepancy between temporal variation of total mRNA levels and synthesis rates. A lack of parallelism between the temporal variation of total mRNA levels and synthesis rates revealed a time delay between total mRNA levels and transcription rates (Molina-Navarro, et al. 2008; Hayles, et al. 2010). It might be a general feature that changes in synthesis rates are more intense and faster than changes in total mRNA abundance, indicating that synthesis rates enable a dynamic monitoring of transcriptional activity in response to osmotic stress (Romero-Santacreu, et al. 2009).

1.1.2 mRNAPs and transcript stability determinants

The two main signals that determine mRNA stability are located at both ends of mRNAs: 5'cap (7-methylguanylate) and poly(A) tail at the 3'end. These stability determenants are introduced cotranscriptionally and function in two ways: First, both act as safeguards by protecting mRNA against exonucleases and therefore ensure a controlled appropriation for translation. The second function is to provide a platform for mRNA binding proteins (mRNPs) wich are involved in regulation of translation, cotranslational processes, storage and, at least, degradation of the transcripts.

Besides the 5'cap and poly(A) tail, there are other elements which influence mRNA stability. In eukaryotes, mRNA stability is regulated by sequence elements predominantly found in the 3'-UTR. The best studied sequence elements are AU-rich elemtens (ARE) (Garnau, et al. 2007). In human cells, Khabar, et al. (2005) showed that more than 8 % of the human transcriptome are mRNA containing AU-rich-elements, which encode e.g. for cytokines, proto-oncogenes, transcription factors and for proteins involved in a variety of cellular processes, such as cell growth, signal transduction as well as transcription and translation control. AU-rich elements are recognized by regulatory proteins, such as human tristetraproline (TTP), AU-rich binding factor-1 (Auf1) and KH splicing regulatory protein (KSRP). This proteins bind to ARE and recruit the mRNA decay machinery to target transcripts. These factors interact directly or indirectly with the mRNA decay machinery. For example, Auf1 interacts with the Exosome (Chen, et al. 2001) and recruit the Exosome for degradation on ARE-containing mRNAs. KSRP binds to both the PARN deadenylase and the Exosome which results in an accelarated decay of selected mRNAs (Gherzi, et al. 2004; Tran, et al. 2004). However, AU-rich elements not only lead to an accelarated decay of certain transcripts, but – in some cases – AREs have a stabilizing effect on selected transcripts. This discrepancy can be explained by a competition between stabilizing and destabilizing factors. It was shown in *S. cerevisiae* that AREs are recognized by the poly(A) mRNA binding protein Pub1 which plays a central role in stabilization of transcripts (Ruiz-Echevarria, et al. 2000).

In addition to AREs, other sequence elements has been identified that modulate mRNA stability. In *S. cerevisiae*, mutation analysis identified sequences which have an intrinsic stabilizing effect on transcripts. These stabilizer elements (STE) are located in the mRNA 5'-region and have been found to modulate stability of the mRNA encoding for transcription factor Gcn4. STEs are recognized preferentially by the poly(A) mRNA binding protein Pub1 which stabilizes the *gcn4* transcript and modulates Gcn4 dependent metabolic processes, such as amino acid biosynthesis. It has been shown that mutations in the STE lead to destabilization of the *gcn4* transcript by targeting mRNA to nonsense-mediated decay (NMD). Similar

observations have been made for the transcript encoding for Yap1, a central regulator of the oxidative stress response in yeast. This observations indicate that post-transcriptional processes contribute to regulation of transcription factors (Hinnebusch et al. 1997;-Ruiz-Echevarria, et al. 2000; Bernard, et al. 2004; Rebbapragada, et al. 2009).

1.1.3 Coregulation and operons

RNPs provide a mechanism to coregulate gene expression, which has been described as post-transcriptional RNA regulons (Keene, et al. 2007). In *S. cerevisiae*, for example, a subset of 154 mRNAs, which encode for mitochondrial proteins, were selectively recognized by Puf3 (Garcia-Rodriguez, et al. 2007). Puf3 interacts with a cis-acting consensus binding motif (UGUANAUA), represses translation of these transcripts and leads to their stabilization (Wickens, et al. 2002). The Puf3 function is coupled with the type of cellular carbonsource: Puf3 mRNAs are unstable in cells grown in glucose but stable when ethanol is provided as carbon source.

Other proteins of the Puf family are involved in coregulation of functional related transcripts and imply that each Puf protein is involved in selevtive cellular processes (Foat, et al. 2005). Each of the Puf family proteins (Puf1-Puf5) bind a distinct subpopulation of mRNAs that encode for proteins with related functions, such as spindle body components, nuleolar regulatory proteins, chromatin remodeling enzymes and membrane proteins. Over 700 mRNAs (approx. 10% of the transcriptome) are targets of the five Puf RNPs (Gerber, et al. 2004; Keene, et al. 2007 and Refs. within). The mechanism of regulating mRNA stability has been investigated in detail for mRNAs of *cox17, tif1, hxk1* and HO endonuclease (Olivas & Parker , 2003, Ulbrecht, et al. 2008). HO endonuclease is involved in mating-type switching within the late G1 cell cycle (Hershkowitz, et al. 2000). HO expression is regulated on the post transcription level: A specific mRNA consensus sequence on the 3'-UTR is recognized by Puf5, which together with Puf4 regulates HO mRNA stability (Goldstrohm, et al. 2006; Tadauchi, et al. 2001; Goldstrohm, et al. 2007). Hook, et al, (2007) could show that in a Puf4 mutant, the mRNA half-live increased from 9 min in wild-type cells to 19 min. The Puf5 mutant shifted the half-live to 35 min, whereas the Puf4-Puf5 double mutant showed an increase of mRNA half-live to 90 min. Obviously, Puf4-Puf5 mark HO mRNA for accelerated degradation and therefore act as negative regulators of HO. Evidence for a potential mechanism cames from the observation, that Puf4 directly binds Pop2, which is member of the Ccr4-Not deadenylase. Interestingly, Puf5 is a target of two MAP kinases (Fus3 and Kss1), and the cell cycle kinase Cdc28, which seems to be the regulatory interface of Puf5 to the signaling pathway of cell cycle control (Wickens, et al. 2002) and might function as connection between gene expression control and mRNA metabolism.

1.1.4 RNA half live and cell cycle time

Several global studies on mRNA half live determination have been performed in bacteria, plants, mammalian and yeast. The median mRNA half lives ranged from 5.7 min in *Escherichia coli* (Bernstein, et al. 2001), 10 min in *Halobacterium salinarium* (Hundt, et al. 2007) to 3.8 h in *Arabidopsis thaliana* (Narsai, et al. 2007). In mammalian cells, the median mRNA half lives varied from 7.1 h in mouse embryonic stem cells (Sharova, et al. 2009) to 10 h in human hepatocellular carcinoma cells (Yang, et al. 2003). In *S. cerevisiae*, transcript half lives were preferentially determined by using a temperature sensitive mutant of the largest Pol II subunit Rpb1 (Rpb1-1) (Nonet, et al. 1987). The median mRNA half live of *S. cerevisiae* was determined by several studies to lies between 19 min to 34 min (Holstege, et al. 1998; Grigull, et al. 2004; Wang, et al.

2002; Shalem, 2008). Since the median mRNA half lives vary considerably throughout the different species, Yang and colleagues postulated the dependence between median transcript half live and cell cycle time (Yang, et al. 2003).

1.1.5 Post-transcriptional regulation of response to osmotic stress

Stability modulation of selected mRNAs has been observed to be one level that is used by MAP kinases to coordinate reorganisation of gene expression in response to environmental changes (Shalem, et al. 2008; Lai, et al. 2002; Molin, et al. 2009; Romero-Santacreu, et al. 2009; Grigull, et al. 2004). The human Hog1 homologue, p38, stabilizes the cytokine mRNAs regulating the binding of destabilization factor TTP (tristetraprolin) to AU-rich elements (ARE) in the 3'-UTR (Sandler, et al. 2008). The yeast mRNA *tif51a*, whose stability is regulated by its ARE, is destabilized when Hog1 function was inhibited (Vasudevan & Peltz, 2001). In *S. cerevisiae*, the *hxt1* (encoding for transmembrane glucose transporter) mRNA was stabilized under osmotic stress conditions (Greatrix, et al. 2006).

Genome wide studies on mRNA stability in yeast suggested that mRNA decay contribute to genetic regulation of stress response and nutrient deprivation (Grigull et al. 2004). During the initial phase, global transcript stability decreases within 6 min after stress induction, whereas stress-responsive transcripts exhibit an increase in stability (Molin, et al. 2009; Romero-Santacreu, et al. 2009). After 30 min, a sharp decrease in mean stability of all initially stabilized stress related transcripts was observed, whereas stress-repressed genes become stabilized, indicating a cellular adaption to stress. The changes in stability between 6 and 30 min correlate with changes in steady-state levels between 30 and 60 min indicating that changes in transcript stability precede steady-state levels after osmotic shock. Hog1 affects both, steady-state levels and stability of stress-responsive transcripts and the modulation is dependent on the applied osmotic pressure (Molin, et al. 2009; Romero-Santacreu, et al. 2009): After treatment with 0.7 M NaCl, the levels of induced mRNAs peak after 45 min (Rep, et al. 2000), while lower salt concentration causes earlier peaking (Posas, et al. 2000).

1.2 mRNA half-live determination

Standard transcriptomics are focused on differentially expressed genes by measuring changes in mRNA abundance. However, mRNA abundance levels are the result from an equilibrium between mRNA synthesis and decay. Therefore, changes of mRNA abundance levels are determined by alterations of mRNA synthesis and decay rates. Since standard transcriptomics monitor relative changes in mRNA levels, expression profiling is unable to measure changes in mRNA synthesis and decay. To overcome this limitation, standard transcriptomics has been combined with additional experimental approaches:

Current experimental methods in yeast follow two distingt strategies for analyzing the mRNA synthesisrates, half-live and decayrates. The first strategy allows for measurement of transcript half-live and decayrates by using transcription inhibitors. The second strategy monitors nascent mRNA synthesis and transcript stabilities by using the genomic-run-on technique. This technique is based on the blockage of cellular functions by treatment with sarkosyl, which is combined with radioactive labeling during a subsequent run-on reaction (Hiroyashi, et al. 1999; Garcia-Martinez, et al. 2004).

However, both strategies use invasive experimental steps which have negative side effects. An alternative approach for unperturbed measurement of mRNA synthesis and decay

rates uses labeled mRNA. While these principles have been successfully used for mammalian, insect and plant cells, this approach is not applicable for yeast.

1.2.1 Inhibitors

The first approach to measure mRNA stability in terms of half-lives and underlying kinetics is achieved by blocking transcription followed by analysis of mRNA abundance at several time points. Under the assumption that mRNA decay is a stochastic process and can be described by an exponential function, the change in mRNA abundance at any given time point is considered as first order process. Therefore, mRNA decay will be described by first derivation dC/dt, where C represents mRNA abundance present at time t. Assuming an idealized situation, in which transcription is completely inhibited at time-point $t=0$, the subsequent reduction of mRNA abundance during time-points $t>0$ is then a direct indication of mRNA half-live. To ensure a complete blockage of transcription at $t=0$, several Pol-II inhibitors have been used for studies in yeast and cultured cell lines of higher eukaryotes (for review see Ross, et al. 1995). As an overview, the predominantly used inhibitors and the temperature-sensitive Pol II mutant Rpb1-1 are described in the following paragraphs. Recent studies, however, revealed that these experimental approaches have some negative side effects on transcriptomics.

Actinomycin-D (ActD)

Several studies on mRNA half-live in yeast as well as in higher eukaryotes made use of Actinomycin-D (ActD), thiolutin and 1,10-Phenantrolin (Phen). For example, Raghavan, et al. (2002) applied ActD to human T lymphocytes and identified short-lived mRNAs encoding for cytokines, cell surface receptors, signal transduction regulators, transcription factors, cell cycle regulators and regulators of apoptosis. ActD was recently used in archaea to analyze mRNA stability to identify novel RNA degrading characteristics (Evguenieva-Hackenbert, et al. 2008). Narsai, et al. (2007) treated cultured arabidopsis thaliana cells with ActD and showed, that genes possessing at least one intron produce significantly more stable transcripts as intron-less genes. However, recent studies revealed some severe drawbacks of ActD. ActD affects the cellular ATP pool and produces therefore significant side effects by influencing other ATP-dependent processes (Ross, et al. 1995). This leads to considerable differences between results obtained with ActD and other methods utilizing less toxic compounds. Harrold, et al. (1991) compared values of mRNA half-lives of immunoglobulin heavy- and light chain encoding transcripts in mouse myeloma cells obtained from different methods. Surprisingly, the values ranged from 2.4 h (ActD) to 5.9 h (DRB). Additionally, actD binds to GC-rich sequences of DNA and inhibits RNA Pol II, which leads to DNA damage response and apoptosis. The DNA damage response activates several RNPs, such as human HuR, and AU-binding factor 1 (Auf1), which stabilize target mRNAs or modulate translation.

1,10-phenanthroline (Phen)

1,10-phenanthroline (Phen) works as a chelating agent that forms stable complexes by coordination of bivalent ions, especially with Ni^{2+}, Zn^{2+} and Mg^{2+}(Chang, et al. 1970; Chang, et al. 1978; Santiago, et al. 1986; Johnston, et al. 1994). The inhibitory effect on RNA polymerases has been described by Scrutton, et al. for *E. coli* (1971). Additionally, Phen has been observed to intercalate DNA, which probably contributes to shut-off transcription (Drew, et al. 1984). Phen has been deployed as inhibitor in a variety of studies on mRNA synthesis and halflive. Yin, et al. (2000) used Phen to analyze changes in mRNA stability encoding for *fbp1* and *pck1* in response at low glucose levels. They could show, that low glucose levels strongly repress transcription of both, *fbp1* and *pck1*, and additionally lead to accelerated degradation of the corresponding mRNAs. In a genome-wide study, Grigull, et al. (2004) compared the changes in mRNA levels between Phen, cordyceptin, actD and thiolution with the temperature-sensitive mutant Rpb1-1 in yeast. Among these inhibitors, Phen showed almost identical expression profile to Rpb1-1. Inhibition of transcription by Phen exhibits some drawbacks: First, Phen works as metalchelator that probably sequesters Mg^{2+} in the active center of RNA polymerases and it is most likely, that other magnesium dependent processes or enzymes are affected by Mg^{2+} depletion. Second, Phen induces heat-shock response in yeast. After treatment with Phen, *hsp82* mRNA reach same levels as in response to heat-shock (Adams, et al. 1991).

Pol-II temperature-sensitive mutant: Rpb1-1

The temperature-sensitive mutant Rpb1-1 has been identified by Nonet, et al. (1987). By shifting the temperature from 24^0C to 36^0C, the authors observed a detectable reduction in mRNA abundance after 15 min and after 45 min, a significant loss in global mRNA abundance (Nonet, et al. 1987). The availability of a ts-mutant which shuts off exclusively Pol-II transcription enabled a number of studies producing interesting results in mRNA turnover and promoted yeast to become a modelorganism for studies on mRNA decay (Herrick, et al. 1990; Moore, et al. 1991; Li, et al. 1999; Grigull, et al. 2004; Wang, et al. 2002; Shalem, et al. 2008). For example, Holstege, et al. (1998) used the Rpb1-1 strain and combined transcriptional shut off with microarray analysis of global mRNA half-lives. With this approach, half-lives of 5735 mRNAs were calculated. However, a major drawback of this strategy lies in the temperature shift which is necessary to shutoff transcription completely. Several studies observed a high induction of heat-shock response genes which might introduce a stress dependent change in mRNA stability and therefore to a potential bias in mRNA half-live determination (Preiss, et al. 2003).

1.2.2 Genomic run on (GRO)

Genomic-run-on (GRO) has been developed to measure transcription rates and quantify mRNA abundance to obtain genomewide mRNA synthesis and decayrates under steady-state conditions (Birse, et al. 1997; Hirayoshi & Lis, 1999; Garcia-Martinez, et al. 2004). GRO is performed in three steps: First, *S. cerevisiae* cells are permeabilized in a cold sarkosyl buffer for 20 min which stops all physiological processes and disrupts all chromatin associated proteins with the exception of elongating RNA polymerases. Second, the run-on reaction is performed for 5 min in the presence of radioactive ^{33}P-UTP label, which is incorporated into nascent mRNA molecules during elongation. Third, transcripts are isolated and hybridized on custom made nylon-microarrays. The values obtained in the GRO-experiment are proportional to the average density of Pol II under the assumption of a constant Pol II elongation rate (Garcia-Martinez, et

al. 2004). However, GRO is an opportunity to measure mRNA kinetics, but there are some limitations: First, GRO requires sarkosyl to permeabilize the cell wall to ensure uptake of the radioactive label. This causes an instantaneous loss of nucleosidetriphosphate and a complete chromatin disruption (Pérez-Ortin, 2008; Hirayoshi & Lis, 1999). Second, GRO measures nascent mRNA synthesis rates. Nascent mRNA undergoes several quality control and processing steps until the mature mRNA is prepared for translation.

1.3 Aim and scope of this project

Cells confronted with threatening environmental changes rapidly reorganize cellular processes to ensure survival. This requires reorganization of the active gene expression program to synthesize specialized proteins and circumvent the pressure of stress. Gene expression is a highly dynamic process, which induces response on different time scales to external perturbations. Dissecting this dynamic process, both functionally and mechanistically, is fundamental to understanding gene regulation. The central question is, what mechanism underlie the dynamic reorganization of gene expression that process the external signal into a specific change in gene expression?

The majority of studies dealing with regulation of gene expression is focused on regulation of transcription and utilize mRNA abundance as a measure of gene expression. However, RNA abundance results from the tightly coordinated balance between transcription and degradation. Therefore, reorganisation of the active gene expression program might be a question of regulating mRNA synthesis and stability. To follow the regulation of gene expression during stress response, dynamics in mRNA synthesis and degradation must be monitored simultanously, without perturbation of the cellular system. This cannot be achieved by standard transcriptomics, which only measure mRNA abundance and cannot resolve relative contributions of transcription and transcript half-lives to total RNA levels.

The aim of this project was to monitor the contribution of RNA synthesis and decay to genetic expression. The yeast *S. cerevisiae* is an ideal model eukaryote for systematic analysis, but mRNA synthesis and decay cannot be measured without cellular perturbation.

In this study, we developed a novel method to measure simultaneously total mRNA abundance, mRNA synthesis and decay rates in the yeast *S. cerevisae*. We report on the development of metabolic labeling of RNA, referred to as dynamic transcriptome analysis (DTA). Metabolic labeling enables selective isolation of newly synthesized transcripts from total cellular RNA. DTA is an easy-to use, non-perturbing method, that allows for global and simultaneous monitoring of synthesisrates and transcript half-lives (section 2.1). We combined the metabolic labeling approach with Affymetrix microarray analysis and an advanced, quantitative dynamic model. DTA revealed changes in synthesis and decay rates at unprecedented sensitivity and temporal resolution (section 2.1.1, 2.1.2 and 2.1.3). Under normal conditions, RNA synthesis and decay rates were obtained under steady-state conditions for normal growth. RNA half-live distribution for more than 4000 genes of *S. cerevisiae* revealed the dynamics of cellular RNA during cell cycle (section 2.1.4). Our work revealed that synthesis and decay are uncoupled under normal growth conditions (section 2.1.5).

In response to environmental changes, cells dynamically reorganize their gene expression programs within minutes. Following the stress stimulus, dynamics of mRNA synthesis and decay were monitored with temperal resolution (section 2.2). DTA was used to monitor the conserved osmotic stress response pathway, to investigate contributions in RNA

synthesis and decay to gene expression during genetic reorganization (section 2.2.1 to 2.2.5). DTA data were combined with Pol II occupancy profiles (ChIP-chip) which investigate connection of mRNA synthesis rates and Pol II redistribution during changes in the active gene expression program (section 2.2.6). Our results establish DTA as a highly valuable tool for the analysis of dynamic changes in mRNA metabolism and as a method that can provide quantitative data for modeling complex gene-regulatory systems.

2. Results & Discussion

2.1 Simultaneous analysis of RNA synthesis and decay rates in yeast

Under normal growth conditions, stable mRNA levels result from transcription and degradation with constant rates, which lead to a dynamic equilibrium which sets total mRNA levels. Therefore, mRNA levels might be the result of a regulated balance between transcript synthesis and degration. To investigate mechanisms that control gene expression, it is essential to analyze the relative contributions mRNA synthesis and decay to total mRNA levels. For simultaneous measurement of RNA synthesis and decay in yeast, we established an experimental strategy for non-perturbing RNA labeling in yeast in combination with RNA microarray analysis and mathematical modeling.

2.1.1 Non-perturbing RNA labeling in yeast

Monitoring of RNA synthesis rates can be achieved by metabolic labeling with nucleoside analogs (Cleary, et al. 2005; Kenzelmann, et al. 2007). Thio-substituated nucleoside analogues are not naturally found in eukaryotes and can be purified from cell lysates. The nucleoside analog 4-thiouridine is readily taken up by many eukaryotic cells and is efficiently incorporated into *de novo* synthesized RNA (Cleary, et al. 2005; Kenzelmann, et al. 2007; Doelken, et al. 2008; Cleary, et al. 2007). This can be used to metabolically label and isolate newly transcribed RNA from total cellular RNA with high specificity (Kenzelmann, et al. 2007; Dolken, et al. 2008). To establish 4-thiouridine labeling in the budding yeast *S. cerevisiae*, we cultured cells in the presence of 100 μM-5 μM 4-thiouridine. Although we observed a concentration dependent, specific incorporation of 4-thiouridine, the efficiency of incorporation was low and the amount of recovered newly transcribed RNA was very small (data not shown). This implied inefficient uptake of 4-thiouridine into yeast cells rather than an intracellular blockage in activation or incorporation by RNA polymerases.

In the fission yeast *Schizosaccharomyces pombe*, expression of the human equilibrative transporter (hEnt1) enables cellular uptake of the nucleoside analog 5-bromo-2'deoxyuridine, resulting in labeling of DNA during replication (Hodson, et al. 2003). To test whether this transporter could also mediate efficient uptake in *S. cerevisiae*, we grew yeast strain BY4741 expressing hEnt1 to mid logarithmic phase, added 4-thiouridine and isolated RNA at different time points (Figure 6). This significantly enhanced 4-thiouridine incorporation to a level similar to that generally achieved in mammalian cells, thereby facilitating efficient separation of total cellular RNA into newly transcribed and pre-existing RNA (Figure 5A).

We next tested whether Pol II incorporates the thionucleotide normally into RNA *in vitro* (Brueckner, et al. 2007; Sydow, et al. 2009). Pol II used the substrates UTP and 4-thiouridine-triphosphate (4sUTP) with very similar kinetics. Whereas k_{cat} was unchanged, K_M increased from 3 nM for UTP to 13 nM for 4sUTP, indicating a slightly decreased substrate affinity that may result from weaker base pairing between 4sUTP and the template (Figure 5B). This minor

difference is likely irrelevant in vivo, where substrate concentration is higher by several orders of magnitude than these K_M values.
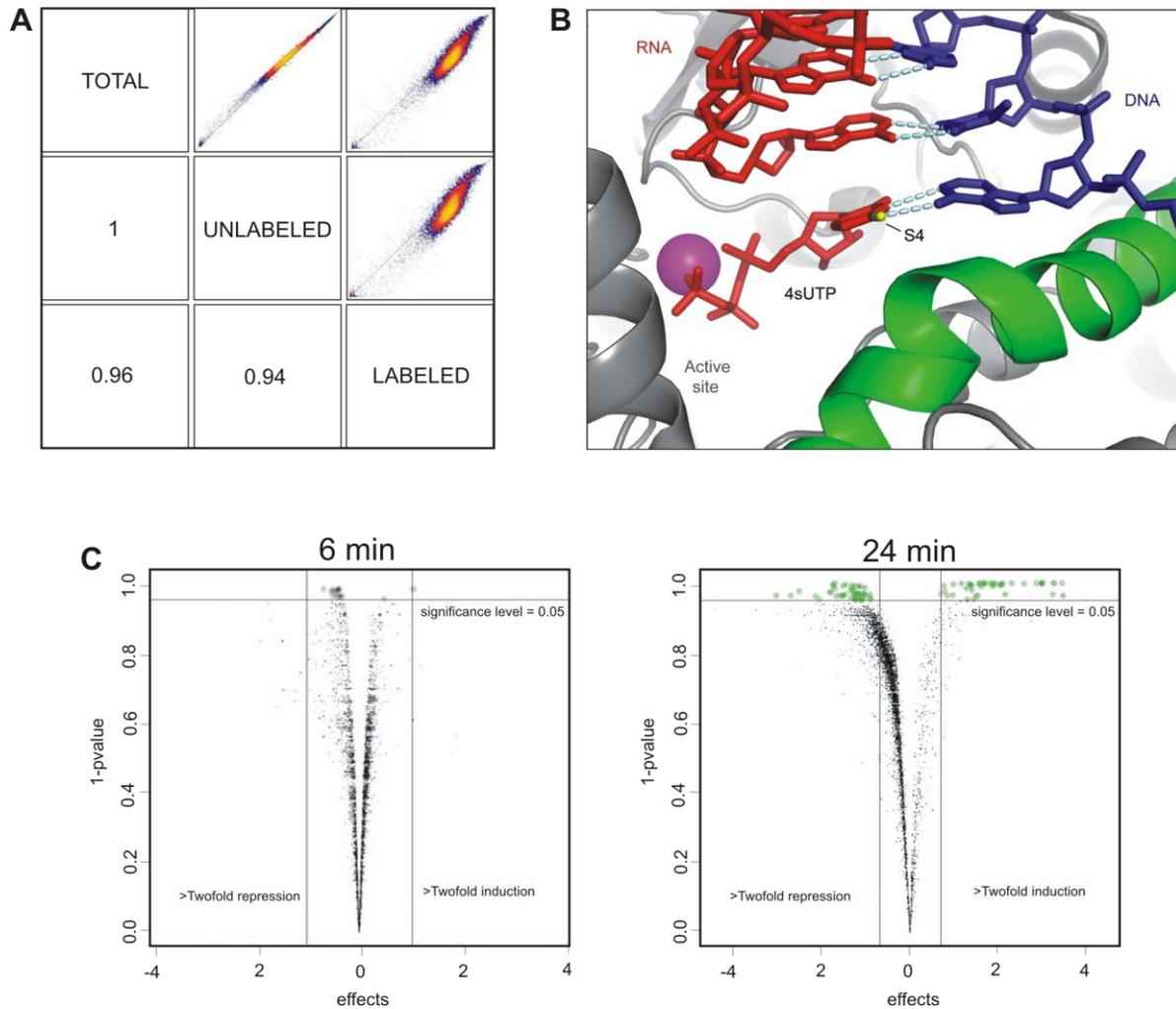
Figure 5: *Non-perturbing RNA labeling in yeast.* (**A**) Scatterplots of log-intensities Tgr, Ugr and Lgr depicted for the 1st replicate of the 6 min labeling time. Numbers represent Spearmean correlations. (**B**) 4sUTP is modeled into the crystal structure of a Pol II transcribing complex (PDB code: 116H). The thio-group at position 4 can form a hydrogen bond with the DNA template strand (blue). Nascent RNA is in red. **(C)** The yeast transcriptome is undisturbed by expression of the human nucleoside transporter hEnt1. The volcano plot compares mRNA levels after 6 min and 24 min labeling versus wild-type cells without labeling. Each dot corresponds to one gene, the x-axis displays the log2(fold) of that gene, the y-axis represents the multiple testing adjusted P-value. In all, 17 genes showed a significant change in mRNA levels (adjusted P-value <5%), only 3 were at least two fold after 6 min labeling time.

To investigate whether RNA labeling perturbed gene expression in vivo, we compared RNA levels in 4-thiouridine treated hEnt1 expressing cells with untreated wild type cells (MATERIALS & METHODS). For a labeling period of 6 min, we observed no significant changes in RNA levels as measured with Affymetrix expression arrays (Figure 5C). Although other cellular processes may be influenced by 4-thiouridine, their effect on mRNA metabolism is apparently not significant, as changes in the total mRNA levels were not observed.
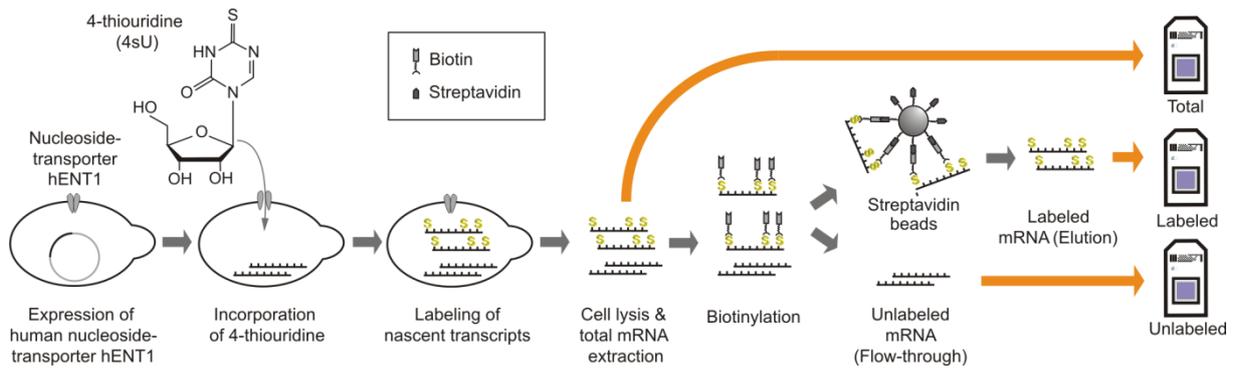
Figure 6: *Dynamic transcriptome analysis in yeast.* Scheme of metabolic mRNA labeling in yeast. Nascent mRNA is labled with 4-thiouridine and thiol specifically biotinylated following cell lysis and preparation of total cellular RNA. Fractionation into pre-existing and nascent mRNA is achieved with streptavidin beads.

2.1.2 Dynamic transcriptome analysis (DTA)

To determine the optimum labeling time, we purified total, newly transcribed (labeled), and pre-existing (unlabeled) RNA at 3, 6, 12, and 24 min after 4-thiouridine addition, and subjected these fractions to expression array analysis (MATERIALS & METHODS). Replicate data always showed correlations above 0.9 for each RNA fraction at each time point (data not shown). To estimate mRNA synthesis and decay rates from individual time point measurements, a new quantitative steady-state model was developed. The model assumes a constant RNA synthesis rate and an exponential decay rate, and no rate changes during the labeling time. The model accounts for exponential cell growth and for variations in RNA extraction efficiencies. It also corrects for differences in the fraction of newly synthesized RNAs that escape labeling. This fraction is larger for shorter RNAs, and depends on the uridine content of the RNA and the labeling efficiency (Figure 8A).

Reproducibility assessment of the data and simulation studies suggested an optimum labeling time of 6 min, which was subsequently used in all experiments. This was short enough to meet the assumption of constant synthesis and decay rates during labeling, but sufficiently long to yield enough labeled RNA for robust measurements. The relative decay rates within an experiment can be estimated reliably, but the absolute values are more difficult to obtain. We refer to this method of deriving mRNA synthesis and decay rates after a short RNA labeling pulse as dynamic transcriptome analysis (DTA) (Figure 6).

2.1.3 Validation of DTA decay-rates under normal conditions

The comparison of replicate experiments revealed that relative mRNA half-lives are estimated reliably by DTA and exhibit a high correlation of 0.95. However, the absolute mRNA half-live values differ by small factors of approx. 1.1 to 1.7. Therefore, the absolute values for decay rates must be validated by complementary experimental data. For this purpose, we measured the decayrates of selected genes with quantitative real-time PCR (qRT-PCR) after inhibition of RNA Pol II by 1,10-phenantroline (Figure 7). Three groups of genes were chosen for qRT-PCR: Housekeeping genes, which are commonly used as reference genes in qRT-PCR are classified in group 1 (rRNA locus *rdn1*, YFL037w/*tub2*, YFL039c/*act1*). Group 2 comprises salt-stress responder genes (YDL022w/*gpd1*, YGR088w/*ctt1*, YDR536w/*stl1*). In group 3 genes were chosen which show a significant stabilization of their mRNA after salt-stress (YGR040w/*kss1*, YOR315w/*sfg1*). The decay of selected transcripts was determined corresponding to the time-

points 0, 2.5, 6, 10 and 16 min relative to Pol II inhibition. From each time-point, C(t)-values resulting from cDNA obtained from total and labeled mRNA were determined. To calculate the decay-profiles from qRT-PCR data, C(t) values were rescaled and used as validation for a decay-model that delivered estimated decay-rates. The amount of labeled and total mRNA as quantified by DTA were confirmed by qRT-PCR , as well as the estimated decay-rates for the wild-type. This results show, that the estimation of decayrates by DTA is generally consistent with values obtained from qRT-PCR. Therefore, DTA provide a method for estimation of absolute mRNA decayrates (Figure 7).
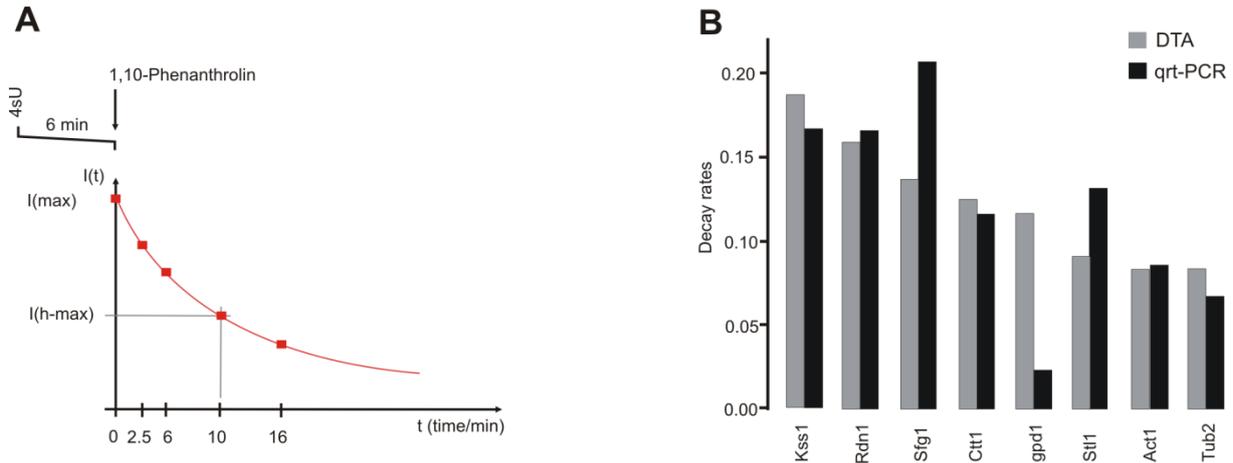
Figure 7: *Validation of DTA data.* (**A**) Design of the qRT-PCR experiments. Samples of total and labeled mRNA were taken (after a labeling period of 6 min) of the wild type. qRT-PCR was performed for a set of selected genes (MATERIALS & METHODS). The mRNA decay rates of selected genes were determined with qPCR by an mRNA decay time series taken at t = 0, 2.5, 6, 10, 16 min after transcriptional shut off. (**B**) Bar plots of the DTA (grey) and qRT-PCR (black) decay rate estimates.

2.1.4 Synthesis rates are low for most mRNAs

We used DTA to derive synthesis rates and decay rates (halflives) for most (4508) of the yeast mRNAs. On the basis of a published rough estimate of 15 000 mRNA transcripts per yeast cell (Hereford and Rosbash, 1977), we calculated the synthesis rate as the number of mRNA molecules produced per cell per cell cycle time (150 min) (Figure 8B). The obtained rates correlated with previously reported rates obtained by nuclear run-on (Pelechano & Perez-Ortin, 2010). Synthesis rates ranged from 1 to 600 mRNAs per cell per cell cycle time. The synthesis rate distribution is strongly right skewed (skewness 5), with a median synthesis rate of 18 RNAs per cell and cell cycle time (mean 31, 1st quartile 11, and 3rd quartile 33). This shows that only a few copies are made for most mRNAs (Figure 8B). This observation is generally consistent with single molecule live-cell imaging (Park et al, 2010). We observed that mRNAs with high synthesis rates encoded ribosomal protein genes and genes involved in ribosome biogenesis, whereas mRNAs with low synthesis rates originated from genes that are silenced during normal growth, including most TFs (Figure 8B).

2.1.5 mRNA decay is not correlated with synthesis

DTA measured a median mRNA half-live of 11 min (mean 14, 1st quartile 9 and 3rd quartile 17 min, Figure 8B). The half-life distribution is strongly right skewed (skewness 8). Thus, most

mRNAs in yeast are synthesized and degraded several times during cell cycle time. Gene ontology (GO) analysis revealed that mRNAs with the shortest half-lives are involved in the regulation of transcription, cell cycle and mRNA processing (Figure 8C). In contrast, mRNAs with long half-lives are involved in carbon and nitrogen metabolism and include many transcripts encoding housekeeping enzymes (Figure 8D).

The decay rates did not correlate with published rates (Holstege, et al. 1998; Wang, et al. 2002; Grigull, et al. 2004; Shalem, et al. 2008), which were obtained with protocols that perturb mRNA metabolism (data not shown). The decay rates did not correlate with mRNA length (data not shown), inconsistent with models that assume stochastic degradation, but consistent with degradation control at the level of mRNA deadenylation and decapping. Many mRNAs with long half-lives contained AU-rich elements in their 3'-untranslated region, consistent with a stabilizing role of these elements (Barreau, et al. 2005). Decay rates correlated weakly with mRNA levels (Spearman correlation -0.59), but synthesis rates correlated well (Spearman correlation 0.84) (data not shown). However, synthesis rates did not correlate with decay rates (Spearman correlation -0.15). This indicates that mRNA synthesis and decay are functionally independent during normal growth, and that both processes contribute to setting cellular mRNA levels.
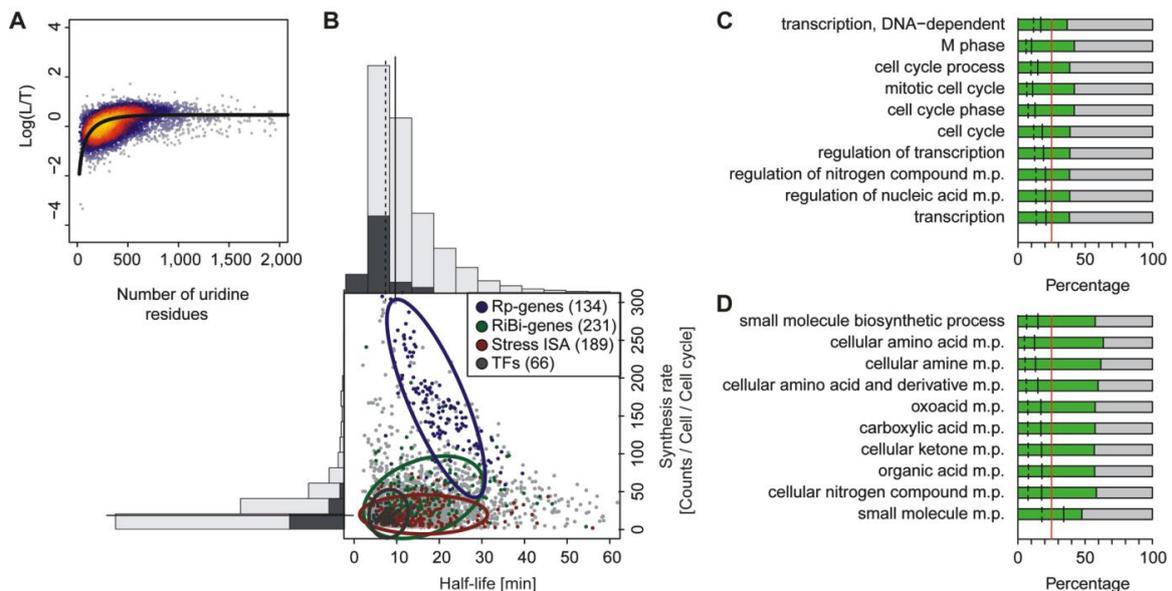
Figure 8: *Determination of mRNA synthesis and decay rates.* **(A)** The comparison of transcript length and DTA decay rates (estimated with DTA) shows that degradation speed (= decay rate =log(2)/half-life) is uncorrelated with transcript length. The spearman correlation coefficient is 0.06. It is noteworthy that a correlation coefficient of 0.64 is obtained, if discrepancies that are due to 4-thiouridine/Biotin labeling are ignored. Without bias removal, the half-lives of 72% of RNAs are artificially elongated by a factor of at least 2, so that the overall ranking of the half-lives is strongly altered. **(B)** Center, scatter plot of the mRNA half-lives and synthesis rates for exponentially growing yeast cells. Colored points belong to the indicated gene sets (green, ribosomal biogenesis genes; violet, ribosomal protein genes; red, stress genes; dark gray, transcription factors (TFs). Assuming Gaussian distributions, ellipses show the 75% regions of highest density for the respective sets. Histograms along the x axis resp. y axis show the global half-life resp. synthesis rate distribution (light gray) and the half-life resp. synthesis rate distribution of the TFs (dark gray). Overall half-lives and synthesis rates are uncorrelated (Spearman correlation 0.06), however some gene groups behave differently (correlations: Ribosomal protein genes (Rp) 0.79, Ribosomal biogenesis genes (RiBi) 0.35, ISA stress module genes 0, TFs 0.07). **(C) (D)** Gene Ontology (GO) analysis of the short-lived mRNAs (lower 25% of the half-life distribution). The 10 most significant categories are displayed, sorted from bottom (most significant) to top. Red line, proportion of short-lived transcripts in the whole population (25% by construction). The number of short-lived transcripts in the resp. GO category is given relative to the GO category size (green bar) and relative to the number of short-lived transcripts (black line). Dashed line, relative size of the GO set in the whole population.

2.2 Stress induced reorganization of gene expression

The above analysis and published studies estimate mRNA synthesis and decay rates only in the steady-state (Doelken, et al. 2008; Amorim, et al. 2010). Under stress conditions, however, the assumption of steady-state mRNA levels cannot be maintained, when cells rapidly change their transcriptional program. To monitor dynamics in mRNA metabolism with altered synthesis and decay rates, the DTA model has to be extended for variations of global mRNA levels. This was achieved by introduction a time-dependent "growth-rate" for each individual mRNA into the steady-state model (MATERIALS & METHODS).
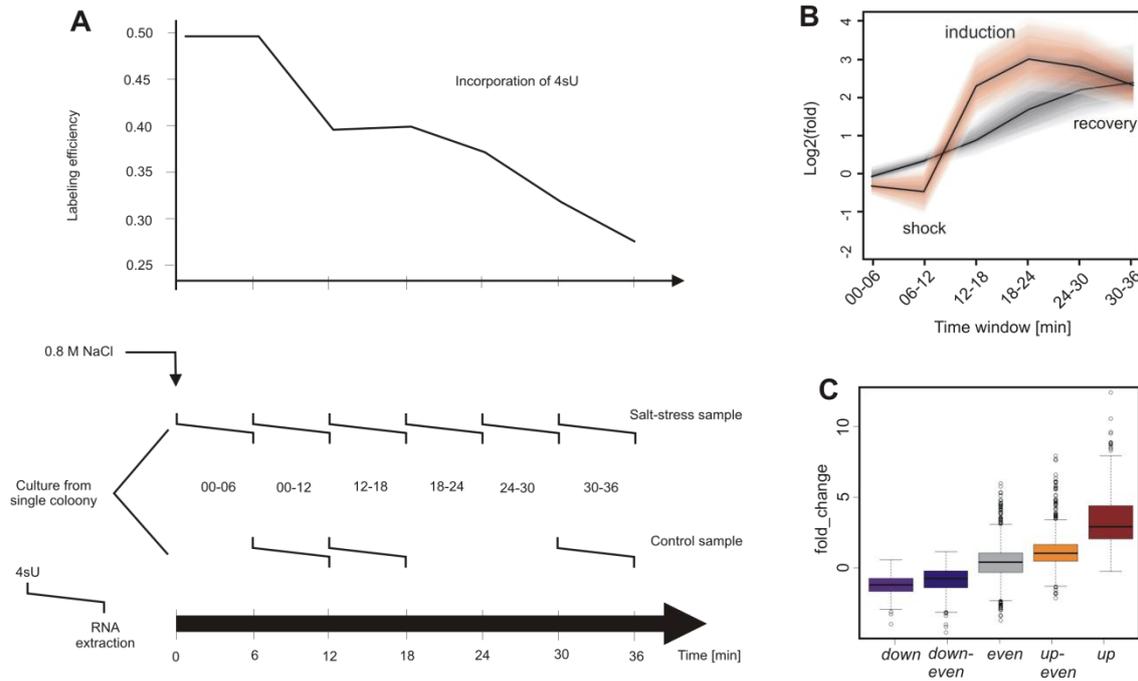
Figure 9: *Design of the time series experiment.* **(A)** Each time window (└─┐) corresponds to one sample, left end marks the start of the 4-thiouridine labeling, right end marks the time of mRNA extraction. Upper panel shows the drop in labeling efficiency from roughly one 4-thiouridine in 200 uridines to one 4-thiouridine in 400 uridines during the osmotic stress response. **(B)** Increased sensitivity and temporal resolution of DTA compared to standard transcriptomics. Grey: Time course of the total mRNA fraction of the Hog1-induced genes (Capaldi, et al. 2008). Red: Time course of the synthesis rates of the same gene set. The solid lines represent the time course of the median, the shaded bands are the central 95% regions, respectively. In contrast to the monotonically increasing total mRNA time course, the synthesis rates clearly show three response phases. **(C)** Expression changes of the five clusters (*up*, *up-even*, *even*, *down-even*, *down* – see Materials and methods) that were defined in a normalization-independent manner. The box plot shows synthesis rate folds (30 min vs. 0 min).

2.2.1 DTA monitors rate changes during osmotic stress

To monitor rate changes, and thus the dynamics in mRNA metabolism, we extended DTA to a time-resolved analysis of the yeast osmotic stress response. Cells were grown to logarithmic phase and split into control and sample cultures (Figure 9A). Sodium chloride was added to the sample culture to a concentration of 0.8 M. Control and sample cultures were divided in aliquots, and 4-thiouridine was added at 0, 6, 12, 18, 24, and 30 min after salt addition. After labeling for 6 min, total, labeled, and unlabeled RNA was purified and analyzed with gene expression arrays. DTA estimated rates within the time windows 0-6, 6-12, 12-18, 18-24, 24-30, and 30-36 min

after stress induction. The results were confirmed for selected genes by quantitative RT-PCR at 12 and 24 min after stress induction (Figure 9).

2.2.2 Three phases of the osmotic stress response

DTA resolved three phases of the osmotic stress response with unprecedented clarity. In the first 12 min after salt addition (shock phase), essentially all synthesis and decay rates decreased, reflecting global transcription down-regulation and mRNA stabilization. Within 12-24 min after salt addition (induction phase), synthesis rates strongly increased for a subset of mRNAs. These stress induced mRNAs show increased decay rates, likely to ensure their rapid removal towards the end of the response. Finally, decay rates were mostly restored, whereas a fraction of the synthesis rates remained at levels distinct from the starting values (recovery phase) (Figure 8B). We could not monitor complete recovery, which takes about two hours (Macia, et al. 2009), but a fraction of synthesisrates apparently remains at values different from the starting values, to ensure continued expression of salt homeostasis genes, and lower expression of housekeeping genes. DTA also revealed a drop of labeling efficiency from 0.5% to 0.27% (Figure 9A), reflecting the known inhibition of cellular uptake of small molecules during stress.

2.2.3 Temporary correlation of mRNA synthesis and decay rates

We transformed all rates to their ranks within the rate distributions, to circumvent an error-prone estimation of an unknown normalization factor between measurements at different time points. By comparing the ranks of synthesis rates in the data sets 6 and 36 min after salt addition, five clusters of genes were defined (Figure 9C): '*up*' (379 genes, rank gain > 2000), '*up-even*' (587 genes, rank gain 1000-2000), '*down-even*' (520 genes, rank loss 1000-2000), '*down*' (416 genes, rank loss > 2000), and '*even*' (all remaining 4074 genes). Although global mRNA synthesis and decay were not correlated before stress, some gene groups showed positive and negative correlations during stress (Figure 8B). An analysis of the changes in synthesis and decay rates reveals a temporary interdependence of the rates of mRNA synthesis and decay during the first two stress phases (Figure 10). During the shock phase, a decrease in synthesis rate is usually accompanied by a decrease in decayrate. During the induction phase, an increase in synthesisrates is generally accompanied by an increase in decayrate. They become again uncorrelated during recovery. The nature of a possible physical coupling underlying this temporary correlation of rates remains to be explored.

2.2.4 High temporal resolution reveals mRNA dynamics

Resolution of the three phases of stress response was dependend on DTA and was not possible by measuring total mRNA levels only (Figure 9B). To test the performance of DTA with an unbiased gene set, we monitored the previously described 305 Hog1-responsive genes (Capaldi, et al. 2008). DTA detected an initial decrease in synthesis rates during shock, whereas total RNA levels increased (data not shown). This was however not due to increased transcriptional activity, but rather due to residual transcription activity combined with mRNA stabilization (Figure 10). Also, the signal-to-noise ratio in detection of changes in synthesis rates was on average two times higher than that of measuring differences in total mRNA levels. Thus conventional transcriptomics fails to unveil the nature of the changes in mRNA metabolism upon stress, which are however monitored by DTA.
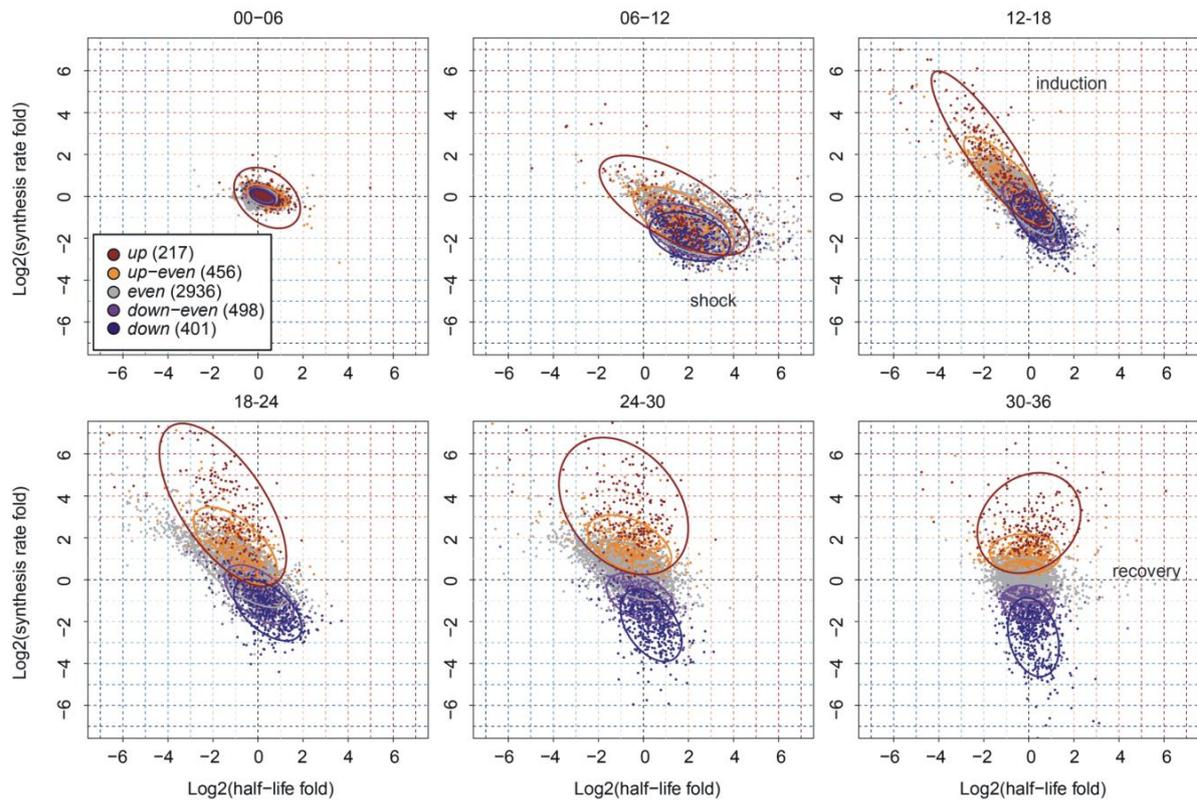
Figure 10: *Dynamics of synthesis and decay rates in the osmotic stress time series.* Each diagram corresponds to one time point. Each point corresponds to one gene, which is colored according to its affiliation with one of the clusters (rank gain analysis) and the ellipses show the 75% regions of highest density within each cluster, assuming Gaussian distributions. The shape of the ellipses indicate the correlation structure within a cluster.

2.2.5 Validation of DTA decay rates by qRT-PCR

To validate the dynamic DTA-model, mRNA levels estimated by DTA were compared to those obtained by qRT-PCR during osmotic-stress response. Cells were grown to mid-logarithmic phase and osmotic stress was induced by adding 0.8 M sodium chloride to the cells. 4-thiouridine was added at 0, 6, 24 and 30 min after salt addition for a constant labeling time of 6 min corresponding to the timewindows 6-12, 24-30 and 30-36 min. Total and labeled mRNA from each timepoint were isolated and analyzed by qRT-PCR. The C(t)-values were processed as described in MATERIALS & METHODS. The mRNA levels were calculated relative to the unstressed control samples at 0 min and the obtained mRNA folds of qRT-PCR were compared to values estimated by the dynamic DTA model (Figure 11). Although the mRNA values quantified by qRT-PCR and DTA show a weak correlation after 12 min, the mRNA values correlated above 0.9 for 30 and 36 min, respectively. This results show that the dynamic DTA model provides a reliable estimation of mRNA values during osmotic stress response, even when constant mRNA levels cannot be assumed.
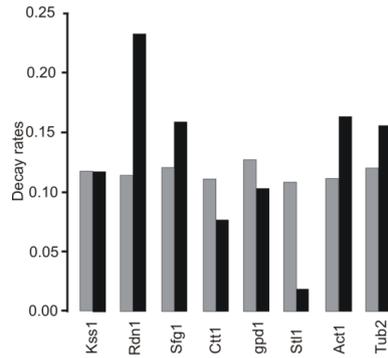
Figure 11: *Validation of DTA decay rates by qRT-PCR.* RT-PCR Bar plots of the DTA (grey) and PCR (black) decay rate estimates, obtained as described in Section 13.2(DTA) resp. Section 15.2(PCR). The left plot shows the wild type, the right plot shows the situation after 12 min of osmotic stress.

2.2.6 High sensitivity detects new stress response genes

Due to the increased sensitivity, DTA reveals many genes that are induced during stress. The *up* cluster contained genes associated with GO terms related to stress response. Of the stress module genes as defined by the iterative structure algorithm (Ihmels et al. 2002), 74% showed a rank gain greater than 1000. The *up* cluster contained only three transcription factors (TFs), consistent with the pre-existence of TFs for stress response and their post-translational activation (Proft & Struhl, 2004, and references therein). The *up* cluster contained 62% genes that were up-regulated in a recent study of the osmotic stress response (Capaldi et al. 2008). However, DTA also detected 58 new genes involved in the osmotic stress response (Figure 12; Table 10; MATERIALS & METHODS). These are mostly genes of unknown function, except Ubc5, which is known to mediate degradation of abnormal proteins during cellular stress. Of genes in the *up* cluster, 35% were uncharacterized, compared to only 16% over all yeast genes. Yeast strains with single knock-outs of the newly revealed stress genes did generally not show growth defects under high salt conditions (data not shown), providing a possible explanation for why they were not discovered previously.
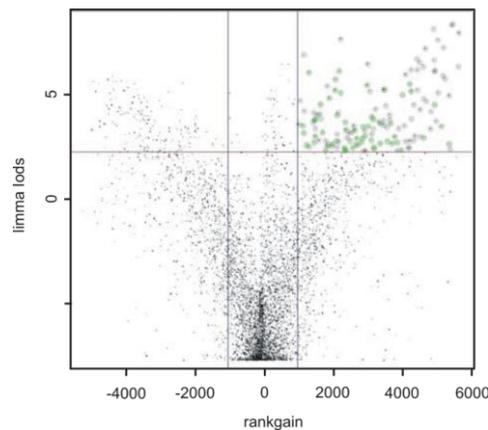
Figure 12: *High sensitivity of DTA detecs new stress response genes.* Volcano plot comparing the synthesis rates 36 min after osmotic stress induction with wild type synthesis rates. The x-axis shows the difference of the ranks of a gene in the 36 min synthesis rates distribution and the wild type synthesis rates distribution. The y-axis shows the significance of a change in synthesis rates, as measured with limma (Smyth, 2004). It is given as the log odds (synthesis rate is different/synthesis rate is unchanged) for each gene. Grey dots: Hog1 and/or Msn2/4 dependent osmotic stress genes identified by (Capaldi et al. 2008). The 58 dots in green are novel genes also clearly involved in the transcriptional response to osmotic stress.

2.2.7 Genomic Pol II redistribution predicts mRNA synthesis rate changes

To investigate whether mRNA synthesis rates correlate with the presence of Pol II at transcribed genes, we determined occupancy profiles for the Pol II subunit Rpb3 by chromatin immunoprecipitation (ChIP) and tiling microarray (chip) analysis, and calculated the mean Pol II occupancy between the transcription start site (TSS) and the polyadenylation site (pA) for each gene (Mayer, et al. 2010). We also measured ChIP-chip profiles 12 and 24 min after salt addition, to investigate whether Pol II is redistributed over the genome upon stress. At all three time points (0, 12, and 24 min), the mean Pol II gene occupancy was calculated. The three resulting Pol II occupancy vectors were compared with the vectors of total RNA, newly synthesized RNA, and synthesis rates at all six 6min time windows of the osmotic stress (Figure 13). Pol II gene occupancies at 0, 12 and 24 min correlated only weakly with mRNA levels, but very well with the levels of labeled mRNA and with the synthesis rates at the corresponding time points (Figure 13). The results also demonstrated the low temporal resolution of standard transcriptomics, as Pol II occupancy 12 and 24 min after stress induction correlated with mRNA levels at a later time point (Figure 13). We averaged Pol II occupancy profiles over genes belonging to the even, down, and up clusters (Figure 14). The even cluster showed a typical gene-averaged profile with elevated Pol II levels on the transcribed region and peaks around the TSS and poly(A) site. This profile persisted during stress, although overall polymerase levels decreased. The down cluster genes apparently lost most if not all Pol II during stress. In contrast, the up cluster genes did not contain detectable amounts of Pol II before stress but gained Pol II during stress. The shape of the averaged profile of up cluster genes after 24 min of salt stress showed an even distribution of Pol II that was very different from the canonical profile (Figure 14), maybe because of a high density of Pol II on these stress-induced genes. Thus, Pol II occupancy predicted mRNA synthesis rates and Pol II redistribution upon stress predicted changes in synthesis rates. On the other hand, the observed correlations confirm that DTA realistically monitors changing transcriptional activity.
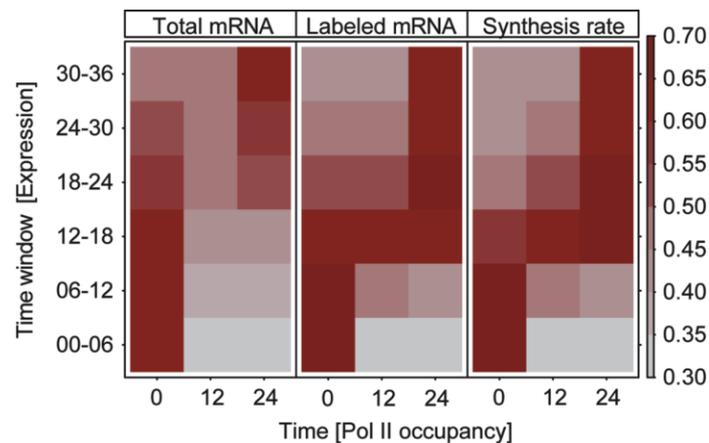
Figure 13: *Pol II gene occupancy predicts mRNA synthesis*. **A)** The vectors of mean Pol II occupancies on transcribed regions were calculated from ChIP-chip data at 0, 12, and 24 min after salt stress and compared with the vectors of total mRNA levels (left), labeled mRNA (middle), and synthesis rates (right) at each time point of the osmotic stress time course experiment. The pair-wise Spearman correlation values are represented by colorcoded squares.
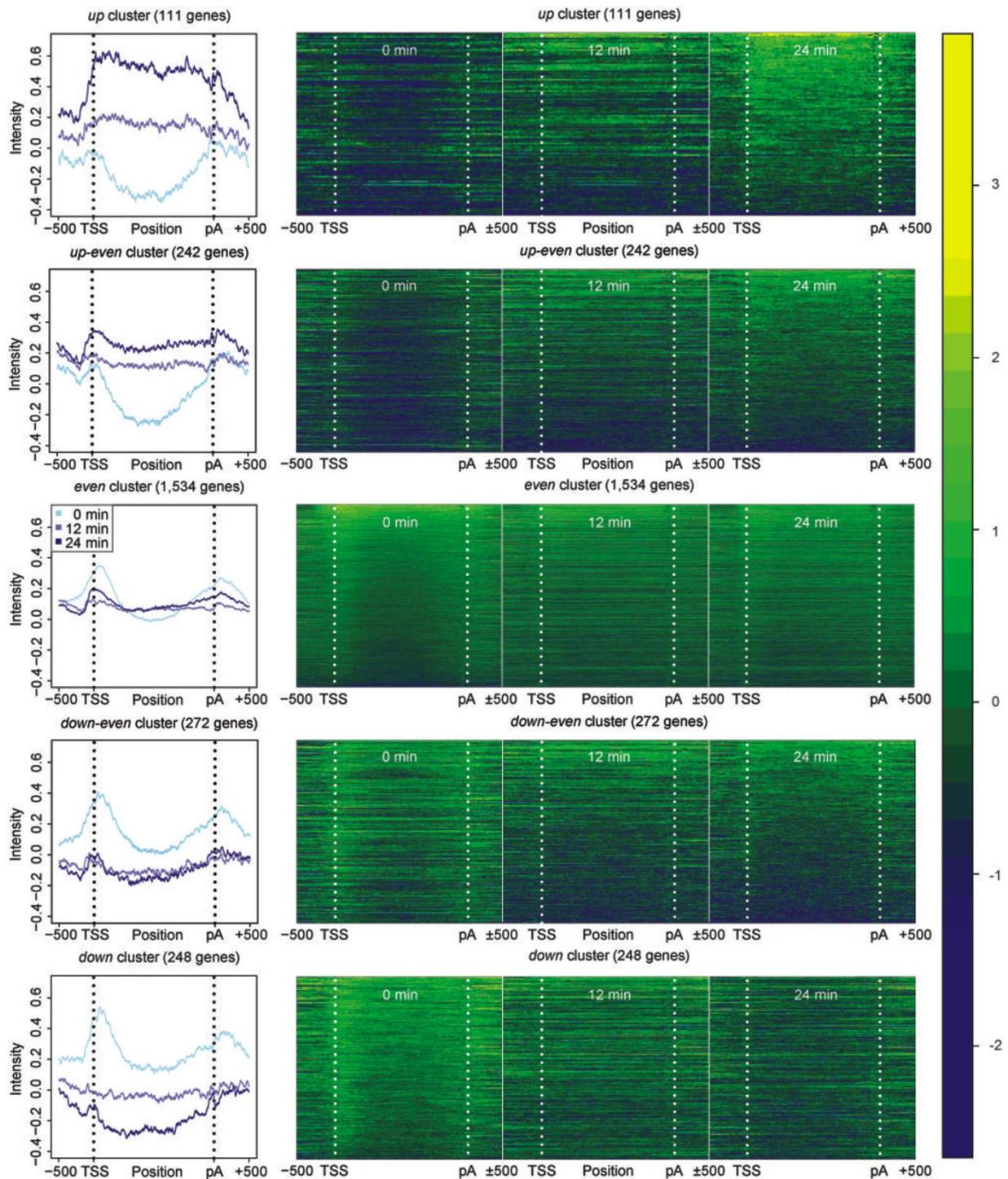
Figure 14: *Osmotic stress induced genomic Pol II redistribution.* **Left:** Mean Pol II occupancy profiles of all selected clusters. Profiles are obtained after 0, 12 and 24 min of osmotic stress (light blue, blue, dark blue lines). Vertical dotted lines are drawn at the TSS and the pA site. **Right:** Heatmaps of the Pol II profiles for all cluster at 0, 12, and 24 min. Each row corresponds to one gene. The vertical dotted lines mark TSS and pA of each gene. Pol II occupancy from low to high is coded with colors ranging from dark to bright.

3. Conclusion and Outlook

We developed Dynamic Transcriptome analysis (DTA) for measuring simultaneously the critical characteristics of mRNA metabolism: mRNA abundance, synthesis rates and half-lives. DTA can monitor mRNA metabolism on a global scale, with a high dynamic range, high sensitivity and temporal resolution and without perturbation of the transcriptome. This was achieved by a metabolic mRNA labeling approach, which comprises genetically facilitated cellular uptake of the nucleoside analog 4-thiouridine, metabolic RNA labeling, separation and microarray analysis of total, newly transcribed and pre-existing RNA. DTA combines the metabolic labeling approach with a quantitative dynamic model, that enables extraction of synthesis and decay rates and mRNA half-lives from the array data. This allows for time-resolved correlation analysis of mRNA synthesis and decay, which revealed the contribution of transcription and post-transcriptional processes to gene expression. To obtain synthesis rates that reflect the production of complete transcripts, the DTA protocol selects for polyadenylated RNA by hybridizing the 3'-region of transcripts on the array. DTA was developed as a tool for simultaneous monitoring of gene expression control on different levels in parallel to get insights into the interplay between transcriptional and post-transcriptional regulation of gene expression.

We applied DTA to wild-type yeast cells to monitor the undisturbed mRNA metabolism. During exponential growth, most genes are transcribed and produce only a few copies per cell and cell cycle time. The median mRNA half-live of 11 min revealed a generally rapid transcript turn-over. Transcript synthesis and decay are generally not correlated, indicating that transcription and mRNA degradation contribute independently to steady-state mRNA levels.

Yeast cells respond to stress situations by an fast reorganization of the gene expression program. To study this fast, efficient and precise change between the normal growth and stress response on a transcriptomic level, we used DTA to monitor mRNA synthesis and decay during osmotic stress. DTA follows dynamic changes in mRNA synthesis and decay and revealed three phases of the stress response: Within the initial shock phase (0-12 min), transcription is globally decreased and mRNA required for normal growth is stabilized, apparently to store them. During the subsequent induction phase (12-24 min), synthesis rates for a subset of mRNA are strongly increased, indicating the induction of the stress response program. The strongly induced transcripts exhibit also severe destabilization, probably thus allowing their rapid removal after adaption to stress. We observed also an extensive redirection of cellular resources, probably to antagonize rapidly the stress situation. During the later adaption phase (24-30 min), decay rates are restored whereas synthesis rates remain at altered values, indicating that the cells undergo a second reorganization of gene expression. Many transcripts required for normal growth exhibit increased synthesis rates, whereas stress responsive genes were still expressed to stabilize to the stress situation.

DTA identified 58 new genes induced by osmotic stress, including many genes of unknown function. DTA followed the dynamic changes in mRNA synthesis and decay during osmotic stress response, with higher sensitivity and temporal resolution than ordinary transcriptomics and thus provides new biological insights. Theoretical considerations show that changes in synthesis rate can more quickly change mRNA levels for low abundant transcripts

(Alon, 2006). Changes in decay rates can only efficiently change mRNA levels for highly abundant transcripts. This is consistent with our observations of the osmotic stress by DTA. Probably, this concept might be also realized in other gene regulatory systems, which require a fast and inducible reprogramming of gene expression.

Parts of our observations are consistent with published data on the osmotic stress response in yeast. After global inhibition of transcription, Molin et al. (2009) observed a sharp decrease in mean stability of all initially stabilized stress related transcripts whereas stress-repressed genes become stabilized within 30 min. Genomic run-on analysis showed that osmotic stress provokes mRNA stabilization and sequestration into P-bodies (Romero-Santacreu, et al. 2009). P-bodies develop at 0.8 M NaCl within minutes (Teixeira & Parker, 2007). Proft & Struhl (2004) observed an immediate dissociation of most proteins from chromatin. This may be causative to the rapid decrease of mRNA synthesis and decay rates during the initial shock phase (Proft & Struhl, 2004; Mettetal, et al. 2008). This may go along with a transient depression of tranlationally active ribosomes (Warringer, et al. 2010). Reprogramming during osmotic stress response is dependent on MAP kinase Hog1, which interact with elongating Pol II. Induction of stress responsive genes goes along with Hog1 dependent phosphorylation of a number transcription factors that are required for transcription.

DTA correlate well with Pol II occupancy profiling during osmotic stress response. We could show that the mRNA synthesis rates obtained by DTA are consistent with the Pol II ChIP-chip profiling. Therefore, Pol II occupancy profiling and synthesis rates obtained by DTA apparently monitor the same biological process and reflect the transcriptional activity of Pol II. Thus, previously obtained correlations of Pol II occupancy with mRNA abundance levels (Andrau et al, 2006; Steinmetz, et al, 2006; Pelechano et al, 2010; Venters and Pugh, 2009; Mayer et al, 2010; Rodriguez-Gil et al, 2010) are only an indirect effect of the correlation of mRNA synthesis rates with mRNA levels.

The combination of DTA and Pol II occupancy profiling imply that the reprogramming of gene expression during stress response may be the result of two steps: First, we could show that the dissociation of most proteins during the initial shock phase lead also to global removal of Pol II from transcription start sites. This is consistent with Proft & Struhl (2004), who observed a dissociation of many chromatin bound proteins immediately after stress response induction. Second, we observed the recruitment of Pol II and the PIC assembly on stress induced promoters during the induction phase, whereas the recruitment to non responder genes was not observed. This observations implies that the fast reprogramming in the induction phase might be the result of a global and unspecific Pol II drop off, followed by a selective recruitment of Pol II to stress responder genes.

Outlook

DTA has great potential for studying processes that regulate gene expression. Since switching between alternative gene expression programs is a multilevel process, DTA provides an important tool for an integrative approach. The simultaneous measurements of mRNA abundance levels, synthesis and decay would provide valuable insights into cellular response to changes in environmental conditions, chemical substances or radiation exposure. By developing DTA as a tool for *S. cerevisiae*, the role of yeast as a model organism for fundamental studies is invigorated. The combination of global analysis, the high dynamic range, high sensitivity and temporal resolution of DTA with Pol II profiling may be used to improve models of the osmotic stress response (Capaldi, et al. 2008; Muzzey, et al. 2009). DTA-derived rates of mRNA synthesis

are averaged over a cell population and a time period of 6 min, suggesting that they are independent of the nature of transcription, which may occur in bursts and discontinuously (Suter, et al. 2011; Zenklusen, 2008; Tan, et al. 2010; Cai, 2008).

DTA has great potential to analyze the mechanisms that underlie mRNA metabolism and turnover. With DTA we could demonstrate global changes in response to high salt concentrations. The next step would be to investigate the detailed mechanisms that couple transcription and post-transcriptional processes. As exemplified for the Pol II subunit RBP4/7 which has been identified in cytosolic P-bodies during stress response (Lotan, et al. 2005; Harel-Sharvit, et al. 2010), the interplay between different levels of the mRNA live-cycle is the key of orchestration the gene expression control network. DTA may be used for decipher the pathways of mRNA decay and the regulation of mRNA half-lives by RNA-binding proteins. Post-transcriptional regulons such as the yeast Puf-proteins (Duttagupta et al. 2005), which integrate mRNA from functionally related genes into context dependent coregultion, might be also analyzed by DTA.

Table 10: Genes identified by DTA during response to osmotic stress.

Name	Gene	Description
AFR1	YDR085C	Protein required for pheromone-induced projection (shmoo) formation; regulates septin architecture during mating; has an RVXF motif that mediates targeting of Glc7p to mating projections; interacts with Cdc12p
ARR2	YPR200C	Arsenate reductase required for arsenate resistance; converts arsenate to arsenite which can then be exported from cells by Arr3p
ATH1	YPR026W	Acid trehalase required for utilization of extracellular trehalose
BOP2	YLR267W	Protein of unknown function
CPS1	YJL172W	Vacuolar carboxypeptidase yscS; expression is induced under low-nitrogen conditions
DAN3	YBR301W	Cell wall mannoprotein with similarity to Tir1p, Tir2p, Tir3p, and Tir4p; member of the seripauperin multigene family encoded mainly in subtelomeric regions; expressed under anaerobic conditions, completely repressed during aerobic growth
DIA1	YMR316W	Protein of unknown function, involved in invasive and pseudohyphal growth; green fluorescent protein (GFP)-fusion protein localizes to the cytoplasm in a punctate pattern
ECI1	YLR284C	Peroxisomal delta3,delta2-enoyl-CoA isomerase, hexameric protein that converts 3-hexenoyl-CoA to trans-2-hexenoyl-CoA, essential for the beta-oxidation of unsaturated fatty acids, oleate-induced
ECM12	YHR021W-A	Non-essential protein of unknown function
FMP23	YBR047W	Putative protein of unknown function; proposed to be involved in iron or copper homeostatis; the authentic, non-tagged protein is detected in highly purified mitochondria in high-throughput studies
FSH1	YHR049W	Putative serine hydrolase that localizes to both the nucleus and cytoplasm; sequence is similar to S. cerevisiae Fsh2p and Fsh3p and the human candidate tumor suppressor OVCA2
GIP1	YBR045C	Meiosis-specific regulatory subunit of the Glc7p protein phosphatase, regulates spore wall formation and septin organization, required for expression of some late meiotic genes and for normal localization of Glc7p
GSM1	YJL103C	Putative zinc cluster protein of unknown function; proposed to be involved in the regulation of energy metabolism, based on patterns of expression and sequence analysis
GSP2	YOR185C	GTP binding protein (mammalian Ranp homolog) involved in the maintenance of nuclear organization, RNA processing and transport; interacts with Kap121p, Kap123p and Pdr6p (karyophilin betas); Gsp1p homolog that is not required for viability

HMX1	YLR205C	ER localized, heme-binding peroxidase involved in the degradation of heme; does not exhibit heme oxygenase activity despite similarity to heme oxygenases; expression regulated by AFT1
ICT1	YLR099C	Lysophosphatidic acid acyltransferase, responsible for enhanced phospholipid synthesis during organic solvent stress; null displays increased sensitivity to Calcofluor white; highly expressed during organic solvent stress
LEE1	YPL054W	Zinc-finger protein of unknown function
MAG1	YER142C	3-methyl-adenine DNA glycosylase involved in protecting DNA against alkylating agents; initiates base excision repair by removing damaged bases to create abasic sites that are subsequently repaired
MST27	YGL051W	Putative integral membrane protein, involved in vesicle formation; forms complex with Mst28p; member of DUP240 gene family; binds COPI and COPII vesicles
PAU2	YEL049W	Member of the seripauperin multigene family encoded mainly in subtelomeric regions, active during alcoholic fermentation, regulated by anaerobiosis, negatively regulated by oxygen, repressed by heme
PCL1	YNL289W	Cyclin, interacts with cyclin-dependent kinase Pho85p; member of the Pcl1,2-like subfamily, involved in the regulation of polarized growth and morphogenesis and progression through the cell cycle; localizes to sites of polarized cell growth
PEP12	YOR036W	Target membrane receptor (t-SNARE) for vesicular intermediates traveling between the Golgi apparatus and the vacuole; controls entry of biosynthetic, endocytic, and retrograde traffic into the prevacuolar compartment; syntaxin
PET10	YKR046C	Protein of unknown function that co-purifies with lipid particles; expression pattern suggests a role in respiratory growth; computational analysis of large-scale protein-protein interaction data suggests a role in ATP/ADP exchange
PFK26	YIL107C	6-phosphofructo-2-kinase, inhibited by phosphoenolpyruvate and sn-glycerol 3-phosphate; has negligible fructose-2,6-bisphosphatase activity; transcriptional regulation involves protein kinase A
PRM8	YGL053W	Pheromone-regulated protein with 2 predicted transmembrane segments and an FF sequence, a motif involved in COPII binding; forms a complex with Prp9p in the ER; member of DUP240 gene family
REC102	YLR329W	Protein involved in early stages of meiotic recombination; required for chromosome synapsis; forms a complex with Rec104p and Spo11p necessary during the initiation of recombination
RNR3	YIL066C	One of two large regulatory subunits of ribonucleotide-diphosphate reductase; the RNR complex catalyzes rate-limiting step in dNTP synthesis, regulated by DNA replication and DNA damage checkpoint pathways via localization of small subunits
SCS22	YBL091C-A	Protein involved in regulation of phospholipid metabolism; homolog of Scs2p; similar to D. melanogaster inturned protein
SGF11	YPL047W	Integral subunit of SAGA histone acetyltransferase complex, regulates transcription of a subset of SAGA-regulated genes, required for the Ubp8p association with SAGA and for H2B deubiquitylation
SPG5	YMR191W	Protein required for survival at high temperature during stationary phase; not required for growth on nonfermentable carbon sources
SPL2	YHR136C	Protein with similarity to cyclin-dependent kinase inhibitors; downregulates low-affinity phosphate transport during phosphate limitation; overproduction suppresses a plc1 null mutation; GFP-fusion protein localizes to the cytoplasm
SRL3	YKR091W	Cytoplasmic protein that, when overexpressed, suppresses the lethality of a rad53 null mutation; potential Cdc28p substrate
STB2	YMR053C	Protein that interacts with Sin3p in a two-hybrid assay and is part of a large protein complex with Sin3p and Stb1p
STF1	YDL130W-A	Protein involved in regulation of the mitochondrial F1F0-ATP synthase; Stf1p and Stf2p may act as stabilizing factors that enhance inhibitory action of the Inh1p protein
TGL2	YDR058C	Protein with lipolytic activity towards triacylglycerols and diacylglycerols when expressed in E. coli; role in yeast lipid degradation is unclear
THO1	YER063W	Conserved nuclear RNA-binding protein; specifically binds to transcribed chromatin in a THO- and RNA-dependent manner, genetically interacts with shuttling hnRNP NAB2; overproduction suppresses transcriptional defect caused by hpr1 mutation
UBC5	YDR059C	Ubiquitin-conjugating enzyme that mediates selective degradation of short-lived, abnormal, or excess proteins, including histone H3; central component of the cellular stress response; expression is heat inducible
UGX2	YDL169C	Protein of unknown function, transcript accumulates in response to any combination of stress conditions

YBR056W-A	YBR056W-A	Dubious open reading frame unlikely to encode a protein, based on available experimental and comparative sequence data; partially overlaps the dubious ORF YBR056C-B
YDL085C-A	YDL085C-A	Putative protein of unknown function; green fluorescent protein (GFP)-fusion protein localizes to the cytoplasm and nucleus
YER185W	YER185W	Plasma membrane protein with roles in the uptake of protoprophyrin IX and the efflux of heme; expression is induced under both low-heme and low-oxygen conditions; member of the fungal lipid-translocating exporter (LTE) family of proteins
YET1	YKL065C	Endoplasmic reticulum transmembrane protein; may interact with ribosomes, based on co-purification experiments; homolog of human BAP31 protein
YGL010W	YGL010W	Putative protein of unknown function; YGL010W is not an essential gene
YIL046W-A	YIL046W-A	Putative protein of unknown function; identified by expression profiling and mass spectrometry
YIL055C	YIL055C	Putative protein of unknown function
YJL185C	YJL185C	Putative protein of unknown function; mRNA is weakly cell cycle regulated, peaking in G2 phase; YJL185C is a non-essential gene
YKL133C	YKL133C	Putative protein of unknown function; has similarity to Mgr3p, but unlike MGR3, is not required for growth of cells lacking the mitochondrial genome (null mutation does not confer a petite-negative phenotype)
YLR031W	YLR031W	Putative protein of unknown function
YLR108C	YLR108C	Protein of unknown function; green fluorescent protein (GFP)-fusion protein localizes to the nucleus; YLR108C is not an esssential gene
YLR285C-A	YLR285C-A	Putative protein of unknown function; identified by fungal homology and RT-PCR
YMR034C	YMR034C	Putative transporter, member of the SLC10 carrier family; identified in a transposon mutagenesis screen as a gene involved in azole resistance; YMR034C is not an essential gene
YNL040W	YNL040W	Putative protein of unknown function with strong similarity to alanyl-tRNA synthases from Eubacteria; green fluorescent protein (GFP)-fusion protein localizes to the cytoplasm; YNL040W is not an essential gene
YNL130C-A	YNL130C-A	Protein of unknown function; dgr1 null mutant is resistant to 2-deoxy-D-glucose
YNL211C	YNL211C	Putative protein of unknown function; green fluorescent protein (GFP)-fusion protein localizes to mitochondria; YNL211C is not an essential gene
YNR068C	YNR068C	Putative protein of unknown function
YOL024W	YOL024W	Putative protein of unknown function; predicted to have thiol-disulfide oxidoreductase active site
YPR098C	YPR098C	Protein of unknown function, localized to the mitochondrial outer membrane
YPR172W	YPR172W	Protein of unknown function, transcriptionally activated by Yrm1p along with genes involved in multidrug resistance

CHAPTER IV:

MEDIATOR PHOSPHORYLATION PREVENT STRESS RESPONSE TRANSCRIPTION DURING NON-STRESS CONDITIONS

Miller, et al. **(2012)** *Journal of Biological Chemistry*, 287(53), 44017-26

1. Introduction

1.1 The Mediator Coactivator complex

Regulation of transcriptional activity is dependent on gene-specific transcription factors that respond to environmental signals. In eukaryotic cells, these transcription factors require co-activator complexes to transmit signals to the RNA polymerase II machinery. Among these co-activators, the Mediator complex plays a key role by interacting with transcription factors and the Pol II machinery. Mediator dysfunction leads to a variety of diseases, including mental retardation and cancer (Malik, et al. 2010).

1.1.1 Discovery and conservation of Mediator complexes

First evidence for an intermediary function between transcription activators and Pol II arose from squelching experiments in yeast (Gill & Ptashne, 1988) and mammalian cells (Triezenberg, et al. 1988). Squelching experiments investigate the interference of one activator by overexpression of another activator for the potential to activate Pol II transcription. One try to explain this phenomenon was that both activators compete for binding the same target within the basal transcription machinery. However, neither the addition of an excess of Pol II, nor any of the GTFs were able to relieve squelching. Since addition of a crude yeast extract was able to relieve squelching, the conclusion was drawn that an additional functionality is required that mediate between activators and the basal transcription machinery (Flanagan, et al. 1991; Kelleher, et al. 1990). Genetic screens in yeast identified genes by their ability to suppress the cold-sensitive phenotype of Pol II mutant with truncated CTD. These genes were termed "suppressors of RNA polymerase B" (Srb) and all 9 Srb proteins turned out to be subunits of the coactivator complex Mediator (Nonet & Young, 1989). Mediator is a highly conserved multiprotein complex, which has been identified in yeast (Kelleher, et al. 1990; Flanagan, et al. 1991), plants (Bächström, et al. 2007) and metazoans (Malik, et al. 2010). An ancient 17-subuint Mediator core complex has been identified, which is conserved in all eukaryotes (Bourbon, et al. 2008). Mediator complexes in higher eukaryotes contain additional subunits (Table 12).

1.1.2 Modular structure of Mediator complexes

In *S. cerevisiae*, the Mediator complex consists of 25 subunits and accumulates a mass of 1.4 MDa. The subunits are organized in four functional modules, named head-, middle-, tail- and kinase-module (Björklund, et al. 2005; Cai, et al. 2009). Each module provides a dedicated function. The head-module has been identified to provide an interface for binding Pol II-TFIIF (Takagi, et al. 2006), the kinase module harbors enzymatic function which is involved in phosphorylation of Pol II C-terminal domain (CTD) (Kang, et al. 2001, Näär, et al. 2002). The middle and more evidently the tail module are interaction platforms for regulatory proteins and transcription factors. Structural information on the Mediator shape came from several electron

microscopy data, that revealed a conformational change between a closed conformation and a open conformation, when bound to Pol II (Asturias, et al. 1999; Cai, et al. 2010; Davis, et al. 2002; Dotson, et al. 2000; Elmlund, et al. 2006; Näär, et al. 2002; Taatjes, et al. 2002; Taatjes, et al. 2004). Biochemical studies (Kang, et al. 2001), gene expression profiling (van de Peppel, et al. 2005), yeast two-hybrid screen (Gulielmi, et al. 2004) and deletion studies (Koschubs, et al, 2010) revealed many details of subunit composition within the Mediator. Crystal structures are available for CycC (Hoeppner, et al. 2005), Med7C/Med21 (Baumli, et al. 2005), Med7N/Med31 (Koschubs, et al. 2009), Med8C/Med18/Med20 (Larivière, et al. 2006) and Med15-KIX domain (Thakur, et al. 2005; Yang, et al. 2006; Bontems, et al. 2010). Very recently, the crystal structure of the Mediator head module has been solved and revealed the architecture of *S. pombe* head consisting of Med6, Med8, Med11, Med17, Med18, Med20 and Med22 (Larivière, et al. 2012).
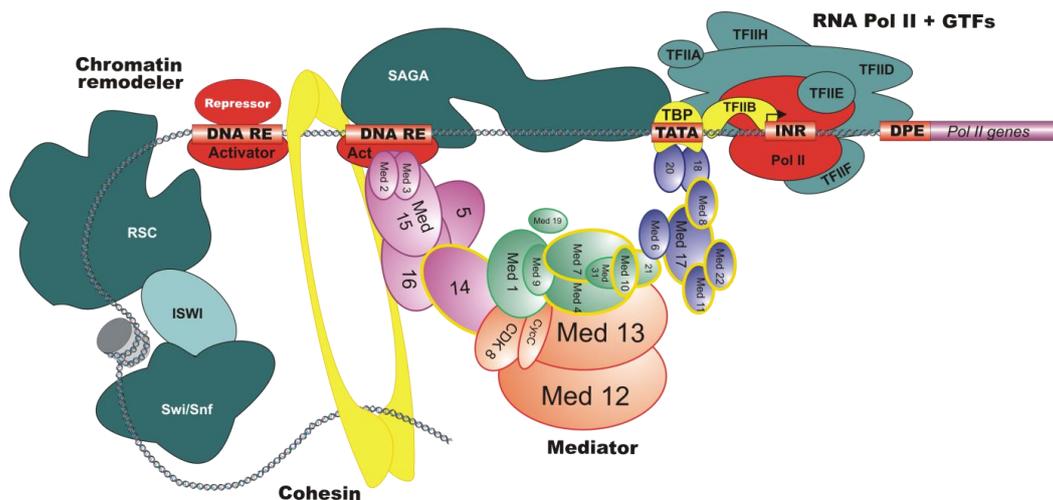
Figure 15: *Model for assembly of basal transcription machinery on the promoter*. In response to cellular signals, gene specific regulatory factors recognize DNA recognition elements (DNA RE). DNA bound transcription factors serve as nucleation point for recruitment of coactivators (RSC, ISWI, Swi/Snf, NuA4, Chd1, INO80, Swr1), which change the chromatin environment and facilitate PIC assembly on the promoter (TATA = TATA box; INR = Initator element; DPE = downstream promoter element; the transcription start site is represented by arrow). The Mediator and SAGA form an interface between gene specific activators/repressors and the Pol II transcription initiation machinery. The Mediator is involved in gene-looping by interaction with cohesins. The Mediator head module is colored in blue, the middle module in green, the tail module in magenta and kinase module in orange. Mediator subunits essential for yeast viability are outlined in yellow (own illustration, adapted from Martin Seizl & Tobias Koschubs, both Gene Center Munich).

1.1.3 Mediator function in regulation of Pol II transcription

Mediator connects the gene specific set of transcriptional activators to the Pol II initiation complex and forms an interface between gene-specific factors and the general transcription machinery (Cantin, et al. 2003; Malik & Roeder, 2010). Mediator is a target of cellular signaling pathways. The human Mediator subunit Med1 is targeted by thyroid hormone receptor (Ranchez, et al. 1999) and Med1 phosphorylation by the ERK kinase is involved in thyroid receptor pathway (Belakavadi, et al. 2008). Human Med23 is an endpoint of the insulin-signaling pathway, which induces MAP kinase-dependent activation of Elk1 (Wang, et al. 2005; Wang, et al. 2009). The yeast subunit Med15 is targeted by Oaf1, a transcription activator involved in sensing fatty acid levels (Thakur, et al. 2008). Subunit Med15 also interacts with Pdr1, a factor involved in multidrug resistance (Thakur, et al. 2008; Jedidi, et al. 2010).

Table 11: Mediator subunits

S. cerevisae	Module	alias	*S.c.*-Theoretical mass [kDa]	*H. sapiens*
Med1	Middle	Med1	64,251	Tap220 Arc/Drip200
Med2	Tail	Med2	47,717	
Med3	Tail	Pgd1, Hrs1, Med3	43,079	
Med4	Middle	Med4	32,205	Trap36 Arc/Drip36
Med5	Tail	Nut1	128,793	
Med6	Head	Med6	32,819	hMed6 Arc/Drip33
Med7	Middle	Med7	25,585	hMed7 Arc/Drip34 Arc32
Med8	Head	Med8	25,268	Arc32
Med9	Middle	Cse2, Med9	17,376	
Med10	Middle	Nut2, Med10	17,908	hNut2 hMed10
Med11	Head	Med11	15,168	
Med12	Kinase	Srb8	166,859	Trap230 Arc/Drip240
Med13	Kinase	Ssn2, Srb9	159,999	Trap240 Arc/Drip250
Med14	Middle/Tail	Rgr1	123,357	Trap170 Arc/Drip250 Arc105
Med15	Tail	Gal11, *RAR3, SDS4, SPT13, ABE1*	120,308	Trap95 Drip92
Med16	Tail	BEL2, GAL22, SDI3, SSF5, SSN4, TSF3, RYE1	111,296	Trap95 Drip92
Med17	Head	Srb4, Med17	78,475	Trap80 Arc/Drip77
Med18	Head	Srb5, Med18	34,288	P28b
Med19	Head/Middle	Rox3, Nut3, Ssn7	24,857	LCMR1
Med20	Middle	Srb2, Hrs2	22,894	hTrfp
Med21	Middle	Srb7	16,071	hSrb7
Med22	Head	Srb6	13,863	Surf5
Med31	Middle	Soh1	14,741	hSoh1
Cdk8	Kinase	Ssn3, GIG2, NUT7, SRB10, UME5, RYE5, CDK8	62,847	Cdk8 hSrb10
CycC	Kinase	Srb11, Ssn8, Ume3	37,790	CyC hSrb11 Med25 Arc92/Acid1 Med26 Arc70/Crsp70 Med28 Fksg20 Med30 Trap25

The yeast Mediator subunits Med2, Med4, and Med13 are phosphorylated, and these phosphorylation events play a role in transcription, Kin28-dependent processes, and the Ras/PKA pathway, respectively (Chang, et al. 2004; Guidi, et al. 2004; Hallberg, et al. 2004; Lui, et al. 2004.

In *S. cerevisiae*, the Mediator is generally required for Pol II transcription. Mediator promotes assembly of complexes required for transcription initiation on the promoter. The mechanism is most likely through physical interactions to Pol II, GTFs and transcription activators (Cantin, et al. 2003). Meditator recruitment to the promoter requires DNA bound activators and this is independent of Pol II recruitment (Cosma, et al. 2001). The Mediator and other factors built up the reinitiation scaffold, which remain on the promoter during transcription elongation to enable a rapid reinitiation of actively transcribed genes (Yudkovsky, et al. 2000). In higher eukaryotes, distant enhancers contribute to regulation of transcription by cooperative activation (Spitz & Furlong, 2012). To achieve cooperative activation, enhancers and activators must be positioned to enable physical interaction. This is achieved by gene looping and a recent study revealed a direct interaction between Mediator and cohesions, which brings distal enhancers in close proximity to the promoter (Kagey, et al. 2010)(Figure 15). The tail module has been identified to be involved in histone acetylation. ScMed5 show intrinsic histone acetyltransferase activity (HAT), which might be involved in preparation the nucleosome environment for transcription (Lorch, et al. 2000).

There is some evidence that Mediator have a negative effect on transcription. The kinase module is reversibly associated with the Mediator and the Cdk8 kinase is involved in phosphorylation of the CTD. It has been shown that the *S. pombe* kinase module sterically blocks interaction between Mediator and Pol II (Elmlund, et al. 2006). Mediator mutants led to increased transcriptional activity at selected genes (van de Peppel, et al. 2005). One mechanism might be through the Mediator interaction to the general corepressor Ssn6-Tup1 complex (Papmichos-Chronakis, et al. 2000).

1.1.4 Mediator and human diseases

The Mediator functions as integrator of cellular information and contributes to spatiotemporal control of Pol II transcription. As an endpoint of cellular signaling, the Mediator combines the determinative set of intrinsic and extrinsic signals to a defined output for the basal transcription machinery. Several studies in mice revealed that Mediator mutations are invariably lethal or lead to distinctive changes in organogenesis and altered gene expression programs similar to defects in essential developmental transcription factors (Spaeth, et al. 2011 and references within).

Mediator and cancer

As an endpoint of several signaling pathways, the Mediator is functionally linked to regulation of cellular growth, development and differentiation. Recent studies revealed associations between specific cancers and individual Mediator subunits. The human Med1 is linked to breast cancer, which is the leading cause of cell deaths among women (Jemal, et al. 2011). The steroid hormone estrogen (17-ß-estradiol; E2) has been shown to induce and promote breast cancer in the animal model (Russo, et al. 2006). Mediator is a functional coregulator for members of the nuclear receptor superfamiliy. It has been shown, that the breast cancer related subtype of estrogen receptor (ERα) interacts with Med1, which is the primarily receptor interface to the Mediator (Spaeth, et al. 2011). Med1 plays also a role in prostate cancer, which is the second

most frequently diagnosed cancer (Jemal, et al. 2011). Prostate cancer is driven by androgens through their interactions with the androgen receptor (AR). Androgen responsive genes are activated by a ligand-activated transcription factor that control prostate cancer cell growth and survival (Heinlein, et al. 2007; Lupien, et al. 2009). Med1 is critical for AR-dependent signaling and activation of AR response genes. It has been hypothesized that phosphorylation of Med1 by MAP kinase can be involved in the AR-dependent activation mechanism, as MAP kinases itself are constitutively activated in many prostate cancers (Beklavadi, et al. 2008; Pandey, et al. 2005). Other Mediator subunits have been indentified to be associated with cancers, as Med28 and breast cancer, Cdk8 and colon cancer and melanoma (Spaeth, et al. 2011 and references within).

Table 12: Molecular disposition of human Mediator subuints linked to pathological disorders (Spaeth, et al., 2011)

Disease/disorder	Mediator subunit
Neurodevelopmental disorders	
X-linked mental retardation syndromes FG syndrome Lujan syndrome	Med12 (Missense mutation) Med12 (Missense mutation)
Infantile cerebral and cerebellar atrophy	Med17 (Missense mutation)
Autosomal recessive axonal Charcot-Marie-Tooth disease	Med25(Missense mutation)
Cardiovascular disorders	
Transpostion of the great arteries (TGA)	Med13 (Haploinsufficiency, (Missense mutation)
22q11.2 deletion syndrome	Med15 (deletion)
Behavioral disorders	
Shizophrenia; psychosis	Med12 (Polymorphism)
Cancer	
Bladder	Med19 (overexpression)
Breast	Med1 (overexpression) Med19 (overexpression) Med28 (overexpression)
Colon	Med28 (overexpression) Cdk8 (overexpression) Med1 (reduced expression)
Lung	Med19 (overexpression)
Melanoma	Med1 (reduced expression) Med23 (chromosomal deletion) Cdk8 (overexpression)
Pancreas	Med29 (overexpression)
Prostate	Med1 (overexpression) Med28 (overexpression)

1.2 Aim and scope of this project

Mediator is a target of cellular signaling pathways, but it is poorly understood how it integrates regulatory signals, and how it transfers the output to the Pol II machinery. However, a functional influence of posttranslational modification of the Mediator has not been investigated systematically.

A paradigm for a conserved signaling pathway is the response of yeast cells to high salt concentrations. Osmotic stress activates the conserved mitogen-activated protein (MAP) kinase cascade, which leads to cell cycle arrest (Alexander, et al. 2001; Escote, et al. 2001), affects interaction between proteins and chromatin (Proft, et al. 2004), and induces transcription of stress-responsive genes (Causton, et al, 2001; Gasch, et al, 2002; Melamed, et al. 2008; Macia, et al. 2009). Osmotic stress response includes three phases (shock-, induction- and recovery phase)(Molin, et al. 2009; Romero-Santacreu, et al. 2009; Miller, et al. 2011). Transcription activity is initially reduced (shock phase), but stress-induced genes are heavily transcribed within 12-24 min (induction phase), and cells then fully adapt to growth in high-salt conditions (recovery phase). Response to osmotic stress goes along with significant changes in the phosphoproteome (Soufi, et al. 2008).

Due to recent technological and methodological advances, mass spectrometry (MS)-based proteomics has established itself as a powerful and versatile approach for global and quantitative investigation of many aspects of biology (Cox, et al. 2011). Stable isotope labeling of amino acids in culture (SILAC) (Ong, et al. 2002) is one of the most popular quantitative proteomics methods with a wide range of biological applications (Mann, 2006). Although mass spectrometry is well suited for the study of nearly all post-translational modifications (Witze, et al. 2007), it has proven particularly successful in characterizing phosphorylation dynamics (Macek, et al. 2009). Due to the availability of efficient techniques for phosphopeptide enrichment, tens of thousands of phosphorylation sites can be identified in a single experiment (Holt, et al. 2009; Huttlin, et al. 2010; Olsen, et al. 2010; Ringbolt, et al. 2011).

The aim of this study was to identify new Mediator phosphosites, observe phosphorylation dynamics in response to osmotic stress and characterize the impact of Mediator phosphosites to transcription. Here we used affinity purification and MS to show that yeast Mediator is phosphorylated at 17 of its 25 subunits *in vivo*. We then used SILAC to show that the phosphorylation level at some of the identified sites changes during the osmotic stress response. Finally we used mutagenesis and dynamic transcriptome analysis (DTA) to show that phosphorylated amino acid residues on the Mediator subunit Med15 are required for setting cellular mRNA synthesis rates during stress. These results demonstrate that Mediator is extensively modified post-translationally, and that Mediator phosphorylation contributes to transcription regulation during cellular stress response.

2. Results & Discussion

2.1 Systematic analysis of Mediator phosphorylation

2.1.1 Mediator is phosphorylated on many sites *in vivo*

To obtain endogenous Mediator, we generated a yeast strain carrying an N-terminal tandem affinity purification (TAP)-tagged version of Med17. Cells were grown in YPD medium to late-logarithmic phase, and Mediator was affinity-purified in the presence of phosphatase inhibitors (Puig, et al. 2001) (Figure 16A; MATERIALS & METHODS). This preparation was active in promoter-dependent transcription in vitro (data not shown). Pure Mediator was digested with trypsin to generate peptides that were subjected to a phosphoenrichment procedure (Larsen, et al. 2005). Phosphopeptides were analyzed by liquid chromatography-tandem mass-spectrometry (LC-MS/MS) on a high-resolution linear ion trap Orbitrap instrument (Figure 16B; MATERIALS & METHODS).

The phosphopeptides contained 125 unique phosphorylated sites that were heterogeneously distributed over 17 different Mediator subunits (Figure 16C). Phosphosites were concentrated in the Mediator middle (36%) and tail (48%) modules. Of the 125 phosphosites, 37 have previously been reported (Guidi, et al. 2004; Hallberg, et al. 2004; Gruhler, et al, 2005; Chi, et al. 2007; Li, et al. 2007; Smolka, et al. 2007; Albuquerque, et al. 2008; Soufi, et al. 2008), whereas 88 were novel (Table 14). Because phosphosite localization can be challenging when a peptide contains multiple serine, threonine, or tyrosine residues, we assigned each phosphosite to one of three localization classes. Phosphosites were categorized into p(STY)-class I, II, or III, if the localization probability value for the phospho group was above 0.75, between 0.25 and 0.75, or below 0.25, respectively (Olsen, et al. 2006; Macek, et al. 2009). Of the 125 phosphosites, 82, 38, and 5 were ascribed to class I, II and III, respectively (Figure 16D-E). These results reveal that Mediator is phosphorylated on many sites during exponential cell growth *in vivo* (Figure 17A-C; Table 14).

2.1.2 Mediator phosphorylation changes during stress

We next tested whether the phosphorylation status of Mediator changes in response to an external stimulus. We used SILAC to monitor the response of yeast cells to osmotic stress. Yeast cells auxotrophic for lysine were grown either in light or heavy ($^{13}C_6/^{15}N_2$) lysine containing SILAC medium to mid-logarithmic phase (MATERIALS & METHODS). Sodium chloride was added to a concentration of 0.5 M to the culture grown on heavy lysine, whereas the culture grown on light lysine was left untreated. Cells were harvested 20 min after salt addition, when expression of stress mRNAs is highly induced (Molin, et al. 2009; Miller, et al. 2011). Equal amounts of the cultures were combined and Mediator was isolated. Proteins were digested with endopeptidase Lys-C, to ensure that a majority of peptides contained at least one lysine (Ong, et al. 2003) (Figure 18A-B). The obtained peptides cover 53% of the amino-acid sequence of Mediator-core

proteins. Levels of 20 Mediator subunits were unchanged, providing an accurate basis for data normalization.

Phosphopeptides were enriched and analyzed by mass spectrometry (MATERIALS & METHODS). We detected peptides from 21 Mediator subunits. These peptides contained 29 unique phosphosites, which derived from subunits Med1, 2, 3, 4, 5, 6, 7, 14, 15, and 17. A replicate experiment revealed 23 additional sites, resulting in a total of 52 unique phosphosites (Figure 18C; Table 15). Of these, 15 sites in Med5 and Med15 showed significantly decreased phosphorylation with a ratio of heavy to light lysine-containing peptide intensities between 0.2 and 0.6, whereas one site in Med14 showed significantly increased phosphorylation (Table 13). All of these dynamically phosphorylated sites were located in predicted loops of the Mediator tail module, which interacts with transcription regulators (Park, et al. 2000; Jedidi, et al. 2010).
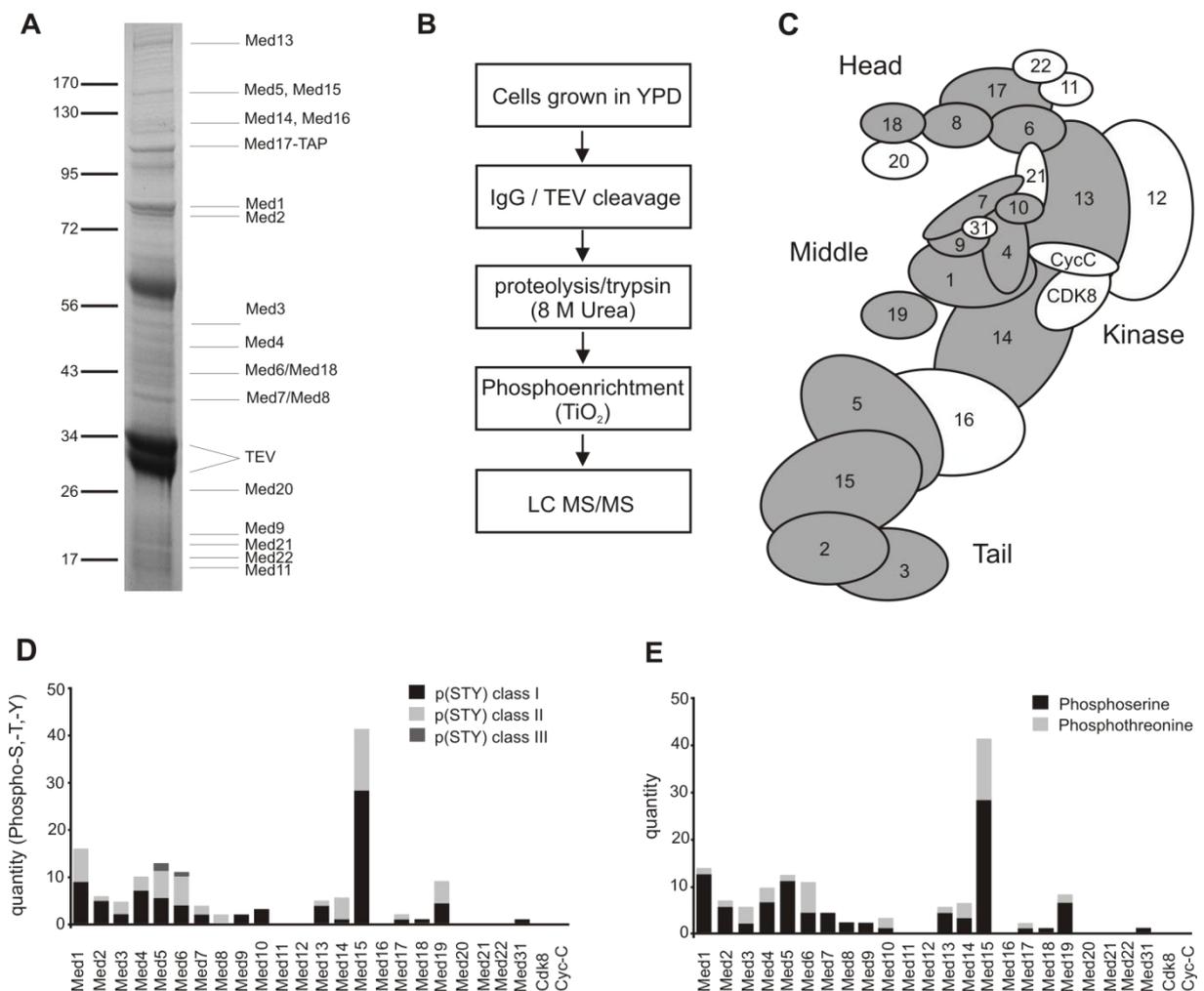
Figure 16: *Mediator is highly phosphorylated in vivo.* **(A)** SDS-PAGE analysis of endogenous Mediator proteins that were co-purified with TAP-Med17 from wild-type *S. cerevisiae*. Protein bands were stained with Coomassie blue and identified by mass spectrometry (TEV, TEV protease bands). **(B)** Diagram illustrating the workflow for analysis of Mediator phosphosites by high-performance LQ MS/MS. **(C)** Schematic view of Mediator with Med subunits labeled with numbers and highlighted in grey if they were found to be phosphorylated under normal growth conditions. The four modules of Mediator are also indicated. **(D)** Bar chart showing the number of phosphosites classified into p(STY) classes A (black), B (light grey), and C (dark grey). **(E)** Bar chart showing the number of phosphorylated serine (black), threonine (light grey), and tyrosine (dark grey) residues in Mediator proteins.

Figure 17: *Distribution of phosphorylation sites in Mediator subunits.* **(A-C)** Schematic illustration of phosphosite positions on the primary structure of Mediator subunits belonging to the head **(A)**, middle **(B)**, and tail **(C)** modules. Phosphosites classified in p(STY)-class I (high localization probability) are highlighted in black and p(STY)-class II (medium localization probability) in white, respectively.

Figure 18: *Mediator phosphorylation changes during osmotic stress.* **(A)** Schematic diagram of SILAC experiment workflow. **(B)** SDS-PAGE analysis of endogenous yeast Mediator preparation (SILAC) that was used as input for mass spectrometry analysis. Copurified proteins were stained with Coomassie blue (TEV, TEV protease bands). **(C)** Schematic view of Mediator with subunits that were detected to be phosphorylated under osmotic stress conditions. Subunits with unaltered phosphorylated sites are in grey, subunits with phosphorylated sites that show altered levels of phosphorylation are in black.

Table 13: Mediator sites that change phosphorylation level during salt stress

Subunit	Amino acid	Position	Sequence window	pSTY-class	Localization p-value	PTM Score	Ratio H/L normalized by proteins
Med5	S	257	TNEFVGSPSLTSP	II	0,504487	35,82	0,60258
Med5	S	259	EFVGSPSLTSPQY	II	0,349267	35,82	0,60258
Med5	T	261	VGSPSLTSPQYIP	II	0,351505	35,82	0,60258
Med5	S	262	GSPSLTSPQYIPS	II	0,728166	35,82	0,60258
Med5	S	268	SPQYIPSPLSSTK	III	0,188482	35,82	0,60258
Med5	S	271	YIPSPLSSTKPPG	III	0,190959	35,82	0,60258
Med5	S	272	IPSPLSSTKPPGS	II	0,306	35,82	0,60258
Med5	T	273	PSPLSSTKPPGSV	II	0,306287	35,82	0,60258
Med14	T	1036	DTKRLGTPESVKP	I	0,999212	40,65	1,4734
Med15	S	746	TPKVPVSAAATPS	I	1	139,73	0,59134
Med15	T	750	PVSAAATPSLNKT	I	0,75299	139,73	0,59134
Med15	S	796	QQPTPRSASNTAK	II	0,431756	62,19	0,28888
Med15	S	798	PTPRSASNTAKST	II	0,431756	62,19	0,28888
Med15	T	769	GRTKSNTIPVTSI	I	0,999999	121,83	0,23904
Med15	S	767	VNGRTKSNTIPVT	I	1	121,83	0,23904
Med15	T	800	PRSASNTAKSTPN	II	0,328631	62,18	0,28888

2.2 Mediator phosphorylation is involved in Stress response Transcription

2.2.1 Med15 phosphosites contribute to suppression of stress-induced changes in gene expression under non-stress conditions.

The above analysis identified 30 phosphorylated sites that cluster in the Med15 C-terminal region (Figure 17C). Seven of these sites are dynamically changed in response to osmotic stress. To test whether the phosphorylated sites are functionally involved in the regulation of transcription, we created two mutant strains that carry point mutations on selected sites (Figure 20A; Tables 16-17). The first mutant, referred to as *D7P*, carries alanine mutations on the seven dynamically phosphorylated sites, whereas in the second mutant, *D30P*, all 30 phosphorylated sites clustering near the C-terminus of Med15 were mutated to alanine (Figure 20A). Mutation of phosphorylated serine and threonine residues to alanine is functionally similar to the dephosphorylated state (Thorsness, et al. 1987). The clustering of 30 phosphosites in the Med15 C-terminus suggested that combinatorial phosphorylation on multiple sites affect biological outcome (Thomson, et al. 2009; Barik, et al. 2010), as was shown for cell cycle control (Kovomägi, et al. 2011) and for transcription regulation (Holmberg, et al. 2002).

We performed dynamic transcriptome analysis (DTA) for *D30P* mutant and wild-type cells under normal conditions. DTA uses metabolic RNA labeling to globally monitor mRNA synthesis and decay rates with high sensitivity (Miller, et al. 2011). We carried out metabolic RNA labeling by addition of 4-thiouridine for 6 min, extracted RNA, separated labeled RNA from pre-existing RNA and analyzed the labeled RNA to generate expression profiles on Affymetrix microarrays (Miller, et al. 2011). We performed comparative DTA (cDTA) under identical experimental conditions for the *D7P* mutant, a strain lacking subunit Med15 (*Δmed15*) and the wild-type strain under normal conditions. cDTA allows for direct comparison of synthesis and decay rates in different yeast strains (Sun, et al. 2012).

Mutation of the seven dynamically phosphorylated sites in the *D7P* strain significantly altered the expression of 64 genes. We found 53 genes induced, suggesting a mild negative effect of the dynamic phosphosites on transcription. We searched for significantly enriched GO terms, which are ranked by Fisher's exact test. Among the subset of 53 induced genes, we identified a significant enrichment of genes involved in response to temperature stimulus, autophagy, and carbohydrate metabolism. We found stress markers induced by mutation of dynamically phosphorylated sites under physiological conditions. For example, we detected Hsp12, a responder to heat shock, oxidative and osmotic stress (Welker, et al. 2010; Morano, et al. 2012), Ddr2, which is induced under environmental stress conditions (Kobayashi, et al. 2012; Treger, et al. 1998; Hirata, et al. 2003), and the glycogen synthases Gsy1 and Gsy2, which are also induced under several environmental stress conditions (Unnikrishnan, et al. 2003; Enjalbert, et al. 2004; Zähringer, et al. 2000). These observations indicate that the dynamic phosphosites contribute to the repression of genes involved in response to stress conditions under non-stress conditions (Figure 20B).

The expression profile of the strain carrying thirty mutated phosphosites in the Med15 C-terminal region (*D30P*) showed significantly altered transcription for 326 genes under normal growth conditions. The loss of function caused by the *D30P* mutation led to the induction of 240 genes, indicating that native phosphorylation of these sites has a negative effect on transcription. In comparison to the genes induced by the mutated dynamic phosphosites (*D7P*), the stable phosphosites act on additional pathways. A GO term analysis revealed the induction of genes

involved in response to stimulus, vacuolar protein catabolic process, autophagy and oxidation and reduction (Table 22). These GO terms reflect the cellular adaption to environmental changes (Rubinsztein, et al. 2011; Singh, et al. 2011; Murray, et al. 2011). Taken together, the overall transcriptome changes observed in the *D30P* mutant strain are similar to those observed in the *D7P* strain, albeit more pronounced.

We next compared the *D7P* and *D30P* profiles to the *Δmed15* profile under normal growth conditions. Med15 deletion altered the expression of 1743 genes. The transcriptome changes observed in the *Δmed15* mutant strain resemble those observed during a salt stress response, although it was less pronounced (Figure 20C). We analyzed this subset of genes for enriched regulatory factors and ranked the factors by Fisher`s exact test. Among the induced genes, targets of Sok2 and Rap1 were significantly enriched. We also found a general dependence on the general coactivator SAGA and transcription factor Msn2 (Figure 19).

We next tested whether the observed *D7P*- and *D30P*-dependent induction of genes contributes to the cellular response to osmotic stress. We focused on the expression profile of the wild type within the stress induction phase (18-24 min after addition of salt). The GO terms associated with carbohydrate metabolism and response to stimulus were enriched in the wild-type profile under osmotic stress conditions, but also in the mutants *D7P*, *D30P* and *Δmed15* under non-stress conditions (Figure 20D). We calculated the induction level of each GO term by the percentage of genes induced by *D7P* relative to the whole set of genes in the corresponding GO term. We found the highest induction by *D7P* mutations for the GO term response to temperature stimulus (15%) and for hexose transport (20%) (Figure 20D). Taken together, both dynamically and stably phosphorylated sites in Med15 contribute to the repression of genes involved in the response to environmental changes under non-stress conditions.
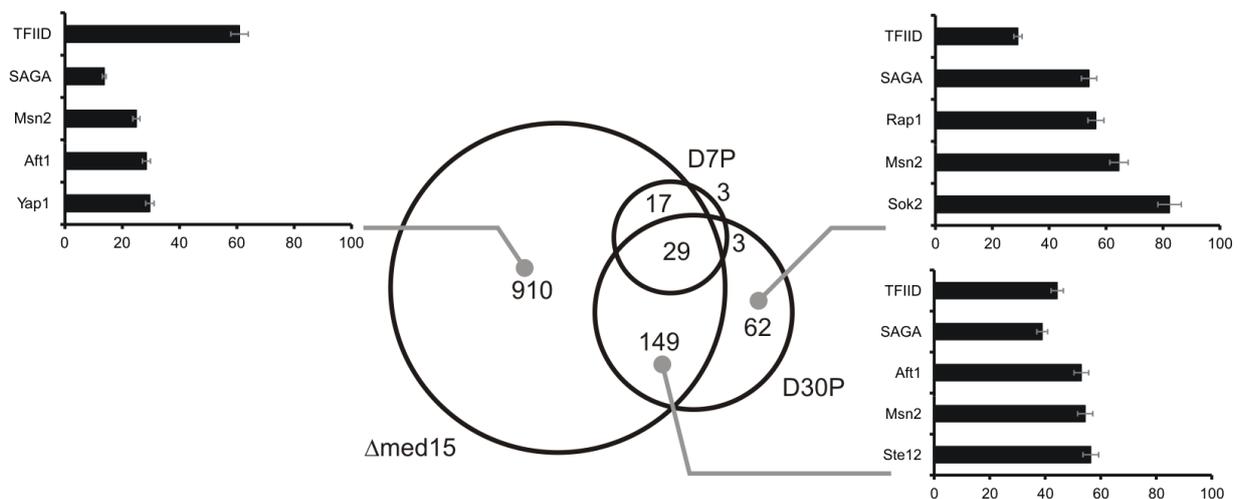
Figure 19: *The D30P phosphosites act on different genes as Δmed15.* Venn diagram of the induced datasets of *D7P*, *D30P* and *Δmed15* under normal growth conditions. The mutation of the 30 phosphosites induces expression of 62 genes, which are not induced in the Med15 knock-out. Bar plots represent the relative enrichment (fisher's exact test) of transcription factor targets from a total set of 110 transcription factors (Abdulrehman, et al. 2011; Teixeira, et al, 2005) and TFIID, SAGA (Huisigna, et al, 2004). The length of the bars represent the percentage of genes in the subset regulated by the respective factor.

2.2.2 Med15 contributes to activation of genes involved in ribosome biogenesis during non-stress conditions

The *Δmed15* mutation caused a selective repression of a subset of genes, which are involved in ribosomal biogenesis. The highest ranked GO terms are ribosome biogenesis, ribonucleoprotein complex biogenesis, RNA metabolic process, gene expression, ribosomal large subunit biogenesis and RNA modification (Tables 18-19). We performed MGSA analysis (Bauer, et al. 2011) to identify a selective enrichment of transcription factor targets. Among the subset of repressed genes we found a significant enrichment of genes regulated by Leu3 and Fhl1 (data not shown). Leu3 regulates expression of genes that are involved in branched amino acid synthesis and it is functionally related to Gcn4 (Hinnebusch, et al. 2002). Fhl1 regulates transcription of ribosomal protein genes and is regulated under different growth and stress conditions (Martin, et al. 2004). Fhl1 function links gene expression of ribosomal protein genes to the TOR pathway (Martin, et al. 2004). We next compared the subset of repressed genes of the *Δmed15* dataset to the dataset of response of wild-type cells to osmotic stress. The down-regulation of ribosome biogenesis genes in the *Δmed15* mutant under normal conditions is to a large extent similar to the repression under osmotic stress conditions in wild type cells (Figure 20D). These observations indicate a functional role of Med15 in the expression of ribosome biogenesis genes and thus cell growth that is suppressed during salt stress (Figure 20B and 20D).

2.2.3 Mutated dynamic phosphosites do not alter osmotic stress-induced gene expression

Recent work revealed that Med15 interacts with the general stress regulatory factors Msn2/Msn4 (Lallet, et al. 2006; Sadeh, et al. 2012) and that mutations of Med15 had a strong effect on TATA-containing and SAGA-regulated genes (Ansari, et al. 2012). Based on these findings, we searched the cDTA datasets for *D7P*, *D30P*, *Δmed15*, and the wild type data set at 0.8 M NaCl (induction phase 18-24 min) for enrichment of TATA-containing promoters (Seizl, et al. 2011) and Msn2/4 and Hog1 targets. Consistent with previous findings, we found general enrichment of TATA-containing genes in both, induced and repressed genes (p-value: 6.25E-11). Furthermore we observed a predominance of Msn2/Msn4 regulated genes within the subset of induced genes (p-value: 6.32E-42) (Figure 21). Because the *Δmed15* strain exhibits a slow-growth phenotype sensitive to temperature changes and osmotic stress (MATERIALS & METHODS) we tested the *D7P* and *D30P* mutant strains for sensitivity to temperature and salt stress (data not shown). Whereas the *D7P* mutant strain exhibited no significant growth phenotype, the *D30P* mutant exhibits a weak slow-growth phenotype under temperature and salt stress conditions (data not shown). We performed a liquid growth assay to determine the doubling times under stress conditions (YPD; 0.8 M NaCl). Relative to wild type and *D7P* cells (145 min), the doubling time slightly increased from *D30P* (193 min) to *Δmed15* (205 min). To investigate whether this phenotype is a result of impaired transcription regulation, we performed DTA (for *D30P* & wild type) and comparative DTA (for *D7P*, *Δmed15* & wild type) under osmotic stress conditions. Cells were grown to mid-log phase and divided into control and stress samples. For the control samples, we carried out metabolic RNA labeling as described (Miller, et al. 2011; Sun, et al. 2012). For the stress samples, we induced osmotic stress by addition of sodium chloride to a final concentration of 0.8 M, added 4-thiouridine (DTA) after 18 min and extracted RNA after 6 min of labeling (MATERIALS & METHODS). The time frame 18-24 min is consistent with the previous observation of the induction phase, when cells activate the gene expression program to antagonize osmotic pressure (Miller, et al. 2011; Molin, et al. 2009) (MATERIALS & METHODS).
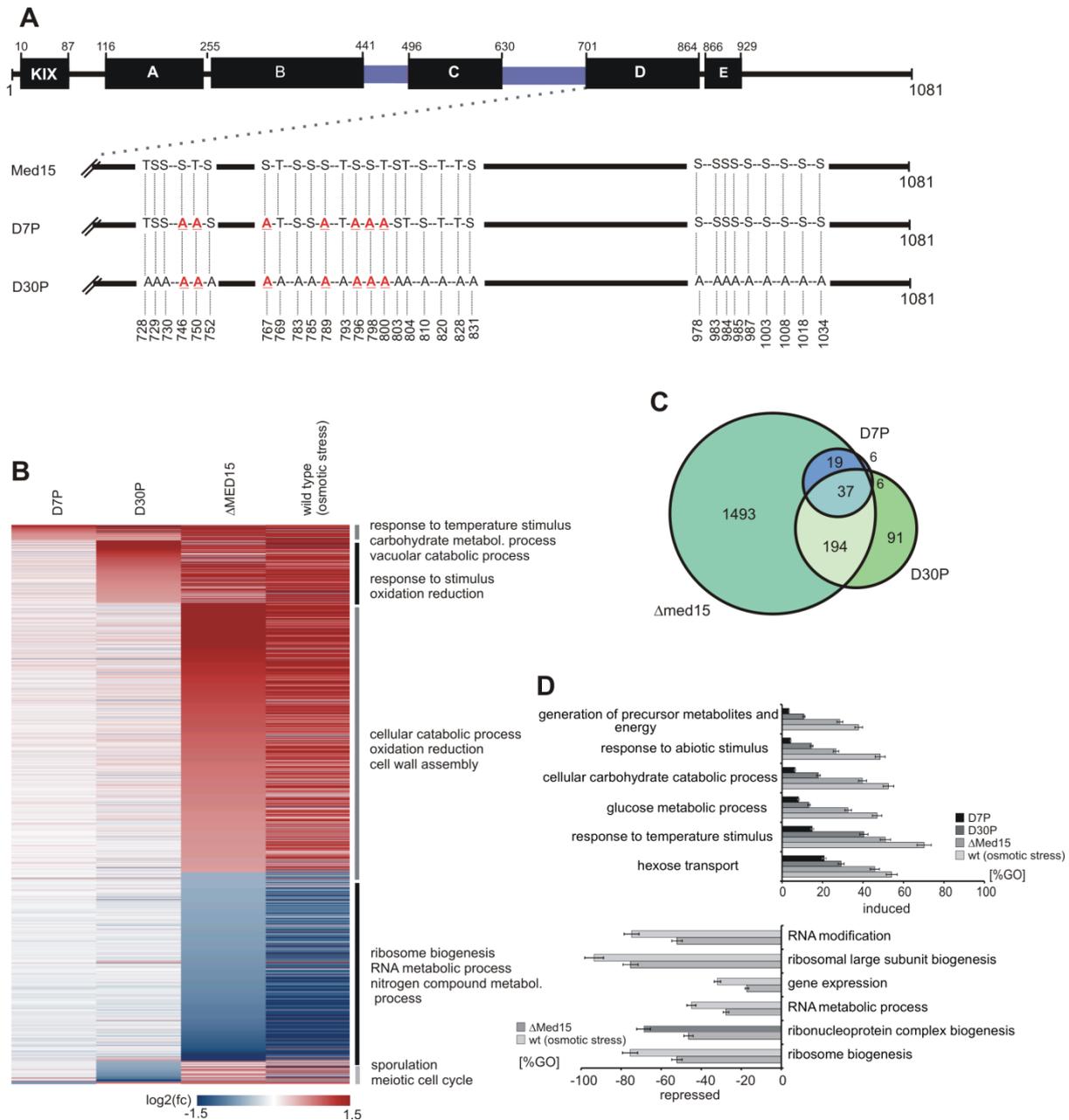
Figure 20: *Effect of mutated phosphosites on global gene expression under normal growth conditions*. **A)** Functional organization of *S.cerevisiae* Med15. Med15 is organized in several regions as described previously (KIX-domain; A-E; black bars, which interact with different transcription factors (Jedidi, et al. 2010; Herbig, et al. 2010), Msn2 (Lallet, et al. 2006), Gal4 (Jeong, et al. 2001), Gcn4 (Herbig, et al. 2010; Brzovic, et al. 2011), Pdr1 (Thakur, et al. 2009; Thakur, et al. 2008), Oaf1(Thakur, et al. 2009)). Q-rich regions are colored in blue. Mutant sequence features are shown below. The *D7P* mutant harbors genomic point mutations of the seven serine and threonine positions to alanine, which are dynamically phosphorylated during response to high salt concentrations. The *D30P* mutant harbors the complete set of all 30 phosphosites (identified during this study), which mimic the dephosphorylated state of the Med15 C-terminus. **B)** Heatmap illustrating the effect of the mutated phosphosites on global gene expression (labeled mRNA fraction, 6 min labeling time). The genes are arranged by the highest induction or repression fold changes in order of *D7P*, *D30P* and *Δmed15*. The horizontal lines represent genes, which are differentially expressed at least 1.5-fold in at least one of the data sets. Red color indicates genes, which are induced compared to the wild type control. Blue color indicates repressed genes. Genes were ranked by highest/lowest fold-change in order of *D7P*, *D30P* and *Δmed15*. **C)** Venn diagram illustrating the overlap between the data sets of *D7P, D30P* and *Δmed15*. **D)** Diagram representing enriched GOterms ranked by Fisher`s exact test. (upper diagram): The bars represent the percentage of genes induced in the *D7P* (black), *D30P* (dark gray) and *Δmed15* (middle gray) strains relative to all genes in the GO term. (lower diagram): The bars represent the percentage of genes repressed in the *D7P* (black)-, *D30P* (dark-grey)- and *Δmed15* (fair-grey) mutant relative to all genes in the GO term.

Upon stress, levels of 3516 newly transcribed (labeled) mRNAs exhibit at least a 1.5-fold change in at least one of the data sets. We compared the labeled RNA fraction of *D7P*, *D30P*, *Δmed15* and wild type responding to 0.8 M sodium chloride within the Time frame of 18-24 min after salt addition. The response to osmotic stress changed about 50% of newly synthesized RNAs (Figure 21A).

To identify gene expression changes during the stress response caused by the mutated phosphosites, we calculated a linear model. We used all data sets as dependent variables and regressors according to their condition in a linear regression analysis. We found that mutations *D7P*, *D30P* and *Δmed15* do not have any additional effect on salt stress-induced expression changes (Figure 21B). We conclude that Med15 phosphosites are involved in repression of genes under non-stress conditions, but do not have additional, specific effects on gene expression under osmotic stress conditions.
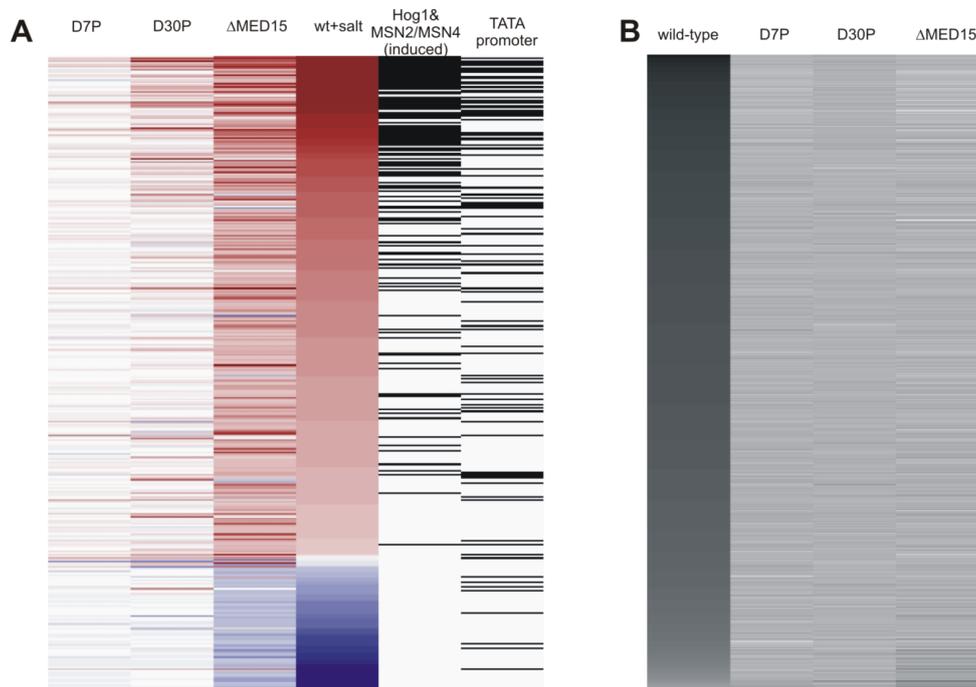
Figure 21: *Linear regression analysis: Effect of Med15 phosphosite mutants on osmotic stress response.* **A)** Global changes in labeled mRNA expression under normal conditions and response to osmotic stress. Heatmap illustrating the effect of the mutated phosphosites on global gene expression (labeled mRNA fraction, 6 min labeling time). The horizontal lines represent genes, which are differentially expressed at least 1.5 fold in at least one of the datasets. Red color indicates genes, which are relative induced compared to the wild-type control. Blue color indicates relative repressed genes. Black bars mark the genes, which are regulated by Msn2/4 (p-value: 6.32E-42) (second right column) or TATA containing promoter genes (p-value: 6.25E-11) (Melamed, et al. 2008) (right column). **B)** linear regression analysis to decipher the influences of the mutation (*D7P & D30P*) and *Δmed15* strains under non-stress and salt stress conditions.

3. Conclusion & Outlook

Mediator functions by receiving signals from different pathways to generate an output for the general transcription machinery (Malik & Roeder, 2010). However, a functional influence of posttranslational modification of the Mediator has not been investigated systematically. By combining high-resolution MS, quantitative proteomics (SILAC), and dynamic transcriptome analysis, we demonstrate here an extensive phosphorylation of Mediator and a contribution of Mediator phosphorylation to gene regulation.

Earlier work had shown that Mediator is phosphorylated on subunits Med2, Med4, Med13 and Med14 and that Med2 phosphorylation can influence Mediator function (Chang, et al.l, 2004; Guidi, et al. 2004; Hallberg, et al. 2004; Liu, et al. 2004). Previous proteomic analysis additionally revealed that subunits Med1, Med5, Med6, Med15 and Med17 are phosphorylated (Gruhler, et al. 2005; Chi, et al. 2007; Li, et al. 2007; Smolka, et al. 2007; Albuquerque, et al. 2008, Soufi, 2008). Here we used affinity purification and high-resolution MS to map 125 sites on 17 Mediator subunits that are phosphorylated *in vivo* under normal growth conditions. Of these, 88 were novel, whereas 37 were previously reported (Chang, et al. 2004; Guidi, et al. 2004; Hallberg, et al. 2004; Liu, et al. 2004, Gruhler, et al. 2005; van de Peppel, et al. 2005; Chi, et al. 2007, Li, et al. 2007; Smolka, et al. 2007; Albuquerque, et al. 2008; Soufi, et al. 2008; Jain, et al. 2009; Consortium, 2010) and confirmed here. The majority of these phosphosites is located in the middle and tail modules. Quantitative proteomics using SILAC revealed that a subset of these sites has different levels of phosphorylation during the osmotic stress response. Phosphorylation levels generally decrease during osmotic stress, consistent with previous observations (Soufi, et al. 2009). In particular, we identified 30 phosphorylated sites near the Med15 C-terminus, of which seven changed phosphorylation levels during stress

The number of clustered phosphosites in Med15 suggests an important role of this tail module subunit for the transcriptional response to stress. Consistent with this view, Med15 binds to transcription factors Gcn4, Pdr1, Oaf1, Hsf1, and Ace1 (Thakur, et al. 2008; Herbig, et al. 2010; Jedidi, et al. 2010), and a *med15* knockout strain (Δ*med15*) exhibits a growth defect under hyperosmotic stress conditions (Fan, et al. 2006; Zapater, et al. 2007).

To investigate whether these phosphosites contribute to Mediator function in gene regulation, we mutated a phosphorylation sites in Med15, and used DTA to investigate their contribution to gene regulation during the osmotic stress response. This revealed that the 30 clustered phosphosites in Med15 are involved in suppression of stress-induced alteration of transcription from genes responding to environmental changes. The seven dynamically phosphorylated sites were required for the repression of genes involved in temperature stimulus, autophagy and carbohydrate metabolism under normal growth conditions. Under osmotic stress conditions, however, we found no significant contribution of the Med15 phosphosites to gene expression.

Taken together, our results show that Mediator is phosphorylated at multiple sites in vivo, that the level of phosphorylation can change during stress, and that a phosphorylated subunit region can contribute to transcription regulation by repressing stress genes under normal growth conditions. One possible explanation for our observations is that Med15 phosphorylation suppresses the association of Mediator with various activators that stimulate the expression of stress-induced genes. Consistent with this model, Med15 binds to transcription factors Msn2, Gcn4, Pdr1, Oaf1, Hsf1, and Ace1 (Thakur, et al. 2009; Jedidi, et al. 2010; Lallet, et al. 2006; Herbig, et al. 2010). Alternatively, transcriptional repressors that normally repress stress gene transcription would require specific Mediator phosphorylations for their function.

The combination of SILAC and mass spectrometry, to identify post-translational modification and the systematic investigation of combinations fo multiple phosphorylation by synthetic genes and DTA might be an experimental strategy even for other regulatory modifications. Sumolyation, Acetylation or ubiquitination are involved in tunig specific protein functions in regulation of gene expression.

Further effort is needed to answer future questions of how information is transmitted from sigalling pathways, the Mediator and the Pol II transcription machinery to regulate genetic information. As shown, Mediator phosphorylation is involved in regulation of stress response genes in yeast. In human, recent studies have shown that phosphorylation of Med1 is associated with prostate cancer in a hormone induced nuclear receptor dependent mechanism. Additional to cancer, Mediator dysfunction leads to cardiovascular diseases, metabolic disorders and mental retardation. Further studies on mechanisms that regulate Mediator function could reveal detailed mechanisms that underly these deseases.

4. Tables

4.1 Mediator phosphosites

Table 14: Phosphopeptides from endogenous Mediator identified by mass spectrometry

Mediator subunit	Phosphorylated amino acid	Relative position	Phospho-peptide sequence	Number of phospho (STY)	pSTY-class	Localization p-value	PTM Score	Literature (Jain 2009; Consortium 2010)
Med1	148	S	S(1)LDSSNASFNNQGK	1	I	0,999997	256,36	
Med1	151	S	S(0.002)LDS(0.869)S(0.129)NAS(0.001)FNNQGK	1	I	0,868889	256,36	
Med1	152	S	S(0.001)LDS(0.018)S(0.981)NAS(1)FNNQGK	2	I	0,980961	278,37	
Med1	155	S	SLDSSNAS(1)FNNQGK	1	I	0,999764	256,36	Albuquerque, 2008
Med1	363	S	LVS(0.069)T(0.069)PS(0.315)S(0.315)NS(0.315)NS(0.458)S(0.458)ELEPDYQAPFSTSTK	2	I I	0,315399	154,07	
Med1	364	S	LVS(0.069)T(0.069)PS(0.315)S(0.315)NS(0.315)NS(0.458)S(0.458)ELEPDYQAPFSTSTK	2	I I	0,315399	154,07	
Med1	366	S	LVS(0.001)T(0.003)PS(0.02)S(0.142)NS(0.793)NS(0.02)S(0.02)ELEPDYQAPFSTSTK	1	I	0,793442	225,11	
Med1	368	S	LVS(0.069)T(0.069)PS(0.315)S(0.315)NS(0.315)NS(0.458)S(0.458)ELEPDYQAPFSTSTK	2	I I	0,458234	154,07	
Med1	369	S	LVS(0.021)T(0.07)PS(0.281)S(0.281)NS(0.309)NS(0.313)S(0.717)ELEPDY(0.005)QAPFSTSTK	2	I I	0,717215	154,07	
Med1	389	S	NS(0.077)S(0.855)T(0.059)S(0.008)NTEPIPR	1	I	0,855457	139,39	
Med1	391	S	NS(0.025)S(0.116)T(0.096)S(0.382)NT(0.382)EPIPR	1	I I	0,381914	139,39	
Med1	393	T	NS(0.025)S(0.116)T(0.096)S(0.382)NT(0.382)EPIPR	1	I I	0,381914	139,39	
Med1	404	S	HGS(1)VVEASR	1	I	1	149,55	Albuquerque, 2008 Smolka, 2007
Med1	419	S	S(1)KRPS(0.999)IT(0.001)EAMMLK	2	I	1	238,08	
Med1	423	S	RPS(0.998)IT(0.002)EAMMLK	1	I	0,998231	212,14	Li, 2007 Soufi, 2009
Med2	6	S	VVQNS(0.989)PVS(0.002)S(0.009)VHTANFSER	1	I	0,989191	298,44	Albuquerque, 2008
Med2	9	S	VVQNS(0.206)PVS(0.703)S(0.26)VHT(0.831)ANFS(0.001)ER	2	I I	0,702841	243,05	

Med2	10	S	VVQNS(0.985)PVS(0.154)S(0.859)VHT(0.002)ANFSER	2	I	0,858722	243,05	
Med2	13	T	VVQNS(0.206)PVS(0.703)S(0.26)VHT(0.831)ANFS(0.001)ER	2	I	0,830722	243,05	
Med2	208	S	ENYQELGSLQSSSQTQLENANAANNGAAFS(0.999)PLT(0.001)TTR	1	I	0,999232	235,08	Van de Peppel, 2005 Hallberg, 2004
Med2	266	S	GFDDNDS(0.995)GNNY(0.005)NDINISSIENNINNNINSTK	1	I	0,995136	346,28	

Med3	189	S	S(0.796)GS(0.193)T(0.011)MGTPTVHNSTAAAPIAAPK	1	I	0,795633	246,24	
Med3	191	S	S(0.09)GS(0.807)T(0.104)MGTPTVHNSTAAAPIAAPK	1	I	0,806632	246,24	
Med3	192	T	S(0.145)GS(0.799)T(0.526)MGT(0.526)PT(0.004)VHNSTAAAPIAAPK	2	II	0,525873	174,85	
Med3	195	T	S(0.02)GS(0.024)T(0.024)MGT(0.925)PT(0.007)VHNSTAAAPIAAPK	1	I	0,924891	246,24	
Med3	197	T	S(0.145)GS(0.173)T(0.035)MGT(0.035)PT(0.611)VHNSTAAAPIAAPK	1	II	0,611461	246,24	

Med4	18	S	S(0.73)S(0.131)S(0.131)VS(0.007)LVAEATSNTNSEDK	1	II	0,729971	269,14	
Med4	19	S	S(0.094)S(0.764)S(0.118)VS(0.024)LVAEATSNTNSEDK	1	I	0,764367	269,14	
Med4	20	S	S(0.597)S(0.597)S(0.597)VS(0.189)LVAEAT(0.01)S(0.003)NT(0.003)NS(0.003)EDK	2	II	0,596842	234,73	
Med4	22	S	S(0.334)S(0.334)S(0.333)VS(0.998)LVAEATSNTNSEDK	2	I	0,99797	234,73	
Med4	222	S	IPGEEVEETEVPTVPPS(0.5)QS(0.5)EEQK	1	II	0,499999	161,68	Albuquerque, 2008
Med4	224	S	IPGEEVEETEVPTVPPS(0.163)QS(0.837)EEQK	1	I	0,837069	161,68	
Med4	237	T	EGT(1)PKTDSFIFDGTAK	1	I	0,99957	246,71	Albuquerque, 2008 Guidi, 2004 Li, 2007 Chi, 2007 Smolka, 2007 Hallberg, 2004 Soufi, 2009
Med4	240	T	KEGT(0.004)PKT(0.969)DS(0.026)FIFDGT(0.001)AK	1	I	0,968929	246,71	
Med4	242	S	T(0.019)DS(0.981)FIFDGTAK	1	I	0,980673	246,71	Albuquerque, 2008 Chi, 2007 Smolka, 2007 Soufi, 2009
Med4	248	T	KEGT(0.001)PKTDSFIFDGT(0.999)AK	1	I	0,998687	246,71	

Med5	64	T	ASDLVDT(0.978)PS(0.021)NNTAATADTTHLHEALDIVCSDFVK	1	I	0,978365	275,96	Albuquerque, 2008
Med5	66	S	KAS(0.001)DLVDT(0.499)PS(0.499)NNT(0.001)AATADTTHLHEALDIVCSDFVK	1	II	0,498934	275,96	
Med5	257	S	DS(0.031)T(0.031)NEFVGS(0.773)PS(0.092)LT(0.031)S(0.031)PQY(0.01)IPSPLSSTKPPGSVNSAAK	1	I	0,772976	253,18	
Med5	259	S	DS(0.024)T(0.024)NEFVGS(0.183)PS(0.587)LT(0.069)S(0.069)PQY(0.024)IPS(0.005)PLS(0.004)S(0.005)T(0.005)KPPGS(0.001)VNS(0.001)AAK	1	II	0,586881	253,18	
Med5	262	S	DS(0.001)T(0.001)NEFVGS(0.977)PS(0.147)LT(0.147)S(0.725)PQY(0.002)IPSPLSSTKPPGSVNSAAK	2	I	0,724792	215,35	Albuquerque, 2008

Med5	268	S	DSTNEFVGSPSLTSPQY(0.001)IPS(0.967)PLS(0.012)S(0.01)T(0.01)KPPGSVNSAAK	1	I	0,966826	253,18	Albuquerque, 2008
Med5	271	S	DSTNEFVGS(0.952)PS(0.051)LT(0.147)S(0.147)PQY(0.146)IPS(0.573)PLS(0.662)S(0.16)T(0.16)KPPGS(0.001)VNSAAK	3	II	0,662499	195,1	
Med5	278	S	DS(0.033)T(0.033)NEFVGS(0.429)PS(0.429)LT(0.036)S(0.034)PQY(0.018)IPS(0.071)PLS(0.179)S(0.179)T(0.18)KPPGS(0.186)VNS(0.192)AAK	2	III	0,185502	215,35	
Med5	281	S	DS(0.033)T(0.033)NEFVGS(0.429)PS(0.429)LT(0.036)S(0.034)PQY(0.018)IPS(0.071)PLS(0.179)S(0.179)T(0.18)KPPGS(0.186)VNS(0.192)AAK	2	III	0,191816	215,35	
Med5	682	S	YYLEESNVNDS(0.996)DMLT(0.004)K	1	I	0,995628	286,16	
Med5	838	S	VQSQS(0.002)NY(0.002)GIY(0.044)S(0.476)S(0.476)DAQGDPNLEPLIAK	1	II	0,476154	256,79	
Med5	839	S	VQSQS(0.002)NY(0.002)GIY(0.044)S(0.476)S(0.476)DAQGDPNLEPLIAK	1	II	0,476154	256,79	
Med5	1014	S	NDS(1)AEVRQETQPK	1	I	1	154,46	

Med6	225	S	VPTDTSTTATAATNGNNAGGGS(1)NK	1	I	1	341,32	
Med6	228	S	S(0.181)S(0.181)VRPT(0.181)GGANMAT(0.184)VPS(0.187)T(0.187)T(0.187)NVNMT(0.23)VNT(0.228)MGT(0.242)GGQT(0.011)IDNGT(0.002)GR	2	III	0,181253	209,5	
Med6	229	S	S(0.181)S(0.181)VRPT(0.181)GGANMAT(0.184)VPS(0.187)T(0.187)T(0.187)NVNMT(0.23)VNT(0.228)MGT(0.242)GGQT(0.011)IDNGT(0.002)GR	2	III	0,181253	209,5	
Med6	233	T	S(0.181)S(0.181)VRPT(0.181)GGANMAT(0.184)VPS(0.187)T(0.187)T(0.187)NVNMT(0.23)VNT(0.228)MGT(0.242)GGQT(0.011)IDNGT(0.002)GR	2	III	0,181253	209,5	
Med6	240	T	S(0.005)S(0.005)VRPT(0.012)GGANMAT(0.864)VPS(0.576)T(0.175)T(0.186)NVNMT(0.052)VNT(0.056)MGT(0.055)GGQT(0.013)IDNGT(0.001)GR	2	I	0,863718	209,5	
Med6	243	S	S(0.005)S(0.005)VRPT(0.007)GGANMAT(0.013)VPS(0.593)T(0.593)T(0.568)NVNMT(0.462)VNT(0.46)MGT(0.198)GGQT(0.094)IDNGT(0.002)GR	3	II	0,592586	171,88	
Med6	244	T	S(0.005)S(0.005)VRPT(0.007)GGANMAT(0.013)VPS(0.593)T(0.593)T(0.568)NVNMT(0.462)VNT(0.46)MGT(0.198)GGQT(0.094)IDNGT(0.002)GR	3	II	0,592586	171,88	
Med6	250	T	S(0.005)S(0.005)VRPT(0.007)GGANMAT(0.013)VPS(0.593)T(0.593)T(0.568)NVNMT(0.462)VNT(0.46)MGT(0.198)GGQT(0.094)IDNGT(0.002)GR	3	II	0,461857	171,88	
Med6	253	T	SSVRPTGGANMATVPS(0.004)T(0.003)T(0.004)NVNMT(0.077)VNT(0.926)MGT(0.969)GGQT(0.017)IDNGTGR	2	I	0,925921	209,5	
Med6	256	T	SSVRPTGGANMATVPSTTNVNMTVNT(0.009)MGT(0.939)GGQT(0.052)IDNGTGR	1	I	0,938822	214,26	Albuquerque, 2008
Med6	260	T	SSVRPTGGANMATVPSTTNVNMT(0.041)VNT(0.036)MGT(0.145)GGQT(0.773)IDNGT(0.005)GR	1	I	0,773043	214,26	

Med7	214	S	LTSIQDTLRT(0.249)GS(0.751)QS(0.999)PPS(0.001)SSQ	2	I	0,751232	239,75	
Med7	219	S	LT(0.001)S(0.001)IQDT(0.028)LRT(0.106)GS(0.251)QS(0.805)PPS(0.55)S(0.481)S(0.776)Q	3	II	0,550011	240,65	
Med7	220	S	LT(0.001)S(0.001)IQDT(0.028)LRT(0.106)GS(0.251)QS(0.805)PPS(0.55)S(0.481)S(0.776)Q	3	II	0,481251	240,65	
Med7	221	S	LTSIQDTLRTGSQS(0.999)PPS(0.002)S(0.037)S(0.961)Q	2	I	0,961147	239,75	

Med8	220	S	FTFTGEKPIITGSTST(0.001)S(0.45)S(0.45)S(0.098)N	1	II	0,450021	210,67	
Med8	221	S	FTFTGEKPIITGSTST(0.001)S(0.45)S(0.45)S(0.098)N	1	II	0,450021	210,67	

Med9	118	S	S(1)PSEWQDIIHQR	1	I	0,999948	279,51	
Med9	120	S	DLLS(0.084)KS(0.097)PS(0.819)EWQDIIHQR	1	I	0,819416	279,51	

Med10	147	T	RT(0.949)S(0.051)PIDNVSNTH	1	I	0,949122	180,17	
Med10	148	S	RT(0.187)S(0.813)PIDNVSNTH	1	I	0,813052	180,17	
Med10	156	T	RTSPIDNVS(0.024)NT(0.976)H	1	I	0,975873	180,17	

Med13	425	S	QTTVSNDLENS(1)PLK	1	I	1	159,17	Albuquerque, 2008 Smolka, 2007
Med13	472	S	EQNENLPS(1)DKS(0.997)DS(0.003)MVDK	2	I	0,999986	162,71	
Med13	475	S	EQNENLPS(1)DKS(0.997)DS(0.003)MVDK	2	I	0,997092	162,71	
Med13	477	S	EQNENLPS(0.095)DKS(0.948)DS(0.957)MVDK	2	I	0,956694	162,71	
Med13	746	T	IPQNDIPQT(0.569)ES(0.431)PLK	1	II	0,568941	176,38	

Med14	2	T	T(0.456)T(0.102)T(0.102)IGS(0.34)PQMLANEER	1	II	0,455663	314,92	
Med14	3	T	T(0.279)T(0.32)T(0.32)IGS(0.08)PQMLANEERLS(0.001)NEMHALK	1	II	0,320262	314,92	
Med14	4	T	T(0.279)T(0.32)T(0.32)IGS(0.08)PQMLANEERLS(0.001)EMHALK	1	II	0,320262	314,92	
Med14	7	S	TTTIGS(1)PQMLANEER	1	I	1	314,92	Albuquerque, 2008
Med14	18	S	T(0.075)T(0.086)T(0.086)IGS(0.319)PQMLANEERLS(0.434)NEMHALK	1	II	0,434133	170,08	
Med14	48	S	NTQLHGPS(0.499)AT(0.499)DPET(0.002)TATQK	1	II	0,498769	132,93	

Med15	163	T	RQLT(1)PQQQQLVNQMK	1	I	1	193,14	Albuquerque, 2008
Med15	398	T	AQNVPMNIIQQQQQQNT(0.004)NNNDT(0.001)IAT(0.014)S(0.05)AT(0.926)PNAAAFS(0.004)QQQNAS(0.001)S(0.001)K	1	I	0,925814	203,97	
Med15	728	T	NT(0.462)S(0.076)S(0.462)MDFLNSMENTPK	1	II	0,462191	245,93	
Med15	729	S	NT(0.158)S(0.727)S(0.115)MDFLNSMENTPK	1	II	0,727063	245,93	
Med15	730	S	NT(0.013)S(0.104)S(0.883)MDFLNSMENTPK	1	I	0,882932	245,93	Albuquerque, 2008
Med15	746	S	VPVS(1)AAATPSLNK	1	I	0,999759	205,99	Albuquerque, 2008
Med15	750	T	VPVS(0.999)AAAT(0.997)PS(0.004)LNK	2	I	0,997081	178,35	Albuquerque, 2008
Med15	752	S	VPVSAAAT(0.008)PS(0.992)LNK	1	I	0,991966	205,99	Albuquerque, 2008
Med15	767	S	S(0.997)NT(0.003)IPVTSIPSTNKK	1	I	0,996723	154,81	Soufi, 2009
Med15	783	S	KLS(0.998)IS(0.002)NAASQQPTPRSASNTAK	1	I	0,998448	238,32	Albuquerque, 2008 Gruhler, 2005

Med15	785	S	KLSIS(1)NAAS(1)QQPTPR	2	I	1	293,6	Smolka, 2007 Albuquerque, 2008 Soufi, 2009
Med15	789	S	KLSISNAAS(1)QQPTPR	1	I	0,999996	238,32	
Med15	793	T	LSISNAASQQPT(1)PR	1	I	0,999998	238,32	Albuquerque, 2008
Med15	796	S	S(0.847)AS(0.17)NT(0.901)AKS(0.086)T(0.206)PNT(0.738)NPS(0.052)PLK	3	I	0,847316	223,49	
Med15	798	S	KLS(0.132)IS(0.014)NAAS(0.543)QQPT(0.194)PRS(0.266)AS(0.665)NT(0.188)AK	2	II	0,664764	203,01	
Med15	800	T	S(0.028)AS(0.189)NT(0.785)AKS(0.841)T(0.156)PNT(0.001)NPSPLK	2	I	0,785459	203,01	
Med15	803	S	SASNTAKS(1)T(0.992)PNT(0.008)NPSPLK	2	I	0,999583	203,01	Albuquerque, 2008 Soufi, 2009
Med15	804	T	SASNTAKS(1)T(0.992)PNT(0.008)NPSPLK	2	I	0,99188	203,01	Albuquerque, 2008
Med15	810	S	STPNTNPS(1)PLK	1	I	0,99995	140,69	Soufi, 2009
Med15	820	T	NGT(1)PNPNNMK	1	I	1	194,11	
Med15	828	T	T(0.934)VQS(0.066)PMGAQPSYNSAIIENAFRK	1	I	0,933878	248,59	Albuquerque, 2008 (Albuquerque 2008) Soufi, 2009 (Soufi 2008)
Med15	831	S	T(0.094)VQS(0.906)PMGAQPSYNSAIIENAFR	1	I	0,906148	248,59	Albuquerque, 2008 Soufi, 2009
Med15	978	S	DLS(0.399)T(0.399)LVHS(0.067)S(0.067)S(0.067)PS(0.027)T(0.022)S(0.476)S(0.476)NMDVGNPR	2	II	0,399447	220,7	
Med15	983	S	DLS(0.003)T(0.003)LVHS(0.926)S(0.525)S(0.525)PS(0.009)T(0.009)SSNMDVGNPR	2	I	0,925609	220,7	Albuquerque, 2008
Med15	984	S	DLSTLVHS(0.001)S(0.994)S(0.976)PS(0.027)T(0.001)SSNMDVGNPR	2	I	0,994309	220,7	Albuquerque, 2008
Med15	985	S	DLSTLVHS(0.001)S(0.994)S(0.976)PS(0.027)T(0.001)SSNMDVGNPR	2	I	0,975761	220,7	Gruhler, 2005 Smolka, 2007 Albuquerque, 2008
Med15	987	S	DLS(0.016)T(0.034)LVHS(0.107)S(0.742)S(0.121)PS(0.978)T(0.002)SSNMDVGNPR	2	I	0,978318	220,7	Albuquerque, 2008
Med15	1003	S	RKAS(1)VLEISPQDSIASVLSPDSNIMSDSK	1	I	0,999833	279,49	Smolka, 2007 Albuquerque, 2008
Med15	1008	S	ASVLEIS(0.956)PQDS(0.042)IAS(0.004)VLS(0.975)PDS(0.014)NIMS(0.008)DS(0.002)KK	2	I	0,955844	275,02	
Med15	1018	S	ASVLEISPQDSIASVLS(0.973)PDS(0.027)NIMSDSKK	1	I	0,97272	279,49	Smolka, 2007
Med15	1021	S	ASVLEISPQDSIASVLS(0.011)PDS(0.976)NIMS(0.011)DS(0.002)K	1	I	0,975597	279,49	
Med15	1034	S	VDS(1)PDDPFMTK	1	I	1	235,28	Smolka, 2007 Li, 2007 Chi, 2007 Albuquerque, 2008

Med17	56	T	ADT(0.879)S(0.121)IRLEGDELENK	1	I	0,87863	194,24	
Med17	57	S	ADT(0.003)S(0.997)IRLEGDELENK	1	I	0,997496	194,24	Smolka, 2007 Albuquerque, 2008

Med18	129	S	NILHNTVPQVTNFNSTNEDQNNS(1)K	1	I	1	258,12	

Med19	197	S	S(0.611)S(0.611)GS(0.362)S(0.362)MAT(0.044)PT(0.007)HS(0.003)DS(0.001)HEDMK	2	II	0,610692	199,85	

Med19	198	S	S(0.611)S(0.611)GS(0.362)S(0.362)MAT(0.044)PT(0.007)HS(0.003)DS(0.001)HEDMK	2	II	0,610692	199,85	
Med19	200	S	S(0.049)S(0.056)GS(0.747)S(0.146)MAT(0.002)PT(0.001)HSDSHEDMK	1	II	0,746841	220,76	
Med19	201	S	S(0.447)S(0.447)GS(0.451)S(0.447)MAT(0.021)PT(0.085)HS(0.1)DS(0.002)HEDMK	2	II	0,44693	199,85	
Med19	204	T	SSGSS(0.003)MAT(0.813)PT(0.172)HS(0.01)DS(0.002)HEDMK	1	I	0,81314	220,76	
Med19	206	T	S(0.001)S(0.001)GS(0.005)S(0.005)MAT(0.113)PT(0.763)HS(0.113)DSHEDMK	1	I	0,763434	220,76	
Med19	208	S	S(0.016)S(0.016)GS(0.013)S(0.02)MAT(0.435)PT(0.558)HS(0.941)DS(0.001)HEDMK	2	I	0,940917	199,85	
Med19	210	S	SSGSSMAT(0.004)PT(0.15)HS(0.032)DS(0.814)HEDMK	1	I	0,814275	220,76	

Med31	11	T	SSTNGNAPAT(0.851)PS(0.149)SDQNPLPTR	1	I	0,850876	182,11	

4.2 Mediator phosphosites under normal and stress conditions

Table 15: Phosphopeptides from endogenous Mediator (SILAC) identified by quantitative mass spectrometry

Subunit	Phosphorylated Amino acid	Relative position	Phosphopeptide sequence	Number of phospho (STY)	pSTY-class	Localization p-value	PTM Score	Ratio H/L normalized by protiens	Ratio H/L Protein	Experiment (replicate)
Med1	S	155	LDSSNASFNNQGK	1	I	0,999988	113,1	1,1403	0,93111	[8]
Med2	S	266	GFDDNDSGNNYND	1	I	0,999916	91,06	1,2889	1,0173	[8]
Med3	S	189	GKRGPKSGSTMGT	2	II	0,520948	110,2	0,67404		[5]
Med3	T	195	SGSTMGTPTVHNS	2	II	0,483304	110,2	0,67404		[5]
Med3	T	197	STMGTPTVHNSTA	2	I	1	110,2	0,67404		[5]
Med4	S	2	MSVQDTKA	2	II	0,375866	42,7	0,89538		[5]
Med4	S	29	LVAEATSNTNSED	2	II	0,427697	42,7	0,89538		[5]
Med4	T	237	MAKKEGTPKTDSF	1	I	0,895187	63,90	0,88859	0,97272	[8]
Med4	T	240	KEGTPKTDSFIFD	1	II	0,466767	63,90	0,87087	0,97272	[8]
Med5	T	64	ASDLVDTPSNNTA	1	I	0,711911	44,01	0,75578	0,96689	[8]
Med5	S	66	DLVDTPSNNTAAT	1	II	0,414839	44,01	0,75578	0,96689	[8]
Med5	S	257	TNEFVGSPSLTSP	1	II	0,594324	59,16	1,0164	0,96689	[8]
Med5	S	257	TNEFVGSPSLTSP	2	II	0,504487	35,82	0,60258		[5]
Med5	S	259	EFVGSPSLTSPQY	3	II	0,349267	35,82	0,60258		[5]
Med5	T	261	VGSPSLTSPQYIP	3	II	0,351505	35,82	0,60258		[5]
Med5	S	262	GSPSLTSPQYIPS	3	II	0,728166	35,82	0,60258		[5]
Med5	S	268	SPQYIPSPLSSTK	1	II	0,554887	59,16	1,0164	0,96689	[8]
Med5	S	268	SPQYIPSPLSSTK	3	III	0,188482	35,82	0,60258		[5]
Med5	S	271	YIPSPLSSTKPPG	3	III	0,190959	35,82	0,60258		[5]
Med5	S	272	IPSPLSSTKPPGS	2	II	0,306	35,82	0,60258		[5]
Med5	T	273	PSPLSSTKPPGSV	2	II	0,306287	35,82	0,60258		[5]
Med5	S	1014	LHEKNDSAEVRQE	1	I	1	108,8	1,1616	0,96689	[8]
Med6	S	225	NNAGGGSNKSSVR	1	I	0,999975	68,61	0,75332		[5]
Med6	S	225	NNAGGGSNKSSVR	1	I	1	245,8	0,98941	0,96518	[8]
Med7	S	214	DTLRTGSQSPPSS	1	I	0,965933	162,7			[8]

Med7	S	214	DTLRTGSQSPPSS	1	I	0,999754	112,6			[5]
Med7	S	216	DTLRTGSQSPPSS	1	I	1	162,7			[8]
Med7	S	216	LRTGSQSPPSSSQ	2	I	0,999821	112,6			[5]
Med7	S	219	GSQSPPSSSQ	3	II	0,591076	152,58			[5]
Med7	S	221	QSPPSSSQ	3	II	0,745165	152,58			[5]
Med14	S	7	MTTTIGSPQMLAN	1	I	0,981906	59,61	1,0028	0,93638	[8]
Med14	T	1036	DTKRLGTPESVKP	1	I	0,999212	40,65	1,4734	0,93638	[8]
Med15	S	746	TPKVPVSAAATPS	2	I	1	139,73	0,59134		[5]
Med15	T	750	PVSAAATPSLNKT	2	I	0,75299	139,73	0,59134		[5]
Med15	S	767	VNGRTKSNTIPVT	1	I	0,997779	108,8	0,7847	1,0152	[8]
Med15	S	767	VNGRTKSNTIPVT	2	I	1	121,83	0,23904		[5]
Med15	T	769	GRTKSNTIPVTSI	2	I	0,999999	121,83	0,23904		[5]
Med15	S	783	STNKKLSISNAAS	1	I	0,930035	62,19	1,3327	1,0152	[8]
Med15	S	796	QQPTPRSASNTAK	1	II	0,431756	62,19	0,28888	1,0152	[8]
Med15	S	798	PTPRSASNTAKST	1	II	0,431756	62,19	0,28888	1,0152	[8]
Med15	T	800	PRSASNTAKSTPN	1	II	0,328631	62,18	0,28888	1,0152	[8]
Med15	S	803	ASNTAKSTPNTNP	1	II	0,506016	31,18	0,77543	1,0152	[8]
Med15	T	804	SNTAKSTPNTNPS	1	I	0,821598	31,19	0,62814	1,0152	[8]
Med15	T	820	TQTKNGTPNPNNM	1	I	1	63,85	1,1509	1,0152	[8]
Med15	T	820	TQTKNGTPNPNNM	1	I	1	96,19	0,67499		[5]
Med15	S	831	NMKTVQSPMGAQP	1	I	0,952246	86,1	1,1016	1,0152	[8]
Med15	S	983	LSTLVHSSSPSTS	1	II	0,319945	128,3	0,98032	1,0152	[8]
Med15	S	983	LSTLVHSSSPSTS	1	II	0,467627	100,57	0,80973		[5]
Med15	S	984	STLVHSSSPSTSS	1	II	0,335819	128,3	0,98032	1,0152	[8]
Med15	S	984	STLVHSSSPSTSS	1	II	0,467627	100,57	0,80973		[5]
Med15	S	987	VHSSSPSTSSNMD	1	II	0,335819	128,3	0,98032	1,0152	[8]
Med15	S	1008	ASVLEISPQDSIA	2	I	0,759731	74,54	1		[5]
Med15	S	1018	SIASVLSPDSNIM	2	I	0,974119	74,54	1,0		[5]
Med15	S	1034	KKIKVDSPDDPFM	1	I	1	242,1	1,0116	1,0152	[8]
Med15	S	1034	KKIKVDSPDDPFM	1	I	1	164,05	0,75937		[5]
Med17	S	57	AGKADTSIRLEGD	1	I	0,926108	106,6	1,0224	0,96252	[8]
Med17	T	56	SAGKADTSIRLEG	1	II	0,5	106,6	0,94258	0,96252	[8]

[5], [8] identifier of replicate experiment

4.3 Phosphosite mutants: Genomic point mutations

Table 16: Genomic point mutations in *D7P* mutant strain

	Relative amino-acid position	Point mutation
Med15	746	S→A
Med15	750	T→A
Med15	796	S→A
Med15	798	S→A
Med15	769	T→A
Med15	767	S→A
Med15	800	S→A

Table 17: Genomic point mutations in *D30P* mutant strain

	Relative amino-acid position	Point mutation
Med15	728	T→A
Med15	729	S→A
Med15	730	S→A
Med15	746	S→A
Med15	750	T→A
Med15	752	S→A
Med15	767	S→A
Med15	769	T→A
Med15	783	S→A
Med15	785	S→A
Med15	789	S→A
Med15	793	T→A
Med15	796	S→A
Med15	798	S→A
Med15	800	T→A
Med15	803	S→A
Med15	804	T→A
Med15	810	S→A
Med15	820	T→A
Med15	828	T→A
Med15	831	S→A
Med15	978	S→A
Med15	983	S→A
Med15	984	S→A
Med15	985	S→A
Med15	987	S→A
Med15	1003	S→A
Med15	1008	S→A
Med15	1018	S→A
Med15	1034	S→A

4.4 Gene Ontology analysis

Table 18: *Δmed15* (induced): GO term

GO-ID	p-value	x	n	X	N	Description
7039	3,48E-39	73	118	732	6208	vacuolar protein catabolic process (autophagy)
9056	1,06E-26	190	775	732	6208	catabolic process
44248	3,28E-24	169	680	732	6208	cellular catabolic process
6914	3,68E-15	57	163	732	6208	autophagy
30163	6,10E-14	84	314	732	6208	protein catabolic process
55114	1,19E-13	92	363	732	6208	oxidation reduction
44257	1,27E-13	81	301	732	6208	cellular protein catabolic process
5975	8,80E-11	79	326	732	6208	carbohydrate metabolic process
44262	1,24E-10	73	293	732	6208	cellular carbohydrate metabolic process
44281	2,49E-10	167	912	732	6208	small molecule metabolic process
44282	6,83E-10	45	148	732	6208	small molecule catabolic process
9057	1,20E-08	92	442	732	6208	macromolecule catabolic process
6066	1,43E-08	59	240	732	6208	alcohol metabolic process
5984	2,71E-08	13	20	732	6208	disaccharide metabolic process
44265	4,47E-08	87	421	732	6208	cellular macromolecule catabolic process
5996	7,69E-08	38	132	732	6208	monosaccharide metabolic process
19318	1,12E-07	35	118	732	6208	hexose metabolic process
6112	2,29E-07	18	41	732	6208	energy reserve metabolic process
9266	5,09E-07	19	47	732	6208	response to temperature stimulus
51187	5,52E-07	16	35	732	6208	cofactor catabolic process

Table 19: *Δmed15* (repressed): GO term

GO-ID	p-value	x	n	X	N	Description
42254	1,83E-125	237	372	818	6208	ribosome biogenesis
22613	7,44E-111	240	423	818	6208	ribonucleoprotein complex biogenesis
6364	1,47E-97	173	252	818	6208	rRNA processing
16072	2,02E-94	174	262	818	6208	rRNA metabolic process
34470	1,19E-92	201	350	818	6208	ncRNA processing
34660	2,49E-90	216	409	818	6208	ncRNA metabolic process
6396	8,45E-61	213	532	818	6208	RNA processing
16070	3,16E-56	271	837	818	6208	RNA metabolic process
462	9,41E-55	78	93	818	6208	maturation of SSU-rRNA from tricistronic rRNA transcript (SSU-rRNA, 5,8S rRNA, LSU-rRNA)
10467	4,98E-54	451	1921	818	6208	gene expression
30490	1,14E-53	80	99	818	6208	maturation of SSU-rRNA
44085	1,07E-52	278	903	818	6208	cellular component biogenesis
6417	3,07E-45	106	192	818	6208	regulation of translation
32268	1,19E-42	110	215	818	6208	regulation of cellular protein metabolic process
10608	2,20E-41	106	206	818	6208	posttranscriptional regulation of gene expression
42273	4,76E-40	61	77	818	6208	ribosomal large subunit biogenesis
42255	6,83E-38	56	69	818	6208	ribosome assembly
466	4,95E-32	53	72	818	6208	maturation of 5,8S rRNA from tricistronic rRNA transcript (SSU-rRNA, 5,8S rRNA, LSU-rRNA)
460	4,95E-32	53	72	818	6208	maturation of 5,8S rRNA
51246	5,45E-31	112	279	818	6208	regulation of protein metabolic process

Table 20: *D30P* (induced): GO term

GO-ID	p-value	x	n	X	N	Description
7039	5,92E-23	32	118	183	6208	vacuolar protein catabolic process (autophagy)
9266	2,65E-16	18	47	183	6208	response to temperature stimulus
44257	2,70E-11	33	301	183	6208	cellular protein catabolic process
30163	8,54E-11	33	314	183	6208	protein catabolic process
9628	1,97E-09	22	165	183	6208	response to abiotic stimulus
16052	2,69E-09	16	86	183	6208	carbohydrate catabolic process
44275	5,35E-09	15	78	183	6208	cellular carbohydrate catabolic process
44282	8,92E-09	20	148	183	6208	small molecule catabolic process
9056	1,11E-08	51	775	183	6208	catabolic process
44248	9,11E-08	45	680	183	6208	cellular catabolic process
44265	1,49E-07	33	421	183	6208	cellular macromolecule catabolic process
46164	3,68E-07	12	66	183	6208	alcohol catabolic process
9057	4,66E-07	33	442	183	6208	macromolecule catabolic process
46365	1,25E-06	11	61	183	6208	monosaccharide catabolic process
19320	5,03E-06	10	57	183	6208	hexose catabolic process
6091	6,20E-06	22	259	183	6208	generation of precursor metabolites and energy
44262	1,40E-05	23	293	183	6208	cellular carbohydrate metabolic process
6007	1,44E-05	9	51	183	6208	glucose catabolic process
6066	2,24E-05	20	240	183	6208	alcohol metabolic process
6006	2,66E-05	12	98	183	6208	glucose metabolic process

Table 21: *D30P* (repressed): GO term

GO-ID	p-value	x	n	X	N	Description
42180	6,55E-08	17	391	59	6208	cellular ketone metabolic process
19752	2,46E-07	16	377	59	6208	carboxylic acid metabolic process
43436	2,46E-07	16	377	59	6208	oxoacid metabolic process
6082	4,81E-07	16	396	59	6208	organic acid metabolic process
44281	3,87E-06	23	912	59	6208	small molecule metabolic process
44271	2,61E-05	12	310	59	6208	cellular nitrogen compound biosynthetic process
16053	2,98E-05	9	172	59	6208	organic acid biosynthetic process
46394	2,98E-05	9	172	59	6208	carboxylic acid biosynthetic process
32787	3,54E-05	8	135	59	6208	monocarboxylic acid metabolic process
44283	5,54E-05	13	390	59	6208	small molecule biosynthetic process
6519	1,51E-04	11	315	59	6208	cellular amino acid and derivative metabolic process
44106	1,95E-04	10	270	59	6208	cellular amine metabolic process
6767	3,01E-04	5	63	59	6208	water-soluble vitamin metabolic process
6766	4,02E-04	5	67	59	6208	vitamin metabolic process
6520	4,75E-04	9	247	59	6208	cellular amino acid metabolic process
9308	4,93E-04	10	303	59	6208	amine metabolic process
46942	5,26E-04	5	71	59	6208	carboxylic acid transport
19541	8,72E-04	2	5	59	6208	propionate metabolic process
6865	1,13E-03	4	49	59	6208	amino acid transport
15849	1,20E-03	5	85	59	6208	organic acid transport

Table 22: *D7P* (induced): GO term

GO-ID	p-value	x	n	X	N	Description
7039	2,78E-08	7,98E-06	10	118	51	vacuolar protein catabolic process (autophagy)
9266	8,08E-08	1,16E-05	7	47	51	response to temperature stimulus
6006	1,05E-06	6,64E-05	8	98	51	glucose metabolic process
15749	1,16E-06	6,64E-05	5	24	51	monosaccharide transport
8645	1,16E-06	6,64E-05	5	24	51	hexose transport
6066	2,77E-06	1,33E-04	11	240	51	alcohol metabolic process
19318	4,32E-06	1,77E-04	8	118	51	hexose metabolic process
5996	9,97E-06	3,58E-04	8	132	51	monosaccharide metabolic process
6112	1,84E-05	5,27E-04	5	41	51	energy reserve metabolic process
8643	1,84E-05	5,27E-04	5	41	51	carbohydrate transport
34637	2,97E-05	7,11E-04	6	75	51	cellular carbohydrate biosynthetic process
160	8,91E-05	1,83E-03	6	91	51	carbohydrate biosynthetic process
44257	1,34E-04	2,26E-03	10	301	51	cellular protein catabolic process
30163	1,90E-04	2,98E-03	10	314	51	protein catabolic process
46323	1,97E-04	2,98E-03	2	3	51	glucose import
6091	2,17E-04	3,12E-03	9	259	51	generation of precursor metabolites and energy
5975	2,58E-04	3,53E-03	10	326	51	carbohydrate metabolic process
9628	3,57E-04	4,26E-03	7	165	51	response to abiotic stimulus
44265	4,90E-04	5,41E-03	11	421	51	cellular macromolecule catabolic process
7039	2,78E-08	7,98E-06	10	118	51	vacuolar protein catabolic process

5. Synthesis- decay compensation (Unpublished additional Data)

5.1 Stress induced mRNA synthesis- decay compensation

5.1.1 Osmotic stress induced synthesis rates are compensated by increased mRNA half-lives

We used cDTA to obtain data sets of absolute mRNA synthesis rates and halflives for 5331 genes of the wildtype, *Δmed15* and *D7P* under normal and osmotic stress conditions (Figure 22A-B). Upon high salt concentrations, wild type cells show decreased absolute synthesis rates (median fold: 0.212), which are accompanied by a 4-fold extension of global transcript halflives (Figure 22A). The absolute median synthesis rate decreased from 53 mRNA per cell and cell cycle under normal conditions to 11 under stress condition, and absolute median mRNA half-live increased from 18 to 71.6 min (Table 26). Therefore, osmotic stress induced change of synthesis rates is accompanied by prolonged transcript half-lives, indicating a potential compensation on the post-transcriptional level (Figure 22A). Variation analysis of absolute synthesis and decayrates revealed, that high salt concentrations induce a strong shift in absolute synthesis and decayrates relative to the wild type under normal conditions (Figure 22B). The stress response of *D7P* exhibits a similar shift of median synthesis rates (from 52.5 to 11 mRNA/cell/cell cycle), but an increased median half-live of 106 min in response to osmotic stress conditions (Table 26). Therefore, response to osmotic stress induces absolute mRNA synthesis rate changes, which might be compensated by an increase mRNA half lives.

Table 23: *Median mRNA synthesis rate and transcript half-live.* Median of absolute mRNA synthesis rates and transcript half-lives of wildtype, *D7P* and *Δmed15* under normal or osmotic stress conditions calculated from cDTA data sets.

	Normal conditions		Osmotic stress conditions	
Strain	Median mRNA synthesis rate [mRNA/cell/cell cycle]	Median mRNA half-live [min]	Median mRNA synthesis rate [mRNA/cell/cell cycle]	Median mRNA half-live [min]
wild type	53	18	11.1	71.6
D7P	52.5	20	11	105.7
Δmed15	14.75	108.4	2.4*	443.7*

* Please note that we observed a strong shift of synthesis and decay rates in the *Δmed15* mutant during response to osmotic stress (data not shown). Therefore, the median absolute mRNA synthesis rate and absolute half-live for *Δmed15* are based on the data of 333 genes.
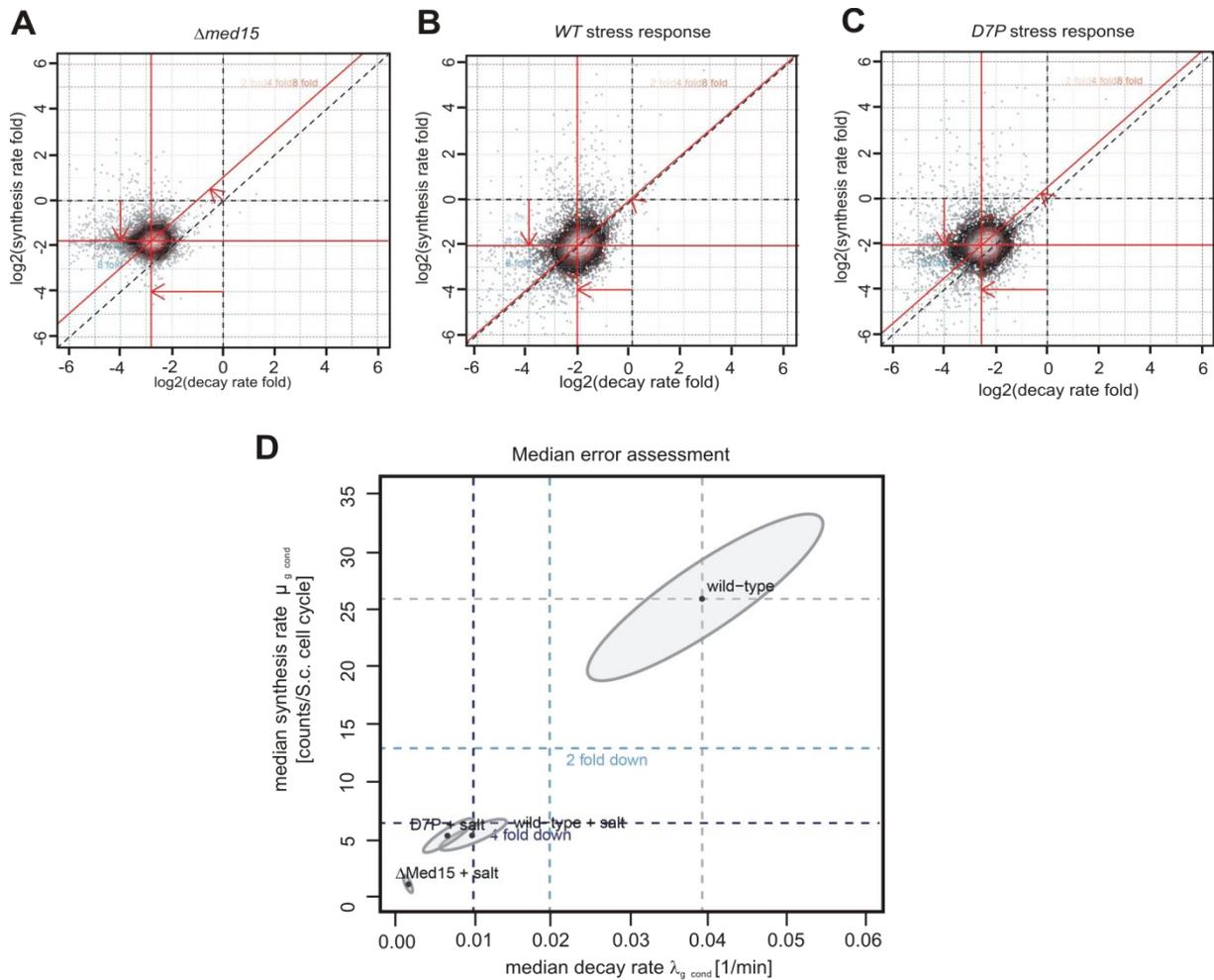
Figure 22: *Osmotic stress induced changes in absolute synthesis rates are compensated by increased mRNA half-lives* **A)** Scatter plots comparing the changes in mRNA synthesis rates (log fold change, x-axis) and decay rates (log fold changes, y-axis). Each dot corresponds to one mRNA and the density is represented by the brightness of grey scale. Contour lines define regions of equal density. Changes of absolute mRNA synthesis and decay rates in *Δmed15* under normal conditions compared to wild type. The center of distribution is located at (log2 fold change: -2.1 and -2.6), which indicates a global shift in the median synthesis rate and a global shift in the median decay rate, which is accompanied by a global change in mRNA levels, which is predicted by the offset of the diagonal red line from the dashed main diagonal. Scatter plot as in A; Osmotic stress response of wild-type cells (induction phase, 18-24 min after salt addition): Median mRNA synthesis and decay rates are decreased by similar factors and exhibit no change in global mRNA levels (no offset of the diagonal red line).The center of distribution is located at (log2fold change: -2 and -2). Scatter plot as in A; Osmotic stress response of *D7P* mutant cells (induction phase, 18-24 min after salt addition): The center of distribution is located at (log2 fold change: -2.1 and -2.6), which indicates a global shift in the median synthesis rate and a global shift in the median decay rate, which is accompanied by a global change in mRNA levels, which is predicted by the offset of the diagonal red line from the dashed main diagonal. **B)** Coupling of absolute synthesis and decay rates in response to osmotic stress. (global shift in mRNA metabolism in response to osmotic stress) The comparison of absolute transcript half-live (x-axis) and mRNA synthesis rate (y-axis) illustrates changes in mRNA metabolism that contribute to gene expression. The black dots represent the center of mRNA distribution (median). The 95%-confidence area is represented by grey ellipses. Osmotic stress leads to a significant decrease of synthesis and decay rates in the wild-type compared to normal conditions (95% region: 5065 transcripts). The *D7P* mutant exhibits a strong decrease in decay rates (95% region: 4220 transcripts). Osmotic stress leads to a strong shift of mRNA synthesis rates, which is partly compensated by a corresponding prolongation of transcript half-lives, indicating a coupling between transcription and post-transcription to adjust global mRNA levels.

APPENDIX (UNPUBLISHED DATA):
FUNCTIONAL CHARACTERIZATION OF THE MEDIATOR SUBUNIT ROX3

Third Research Project

1. Introduction

1.1 Identification of Rox3

Rox3 was identified during a search for factors which are involved in expression of heme-regulated cytocrome c (*cyc7* gene) in *Saccharomyces cerevisiae* (Rosenblum-Vos, et al. 1991). Rox3 was shown to be tightly associated with the Pol II holoenzyme and has been identified as component of the Mediator complex (Gustafsson, et al. 1997). Homologues of *S. cerevisiase* Rox3 has been identified in fungi, metazoan, plants and mammalia (Bourbon, 2008). The high sequence identity between the yeast and human Rox3 homologue suggest a conserved functional role within the Mediator complex.

The human Rox3 homologue is associated with several types of cancer. Med19 knockdown inhibits tumor growth of ovarian cancer (Liu, et al. 2012), decrease cell proliferation of human gastric carcinoma (Ding, et al. 2012), prostate cancer (Cui, et al. 2011), pancreatic cancer (Li, et al. 2011), colorectal cancer (Ji-Fu, et al. 2012), human osteosarcoma cells (Wang, et al. 2011), lung cancer (Sun, et al. 2011), bladder cancer cells (Zhang, et al. 2012), human hepatocellular carcinoma cells (Zou, et al. 2011) and breast cancer cells (Li, et al. 2011).

1.2 Rox3 function in regulation of transcription

Rox3 mutants exhibit temperature sensitivity, osmotic sensitivity and inability to utilize Glycerol as a carbon source (Rosenblum-Vos, et al. 1991, Evangelista, et al 1996) and point mutatuons are floculent in some backgrounds (Song, et al 1996). Med19/Rox3 plays a role in regulation of transcription. Mediator complexes lacking Rox3 have severe defects in basal transcription (Baidoonbonso, et al. 2006). Rox3 is required for increased levels of the lipase Yeh1, which catalyses steryl ester hydrolysis under heme-deficient conditions (Köffel, et al. 2006) and Rox3 is involved in transcription of genes required for growth under aerobic and hypoxic conditions (Beccera, et al. 2002). Rox3 mutants are defective in activation of Gcn4 and Gal4 induced genes and lead to derepression of HO-genes (Tabtiang, et al. 1998). Rox3 is involved in regulation of stress response genes. Activation of oxidative stress genes by the transcription factor Yap1 in present of H_2O_2 is dependent on proper recruitment of Rox3 (Gulshan, et al. 2005) and Rox3 mutant derepress expression of heat-shock genes (Singh, et al. 2006) and led to severe reduction of TBP, SAGA and SWI/SNF recruitment on selected promoter (Govind, et al. 2005).

Initially, Rox3 has been described as an essential factor for yeast viability. However, several recent studies revealed that Rox3 knockout strains have a severe growth defect, but cells are still viable. A Mediator complex could be purified from a Rox3 deletion strain (Baidoonbonso, et al. 2006). The purified Mediator complex lacking Rox3 lost the middle module under stringent buffer conditions. The current model of Rox3 function suggest a requirement for interactions between Mediator subunits and its participation in transcription factor interaction with the Mediator (Baidoonbonso, et al. 2006; Singh, et al. 2006).

1.3 Aim & Scope

Rox3 function is associated with several types of human cancers. Knock-down of Rox3 inhibits cellular growth of tumors and cancer cell lines. Rox3 is a promising candidate for studies to investigate the functional connection between the Mediator and regulation of transcription. Although it has been shown that Rox3 is part of the Mediator complex, there is a lack of knowledge concerning the functional role of Rox3 in regulation of transcription. Because of the high sequence conservation between human and *S. cerevisiae*, studies on yeast Rox3 is promising for getting insights into the functional role of Rox3 in regulation cell growth.

The first part of our study focuses on endogenous Rox3. To identify potential interaction partners within the Mediator complex, we used TAP-tagged Rox3 in combination with mass-spectrometry (section 2.1). In the second part, we investigated the functional organization of Rox3. We used limited proteolysis experiments in combination with bioinformatic sequence analysis to model the domain architecture of Rox3. Based on these model, we designed several Rox3 constructs and tested the potential of Rox3 to activate transcription *in vitro* (section 2.3). The third part focus on the functional role of the Rox3 C-terminus. During the bioinformatic sequence analysis, we found evidence for a conserved nuclear localization sequence (NLS) in Rox3. We extended our analysis to all Mediator subunits and revealed a second potential NLS at the Gal11/Med15 C-terminus. To test the NLS functionality *in vivo*, we combined Rox3 and Gal11/Med15 with reporter proteins (GFP and mCherry) and analysis by fluorescent microscopy. We used Rox3 and Gal11/Med15 C-termini to find evidence for the functional C-terminal NLS (section 2.3).

2. Results

2.1 Rox3 is associated with the middle module and the Gal11-subcomplex

Rox3 has been identified as subunit of the Mediator complex (Gustafsson, et al. 1997), however the available data on Rox3 interactions to Mediator subunits are contradictive. The physical and functional interaction of Rox3 to SRB4/MED17 suggested, that Rox3 might be part of the head module (Guglielmi, et al. 2004; Kang, et al. 2001). Surprisingly, recombinant Rox3 had no influence on the assembly of the 7-subunit head-module from its recombinantly expressed subunits and showed no interaction to any of the head module subunits in vitro (Takagi, Kornberg, 2006).

To test whether Rox3 is stably associated with the Mediator complex, we extracted TAP-Rox3 from yeast and analyzed the copurified proteins. We generated a yeast strain carrying an N-terminal tandem affinity purification (TAP)-tagged version of Rox3. Cells were grown in YPD medium to late-logarithmic phase, and Rox3 was purified by tandem-affinity purification as described previously (Puig, et al. 2001). The proteins eluted from Calmodulin beads were digested with Trypsin and analyzed by mass spectrometry on a high-resolution linear ion trap – Orbitrap spectrometer (MATERIALS & METHODS). The head, middle and tail subunits are copurified with TAP-Rox3 (Figure 23). However, the kinase-module was not associated with the copurifed Mediator core subunits. Consistent with previous findings, the kinase module is transiently associated with the Mediator core complex and can be released from the complex

(Elmlund, et al. 2006). The complete Mediator core subunits copurify with TAP-Rox3 and confirm the stable association with Mediator core complex.
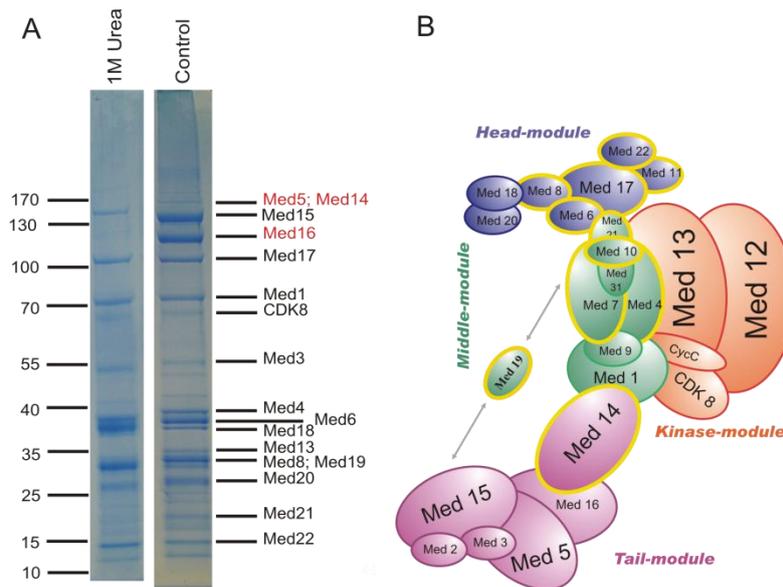

Figure 23: *Rox3 is associated with the middle module and the Gal11-subcomplex.* **(A)** SDS-PAGE of TAP-Rox3 purification. Med5, Med14 and Med16 are dissociated from the Mediator complex after treatment with 1 M Urea. **(B)** Model of the Mediator complex. Based on our and previous findings, Rox3 might interact with Med15 submodule (Med15, Med2, Med3) and the middle module.

To search for potential interaction partners, the TAP-Rox3-Mediator core complex was treated with Urea to remove weakly bound Mediator subunits and identify strong interactions to Rox3. The endogeneous Mediator core complex was divided into 4 fractions and immobilized on IgG beads by TAP-Rox3. Each of the Mediator fractions were treated with either 0 M, 1 M, 3 M, 4 M Urea, eluted from IgG beads by TEV proteolysis and isolated by using Calmodlin beads. The proteins from each of the fractions were separated by SDS-PAGE on a 4-12% gradient gel and protein bands were analysed by standard mass spectrometry (MATERIALS & METHODS). The fractions which were treated with 3 M and 4 M Urea contained no proteins, probably due to Rox3 removal from the beads by unfolding of protein A. However, the fraction treated with 1 M Urea revealed the dissociation of Med5, Med14 and Med16 from the Mediator complex (Figure 23). This results suggest, that Med14 and the tail module subunits Med5 and Med16 might probably not be involved in Rox3 interactions to the Mediator core complex.

This results confirmed the previously observed dissociation of Rgr1/Med14 from Mediator after Urea treatment (Baidoonbonso, et al. 2006). However the additional loss of Med5 and Med16 but non of the other tail module proteins Gal11/Med15, Med3 and Med2 support our hypothesis, that Rox3 interact with the Gal11 subcomplex, which consists of Gal11/Med15, Med3 and Med2. This hypothesis is supported by previous observations: First, the whole middle module is released from the *Δrox3* Mediator complex by treatment with 1 M Urea and leave a subcomplex composed of stable associated head- and tail complex (Baidoonbonso, et al. 2006). Second, Rox3 is not associated with the head module *in vitro* (Takagi & Kornberg, 2006). Taken together, our and previous results suggest physical interactions of Rox3 to the middle module and the Gal11-subcomplex.
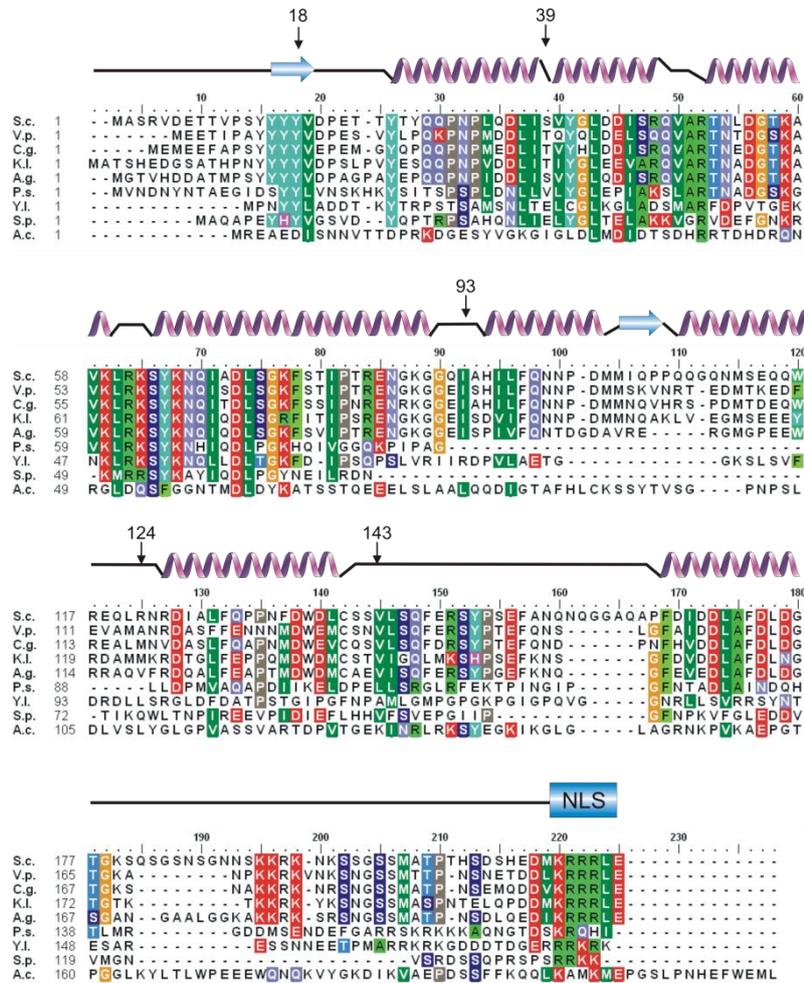
Figure 24: *Multiple Sequence Alignment of Rox3 from mycetes.* Bioinformatic analysis and limited proteolysis of recombinantly expressed Rox3 (trypsin and chymotrypsin) is combined to model the domain architecture of *S. cerevisiae* Rox3. Arrows indicate the fragments identified by Edman-sequencing after proteolysis by trypsin or chymotrypsin.

2.2 Rox3 domain architecture and in vitro transcription assay[3]

To identify the domain architecture of *S. cerevisiae* Rox3, we expressed Rox3 in *E. coli*, optimized the purification procedure and performed limited proteolysis time course using trypsin and chymotrypsin. In combination with multiple sequence alignment of Rox3 homologues, in silico secondary structure prediction and limited proteolysis, we concluded a domain architecture which is connected to an flexible N-termial region (Figure 24).

To characterize the function of the Rox3 domains, we performed *in vitro* transcription assay to quantify the ability of different truncated Rox3 variants to stimulate Pol II transcription. For this purpose, we tested the nuclear extract of the complete Rox3 kock-out strain for the background signal. Since the nuclear extract of Rox3 knock-out strain exhibit no activity, the signal can be restored by titration of recombinantly expressed Rox3 to the reaction (Figure 25).

Next we generated different Rox3 variants by molecular cloing (MATERIALS & METHODS). The constructs were expressed in *E.coli,* isolated by Streptactin and tested for relative expression levels, purification efficiency, stability against degradation and solubility (Figure 25). We choosed the constructs *Rox3-8-180*, *Rox3-18-180*, *Rox3-30-180*, *Rox3-8-160* and *Rox3-8-101* and

---

[3] The in vitro transcription assays were performed in collaboration with Martin Seizl (Gene Center Munich).

tested these constructs for their potential to activate transcription. Based on the *in-vitro* transcription assay designed by Ranish, et al. (1999), we used a plasmid-based assay with a *his4* core promoter and single upstream Gal4-binding site. Depletion of the Mediator complex from wild type nuclear extract reduced signal intensity by 95% and is therefore defective for transcription *in-vitro* (negative control) (Figure 25C, lane 1&2). The TAP-Mediator lacking Rox3 was significantly reduced transcription activity and addition of recombinant Rox3 was able to fully restore the signal to the wild type level (data not shown). Addition of recombinant Rox3 to the ΔRox3 nuclear extract is able to restore transcription up to the level of the native (TAP) Mediator (Figure 25C, lane 3). The truncated Rox3 variants are added in two different concentrations. The truncated Rox3 variants are able to restore transcription, dependent on their concentration (Figure 25C, lanes 3-13). Surprisingly, even the shortest Rox3 variant (8 to101) is able to activate *in-vitro* transcription in this assay. To summarize this results, recombinant Rox3 is able to restore transcription and the region between amino acid 30 and 101 is sufficient for Rox3 functionality to activate transcription *in-vitro*.
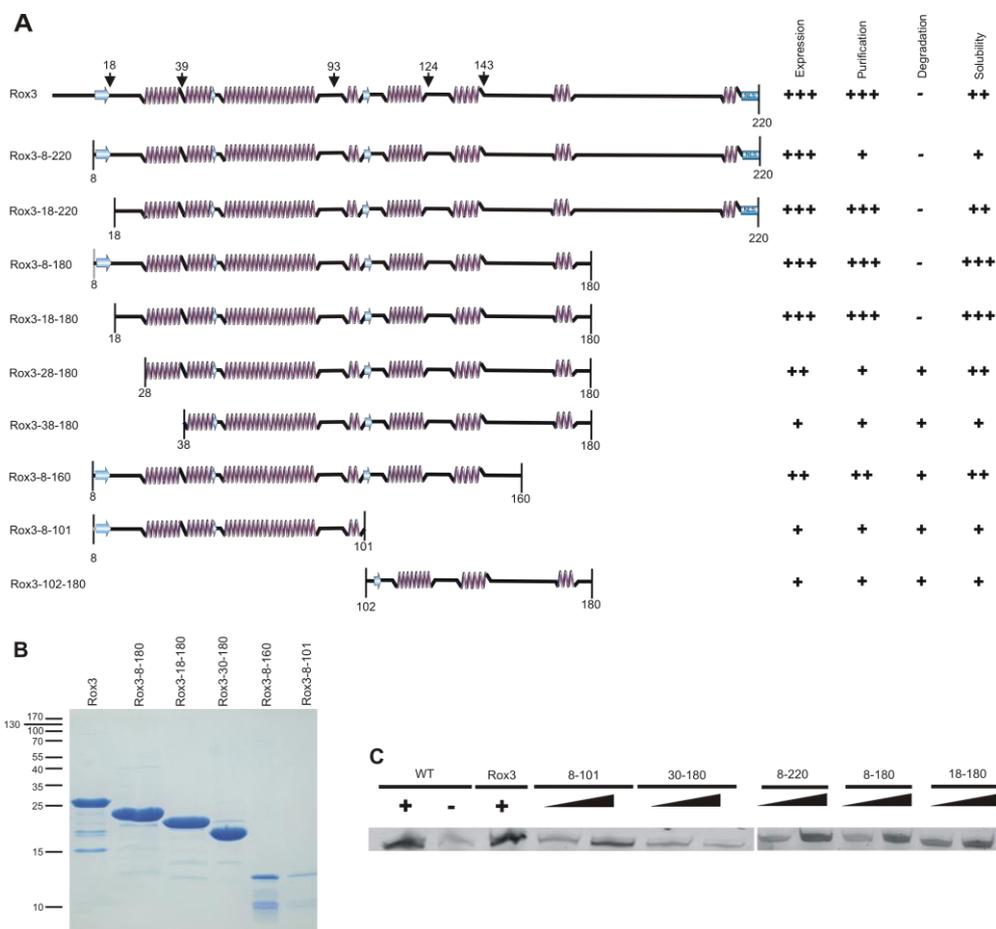

Figure 25: *Functional organization of S. cerevisiae Rox3.* **(A)** Recombinantly expressed Rox3 variants used in this study. Each fragment was tested for expression in *E. coli*, purification yield, spontaneous degradation and solubility. **B)** SDS-PAGE of recombinantly expressed Rox3 variants used for in-vitro transcription assay. **(C)** Results of *in-vitro* transcription assay of Rox3 constructs; **Lane 1**: Wild type nuclear extract (100 µg) for signal normalization; **Lane 2**: Nuclear extract from ΔRox3 strain; **Lane 3**: Recombinant expressed full length Rox3 added to ΔRox3 nuclear extract; **Lanes 4 & 13**: Recombinant expressed Rox3 variants added to ΔRox3 nuclear extract in two different concentrations each.

2.3 Nuclear localization sequences in Mediator subunits Rox3 and Med15

We searched each sequence of Mediator subunits for potential consensus sequences. By comparison of potential nuclear localization signals previously found in different organisms, we identified a nuclear localization sequence at the C-terminus of Rox3. The sequence motif (*KRRRL*) consists of a arginine-rich region, which is conserved among Rox3 homologues in fungi (Figure 26). To confirm this prediction and to test whether the NLS is functional *in vivo*, we used fluorescence microscopy for localization studies[4]. For this purpose, we created GFP fusion proteins of Rox3 (full length), *Rox3ΔNLS* (1-180) and *Rox3-NLS* (181-220). The plasmid encoding for the GFP-fusion variants were transformed to yeast BY strain, grown in YPD with selectivity marker and fixed with paraformaldehyde (MATERIALS & METHODS) and analyzed by microscopy. For the full length Rox3, fluorescence is resticted to the nucleus, indicating a accumulation of Rox3 within the nucleus, as expected. For Rox3 lacking the potential NLS sequence (*Rox3ΔNLS*), we observed an accumulation of the fluorescence singal within the cytoplasm. The isolated *Rox3-NLS* (181-220) was sufficient to direct GFP into the nucleus (Figure 26). This results demonstrate that the identified NLS is sufficient to direct Rox3 into the nucleus.

The Mediator (1.2 MDa) is one of the largest protein complexes inside the nucleus and it is unclear whether the Mediator proteins are assembled within the cytoplasmn or within the nucleus. Because of the Mediator's modular structure, it could be hypothezied that the passage through the nuclear pore complexes (NPC) happen separately for individual modules. Based on these assumptions, we searched all Mediator protein sequences for additional NLS. We found an potential NLS motif (*[KR]{2}x{0,1}[KR]{2,4}x{25,34}K{2,4}x{1,2}K*) at the C-terminus of Gal11/MED15. However, no NLS motif was found within the head-, middle- and kinase-modules. To test the Gal11/MED15 NLS *in vivo*, we generated a fusion protein of Gal11-NLS (974-1044) and mCherry and anlyzed the fluorescence signal by microscopy (Shaner, et al. 2004; MATERIALS & METHODS). Whereas the fluorescence of mCherry is accumulated within the cytoplasm, the fusion protein Gal11-NLS-mCherry result in accumulation within the nucleus. This result demonstrate that Gal11/Med15-NLS sufficient for nuclear localization *in vivo* and this is the first evidence for NLS function in Med15. However, further experiments are required to demonstrate whether the Gal11-NLS would be able to direct additional protiens, e.g. Med2 and Med3 which are members of the Gal11 subcomplex, into the nucleus and details of the context dependent NLS regulation.

---

[4] The Rox3-GFP localization experiment was performed in collaboration with Sonja Baumli (Cramer lab, Gene Center Munich) and Stephan Jellbauer (Jansen Lab, Gene Center Munich).
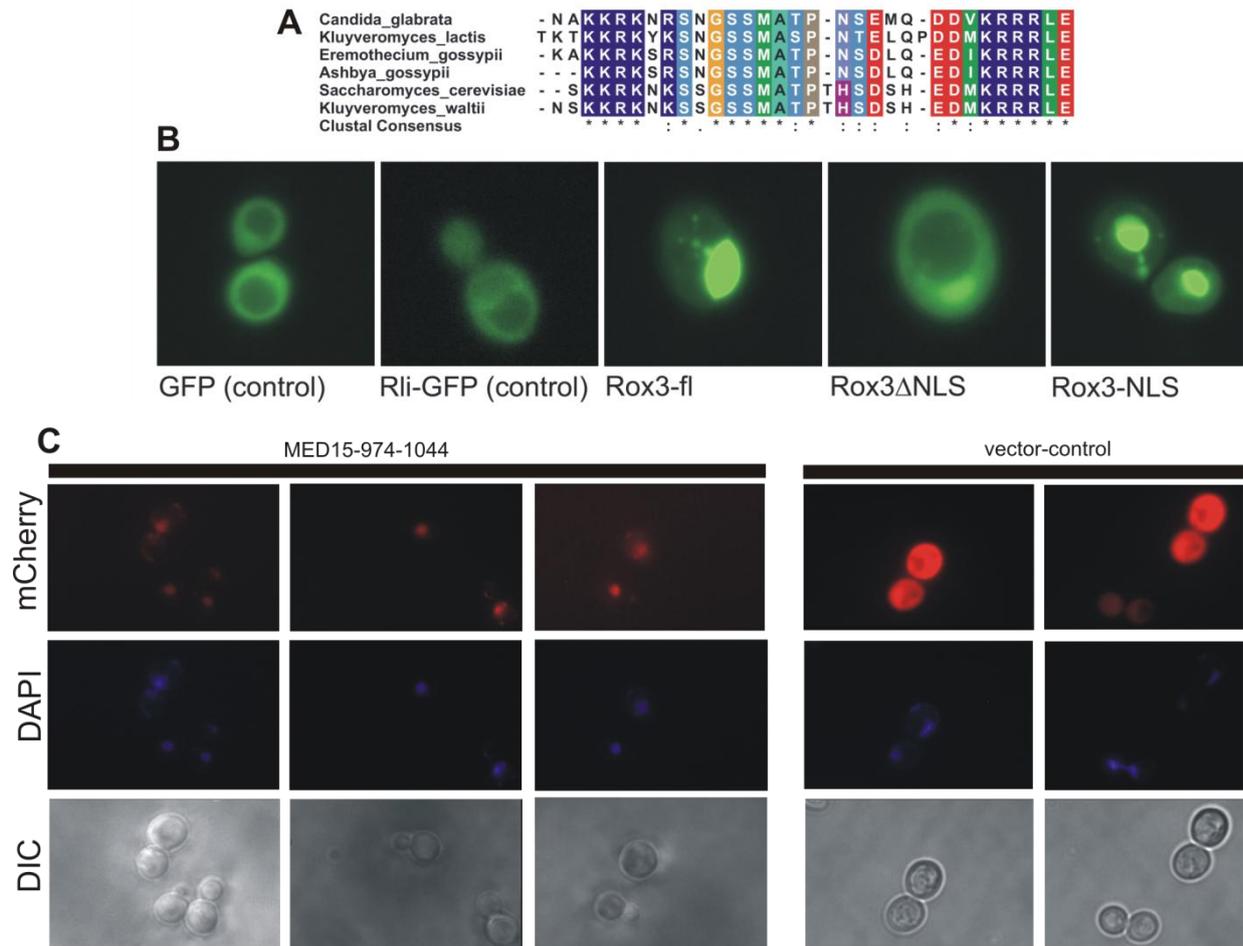
Figure 26: *Nuclear localization sequence in Mediator subunits Rox3 and Med15.* **A)** Muliple sequence alingment of selected nuclear localization sequence of Rox3 homologues identified in mycetes. **B)** Functional nuclear localization sequence of S. cerevisiae Rox3. Left: Green fluoresent protein (GFP) has no intrinsic localization functionality. Second-left: Cytoplasmic protein Rli1 fused to GFP as control experiment for cytoplasmic localization. Middle: Full length Rox3-GFP localizes to the nucleus. Second-right: Rox3 lacking the putative NLS localizes to the cytoplasm. Right: The putative nuclear localization sequence is sufficient to localize GFP to the nucleus. **C)** Localization studies of med15-974-1044 (Med15-NLS) in yeast. The C-terminal sequence ob Med15-974-1044 is suffiecient to localize mCherry to the nucleus.

REFERENCES

Abdulrehman, D., Monteiro, P. T., Teixeira, M. C., Mira, N.P., Lourenco, A.B., Costa dos Santos, S., Cabrito, T.R., Franscisco, A.P., Madeira, S.C., Aires, R.S., Oliveira, A.L., Sa-Correia, I., Freitas, A.T. (2011) YEASTRACT: providing a programmatic access to curated transcriptional regulatory associations in Saccharomyces cerevisiae through a web services interface. *Nucleic Acids Res.* **39**, doi:10.1093/nar/gkq1964

Adams, C., C.; Gross, D.S. (1991) The Yeast Heat Shock Response Is Induced by Conversion of Cells to Spheroblasts and by Potent Transcriptional Inhibitors. *J. Bacteriol.*, **173(23)**, 7429-7435.

Albert, I.; Marvrich, T.N., Thomsho, L.P., Qi, J., Zanton, S.J.; Schuster, S.C., Pugh, B.F. (2007) Translational and rotational settings of H2A.Z nucleosomes across the Saccharomyces cerevisiae genome. *Nature*, 572-576.

Albuquerque, C., P., S.; Payne, M., B.; Bafna, S.H.; Eng,V.; Zhou, H. (2008). A multidimensional chromatography technology for in-depth phosphoproteome analysis. *Mol. Cell. Proteomics*, **7**: 1389-1396.

Alepuz, P.M.; Jovanovic, A.; Reiser, V.; Ammerer, G. (2001) Stress induced map kinase Hog1 is part of transcription activation complexes. *Mol Cell*, **7**, 767–777.

Alexander, M. R., Tyers, M., Perret, M., Craig, M. B., Fang, K. S., Gustin, M. C. (2001). "Regulation of Cell Cycle Progression by Swe1p and Hog1p Following Hypertonic Stress. *Mol.Biol.Cell*, **12**: 53-62.

Allmang, C, Kufel, J, Chanfreau, G, Mitchell, P, Petfalski, E, Tollervey, D (1999) Functions of the Exosome in rRNA, snoRNA and snRNA synthesis. *EMBO J.*, **18**,5399-5410.

Alon, U. (2006) An Introduction to Systems Biology: Design Principles of Biological Circuits. Boca Raton, Florida: Chapman&Hall/CRC Press.

Amorim, M.J.; Cotobal, C.; Duncan, C.; Mata, J. (2010) Global coordination of transcriptional control and mRNA decay during cellular differentiation. *Mol. Sys. Biol.*, **6** (380), doi:10.1038/msb.2010.38, 1-11.

Andersson, A.F.; Lundgren, M.; Eriksson, S.; Rosenlund, M.; Bernader, R.; Nilsson, P. (2006) Global analysis of mRNA stability in the archaeon Sulfolobus. *Genome Biol.*, **7(R99),** doi:10.1186/gb-2006-7-10-r99, 1-10.

Andrau, J.-C.; van de Pasch, L.; Lijnzaad, P.; Bijma, T.; Koerkamp, M.G.; van de Peppel, J.; Wernder, M.; Holstege, F.C.P. (2006) Genome-Wide Location oft he Coactivator Mediator: Binding without Activation and Transient CdK8 Interaction on DNA. *Mol. Cell*, **22**, 179-192.

Ansari, S. A., Ganapathi, M., Benschop, J.J., Holstege, F.C.P., Wade, J.T., Morse, R.H. (2012) Distinct role of Mediator tail module in regulation of SAGA-dependent, TATA-containing genes in yeast. *EMBO J.* **31**, 44-57

Apponi, L., H.; Kelly, S.M.; Harreman, M.T.; Lehner, A.N.; Corbett, A.H.; Valentini, S.R. (2007) An Interaction between Two RNA Binding Proteins, Nab2 and Pub1, Links mRNA Processing/Export and mRNA Stability. *Mol. Cell. Biol.*, **27(18)**, 6569-6579.

Araki Y, Takahashi S, Kobayashi T, Kajiho H, Hoshino S, Katada T. (2001) Ski7p G protein interacts with the Exosome and the Ski complex for 3'-to-5' mRNA decay in yeast. *EMBO J.*; **20**, 4684

Armache, K.-J., Mitterweger, S., Meinhardt, A., Cramer, P. (2005) Structures of Complete RNA Polymerase II and Its Subcomplex, Rpb4/7. *J. Biol. Chem.,* **260(8)**, 7131-7134.

Ashe, M.P., De Long, S.K., and Sachs, A.B. (2000) Glucose depletion rapidly inhibits translation initiation in yeast. *Mol. Biol. Cell* **11:** 833–848.

Ashe, M.P., Slaven, J.W., De Long, S.K., Ibrahimo, S., and Sachs, A.B. (2001) A novel eIF2B-dependent mechanism of translational control in yeast as a response to fusel alcohols. *EMBO J.* **20**, 6464–6474;

Atkinson, G., C.; Baldauf, S., L.; Haurylik, V. (2008) Evolution of nonstop, no-go and nonsense mediated decay and their termination factor-derived components. *BMC Evolutionary Biology*, **8**, 290.

Singh, B.N.; Hampsey, M. (2007), A transcription-independent role for TFIIB in gene looping, *Mol. Cell* , **27** (2007) 806–816.

Bäckström, S., Elfving, N., Wingsle, G., Björklund, S. (2007). Purification of a Plant Mediator from Arabidopsis identifies PFT1 as the Med25 subuint. *Mol.Cell*, **26**, 436-438.

Baker, S.P.; Grant, P.A. (2007) The SAGA continues: expanding the cellular roel of a transcriptional co-activator complex. *Oncogene,* **26(37),** 5329-5340.

Bakshi, R.; Prakash, T., Dash, D.; Brahmachari, V. (2004) In silico characterization of the INO80 subfamily of SWI2/SNF2 chromatin remodeling proteins. *Biochem. Biophys. Res. Commun*., **320(1)**, 197-204.

Balasubramanian, B.; Lowry, C.V.; Zitomer, R.S (1993) The Rox1 repressor of the Saccharomyces cerevisiae hypoxic genes is a specific DNA-binding protein with a high-mobility-group motif. *Mol.Cell. Biol*. **13**, 6071-6078.

Bannister, A.J.; Zegermann, P.; Partridge, J.F.; Miska, E.A.; Thomas, J.O.; Allshire, R.C.; Kouszarides, T. (2001) Selective recognition of methylated lysine 9 on histone H3 by the HP1 chromo domain. *Nature*, **410**, 120-124.

Barbet, N.C., Schneider, U., Helliwell, S.B., Stansfield, I., Tuite, M.F., and Hall, M.N. (1996) TOR controls translation initiation and early G1 progression in yeast. *Mol. Biol. Cell,* **7**, 25–42;

Barik, D., Baumann, W.T., Paul, M.R., Nova, B., Tyson, J.J. (2010) A model of yeast cell-cycle regulation based on multisite phosphorylation. *Mol. Sys. Biol.* **6**, 1-18

Basehoar, A. D., Zanton, S., J., Pugh, F.,B. (2004) Identification and distinct regulation of yeast TATA box-containing genes. *Cell,* 116, 699–709.

Baudin A, Ozier-Kalogeropoulos O, Denouel A, Lacroute F, Cullin C (1993) A simple and efficient method for direct gene deletion in Saccharomyces cerevisiae. *Nucleic Acids Res* **21**(14)**:** 3329-3330

Bauer, S. R., P.N., Gagneur, J. (2011) Model-based Gene Set Analysis for Bioconductor. *Bioinformatics* **27(13)**, 1882-1883

Becskei A.; Serrano, L. (2000) Engineering stability in gene networks by autoregulation. *Nature,* **405**, 590–593.

Belakavadi, M., Pandey, P. K., Vijayvargia, R., Fondell, J. D (2008). MED1 Phosphorylation Promotes Its Association with Mediator: Implications for Nuclear Receptor Signaling. *Mol. Cell. Biol*, 3932-3942.

Bernard, L. (2004) Inhibition of 5' to 3' mRNA degradation under stress conditions in Saccharomyces cerevisiae: from GCN4 to MET16. *RNA*, **10**, 458-468.

Bernstein, J.; Kodursky, A.B.; Lin, P.-H.; Lin-Chao, S.; Cohen, S.N. (2002) Global analysis of mRNA decay and abundance in Escherichia coli at single-gene resolution using two-color fluorescent DNA microarrays. *PNAS*, **99(15)**, 9697-9702.

Berti, L., Mittler, G., Przemeck, G.K.H., Stelzer, G., Günzler, B., Amati, F., Conti, E., Dallapiccola, B., de Angelis, M.H., Novelli, G., Meisterernst, M. (2001) Isolation and Characterization of a Novel Gene from the DiGeorge Chromosomal Region That Encodes for a Mediator Subunit. *Genomics* **74(3)**, 320-332

Bhaumik, S.R. (2011) Distinct regulatory mechanisms of eukaryotic transcriptional activation by SAGA and TFIID. *Biochem. Biophys. Acta*, **1809**, 97-108.

Bhaumik, S.R., Green, M.R. (2002) Differential requirement of SAGA components for recruitment of TATA-box-binding protein to promoters in vivo. *Mol. Cell Biol.*, **22(21)**, 7365-7371.

Bhaumik, S.R.; Green, M.R. (2001) SAGA is an essential in vivo target of the yeast acidic activator Gal4p. *Genes & Dev.*, **15**, 1935-1945.

Bhoite, L. T., Y. Yu, and D. J. Stillman (2001) The Swi5 activator recruits the Mediator complex to the HO promoter without RNA polymerase II. *Genes Dev.* 15: 2457–2469.

Biegert A., Mayer C., Remmert M., Söding J., Lupas A. N. (2006) The MPI Bioinformatics Toolkit for protein sequence analysis. *Nucleic. Acids. Res.* **34**, W335-339.

Bilsland-Marchesan, E., Arin~o, J., Saito, H., Sunnerhagen, P., and Posas, F. 2000. Rck2 kinase is a substrate for the osmotic stress activated mitogen-activated protein kinase Hog1. *Mol. Cell. Biol.* **20**, 3887–3895.

Björklund, S., Gustafsson, C. M. (2005) The yeast Mediator complex and its regulation. *Trends in Biochem. Sciences* **30(5)**, 240-244

Bonneau, F.; Basquin, J.; Ebert, J.; Lorentzen, E.; Conti, E. (2009) The Yeast Exosome Functions as a Macromolecular Cage to Channel RNA Substrates for Degradation. *Cell*, **139**, 547–559.

Bonnerot, C.; Boeck, R.; Lapeyre, B. (2000) The Two Proteins Pat1p (Mrt1p) and Spb8p Interact in Vivo, Are Required for mRNA Decay, and Are Funtionally Linked to Pab1p. *Mol. Cell. Biol.*, **200(16)**, 5939-5946.

Bradford, M.M. (1976) A rapid and sensitive method for the quantitation of microgram quantities of protein utilizing the principle of protein-dye binding. *Anal Biochem.*, **72**, 248-254.

Breitkreutz, B.J., Stark, C., Reguly, T., Boucher, L., Breitkreutz, A., Livstone, M., Oughtred, R., Lackner, D.H., Bähler, J., Wood, V., Dolinski, K., Tyers, M. (2008) The BioGRID Interaction Database: 2008 update. *Nucleic Acids Res.*, **36**(Database issue), D637-40.

Brennan, C.M., Steitz, J. A., (2001) HuR and MRNA stability, *Cell Mol. Life Sci.*, **58**, 266-277.

Brewster, J.L., de Valoir, T., Dwyer, N.D., Winter, E., and Gustin, M.C. 1993. An osmosensing signal transduction pathway in yeast. *Science*, **259**, 1760–1763.

Briggs, S.D.; Bryk, M.; Strahl, B.D. (2001) Histone H3 lysine 4 methylation is mediated by Set1 and required for cell growth and rDNA silencing in Saccharomyces cerevisiae. *Genes&Dev*, **15**, 3286-3295.

Brivanlou, A.H.; Darnell, J.E. (2002) Signal Transduction and the Control of Gene Expression. *Science*, **295**, 813.

Brown, C.E.; Howe, L.; Sousa, K.; Alley, S.C.; Carrozza, M.J.; Tan, S.; Workman, J.L. (2001) Recruitment of HAT Complexes by Direct Activator Interactions with the ATM-Related Tra1 Subunit. *Science*, **292,** 2333.

Brown, C.E.; Sachs, A.B. (1998) Poly(A) Tail Length control in Saccharomyces cerevisiae Occurs by Message-Specific Deadenylation. *Mol. Cell. Biol.*, **18(11)**, 6548-6559.

Bryson, K., McGuffin, L.J., Marsden, R.L., Ward, J.J., Sodhi, J.S., Jones, D.T. (2005) Protein structure prediction servers at University College London. *Nucl. Acids Res.*, **33**, W36-38.

Brzovic, P. S. H., C.C., Kisselev, L., Vernon, R., Herbig, E., Pacheco, D., Warfield, L., Littlefield, P., Baker, D., Klevit, R.E., Hahn, S. (2011) The Acidic Transcription Activator Gcn4 Binds the Mediator Subunit Gal11/Med15 Using a Simple Protein Interface Forming a Fuzzy Complex. *Mol.Cell* **44**, 942-953

Burley, S., K. (1996) The TATA box binding protein. *Current Opinion in Structural Biology,* 6, 69–75.

Cai, G., Imasaki, T., Takagi, Y., Asturias, J.F. (2009) Mediator Structural Conservation and Implications for the Regulation Mechanism. *Structure* **17(1)**, 559-567

Calvo, O.; Manley, J., L. (2003) Strange bedfellows: polyadenylation factors at the promoter. *Genes Dev.* **17**, 1321–1327.

Capaldi, A.P.; Kaplan, T.; Liu, Y.; Habib, N.; Regev, A.; Friedman, N., O'Shea, E. (2008) Structure and function of a transcriptional network activated by the MAPK Hog1. *Nat. Genet.*, doi:10.1038/ng.235; 1-7;

Carey, M. Li, B. Workman, J. L. (2006) RSC exploits histone acetylation to abrogate the nucleosomal block to RNA polymerase II elongation. *Mol. Cell*, **4(3)**, 481-487.

Carlson, M. (1997) Genetics of transcriptional regulation in yeast: connections to the RNA polymerase II CTD. *Annu. Rev. Cell Dev. Biol.*, **13**, 1-23.

Causton, H. C., Ren, B., Koh, S.S., Harbison, C.T., Kanin, E., Jennings, E.G., Lee, T.I., True, H.L., Lander, E.S., and Young, R.A. (2001) Remodeling of yeast genome expression in response to environmental changes. *Mol. Biol. Cell* **12**, 323-327

Chandy, M.; Gutiérrez, J.L.; Prochasson, P.; Workman, J.L. (2006) SWI/SNF displaces SAGA-acetylated nucleosomes. *Eukaryot. Cell, 5(10)*, 1738-47.

Chang, C.-H.; Yarbro, J.W.; Mann, D.E.; Gautiery, R.F. (1978) Effects of 1,10-Phenanthroline and a Zinc Complex of 1,10-Phenanthroline on Nucleic Acid Synthesis in Mouse Liver and Spleen. *The Journal of Pharmacology and Experimental Therapeutics*, **205(1)**, 27-33.

Chang, L.M.S.; Bollum, F.J. (1970) Deoxynucleotide-Polymerizing Enzymes of Calf Thymus Gland, IV. Inhibition of Terminal Deoxynucleotidyl Transferase by Metal Ligands. *PNAS*, **65(4)**, 1041-1048.

Chang, Y.-W., Howard, S. C., Herman, P. K. (2004). The Ras/PKA Signaling Pathway Directly Targets the Srb9 Protein, a Component of the General RNA Polymerase II Transcription Apparatus. *Mol. Cell. Biol* , **15**, 9.

Chellappan, S.P. (2001) HOG on the promoter: regulation of the osmotic stress response. *Sci STKE* , **2001**, E1

Chen, C.-Y.; Gherzi, R.; Ong, S.-E.; Chan, E.L.; Raijmakers, R.; Pruijn, G.J.M.; Stoeckling, G.; Moroni, C.; Mann, M.; Karin, M. (2001). AU binding proteins recruit the Exosome to degrade ARE-containing mRNAs. *Cell*, **107**, 451-464.

Cherry, J. M., Ball, C., Weng, S., Juvik, G., Schmidt, R., Adler, C., Dunn, B., Dwight, S., Riles, L., Mortimer, R.K., Botstein, D. (1997). Genetic and physical maps of Saccharomyces cerevisiae. *Nature,* **387**, 67-73.

Cheung, P.; Tanner, K.G.; Cheung, W.L.; Sassone-Corsi, P.; Denu, J.M. (2000) Synergistic Coupling of Histone H3 Phosphorylation and Acetylation in Response to Epidermal Growth Factor Stimulation. *Mol. Cell* , **5**, 905-915.

Chi, A., Huttehhower, C., Geer, L. Y., Coon, J. J., Syka, J. E. P., Bai, D. L., Shabanowitz, J., Burke, D. J., Troyanskaya, O. G., Hunt, D. F. (2007) Negative regulation of Gcn4 and Msn2 transcription factors by Srb10 cyclin-dependent kinase. *Genes Dev.* **15**, 1078-1092

Clayton, A.L.; Hazzalin, C.A.; Mahadevan, L.C. (2006) Enhanced Histone Acetylation and Transcription: A Dynamic Perspective. *Mol. Cell*, **23**, 289-296.

Cleary, M.C.; Meiering, C.D.; Jan, E.; Guymon, R.; Boothroyd, J. (2005) Biosynthetic labeling of RNA with uracil phosphoribosyltransferase allows cell-specific microarray analysis of mRNA synthesis and decay. *Nat. Biotechn.*, **23(2)**, 232-238.

Cole, C., Barber, J.D., Barton, G.J. (2008) The Jpred 3 secondary structure prediction server. *Nucleic acid research*, **36**, W197-W201

Collart, M.A. (2003) Global control of gene expression in yeast by the Ccr4-Not complex. *Gene*, **313**, 1-16.

Coller, J.; Parker, R. (2004) Eukaryotic mRNA Decapping. *Ann. Rev. Biochem.,* **73**, 861-890.

Consortium, T. U. (2010). Ongoing and future developments at the Universal Protein Resource. *Nucleic Acids Res.*, **39**, D214-D219.

Cormack BP, Struhl K. (1992) The TATA-binding protein is required for transcription by all 3 nuclear-RNA polymerases in yeast-cells. *Cell*, 69, 685–696.

Cox, J., Mann, M. (2008) MaxQuant enables high peptide identificationrates, individualized p.p.b.-range mass accurancies and proteome-wide protein quantification. *Nat. biotech.* **26**, 1367-1372

Cox, J., Mann, M. (2011) Quantitative, High-Resolution Proteomics for Data-Driven Systems Biology. *Annu. Rev.* 10.1146/annurev-biochem-061308-093216

Cox, J., Matic, I., Hilger, M., Nagaraj, N., Selbach, M., Olsen, J. V., Mann, M. (2009) A practical guide to the MaxQuant

computational platform for SILAC-based quantitative proteomics. *Nat. protocols* **4**, 698-705

Cramer, P., Bushnell, D.A., and Kornberg, R.D. (2001). Structural basis of transcription: RNA polymerase II at 2.8 angstrom resolution. *Science,* **292**, 1863–1876.

Crick, F. (1958) The Biological Replication of Macromolecule. Symp. Soc. Exp. Biol. XII, 138

Crick, F. (1970) Central Dogma of Molecular Biology. Nature, 227 (8), 561-563

Daniel, J., A.; Grant, P., A. (2007), Multi-tasking on chromatin with the SAGA coactivator complexes. *Mutat. Res*. 618, 135–148.

Daniel, J.A.; Pray-Grant, M.G., Grant, P.A. (2005) Effector proteins for methylated histones: an expanding family. *Cell Cycle*, **4(7),** 919-926.

Darieva, Z.; Clancy, A.; Bulmer, R.; Williams, E.; Pic-Taylor, A.; Morgan, B.A.; Sharrocks, A.D. (2010) A competitive transcription factor binding mechanism determines the timing of late cell cycle-dependent gene expression. *Mol. Cell*, **38(1)**, 29-40.

De Nadal, E.; Zapater, M.; Alepuz, P.M.; Sumoy, L.; Mas, G.; Posas, F. (2004) The MAPK Hog1 recruits Rpd3 histone deacetlyse to activate osmoresponsive genes. *Nature*, **427**, 370-375.

De Nadal., Posas, F. (2010) Multilayered control of gene expression by stress-activated protein kinases. *EMBO J.,* **29**, 4-13.

De Vit, M.J., Waddle, J.A.; Johnston, M. (1997) Regulated nuclear translocation of the Mig1 glucose repressor. *Mol. Biol. Cell*, **8**, 1603-1618.

Delaunay, A.; Isnard, A.-D.; Tolendano, M.B. (2000) H_2O_2 sensing through oxidation of the Yap1 transcription factor. *EMBO J*., **19(19)**, 5157-5166.

Delepierre, M., Van Heijenoort, C., Igolen, J., Pothier, J., Le Bret, M. Roques, B.P. (1989) Reassesment of structural characteristics of th d(CGCG)2 actinomycin D complex from complete 1H and 31P NMR. *J. Biomol. Struct. Dyn.*, **7(3),** 557-89.

Denisenko, O., Bomsztyk, K. (2008). Epistatic Interaction Between the K-Homology Domain Protein HEK2 and SIR1 at HMR and Telomeres in Yeast. *J. Mol. Biol,*. **375**, 1187-1178.

Deroo, B.J.; Archer, T.K. (2001) Glucocorticoid receptor-mediated chromatin remodeling in vivo. *Ocogene*, **20**, 3039-3046.

Dikstein, R. (2011) The unexpected traits associated with the core promoter elements. *Transcription*, 2(5), 201-206.

Dolken, L.; Ruzsics, Z.; Rädle, B.; Friedel, C.C.; Zimmer, R.; Mages, J.; Hoffmann, R.; Dickinson, P.; Forster, T.; Ghazal, P.; Koszinowski, U.H. (2008) High-resolution gene expression profiling for simultaneous kinetic parameter analysis of RNA synthesis and decay. *RNA*, **14**, 1959-1972.

Ducker, C.E.; Simpson, R.T. (2000) The organized chromatin domain of the repressed yeast a specific gene STE6 contains two molecules of the corepressor TUP1p per nucleosome. *EMBO J*., **19**, 400-409.

Duttagupta, R.; Tian, B.; Wilusz, C.J.; Khounh, D.T.; Soteropoulos, P.; Ouyang, M.; Doughtery, J.P.; Peltz, S.W. (2005). Global Analysis of Pub1p Targets Reveals a Coordinate Control of Gene Expression through Modulation of Binding and Stability. *Mol. Cell. Biol.,* **25(13),** 5499-5513.

Edmondson, D.G.; Smith, M.M., Roth, S.Y. (1998) Repression domain of the yeast global repressor TUP1 interactions directly with histonse H3 and H4. *Genes & Dev*., **10**, 1247-1259.

Eisen, J.A.; Sweder, K.S.; Hanawalt, P.C. (1995) Evolution of the SNF2 family of proteins: subfamilies with distinct sequences and functions. *Nucleic. Acids. Res*., **23(14)**, 2715-2723.

Elmlund, H.; Baraznenok, V.; Lindahl, M.; Samuelsen, C. O.; Koeck, P., J., Holmberg, S.; Hebert, H.; Gustafsson, C.M. (2006) The cyclin-dependent kinase 8 module sterically blocks Mediator interactions with RNA polymerase II. *Proc. Natl. Acad. Sci. USA*, **103(43),** 15788-93.

Enjalbert, B., Parrou, J.L., Teste, M.A. Francois, J. (2004) Combinatorial control by the protein kinases PKA, PHO85 and

SNF1 of transcriptional induction of the Saccharomyces cerevisiae GSY2 gene at the diauxic shift. *Mol. Gen. Genomics* **271(6),** 697-708

Escote, X., Zapater, M., Clotet, J., and Posas, F. (2004). "Hog1 mediates cell-cycle arrest in G1 phase by the dual targeting of Sic1. *Nat.Cell Biol.,* **6**, 997-1002.

Evguenieva-Hackenberg, E.; Wagner, S.; Klug, G. (2008) Chapter 19 In Vivo and In Vitro Studies of RNA Degrading Activities in Archae. *Methods in Enzymology*, **447**, 381-416.

Fan, J.; Yang, X.; Wang, W.; Wood, W.H.; Becker, K.G.; Gorospe, M. (2002) Global analysis of stress-regulated mRNA turnover by using cDNA arrays. *PNAS*, **99(16)**, 10611-10616.

Fan, X., Chou, D. M., Struhl, K. (2006). Mediator is recruited by many activators involved in stress-response. *Nat. Struct. Mol. Biol.*, **13**, 4.

Femino, A. M., Fay, F. S., Fogarty, K., Singer, R. H. (1998) Visualization of single RNA transcripts in situ. *Science*, **280**, 585-590.

Fernandes, L.; Rodrigues-Pousada, C., Struhl, K. (1997) Yap, a Novel Family of Eight bZIP Proteins in *Saccharomyces cerevisiae* with distinct Biological Functions. *Mol. Cell. Biol.,* **17(12)**, 6982-6993.

Ferrigno, P., Posas, F., Koepp, D., Saito, H., Silver, P.A. (1998) Regulated nucleo/cytoplasmic exchange of HOG1 MAPK requires the importin ß homologs NMD5 and XPO1. *EMBO J.*, **17**, 5606-5614.

Flanagan, J.F.; Mi, L.Z.; Chruszcz, M.; Cymborowski, M., Clines, K.L.; Kim, Y.; Rastinejad, F.; Khorasanizadeh, S. (2005) Double chromodomains cooperate to recognize the methylated histone H3 tail. *Nature*, **438**, 1181-1185.

Flanagan, P. M., Kelleher, R. J., Sayre, M. H., Tschochner, H., Kornberg, R. D. (1991) A Mediator required for activation of RNA polymerase II transcription in vitro. *Nature* **350(6317),** 436-438

French, S.L., Osheim, Y.N., Cioci, F., Nomura, M., and Beyer, A.L. (2003). In exponentially growing Saccharomyces cerevisiae cells, rRNA synthesis is determined by the summed RNA polymerase I loading rate rather than by the number of active genes. *Mol. Cell. Biol*,. **23**, 1558–1568.

Friedel, C.C.; Dölken, L.; Ruzsics, Z.; Koszinowski, U.H. (2009) Conserved principles of mammalian transcriptional regulation revealed by RNA half-life. *Nucleic. Acid. Res.*, doi:10.1093/nar/gkp542, 1-12.

Fuchs, S.M.; Laribee, R.N.; Strahl, B.D. (2009) Protein modifications in transcription elongation. *Biochim. Biophys. Acta*, **1789**, 26-36.

Fuda, N. J., Ardehali, M. B. & Lis, J. T. (2009). Defining mechanisms that regulate RNA polymerase II transcription *in vivo. Nature,* **461**, 186–192

Fuge, E.K., Braun, E.L., and Werner-Washburne, M. (1994) Protein synthesis in long-term stationary-phase cultures of Saccharomyces cerevisiae. *J. Bacteriol.* , **176**, 5802–5813;

Gandhi, S.J., Zenklusen, D., Lionnet, T., Singer, R.H. (2011) Transcription of functionally related constitutive genes is not coordinated. *Nat. struct. Mol. Biol.*, **18(1)**, 27-35.

Ganggaraju, V.K.; Bartholomew, B. (2007) Mechanisms of ATP-dependent chromatin remodeling. *Mutat. Res.*, **618**, 3-17.

Garbett, K.A.; Tripathi, M.K.; Cencki, B.; Layer, J.H.; Weil, P.A. (2007) Yeast TFIID serves as a coactivator for Rap1p by direct protein–protein interaction. *Mol. Cell. Biol.*, 27,297–311.

Garcia-Marinez, J.; Aranda, A.; Pérez-Ortin, J.E. (2004) Genomic Run-On Evaluates Transcription Rates for All Yeast Genes and Identifies Gene Regulatory Mechanisms. *Mol. Cell*, **15**, 303-313.

Garcia-Rodriguez, L.J., Gay, A.C., Pon, L. A. (2007) PUF3, a Pumilio family RNA binding protein localizes to mitochondria and regulate mitochondrial biogeneisis and motility in budding yeast. *J. Cell Biol*, **176**, 197-207.

Gardner, T.S.; Collins, J.J. (2000) Neutralizing noise in gene networks. *Nature*, **405**, 520–521.

Garneau, N., L.; Wilusz, J.; Wilusz, C. (2007) The highways and byways of mRNA decay. *Nat. Rev. Mol. Cell Biol.*, **8**, 113-126.

Gasch, A. P., and Werner-Washburne, M (2002). The genomics of yeast responses to environmental stress and starvation. *Funct Integr Genomics* , **2**, 181-192.

Gasch, A.P.; Spellman, P.T.; Kao, C.M.; Carmel-Harel, O.; Eisen, M.B.; Storz, G.; Botstein, D.; Brown, P.O. (2000) Genomic Expression Programs in the Response of Yeast Cells to Environmental Changes. *Mol. Biol. Cell*, **11**, 4241-4257.

Gasteiger, E., Hoogland, C., Gattiker, A.,Duvaud, S., Wilkins, M.R., Appel, R.D., Bairoc, A. (2005) Protein Identification and Analysis Tools on the Expasy server: *Humana Press*.

Gasteiger, E.; Hoogland, C.; Gattiker, A.; Duvaud, S.; Wilkins, M.R.; Appel, R.D.; Bairoch, A. (2005) Protein Identification and Analysis Tools on the ExPASy Server: Humana Press.

Gentleman, R. C., Carey, V. J., Bates, D. M., Bolstad, B., Dettling, M., Dudoit, S., Ellis, B., Gautier, L., Ge, Y., Gentry, J., Hornik, K., Hothorn, T., Huber, W., Iacus, S., Irizarry, R., Leisch, F., Li, C., Maechler, M., Rossini, A. J., Sawitzki, G., Smith, C., Smyth, G., Tierney, L., Yang, J. Y., Zhang, J. (2004). Bioconductor: open software development for computational biology and bioinformatics. *Genome biology*, **5(10)**, R80+

Georgiou, G. (2002) How to Flip the (Redox) Switch. *Cell*, **111**, 607-610.

Gerber, A. P.; Herschlag, D.; Brown, P. O. (2004) Extensive Association of Functionally and Cytotopically Related mRNAs with Puf Familiy RNA-Binding Proteins in Yeast. *PlosBiology,* **2(3)**, 0342-0354

Gherzi, R.; Lee, K.-Y.; Briata, P.; Wegmüller, D.; Moroni, C.; Karin, M.; Chen, C.-Y. (2004) A KH Domain RNA Binding Protein, KSRP, Promotes ARE-directed mRNA Turnover by Recruiting the Degradation Machinery. *Mol. Cell,* **14**, 571-583.

Giardina, C.; Lis, J., T. (1993) DNA melting on yeast RNA polymerase II promoters. *Science*, 261, 759–762.

Gill, T.; Cai, T.; Aulds, J. (2004) RNAse MRP Cleaves the CLB2 mRNA To Promote Cell Cycle Progression: Novel Method of mRNA Degradation. *Mol. Cell. Biol.*, **24(3)**, 945-953.

Goldstrohm, A.C.; Wickens, M. (2006) Multifunctional deadenylase complexes diversify mRNA control. *Nat. Rev. Mol. Cell Biol.*, **9**, 337-345.

Gonzalez, C. I., Ruiz-Echevarria, M. J., Vasudevan, S., Henry, M. F. & Peltz, S. W. (2000) The yeast hnRNP-like protein Hrp1/Nab4 marks a transcript for nonsense-mediated mRNA decay. *Mol. Cell* **5**, 489–499.

Gorospe, M. (2003) HuR in the Mammalian Genotoxic Response. *Cell Cycle*, **2(5)**, 412-414;

Gottesfeld, J.M., Luger, K. (2001) Energetics and affinity of the histone octamer for defined DNA sequences. *Biochemistry*, **40(37)**, 10927-10933.

Gouet, P., Courcelle, E., Stuart, D.I. and Metoz, F. (1999). ESPript: multiple sequence alignments in PostScript. *Bioinformatics*. **15** 305-8

Gray, N.K.; Wickens, M. (1998) Control of Translation Initiation in Animals. *Ann. Rev. Cell. Dev. Biol.*, **14**, 399-458.

Greatrix, B.W.; van Vuuren, H.J.J. (2006) Expression of the HXT13, HXT15 and HXT17 genes in Saccharomyces cerevisiae and stabilization of the HXT1 gene transcript by sugar-induced osmotic stress. *Curr. Genet.*, **49**, 205-217.

Greeenbaum, D., Colangelo, C., Williams, K., Gerstein, M. (2003) Comparing protein abundance and mRNA expression levels on a genomic scale. *Genome Biol.*, **4**, 117.

Greger, I.H., and Proudfoot, N.J. (1998). Poly(A) signals control both transcriptional termination and initiation between the tandem GAL10 and GAL7 genes of Saccharomyces cerevisiae. *EMBO J.* 17, 4771– 4779.

Grigull,, J.; Mnaimneh, S.; Pootoolal, J.; Robinson, M.D.; Hughes, T.R. (2004) Genome-Wide Analysis of mRNA Stability Using Transcription Inhibitors and Microarrays Reveals Posttranscriptional Control of Ribosome Biogenesis Factors. *Mol. Cell. Biol.*, **24(12)**, 5534-5547.

Gruhler, A., Olsen, J. V., Mohammed, S., Mortensen, P., Faergeman, N. J., Mann, M., Jensen, O. N. (2005). Quantitative Phosphoproteomics Applied to the Yeast Pheromone Signaling Pathway. *Mol. Cell Proteomics*, 310-313: 310.

Grunberg-Manago, M. (1999) Messenger RNA Stability and Its Role in Control of Gene Expression in Bacteria and Phages. *Annu. Rev. Genet.*, **33**, 193-227

Grüne, T.; Brzeski, J.; Eberharter, A.; Clapier, C.R.; Corona, D.F.; Becker, P.B.; Müller, C.W. (2003) Crystal structure and functional analysis of a nucleosome recognition module ot the remodeling factor ISWI. *Mol. Cell,* **12(2)**, 449-460.

Guidi, B. W., Bjornsdottir, G., Hopkins, D. C., Lacomis, L., Erdjument-Bromage, H., Tempst, P., Myers, L. C. (2004). Mutual targeting of Mediator and the TFIIH kinase Kin28. *J. Biol. Chem.,* **279**, 29114-29120.

Gutiérrez, R. A.; Ewing, R.M.; Cherry, J.M., Green, P.J. (2002) Identification of unstable transcripts in Arabidopsis by cDNA microarray analysis: Rapid decay is associated with a group of touch- and specific clock-controlled genes. *PNAS*, **99(17)**, 11513-11518.

Haberland, M.; Montgomery, R.L., Olson, E.N. (2009) The many roles of histone deacetylases in development and physiology: implications for disease and therapy. *Nat. Rev. Genet.*, **10**, 32-42.

Hahn, S. (2004) Structure and mechanism of the RNA polymerase II transcription machinery. *Nat. Struct. Mol. Biol.*, 11(5), 394-403

Hahn, S., Buratowski, S., Sharp, P., A., Guarente, L. (1989) Yeast TATA-binding protein TFIID binds to TATA elements with both consensus and nonconsensus DNA-sequences. *Proc. Natl Acad.Sci. USA*, 86, 5718–5722.

Halbeisen, R.E., Galgano, A., Scherrer, T., Gerber, A. P. (2006) Post transcriptional gene regulation: from genome-wide studies to principles. *Cell. Mol. Life Sci.*, **65**, 798-813.

Halbeisen, R.E., Gerber, A. P. (2009) Stress dependent Coordination of Transcriptome and Translatome in Yeast. *PLOS biology*, **7(5)** e1000105, 1-15;

Hall, T.A. (1999). BioEdit: a user-friendly biological sequence alignment editor and analysis program for Windows 95/98/NT*. Nucl. Acids. Symp. Ser.* **41**, 95-98.

Hallberg, M., Polozkov, G.V., Hu, G.-Z., Beve, J., Gustafsson, C.M., Ronne, H., Bjoerklund, S. (2004). Site specific Srb10-dependent phosphorylation of the yeast Mediator subunit Med2 regulates gene expression from the 2-micrometer plasmid. *Proc. Natl. Sci. USA,* **101**, 3370-3376.

Hampsey, M. (1998) Molecular genetics of the RNA polymerase II general transcriptional machinery. *Microbiol. Mol. Biol. Rev.*, **62**, 465–503.

Han, J.; Lee, J.-D.; Bibbs, L.; Ulevitch, R.J. (1994) A MAP Kinase Targeted by Endotoxin and Hypersomolarity in Mammalian Cells. *Science*, **265**, 803-811.

Hao, N.; Behar, M.; Parnell, S.C.; Torres, M.P.; Borchers, C.H.; Elston, T.C.; Dohlman, G.H. (2007) A Systems-Biology Analysis of Feedback Inhibition in the Sho1 Osmotic-Stress-Response Pathway. *Curr. Biol.,* **17**, 659-667.

Harel-Sharvit, L., Eldad, N., Haimovich, G., Barkai, O., Duek, L., Choder, M. (2010) RNA Polymerase II Subunits Link Transcription and mRNA Decay to Translation. *Cell,* **143**, 552-563.

Harigaya, Y., Jones, B.N.; Muhlrad, D., Gross, J.D.; Parker, R. (2010) Identification and Analysis of the Interaction between Edc3 and Dcp2 in *Saccharomyces cerevisiae*. Mol. Cell. Biol., **30(6)**, 1446-1456.

Hassan, A.H.; Neely, K.E.; Vignali, M., Reese, J.C.; Workman, J.L. (2001) Promoter Targeting of Chromatin-Modifying Complexes. *Frontiers in Bioscience*, **6**, 1054-1064.

Hassan, A.H.; Prochasson, P.; Neely, K.E.; Galasinski, S.C.; Chandy, M.; Carrozza, M.J., Workman, J.L. (2002) Function and Selectivity of Bromodomains in Anchoring Chromatin-Modifying Complexes to Promoter Nucleosomes. *Cell*, **111**, 369-379.

Hayles, B., Yellaboina, S., Wang, D. (2010) Comparing Transcription Rate and mRNA abundance as Parameters for Biochemical Pathway and Network Analysis. *PlosONE*, **5**.

Herbig, E., Warfield, L., Fish, L., Fishburn, J., Knutson, B. A., Moorefield, B., Pacheco, D., Hahn, S. (2010) Mechanism of Mediator Recruitment by Tandem Gcn4 Activation Domains and Three Gal11 Activator-Binding Domains. *Mol.*

Biol. Cell **30(10)**, 2376-2390.

Herrick, D.; Parker, R.; Jacobson, A. (1990) Identification and Comparison of Stable and Unstable mRNAs in Saccharomyces cerevisiae. *Mol. Cell Biol.,* **10(5),** 2269-2284.

Hilgers, V., Teiseira, D., Parker R. (2006) Translation-independent inhibition of mRNA deadenylation during stress in Saccharomyces cerevisiae, *RNA*, **12**, 1835-1845.

Hinnebusch, A. G. N., K. (2002) Gcn4p, a master regulator of gene expression, is controlled at multiple levels by diverse signals of starvation and stress. *Eucaryotic Cell* **1**, 22-32

Hirata, Y., Andoh, T., Asahara, T., Kikuchi, A. (2003) Yeast Glycogen Synthase Kinase-3 Activates Msn2pdependent Transcription of Stress Responsive Genes. *Mol. Biol. Cell* **14(1),** 302-12.

Hiroyashi, K., Lis, J.T. (1999) Nuclear run-on assays: assessing by measuring densitiy of engaged RNA polymerases. *Methods Enzymol,.* **304**, 351-362.

Hodson, J.A.; Bailis, J.M.; Forsburg, S.L. (2003) Efficient labeling of fission yeast Schizosaccharomyces pombe with thymidine and BUdR. *Nucleic. Acid. Res.,* **31(21),** DOI: 10.1093/nar/gng134 1-8.

Hohmann, S. (2002) Osmotic Stress Signaling and Osmoadaption in Yeasts. *Microbiol. Mol. Biol. Rev.,* **66(2)**, 300-372.

Holmberg, C., Tran, S.E.F., Erksson, J.E., Sistonen, L. (2002) Multisite phosphorylation provides sophisticated regulation of transcription factors. *Trends in Biochem. Sciences* **27**, 619-627

Holstege, F.C.P., Jennings, E.G.; Wyrick, J.J.; Lee, T.I.; Hengartner, C.J., Green, M.R.; Golub, T.R.; Lander, E.S.; Young, R.A. (1998) Dissecting the Regulatory Circuitry of a Eukaryotic Genome, *Cell,* **95**, 717-728.

Holt, L. J., Tuch, B. B., Villén, J., Jonsen, A. D., Gygi, S. P., Morgan, D. O. (2009). Global Analysis of Cdk1 Substrate Phosphorylation Sites Provides Insights into Evolution. *Science,* **325**, 1682-1686.

Hook, B.A.; Goldstrohm, A.C., Seay, D.J.; Wickens, M. (2007) Two Yeast PUF Proteins Negatively Regulate a Single mRNA. *JBC*, **282(21)**, 15430-15438.

Horak, C. E., N. M. Luscombe, J. Qian, P. Bertone, S. Piccirrillo et al. (2002) Complex transcriptional circuitry at the G1/S transition in Saccharomyces cerevisiae. *Genes Dev*. 16: 3017–3033.

Hoskins, L. (1997) Yeast genomic DNA Prep. http://labs.fhcrc.org/hahn/Methods/mol_bio_meth/ yeast_genom_dna.html

Houseley, J., Tollervey, D., (2009) The Many Pathways of RNA Degradation, *Cell*, **136**, 763-776

Hu, W., Sweet, T.J., Chamnongpol, S., Baker, K.E., Coller, J., (2009), Co-translational mRNA decay in Saccharomyces cerevisiae, *Nature*, **461**, 225, 230

Huang, M.; Zhou, Z.; Elledge, S.J. (1997) The DNA replication and damage checkpioint pathways induce transcription by inhibition oft he Crt1 repressor. *Cell*, **94**, 595-605.

Hundt, S.; Zaigler, A.; Lange, C.; Soppa, J.; Klug, G. (2007) Global Analysis of mRNA Decay in *Halobacterium salinarium* NRC-1 at Single-Gene Resolution Using DNA Microarray. *J. Bacteriol.,* **189(19)**, 6936-6944.

Huisinga, K. L.; Pugh, B. F. (2004) A genome-wide housekeeping role for TFIID and a highly regulated stress-related role for SAGA in Saccharomyces cerevisiae. *Mol. Cell*, **13(4)**, 573-85.

Huttlin, E. L., Jedrychowski, M. P., Elias, J. E., Goswami, T., Rad, R., Beausoleil, S. A., Villén, J., Haas, W., Sowa, M. E., Gygi, S. P. (2010). A Tissue-Specific Atlas of Mouse Protein Phosphorylation and Expression. *Cell*, **143**, 1174-1189.

Hyeon, H.K., Abdelmohsen, K., Gorospe, M. (2010) Regulation of HuR by DNA Damage Response Kinases, *J. Nucleic Acids*, Article ID 981487, 8 pages.

Hyrigaya, Y., Tanaka, H., Yamanaka, S., Tanaka, K., Watanabe, Y., Tsutsumi, C., Chikashige, Y., Hiraoka, Y., Yamashita, A., Yamamoto, M. (2006) Selective elimination of messenger RNA prevents an incincence of untimely meiosis. *Nature*, **442(6)**, 45-50.

Ibrahim, H.; Wilusz, J.; Wilusz, C.J., (2008) RNA recognition by 3'-to-5' exonucleases: the substrate perspective.

Biochim. Biophys. Acta., **1779(4)**, 256-265.

Ihmels, J.; Friedlander, G.; Bergmann, S.; Sarig, O.; Ziv, Y.; Barkai, N. (2002) Revealing modular organization in the yeast transcriptional network. *Nat. Genet.,* **31**, 370-378.

Isken O, Kim YK, Hosoda N, Mayeur GL, Hershey JW, Maquat LE (2008) Upf1 phosphorylation triggers translational repression during nonsense-mediated mRNA decay. *Cell*, **133**:314-27

Ito, T., Bulger, M., Pazin, M.J., Kobayashi, R.; Kodonaga, J.T. (1997) ACF, an ISWI-containing ATP-utilizing chromatin assembly and remodeling factor. *Cell*, **90**, 145-155.

Jain, E., Bairoch, A., Duvaud, S., Phan, I., Redaschi, N., Suzek, B. E., Martin, M., J., McGarvey, P., Gasteiger, E., (2009). Infrastructure for the life sciences: design and implementation of the UniProt website. *BMC Bioinformatics* 10:1036: doi:10.1186/1471-2105-1110-1136.

Jedidi, I., Zhang, F., Qui, H., Stahl, S. J., Palmer, I., Kaufman, J. D., Nadaud, P. S., Mukherjee, S., Wingfield, P. T., Jaroniec, C. P., Hinnebusch, A. G. (2010). Activator Gcn4 Employs Multiple Segments of MED15/Gal11 Including the KIX Domain to Recruit Mediator to Target Genes in Vivo. *J Biol Chem*, **285**, 2438-2442.

Jensen, L.J., Kuhn, M., Stark, M., Chaffron, S., Creevey, C., Muller, J., Doerks, T., Julien, P., Roth, A.,k Somonovic, M., Bork, P., von Mering, C. (2009) STRING 8--a global view on proteins and their functional interactions in 630 organisms. *Nucleic Acid. Res.,* **37** (database issue), D412-6

Jeong, C.-J. Y., S.-H., Xie, Y., Zhang, L., Johnston, S.A., Kodadek, T. (2001) Evidence That Gal11 Protein Is a Target of the Gal4 Activation Domain in the Mediator. *Biochemistry* **40**, 9421-9427

Jiang, C., Pugh, B.F. (2009) Nucleosome positioning and gene regulation: advances through genomics. *Nat. Rev. Genet.,* **10**, 161-172.

Johnson, A.W. (1997) Rat1p and Xrn1p are functionally interchangeable exoribonucleases that are restricted to and required in the nucleus and cytoplasm, respectively. *Mol Cell Biol.,* **17(10)**, 6122-30

Jones, D.T. (1999) Protein secondary structure prediction based on position-specific scoring matrices. *J. Mol. Biol.,* **292**: 195-202

Juven-Gershon, T., Kadonaga, J., T. (2010) Regulation of gene expression via the core promoter and the basal transcriptional machinery. *Dev. Biol.*, 339, 225–229.

Kadonaga, J.T. (2004) Regulation of RNA Polymerase II Transcription by Sequence-Specific DNA Binding Factors. *Cell*, **116**, 247-257

Kalousek, I., Brodska, B., Otevrelova, P., Räselova, P. (2007) Actinomycin D upregulates proapoptotic protein Puma and downregulates Bcl-2 mRNA in normal peripheral blood lymphoscytes. *Anticancer Drugs*, **18(7)**, 763-772.

Karunakaran, S.; Saeed, U.; Mishra, M.; Valli, K.; Joshi, S.D.; Meka, D.P.; Seth, P.; Ravindranath, V. (2008) Selective Activation of p38 Mitogen-Activated Protein Kinase in Pogaminergic Neurons of Substantia Nigra Leads to Nuclear Translocation of p53 in 1-Methyl-4-Phenyl-1,2,3,6-Tetrahydrophyridine-Treated Mice. *J. Neurosci.,* **28(47),** 1250012509.

Kasten, M., Szerlong, H.; Erdjument-Bromage, H.; Tempst, P.; Werner, M.; Cairns, B.R. (2004) Tandem bromodomains in the chromatin remodeler RSC recognize acetylated histone H3 Lys14. *EMBO J.*, **23(6)**, 1348-1359.

Keene, J.D. (2007) RNA regulons: coordination of post-transcriptional events. *Nat. Rev. Genet.*, **8**, 533-543

Keene, J.D.; Tenenbaum, S.A. (2002) Eukaryotic mRNPs May Represent Posttranscriptional Operons. *Mol. Cell*, **9**, 1161-1167.

Kelleher, R. J., Flanagan, P. M., Kornberg, R. D. (1990) A Novel Mediator between Activator Proteins and the RNA Polymerase II Transcription Apparatus. *Cell* **61(17)**, 1209-1221

Kenzelmann, M.; Maertens, S.; Hergenhahn, M.; Kueffer, S.; Hotz-Wagenblatt, A.; Li, L.; Wang, S.; Ittrich, C.; Lemberger, T.; Arribas, R.; Jonnakuty, S.; Hosstein, M.C.; Schmid, W.; Gretz, N.; Gröne, H.J.; Schütz, G. (2007) Micorarray analysis of newly synthesized RNA in cells and animals. *PNAS*, **104(15)**, 6164-6169.

Kim, E.K.; Choi, E.-J. (2010) Pathological roles of MAPK singaling pathways in human deseases. *Biochimica et Biophysica Acta. Biochem. Biophys. Acta*, **1802**, 396-405.

Klipp, E.; Nordlander, B.; Krüger, R.; Gennemark, P.; Hohmann, S. (2005) Integrative model of the response of yeast to omsmotic stress. *Nat. biotech.*, **23(8)**, 975-982.

Knop M, Siegers K, Pereira G, Zachariae W, Winsor B, Nasmyth K, Schiebel E (1999) Epitope tagging of yeast genes using a PCR-based strategy: more tags and improved practical routines. *Yeast* **15**(10B)**:** 963-972

Kobayashi, N., McClanahan, T.K., Simon, J.R., Treger, J.M., McEntee, K. (1996) Structure and Functional Analysis of the Multistress Response Gene DDR2 from Saccharomyces cerevisiae. *Biochem. Biophys. Res. Commun.* **229(2),** 540-7.

Kobayashi, Y.; Inai, T.; Miunuma, M.; Okada, I.; Shitamukai, A.; Hirata, D.; Miyakawa, T. (2008) Identification of Tup1 and Cyc8 mutantions defective in the responses ot osmotic stress. *Biochem. Biophys. Res. Comm.,* **368**, 50-55.

Kobor, M.S.; Venkatasubrahmanyam, S.; Meneghini, M.D.; Gin, J.W.; Jennings, J.L.; Link, A.J.; Madhani, H.D., Rine, J. (2004) A protein complex containing the conserved Swi2/Snf2-related ATPase Swr1p deposits histone variant H2A.Z into euchromatin. *PLoSBiol.*, *2(5)*, E131.

Koivomägi, M., Valk, E., Venta, R., Iofik, A., Lepiku, M., Balog, E.R.M., Rubin, S.M., Morgan, D.O., Loog, M. (2011) Cascades of multisite phosphorylation control Sic1 destruction at the onset of S phase. *Nature* **480**, 128-132

Koleske, A., J., Young, R., A. (1994) An RNA polymerase-II holoenzyme responsive to activators. *Nature*, **368**, 466–469.

Koschubs, T., K. Lorenzen, T.K.; Baumli,S.; Sandstrom, S.; Heck, A.J.; et al. (2010) Preparation and topology of the Mediator middle module. *Nucleic Acids Res.*, **38**, 3186–3195.

Kostrewa, D., Zeller, M., E.; Armache,K., J.; Seizl, M.; Leike , K.; et al. (2009) RNA polymerase II-TFIIB structure and mechanism of transcription initiation. *Nature*, **462**, 323–330.

Kouzarides, T. (2007) Chromatin Modifications and Their Function. *Cell*, *128*, 693-705.

Krogan, N.J.; Keogh, M.C.; Datta, N.; Sawa, C.; Ryan, O.W.; Ding, H.; Haw, R.A.; Pootoolal, J.; Tong, A.; Canadien, V.; Richards, D.P.; Wu, X.; Emili, A.; Hughes, T.R.; Buratowski, S., Greenblatt, J.F. (2003) A Snf2 familiy ATPase complex required for recruitment of the histone H2A variant Htz1. *Mol. Cell*, **12(6)**, 1565-1576.

Kuehner, J. N.; Brow, D., A. (2006) Quantitative analysis of in vivo initiator selection by yeast RNA polymerase II supports a scanning model. *J. Biol. Chem,.* **281**, 14119–14128.

Kuhn, K.M., DeRisi, J.L., Brown, P.O., and Sarnow, P. (2001) Global and specific translational regulation in the genomic response of Saccharomyces cerevisiae to a rapid transfer from a fermentable to a nonfermentable carbon source. *Mol. Cell. Biol.*, **21**, 916–927;

Kultarni, M.; Ozgur, S.; Stoecklin, G. (2010) On the track with P-bodies. *Biochem. Soc. Trans.*, **38**, 242-251.

Kuo, M.H.; Brownell, J.E.; Sobel, R.E.; Ranalli, T.A.; Cook, R.G.; Edmondson, D.G.; Roth, S.Y.; Allis, C.D. (1996) Transcription-linked acetylation by Gcn5p of histones H3 and H4 at specific lysines. *Nature*, **383**, 269-272.

Kuras, L.; Struhl, K. (1999) Binding of TBP to promoters *in vivo* is stimulated by activators and requires Pol II holoenzyme. *Nature*, *399*, 609-613.

Laemmli, U.K. (1970) Cleavage of structural proteins during the assembly of the head of bacteriophage T4. *Nature*, **227**, 680-685.

Lallet, S., Garreau, H., Garmendla-Torres, C., Szestakowska, D., Boy-Marcotte, E., Quevillon-Chéruel, S., Jacquet, M. (2006) Role of Gal11, a component of the RNA polymerase II Mediator in stress-induced hyperphosphoryltion of Msn2 in Saccharomyces cerevisiae. *Mol. Microbiol.* **62(2),** 438-52.

Lalonde MS, Zuo Y, Zhang J, Gong X, Wu S, Malhotra A, Li Z. (2007) Exoribonuclease R in Mycoplasma genitalium can carry out both RNA processing and degradative functions and is sensitive to RNA ribose methylation. *RNA*, **13**:1957.

Lam, L.T.; Pickeral, O.K.; Peng, A.C.; Rosenwald, A., Hurt, E.M.; Giltnane, J.M.; Averett, L.M.; Zhao, H.; Davis, R.E.; Sathyamoorthy, M.; Wahl, L.M.; Harris, E.D.; Mikovits, J.A.; Monks, A.P.; Hollingshead, M.G.; Sausville, E.A.; Staudt, L.M. (2001) Genomic-scale measurement of mRNA turnover and the mechanisms of action of the anti-cancer drug flavopiridol. *Genenome Biology*, **2(10)**, 2-11.

Landschulz, W.H.; Johnson, P.F., McKnight, S.L. (1998) The Lecine Zipper: A Hypothetical Structure Common to a New Class of DNA Binding Proteins. *Science*, **240 (4860),** 1759-1764.

Laprade, L.; Rpose, D.; Winston, F. (2007) Characterization of new Spt3 and TATA-binding protein mutants of Saccharomyces cerevisiae: Spt3 TBP allele-specific interactions and bypass of Spt8. *Genetics*, **177(4)**, 2007-2014.

Larivière, L., Seizl, M., van Wageningen, S., Röther, S., van de Pasch, L., Feldmann, H., Sträßer, K., Hahn, S., Holstege, F. C. P., Cramer, P. (2008) Structure-system correlation identifies a gene regulatory Mediator submodule. *Genes & Dev.* **22**, 872-877

Larschan, W.; Winston, F. (2001) The S. cerevisiae SAGA complex functions in vivo as a coactivator for transcriptional activation by Gal4. *Genes & Dev.,* **15(15)**, 1946-1956.

Larsen, M. R., Thingholm, T. E., Jensen, O. N., Roepstorff, P., Joergensen, T. J. D. (2005) Highly Slective Enrichment of Phosphorylated Ppeptides from Peptide Mixtures Using Titanium Dioxide Microcolumns. *Mol. Cell. Proteomics* **4**, 873-886

Larson, D. R., Zenklusen, D., Wu, B., Chao, J. A., Singer, R. H. (2011) Real-Time Observation of Transcription Initiation and Elongation on an Endogenous Yeast Gene. *Science*, **332**, 475-478.

Leatherwood, J.; Futcher, B. (2010) King of the castle: competition between repressors and activators on the Mcm1 platform. *Mol. Cell*, **38(1)**, 1-2;

Lee, W., Tillo, D., Bray, N.; Morse, R.H., Davis, R.W.; Hughes, T.R., Nislow, C. (2007) A high-resolution atlas of nucleosome accupancy in yeast. *Nat. Genet.*, **39 (10)**, 1235-1244.

Lenhard, B.; Sandelin, A.; Carninci, P. (2012) Metazoan promoters: emerging characteristics and insights into transcriptional regulation. *Nat. Rev. Genetics*, 13, 233-245.

Li, B, Carey, M., Workman, J.L. (2007) The Role of Chromatin during Transcription. *Cell*, **128**, 707-719.

Li, G.; Reinberg, D. (2011) Chromatin higher-order structures and gene regulation. *Curr. Opin. Genetics & Dev.*, **21**, 175-186

Li, X., Gerber, S. A., Rudner, A. D., Beausoleil, S. A., Haas, W., Villén, J., Elias, J. E., Gygi, S. P. (2007) Large-Scale Phosphorylation Analysis of alpha-Factor Arrested Saccharomyces cerevsisae. *J. Proteome* **6**, 1190-1197

Li, X.Y.; Bhaumik, S.R., Green, M.R. (2000) Distinct classes of yeast promoters revealed by differential TAF recruitment. *Science*, **288**, 1242-1244.

Li, X.Y.; Virbasius, A., Zhu, X.; Green, M.R. (1999) Enhancement of TBP binding by activators and general transcription factors. *Nature*, **399**, 605-609.

Lindstrom, K.C.; Vary, J.C.; Parthun, M.R.; Delrow, J.; Tsukiyama, T. (2006) Isw1 functions in parallel with the NuA4 Swr1 complexes in stress-induced gene repression. *Mol. Cell. Biol.*, **26(16)**, 6117-6129.

Liu, Y., Kung, C., Fishburn, J., Ansari, A. Z., Shokat, K. M., Hahn, S. (2004). Two Cyclin-Dependent Kinases Promote RNA Polymerase II Transcription and Formation of the Scaffold Complex. *Mol. Cell. Biol.,* **24**, 1721-1735.

Liu, Y., Kung, C., Fishburn, J., Ansari, A. Z., Shokat, K. M., Hahn, S. (2004) Two Cyclin-Dependent Kinases Promote RNA Polymerase II Transcription and Formation of the Scaffold Complex. *Mol. Cell. Biol.* **24**, 1721-1735

Logan, J., Falck-Pedersen, E., Darnell, J. E., Jr., and Shenk, T. (1987) *Proc. Natl. Acad. Sci. U.S.A.* 84, 8306–8310

López-Maury, L.; Marguerat, S.; Bähler, J. (2008) Tunig gene expression to changing environments: from rapid responses to evolutionary adaption. Nat. Rev. Genet., 9, 583-593

Lopez-Maury, L.; Marguerat, S.; Bähler, J. (2008) Tuning gene expression to changing environments: from rapid responses to evolutionary adaption. *Nat. Rev. Genet.*, **8**, 583-593.

Lotan R, Bar-On VG, Harel-Sharvit L, Duek L, Melamed D, et al. (2005) The RNA polymerase II subunit Rpb4p mediates decay of a specific class of mRNAs. *Genes&Dev,* **19**, 3004–3016.

Lu, P., Bogel, C., Wang, R., Yao, X., Marcotte, E.M. (2007) Absolute protein expression profiling estimates the relative contributions of transcriptional and translational regulation. *Nat. Biotechn.*, **25**, 117-124.

Luger, K.; Mäder, A.W.; Richmond, R.K.; Sargent, D.F.; Richmond, T.J. (1997) Crystal structure of the nucleosome core particle at 2.8 A resolution. *Nature*, **389**, 251-260.

Kenna, M.; Stevens, A.; McCammon, M.; Douglas, M.G. (1993) An essential yeast gene with homology to the exonuclease-encoding Xrn1/Kem1 gene also encodes a protein with exoribonuclease activity. *Mol. Cell. Biol.* **13(1)**, 341-350.

Macek, B., Mann, M., Olsen, J.V. (2009). Global and Site-Specific Quantitative Phsphoproteomics: Principles and Applications. *Annu. Rev. Pharmacol. Toxicol.,* **49**, 199-221.

Macia, J.; Regot, S.; Peeters, T.; Conde, N.; Solé, R.; Posas, F. (2009) Dynamic Signaling in the Hog1 MAPK Pathway Relies on High Basal Signal Transduction. *Sci. Signalling*, **2(63),** DOI: 10.1126/scisignal.2000056.

Maere, S., Heymans, K., Kuiper, M. (2005). BiNGO: a Cytoscape plugin to assess overrepresentation of Gene Ontology categories in Biological Networks. *Bioinformatics* , **21(16)**, 3448-3449.

Malik, S., Roeder, R. G. (2010). The metazoan Mediator co-activator complex as an integrative hub for transcriptional regulation. *Nat. Rev. Genet.*, **11**, 761-772.

Malys, N.; Carroll, K.; Miyan, J.; Tollervey, D.; McCarthy, J.E.G. (2004) The "scavenger" m7GpppX pyrophosphatase activity of Dcs1 modulates nutrient-induced responses in yeast. *Nucleic. Acid. Res.*, **32(12)**, 3590-3600.

Mann, M. (2006). Functional and quantitative proteomics using SILAC. *Nat. Rev. Molecular Cell Biology* ,**7**, 952-958.

Mann, M., and Karin, M. (2001). AU binding proteins recruit the Exosome to degrade ARE-containing mRNAs. *Cell* **107,**451–464.

Maquat L.,E., Carmichael, G.,G .(2001) Quality control of mRNA function. *Cell*, **104**:173-6

Martin, D. E. S., A., Hall, M.N. (2004) TOR regulates ribosomal protein gene expression via PKA and the Forkhead transcription factor FHL1. *Cell* **119**, 969-979

Martinez-Campa, C.; Panagiotis, P.; Moreau, J.-L.; Kent, N.; Goodall, J.; Mellor, J.; Goding, C.R. (2004) Precise Nucleosome Positioning and the TATA Box dictate Requirements for the Histone H4 Tail and the Bromodomain Factor Bdf1. *Mol. Cell,* **15**, 69-81.

Martinez-Montanes, F.; Pascual-Ahuir, A.; Proft, M. (2010) Toward a Genomic View of the Gene Expression Program Regulated by Osmostress in Yeast. *OMICS*, **14(6)**, 619-629.

Martinez-Rucobo, F.W., Sainsbury, S., Cheung, A.C.M., and Cramer, P. (2011). Architecture of the RNA polymerase-Spt4/5 complex and basis of universal transcription processivity. *EMBO J.,* **30**, 1302–1310.

Mavrich, T.N.; Ioshikhes, I.P.; Venters, B.J.; Jiang, C.; Tormsho, L.P.; Qi, J.; Schuster, S.C.; Albert, I.; Pugh, B.F. (2008) A barrier nucleosome model for statistical positioning of nucleosomes throughout the yeast genome. *Genome Res.*, **18(7)**, 1073-83.

Mayer, A.; Lidschreiber, M.; Siebert, M.; Leike, K.; Söding, J.; Cramer, P. (2010) Uniform transitions of the general RNA polymerase II transcription complex. *Nat. Struct. Mol. Biol.*, **17(19)**, 1272-1278.

Melamed, D., Pnueli, L., Arava, Y. (2008) Yeast translational response to high salinity: Global analysis reveals regulation at multiple levels. *RNA* **14**, 1337-1351

Melissa, S. C., Smoot, M., Cerami, E., Kuchinosky, A., Landys, N., Workman, C., Christmas, R., Avila-Campilo, I., Creech, M., Gross, B., Hanspers, K., et al. (2007) *Nature Potocols* **2(10)**, 2366-2382

Mellor, J.; Morillon, A. (2004) ISWI complexes in Saccharomyces cerevisiae. *Biochim. Biophys. Acta,* **1677**, 100-112.

Mettetal, J.T.; Muzzey, D.; Gomez-Uribe, C.; van Oudenaarden, A. (2008) The Frequency Dependence of Osmo-Adaption in Saccharomyces cerevisiae. *Science*, **319**, 482-486.

Mignone, F.; Gissi, C.; Liuni, S.; Pesole, G. (2002) Untranslated regions of mRNAs. *Genome Biology*, **3(3)**: reviews0004.1-0004.10.

Miller, C., Schwalb, B., Maier, K., Schulz, D., Dümcke, S., Zacher, B., Mayer, A., Sydow, J., Marcinowski, L., Dölken, L., Martin, D. E., Tresch, A., Cramer, P. (2011) Dynamic transcriptome analysis measures rates of mRNA synthesis and decay in yeast. *Mol. Sys. Biol.* **7,** 458-465, doi:10.1038/msb.2010.112

Mitchell, P.; Tollervey, D. (2000) mRNA stability in eukaryotes. *Curr. Opin. Genet. Dev.,* **10**, 193-198.

Mizuguchi, G.; Shen, X.; Landry, J.; Wu, W.H.; Sen, S.; Wu, C. (2004) ATP-driven exchange of histone H2AZ variant catalyzed by SWR1 chromatin remodeling complex. *Science*, **303**, 343-348.

Molin, C.; Jauhiainen, A.; Warringer, J.; Nerman, O.; Sunnerhagen, P. (2009) mRNA stability changes precede changes in steady-state mRNA amounts during hyperosmotic stress. *RNA*, **15**, 600-614.

Molina-Navarro, et al. JBC, 2008;Hayles, B., Yellaboina, S., Wang, D. (2010) Comparing Transcription Rate and mRNA abundance as Parameters for Biochemical Pathway and Network Analysis. *PlosONE*, **5(3)**, e9908, 1-8.

Mollapour, M.; Piper, P.W. (2006) Hog1p mitogen-activated protein kinase determines acetic acid resistance in Saccharomyces cerevisiae. *FEMS Yeast Res.*, **6**, 1274-1280.

Mollapour, M.; Piper, P.W. (2007) Hog1 Mitogen-Activated Protein Kinase Phosphorylation Targets the Yeast Fps1 Aquaglyceroporin for Endocytosis. Thereby Rendering Cells Resistant to Acetic Acid. *Mol. Cell. Biol.*, **27(18)**, 6446-6456.

Moore, P.A.; Sagliocco, F.A.; Wood, R.M.C.; Brown, A.J.P. (1991) Yeast Glycolytic mRNAs Are Differentially Regulated. *Mol. Cell. Biol.*, **11(10)**, 5330-5337.

Morano, K. A., Grand, C.M., Moye-Rowley, W.S. (2012) The Response to Heat Shock and Oxidative Stress in *Saccharomyces cerevisiae. Genetics,* **190(4),** 1157-95

Moriguchi, T.; Toyoshima, F.; Gotoh, Y.; Iwamatsu, A.; Irie, K.; Kuroyanagi, N.; Hagiwara, M.; Matsumoto, K.; Nishida, E. (1996) Purification and Identification of a Major Activator for p38 from Osmotically Shocked Cells., *JBC*, **271(3),** 26981-26988.

Morillon, A.; Karabetsou, N.; O'Sullivan, J.; Kent, N.; Proudfoot, N.; Mellor, J. (2003) Isw1 chromatin remodeling ATPase coordinates transcription elongation and termination by RNA polymerase II. *Cell*, **115(4)**, 425-435.

MORRISSEY, J.P., DEARDORFF, J.A.,HEBRON, C., SACHS, A.B., (1999) Decapping of Stabilized, Polyadenylated mRNA in Yeast *pab1* Mutants; *YEAST*, **15**, 687-702

Muhlrad, D.; Parker, R. (2005) The yeast EDC1 mRNA undergoes deadenylation-independent decapping stimulated by Not2p, Not4p, and Not5p. *EMBO J.*, **24**, 1033-1045.

Murray, D. B. H., K., Tomita, M. (2011) Redox regulation in respiring Saccharomyces cerevisiae. *Biochi. et Biophys. Acta* **1810**, 945-958

Muzzey, D.; Gómez-Uribe, C.A.; Mettetal, J.T.; von Oudenaarden, A. (2009) A Systems-Level Analysis of Perfect Adaption in Yeast Osmoregulation. *Cell*, **138**, 160-171.

Myer, V.E.; Young, R.A. (1992) RNA polymerase II holoenzyme and subcomplexes. *JBC*. **273**, 27757-27760.

Nair, R., Carter, P., Rost, B. (2003) NLSdb: database of nuclear localization signals. *Nucleic Acids Res.*, **31(1),**397–399

Narlikar, G.J.; Fan, H.-Y.; Kingston, R.E. (2002) Cooperation between Complexes that Regulate Chromatin Structure and Transcription. *Cell,* **108**, 475-487.

Narsai, R.; Howell, K.A.; Millar, A.H.; O'Toole, N.; Small, I.; Whelan, J. (2007) Genome-Wide Analysis of mRNA Decay Rates and Their Determinants in Arabidopsis thaliana. *The Plant Cell*, **19**, 3419-3436.

Nehlin, J.O.; Carlberg, M., Ronne, H. (1991) Control of yeast GAL genes by MIG1 repressor: a transcriptional cascade in

the glucose response. *EMBO J.*, **10**, 3373-3377.

Ni, L., C. Bruce, C. Hart, J. Leigh-Bell, D. Gelperin et al. (2009) Dynamic and complex transcription factor binding during an inducible response in yeast. *Genes Dev*. **23**, 1351–1363.

Niall, H.D. (1973) Automated Edman degradation: The protein sequenator. *Methods Enzymology*, **27**, 942-1010

Nikolov, D., B.; Chen, H.; Halay, E., D.; Usheva, A., A., Hisatake, K.; Lee, D., K.; Roeder, R., G.; Burley, S., K. (1995) Crystal structure of a TFIIB-TBP-TATA-element ternary complex. *Nature*, **377**, 119-128.

Nonet, M.; Scafe, C.; Sexton, J.; Young, R. (1987) Eucaryotic RNA Polymerase Conditional Mutant That Rapidly Ceases mRNA Synthesis. *Mol. Cell. Biol.*, **7(5)**, 1602-1611.

O'Rourke, S.M.; Herskowitz, I.; O'Shea, E.K. (2002) Yeast go the whole HOG for the hyperosmotic response. *Trends genetics,* **18(8),** 405-412.

Okazaki, S.; Tachibana, T.; Naganuma, A.; Mano, N.; Kuge, S. (2007) Multistep Disulfide Bond Formation in Yap1 Is Required for Snsing and Transduction of H_2O_2 Stress Signal. *Mol. Cell.,* **27**, 675-688.

Olivas, W., Parker, R. (2000) The Puf3 protein is a transcript-specific regulator of mRNA degradation in yeast. *EMBO J.,* **19(23)**, 6602-6611.

Olsen, J. V., Blagoev, B., Gnad, F., Macek, B., Kumar, C., Mortensen, P., Mann, M. (2006) Global, In Vivo, and Site-Specific Phosphorylation Dynamics in Signaling Networks. *Cell* **127**, 635-648

Olsen, J. V., de Godoy, L.M., Li, G., Macek, B., Mortensen, P., Pesch, R., Makarov, A., Lange, O., Horning, S., and Mann, M. (2005) Parts per million mass accuracy on an Orbitrap mass spectrometer via lock mass injection into a C-trap. *Mol. Cell. Proteomics* **4**, 2010-2021

Olsen, J. V., Vermuelen, M., Santamaria, A., Kumar, C., Miller, M., L., Jensen, L., J., Gnad, F., Cox, J., Jensen, T. S., Nigg, E. A., Brunak, S., Mann, M. (2010) Quantitative Phosphoproteomics Reveals Widespread Full Phosphorylation Site Occupancy During Mitosis. *Sci. Signal.* **3(104)**, ra3 1-15

Ong, S. E., Blagoev, B., Kratchmarova, I., Kristensen, D. B., Steen, H., Pandey, A., and Mann, M. (2002) Stable Isotope Labeling by Amino Acids in Cell Culture, SILAC, as a Simple and Accurate Approach to Expression Proteomics. *Mol. Cell Proteomics* **1**, 376-386

Ong, S. E., Kratchmarova, I., Mann, M. (2003) Properties of 13C-Substituted Arginine in Stable Isotope Labelying by Amino Acids in Cell Culture (SILAC). *J. Proteomics* **2**, 173-181

Orphanides, G., Lagrange, T., and Reinberg, D. (1996). The general transcription factors of RNA polymerase II. *Genes Dev.* 10, 2657–2683.

Orphanides, G.; Reinberg, D. (2002) A Unified Theory of Gene Expression. *Cell*, **108**, 439-451.

Ostling, J.; Ronne, H., (1998) Negative control of the Mig1p repressor by Snf1p-dependent phosphorylation in the absences of glucose. *Eur. J. Biochem.*, **252**, 162-168.

Palangat, M.,Renner, D. B., Price, D. H.&Landick, R.A (2005) Negative elongationfactor forhuman RNA polymerase II inhibits the anti-arrest transcript-cleavage factor TFIIS. *Proc. Natl Acad. Sci. USA.*, **102**, 15036–15041.

Palecek, J., Hasek, J., Helmut Ruis, H., (2001) Rpg1p/Tif32p, a subunit of translation initiation factor 3, interacts with actin-associated protein Sla2p. *Biochem Biophys Res Commun,* **282(5)**, 1244-50

Park, J. M., Kim, H.-S., Han, S. J., Hwang, M.-S., Lee, Y. Ch., Kim, Y-J. (2000) In Vivo Requirement of Activator-Specific Binding Targets of Mediator. *Mol. Biol. Cell*, **20(23)**, 8709-8719

Park, J.B.; Levine, M. (2005) Cloning, sequencing, and characterization of alternatively spliced glutaredoxin 1 cDNA and its genomic gene: chromosomal localization, mrna stability, and origin of pseudogenes. *J. Biol. Chem.*, **289(11)**, 10427-10434.

Parker, R.; Song, H. (2004) The enzymes and control of mRNA turnover. *Nat. Struct. Mol. Biol.*, **11(2)**, 121-127.

Pascual-Ahuir, A.; Struhl, K.; Proft, M. (2006) Genome-wide location analysis ot the stress-activated MAP kinase Hog1

in yeast. *Methods*, **40**, 272-278.

Pelechano, V., Chávez, S., Pérez-Ortin, J.E. (2010) A Complete Set of Nascent Transcription Rates for Yeast Genes. *PlosONE*, **5(11),** e15442, 1-10.

Pelechano, V.; Jimeno-González, S.; Rodriguez-Gil, A.; Garcia-Martinez, J.; Pérez-Ortin, J.E.; Chávez, S. (2010) Regulon-Specific Control of Transcription Elongation across the Yeast Geome. *PLoS Genetics*, **5(8)**, e1000614.

Pérez-Ortin, J.E. (2008) Genomics of mRNA turnover. *Brief. Funct. Genom. Proteom.*, **6(4)**, 282-291.

Peterson, R., Lindquist, S. (1988), The Drosophila hsp70 message is rapidly degraded at normal temperatures and stabilized by heath shock, *Gene*, **72**, 161-168

Pokholok, D.K., Zetilinger, J.; Hannett, N.M.; Reynolds, D.B.; Young, R.A. (2006) Activated Signal Transduction Kinases Frequently Occupy Target Genes. *Science*, **313**, 533-536.

Posas, F.; Chambers, J.R.; Heyman, J.A.; Hoeffler, J.P.; de Nadal, E.; Arino, J. (2000) The Transcriptional Response of Yeast to Saline Stress. *JBC,* **275(23)**, 17249-17255.

Pradet-Balade, B., Boulme, F., Beug, H., Mullner, E.W., Garcia-Sanz, J.A. (2001) Translation control: bringing the gap between genomics and proteomics? *Trends in Biochem. Sci.*, **26**, 225-229.

Pray-Grant, M.G.; Daniel, J.A.; Schieltz, D.; Yates, J.R.; Grant, P.A. (2005) Chd1 chromodomain links histone H3 methylation with SAGA- and SLIK-dependent acetylation. *Nature*, **433**, 434-438.

Preiss, T.; Baron-Benhamou, J.; Ansorge, W.; Hentze, M.W. (2003) Homodirectional changes in transcriptome composition and mRNA translation induced by rapamycin and heat shock. *Nat. Struct. Biol.*, **10**, 1039–1047.

Proft, M., and Struhl, K. (2004) MAP kinase-mediated stress relief that precedes and regulates the timing of transcriptional induction. *Cell* **118**, 351-361

Proft, M.; Pascual-Ahuir, A.; de Nadal, E.; Arino, J.; Serrano, R., Posas, F. (2001) Regulation of the Sko1 transcriptional repressor by the Hog1 MAP kinase in response to osmotic stress. *EMBO J.*, **20(5)**, 1123-1133.

Proft, M.; Struhl, K. (2002) Hog1 kinase converts the Sko1-Cyc8-Tup1 repressor complex into an activator that recruits SAGA and SWI/SNF in response to osmotic stress. *Mol. Cell,* **9(6)**, 1307-1317.

Proft, M.; Struhl, K. (2004) MAP Kinase-Mediated Stress Relief that Precedes and Regulates the Timing of Transcriptional Induction. *Cell*, **118**, 351-361.

Proudfoot, N., J.; Furger, A.; Dye, M., J. (2002) Integrating mRNA Processing with Transcription. *Cell*, **108**, 501-512.

Ptashne, M., and A. Gann, (2002) Genes and Signals. Cold Spring Harbor Laboratory Press, Cold Spring Harbor, NY.

Pugh, B., F., Tjian, R. (1991) Transcription from a TATA-less promoter requires a multisubunit TFIID complex. *Genes & Development,* **5**, 1935–1945.

Puig, O., Caspary, F., Rigaut, G., Rutz, B., Bouveret, E., Bragado-Nilsson, E., Wilm, M., Séraphin, B. (2001). The Tandem Affinity Purification (TAP) Method: A Generla Procedure of Protein Complex Purification. *Methods,* **24**, 218-222.

Qiu, H.; Hu, C.; Zhang, F.; Hwang, G.J.; Swanson, M.J.; Boonchird, C.; Hinnebusch, A.G. (2005) Interdependent Recruitment of SAGA and Srb Mediator by Transcriptional Activator Gcn4p. *Mol. Cell. Biol.,* **25(9)**, 3461-3474.

Rachez, C.; Lemon, B.D.; Suldan, Z.; Bromleigh, V.; Gamble, M.; Näär, A.M.; Erdjument-Bromage, H.; Tempst, P.; Freedman, L.P. (1999) Ligand-dependent transcription activation by nuclear receptors requires the DRIP complex. *Nature*, **398**, 824-829.

Raghavan, A.; Ogilivie, R.L.; Reilly, C.; Abelson, M.L.; Raghavan, S.; Vasewani, J.; Krathwohl, M.; Bohjanen, P.R. (2002) Genome-wide analysis of mRNA decay in resting and activated primary human T lymphocytes. *Nucleic. Acid. Res.*, **30(24)**, 5529-5538.

Ranish, J., A., Yudkovsky, N., Hahn, S. (1999) Intermediates in formation and activity of the RNA polymerase II preinitiation complex: holoenzyme recruitment and a postrecruitment role for the TATA box and TFIIB.

Genes & Dev., **13**, 49–63.

Ratnakumar, S., and E. T. Young (2010) Snf1 dependence of peroxisomal gene expression is mediated by Adr1. *J. Biol. Chem*. **285**, 10703–10714.

Rebbapragada, I.; Lykke-Anderson, J. (2009) Execution of nonsense-mediated mRNA decay: what defines a substrate? *Curr. Opin. Cell Biol.*, **21**, 394-402.

Redd, M.J. Stark, M.R.; Johnson, A.D. (1996) Accessibility of alpha2-repressed promoters to the activator Gal4. Mol. *Cell. Biol.*, **16**, 2865-2869.

Reinke, H., Horz, W. (2003) Histones are first hyperacetylated and then lose contact with the activated PHO5 promoter. *Mol. Cell,* **11**, 1599-1607.

Rep, M.; Krantz, M.; Thevelein, J.M.; Hohmann, S. (2000) The Transcriptional Response of Saccharomyces cerevisiae to Osmotic Shock. *JBC*, **275(12)**, 8290-8300.

Richmond, T.J. (2006) Genomics: Predictable packaging. *Nature*, **442**, 750-752.

Rigaut, G., Shevchenko, A., Rutz, B., Wilm, M., Mann, M., Séraphin, B. (1999) A generic protein purification method for protein complex characterization and proteome exploration. *Nat. Biotechnol.* **17(10)**, 1030-1032

Ringbolt, K. T. G., Prokhorova, T. A., Akimov, V., Henningsen, J., Johanson, P. T., Kratchmarova, I., Kassem, M., Mann, M., Olsen, J. V., Blagoev, B. (2011) System-Wide Temporal Characterization of the Proteome and Phosphoproteome of Human Embryonic Stem Cell Differentiation. *Sci. Signal.* **4(164)**, rs3 1-17

Rodriguez-Gabriel, M.A., Burns, G., McDonald, W.H., Yates, M.V., Valer, J. R., Russell, P. (2003) RNA-binding protein CSX1, mediates global control gene expression in response to oxidative stress. *EMBO J.*, **22**, 6256-6266.

Rodriguez-Navarro, S., Hurt, E. (2011) Lining gene regulation to mRNA production and export. *Curr. Opin. Cell Biol.*, **23(3),** 302-309.

Roeder, R.G. (1996). The role of general initiation factors in transcription by RNA polymerase II. *Trends Biochem. Sci.,* **21**, 327–335.

Romero-Santacreu, L., Moreno, J., Perez-Ortin, J.E., and Alepuz, P. (2009) Specific and global regulation of mRNA stability during osmotic stress in Saccharomyces cerevisiae. *RNA,* **15**, 1110-1120

Ross, J. (1995) mRNA Stability in Mammalian Cells. *Microbiol., Rev.*, **59(3)**, 423-450.

Roy, A.; Kucukural, A.; Zhang, Y. (2010) I-TASSER: a unified platform for automated protein structure and function prediction. Nat. Protocols, 5(4), 725-739.

Rubinsztein, D. C., Marino, G., Kroemer, G. (2011) Autophagy and Aging. *Cell* **146**, 682-695

Ruiz-Echevarria, M.J.; Peltz, S.W. (2000) The RNA Binding Protein Pub1 Modulates the Stability of Transcripts Containing Upstream Open Reading Frames. *Cell*, **101**, 741-751.

Sadeh, A. B., D., Volokh, M., Aharoni, A. (2012) Conserved Motifs in the Msn2-Activating Domain are Important for Msn2-Mediated Yeast Stress Response. *J Cell Sci.* **125(Pt 14),** 3333-42. doi: 10.1242/jcs.096446. Epub ahead of print

Saeed, A.I., Sharov, V., White, J., Li, J., Liang, W., Bhagabati, N., Braisted, J., Klapa, M., Currier, T., Thiagarajan, M., Sturn, A., Snuffin, M., Rezantsev, A., Popov, D., Ryltsov, A., Kostukovich, E., Borisovsky, I., Liu, Z., Vinsavich, A., Trush, V., Quackenbush, J. (2003) TM4: a free, open-source system for microarray data management and analysis. *Biotechniques*. **34(2)**, 374-8.

Saha, A.; Wittmeyer, J.; Bradley, R.C. (2006) Chromatin remodeling: the industrial revolution of DNA around histones. *Nat. Rev. Mol. Cell Biol,* **7**, 437-447.

Saha, A.; Wittmeyer, J.; Cairns, B.R. (2006) Mechanisms for nucleosome movement by ATP-dependent chromatinremodelling complexes. *Results Probl. Cell Differ*., **41**, 127-148.

Sandler, H., Stoecklin, G. (2008) Control of mRNA decay by phosphorylation of tristetraprolin. *Biochem. Soc. Trans.,*

36, 491-496.

Santiago, T.C.; Purvis, I.J.; Bettany, A.J.E.; Brown, A.J.P. (1986) The relationship between mRNA stability and length in Saccharomyces cerevisiae. *Nucleic Acids Res.,* **14(21)**, 8347-8361.

Santos-Rosa, H.; Schneider, R.; Bannister, A. J.; Sherriff, J.; Bernstein, B.E.; Emre, N.C.T.; Schreiber, S.L.; Mellor, J.; Kouzarides, T. (2002) Active genes are tri-methylated at K4 of histone H3. *Nature*, **419**, 407-411.

Scrutton, M.C.; Wu, C.W.; Goldthwait, D.A. (1971) The Presence and Possible Role of Zinc in RNA Polymerase Obtained from Escherichia coli. *Proc. Nat. Acad. Sci. USA,* **68(10),** 2497-2501.

Segal, G.; Ron, E.Z. (1995) The groESL Operon of Agrobacterium tumefaciens: Evidence for Heat Shock-Dependent mRNA cleavage. *J. Bacteriology,* **177(3)**, 750-757

Seizl, M. H., H., Hoeg, F., Kurth, F., Martin, D.E., Soeding, J., Cramer, P. (2011) A Conserved GA Element in TATA-Less RNA Polymerase II Promoters. *PLoS one* **6(11),** e27595

Selinger, D.; Saxena, R.M.; Cheung, K.J.; Church, G.M.; Rosenow, C. (2002) Global RNA Half-Life Analysis in Escherichia coli Reveals Positional Patterns of Transcript Degradation. *Genome Res.*, doi/10.1101/ gr.912603, 1-8.

Shalem, O.; Dahan, O.; Levo, M.; Rodriguez-Martinez, Furman, I.; Segan, E.; Pilpel, Y. (2008) Transient transcriptional responses to stress are generated by opposing effects of mRNA production and degradation. *Mol. Sys. Biol.,* **4**, 223-233.

Shandilya, J.; Roberts, S.G.E. (2012) The transcription cycle in eukaryotes: From productive initiation to RNA polymerase II recycling. *Biochim. Biophys. Acta*, **1819**, 391-400.

Shaner, N.C.; Campbell, R.E.; Steinbach, P.A.; Giepmans, B.N.G.; Palmer, A.E.; Tsien, R.Y. (2004) Improved monomeric red, orange and yellow fluorescent proteins derived from Discosoma sp. Red fluorescent protein. *Nat. biotech*., **22(12),** 1567-1573.

Sharova, L.V.; Harov, A.A.; Nedorezov, T.; Piao, Y.; Shaik, N.; Ko, M.S.H. (2009) Database for mRNA Half-Life of 19977 Genes Obtained by DNA Microarray Analysis of Pluripotent and Differentiating Mouse Embryonic Stem Cells. *DNA Research,* **16**, 45-58.

She M, Decker C, Liu Y, SundramurthyK, Parker R, Song H. (2004) Crystal structure of Dcp1p and its functional implications in mRNA decapping; *Nat. Struct. Mol. Biol,.* **11**, 3, 249-256

Shenton, D., Smirnova, J.B., Selley, J.N., Carroll, K., Hubbard, S.J., Pavitt, G.D., Ashe, M.P., and Grant, C.M. (2006) Global translational´responses to oxidative stress impact upon multiple levels of protein synthesis. *J. Biol. Chem.,* **281**, 29011–29021

Sheth, U.; Parker, R. (2003) Decapping and Decay of Messenger RNA Occur in Cytoplasmic Processing Bodies. *Science,* **300**, 805-809.

Shivaswamy, S.; Bhinge, A.; Zhao, Y.; Jones, S.; Hirst, M.; Iyer, V.R. (2008) Dynamic Remodeling o fIndividual Nucleosomes Across a Ekaryotic Genome in Response to Transcriptional Perturbation. *PlosBiol*, **6(3)**, e65. Doi:10.1371 /journal.pbio.0060065.

Shyu, A.-B.; Greenberg, M.E.; Belasco, J.G. (1989) The c-fos transcript is targeted for rapid decay by two distinct mRNA degradation pathways. *Genes & Dev.*, **30**, 60-72.

Sikorski, R. S., Hieter, P. (1989) A System of Shuttle Vectors and Yeast Host Strains Designed for Efficient Maniupulation of DNA in Saccharomyces cerevisiae. *Genetics* **122**, 9

Sikorski, T.W.; Buratowski, S. (2009) The basal initiation machinery: beyond the general transcription factors. *Cur. Opin. Cell Biol.,* **21**, 344-351.

Simon, E., Seraphin, B. A (2007) Specific role for the C-terminal region of the Poly(A)-binding protein in mRNA decay. *Nucleic Acids Res.* , **35(18)**, 6017-6028.

Simon, I., J. Barnett, N. Hannett, C. T. Harbison, N. J. Rinaldi et al. (2001) Serial regulation of transcriptional regulators in the yeast cell cycle. *Cell*, **106**, 697–708.

Singh, R., Cuervo, A.M. (2011) Autophagy in the Cellular Energetic Balance. *Cell Metabolism,* **13**, 495-504

Smale, S., T. (1996) Transcription initiation from TATA-less promoters within eukaryotic protein-coding genes. *Biochim. Biophys. Acta,* **1351**, 73–88.

Smale, S., T.; Kadonaga, J., T. (2003) The RNA Polymerase II Core Promoter. *Annu. Rev. Biochem.*, **72**, 449-479.

Smolka, M. B. A., C.P., Chen, S.H., Zhou, H. (2007) Proteome-wide identification of in vivo targets of DNA damage checkpoint kinases. *Proc. Natl. Acad. Sci. USA* **104**, 10364-10369

Smyth, G. K. (2004). Linear models and empirical bayes methods for assessing differential expression in microarray experiments. *Statistical applications in genetics and molecular biology*, **3(1)**,

Snel, B., Lehmann, G., Bork, P., Huynen, M. A. (2000). STRING: a web-server to retrieve and display the repeatedly occuring neighbourhott of a gene. *Nucleic Acids Res.*, **28**, 12.

Söding, J. (2005) Protein homology detection by HMM-HMM comparison. B*ioinformatics* **21** (7): 951–960

Soufi, B., Kelstrup, C. D., Stoehr, G., Fröhlich, F., Walther, T. C., Olsen, J. V. (2008) Global analysis of the yeast osmotic stress response by quantitative proteomics. *Mol. Bio. Syst.* **5**, 1337-1346

Spaeth, J. M., Kim, N.H., Boyer, T.G. (2011) Mediator and human disease. *Semin. Cell Dev. Biol.* **22(7)**, 776-787

Steinmetz, E. J., Warren, C. L.; Kuehner, J. N.; Panbehi, B.; Ansari, A. Z; et al. (2006) Genome-wide distribution of yeast RNA polymerase II and its control by Sen1 helicase. *Mol. Cell,* **24**, 735–746.

Stockdale, C.; Flaus, A.; Ferreira, H.; Owen-Hughes, T. (2006) Analysis of Nucleosome Repositioning by Yeast ISWI and Chd1 Chromatin Remodeling Complexes. *J. Biol. Chem.*, **281**, 16279-16288.

Sullivan, E.K.; Weirich, C.S., Guyon, J.R.; Sif, S.; Kingston, R.E. (2001) Transcriptional Activation Domains of Human Heat Shock Factor 1 Recruit Human SWI/SNF. *Mol. Cell. Biol.*, **21(17)**, 5826-5837.

Sun, M., Schwalb, B., Schulz, D., Pirkl, N., Etzold, S., Larivière, L., Maier, K., C., Seizl, M., Tresch, A., Cramer, P. (2012) Comparative Dynamic Transcriptome Analysis (cDTA) reveals mutual Feedback between mRNA synthesis and degradation. *Genome Res.* **doi:10.1101/gr.130161.111**

Suter, D.M.; Molina, N.; Gatfield, D.; Schneider, K.; Schibler, U.; Naef, F. (2011) Mammalian Genes Are Transcribed with Widely Different Bursting Kinetics. *Science*, **332**, 472-476.

Svejstrup, J.Q. (2004) The RNA polymerase II transcription cycle: cycling through chromatin. *Biochim. Biophys. Acta*, **1677**, 64-73.

Swaminathan, S., Masek, T., Molin, C., Pospisek, M., and Sunnerhagen, P. 2006. Rck2 is required for reprogramming of ribosomes during oxidative stress. *Mol. Biol. Cell,* **17**, 1472–1482.

Tachibana, C., J. Y. Yoo, J. B. Tagne, N. Kacherovsky, T. I. Lee et al. (2005) Combined global localization analysis and transcriptome data identify genes that are directly coregulated by Adr1 and Cat8. *Mol. Cell. Biol.*, **25**, 2138–2146.

Takekawa, M.; Posas, F.; Saito, H. (1997) A human homolog oft he yeast Ssk2/Ssk22 MAP kinase kinase kinase, MTK1, mediates stress-induced activation oft he p38 and JNK pathways. *EMBO, J.*, **16(16)**, 4973-4982.

Tan, K., H. Feizi, C. Luo, S. H. Fan, T. Ravasi et al. (2008) A systems approach to delineate functions of paralogous transcription factors: role of the Yap family in the DNA damage response. *Proc. Natl. Acad. Sci. USA,* **105**, 2934–2939.

Tatebayashi, K.; Katsuyoshi, Y.; Tanaka, K.; Tomida, T.; Maruoka, T.; Kasukawa, E.; Saito, H. (2006) Adaptor functions of Cdc42, Ste50 and Sho1 in the yeast osmoregulatory HOG MAPK pathway. *EMBO J.*, **25**, 3033-3044.

Teixeira, D.; Sheth, U.; Valencia-Sanchez, M.A.; Brengues, M.; Parker, R. (2005) Processing bodies require RNA for assembly and contain nontranslating mRNAs. *RNA*, **11**, 371-382.

Thakur, J. K. A., H., Yang, F., Chau, K.H., Wagner, G., Näär, A.M. (2008) Mediator subunit Gal11/Med15 is required for fatty acid dependent gene activation by yeast transcription factor Oaf1P. *J. Biol. Chem.* **284**, 4422-4428

Thakur, J. K., Arthanari, H., Yang, F., Pan, S.-J., Fan, X., Breger, J., Frueh, D. P., Gulshan, K., Li, D. L., Mylonakis, E., Struhl, K., Moye-Rowley, W. S., Cormack, B. P., Wagner, G., Näär, A. M. (2008). A nuclear receptor-like pathway regulating multidrug resistance in fungi. *Nature*, **452**, 604-610.

Tharun S, Muhlrad D, Chowdhury A, Parker R. (2005)Mutations in the Saccharomyces cerevisiae LSM1gene that affect mRNA decapping and 3′ end protection. *Genetics*;**170**:33.

The UniProt Consortium (2010) Ongoing and future developments at the Universal Protein Resource. *Nucleic Acids Res.* **39**, D214-D219

Thomson, M., Gunawardena, J. (2009) Unlimited multistability in multisite phosphorylation systems. *Nature* **460**, 274-277

Thorsness, P. E., Koshland D.E. (1987) Inactivation of Isocitrate Dehydrogenase by Phosphorylation Is Mediated by Negative Charge of the Phosphate. *J. Biol. Chem.* **262 (22)**, 10422-10425

Till, D.D.; Linz, B.; Seago, J.E.; Elgar, S.J.; Marujo, P.E.; Elias, de L., E.; Arraiano, C.M.; McClellan, J.A.; McCarthy, J.E.G.; Newbury, S.F. (1998) Identification and developmental expression of a 5′-3′ exoribonuclease from Drosophila melanogaster. *Mechanisms of Developent*, **79**, 51-55.

Tomecki, R.; Dziembowski, A. (2010) Novel endoribonucleases as central players in various pathways of eukaroyotic RNA metabolism, *RNA*, **16**, 1692-1724.

Treger, J. M., Magee, T.R., McEntee, K. (1998) Functional Analysis of the Stress Response Element and Its Role in the Multistress Response of Saccharomyces cerevisiae. *Biochem. Biophys. Res. Commun.* **243**, 13-19

Treitel, M.A.; Kuchin, S.; Carlson, M. (1998) Snf1 protein kinase regulates phosphorylation of the Mig1 repressor in Saccharomyces cerevisiae. *Mol. Cell. Biol.*, **18**, 6273-6280.

Tucker, M.; Valencia-Sanchez, Staples, R.R.; Chen, J.; Denis, C.L.; Parker, R. (2001) The Transcription Factor Associated Ccr4 and Caf1 Proteins Are Components of the Major Cytoplasmic mRNA Deadenylase in Saccharomyces cerevisiae. *Cell*, **104**, 377-386.

Tupler, R.; Perini, G.; Green, M.R. (2001) Expressing the human genome. *Nature*, **409**, 832-833.

Tzamarias, D., Roussou, I., and Thireos, G. (1989) Coupling of GCN4 mRNA translational activation with decreased rates of polypeptide chain initiation. *Cell*, **57**, 947–954

Uesono, Y. and Toh, E.A. (2002) Transient inhibition of translation initiation by osmotic stress. *J. Biol. Chem.*, **277**, 13848–13855.

Ulbricht, R.J.; Olivas, W.M. (2008) Puf1p acts in combination with other yeast Puf proteins to control mRNA stability. *RNA*, **14**, 246-262.

Unnikrishnan, I., Miller, S., Meinke, M., LaPorte, D.C. (2003) Multiple Positive and Negative Elements Involved in the Regulation of Expression of GSY1 in Saccharomyces cerevisiae. *J. Biol. Chem.* **29**, 26450-26457

van de Peppel, J., Kettelarij, N., van Bakel, H., Kockelkorn, T.T.J.P., van Leenen, D., Holstege, F. C. P. (2005) Mediator expression profiling epistasis reveals a signal transduction pathway with antagonistic submodules and highly specific downstream targets. *Mol. Cell* **19**, 511-522

van de Peppel, J., N. Kettelarij, H. van Bakel, T. T. Kockelkorn, D. van Leenen et al. 2005 Mediator expression profiling epistasis reveals a signal transduction pathway with antagonistic submodules and highly specific downstream targets. *Mol. Cell* ,**19**: 511–522.

Van Vugt, J.J.; Ranes, M.; Campsteijn, C.; Logie, C. (2007) The ins and outs of ATP-dependent chromatin remodelling in budding yeast: biophysical and proteomic perspectives. *Biochim. Biophys. Acta,* **1769(3)**, 153-171.

Vannini, A., and Cramer, P. (2012). Conservation between the RNA polymerase I, II, and III transcription initiation machineries. *Mol. Cell,* **45**, 439–446.

Varga-Weisz, P.D., Wilm, M.; Bonte, E.; Dumas, K.; Mann, M.; Becker, P.B. (1997) Chromatin-remodelling factor CHRAC contains the ATPases ISWI and topoisomerase II. *Nature*, **388**, 598-602.

Vasudevan, S.; Peltz, S.W. (2001) Regulated ARE-Mediated mRNA Decay in Saccharomyces cerevisiae. *Mol. Cell*, **7**, 1191-1200.

Venters, B.J.; Pugh, F.B. (2009) How eukaryotic genes are transcribed. *Crit. Rev. Biochem. Mol. Biol.*, **44(2-3)**, 117-141.

Wang L, Lewis MS, Johnson AW (2005) Domain interactions within the Ski2/3/8 complex and between the Ski complex and Ski7p. *RNA*;**11**,1291

Wang, G., Balamotis, M. A., Stevens, J. L., Yamaguchi, Y., Handa, H., Berk, A. (2005) Mediator Requirement for Both Recruitment and Post recruitment Steps in Transcription. *Mol. Cell* **17(5)**, 683-694

Wang, W., Huang, L., Huang, Y., Yin, J.-w., Berk, A. J, Friedman, J. M., Wang, G. . (2009) Mediator MED23 Links Insulin Signaling to the Adiopegenesis Transcription Cascade. *Developmental Cell* **16**, 764-771

Wang, X., P. M. Watt, E. J. Louis, R. H. Borts, and I. D. Hickson. (1996) Pat1: a topoisomerase II-associated protein required for faithful chromosome transmission in *Saccharomyces cerevisiae*. *Nucleic Acids Res*. **24:**4791–4797.

Wang, Y.; Liu, C.L.; Storey, J.D.; Tibshirani, R.J.; Herschlag, D.; Brown, P.O. (2002) Precision and functional specificity in mRNA decay. *PNAS*, **99(9)**, 5860-5865.

Warringer, J.; Hult, M.; Regot, S.; Posas, F.; Sunnerhagen, P. (2010) The HOG Pathway Dictates the Short-Term Translational Response after Hyperosmotic Shock. *Mol. Biol. Cell*, **21**, 3080-3092.

Weake, V.M.; Workman, J.L. (2010) Inducible gene expression: diverse regulatory mechanisms. *Nat. Rev. Genet.*, **11**, 426-437.

Welker, S., Rudolph, B., Frenzel, E., Hagn, F., Liebisch, G., Schmitz, G., Scheuring, J., Kerth, A., Blume, A., Weinkauf, S., Haslbeck, M., Kessler, H., Buchner, J. (2010) Hsp12 Is an Intrinsically Unstructured Stress Protein that Folds upon Membrane Association and Modulates Membrane Function. *Mol. Cell* **39(4),** 507-20.

Werner, F. (2012). A nexus for gene expression-molecular mechanisms of Spt5 and NusG in the three domains of life. *J. Mol. Biol.* **417**, 13–27.

Westfall, P.J.; Patterson, J.C.; Chen, R.E.; Thorner, J. (2008) Stress resistance and signal fidelity independent of nuclear MAPK function. PNAS, 105(34), 12212-12217.

Wickens, M., Bernstein, D.S., Kimble, J., Parker, R. (2002) A PUF family portrait: 3'UTR regulation as a way of life. *Trends Genet.* **18**, 150-157.

Winston, F.; Allis, C.D. (1999) The bromodomain: a chromatin-targeting module? Nat. Struct. Biol., 6(7), 601-604.

Witze, E. S., Old, W., M., Resing, K. A., Ahn, N. G. (2007) Mapping protein post-translational modifications with mass spectrometry. *Nat. Meth.* **4(10)**

Yang, E.; van Nimwegen, E.; Zavolan, M.; Rajewsky, N.; Schroeder, M.; Magnaso, M.; Darnell, J.E. (2003) Decay Rates of Human mRNAs: Correlation With Functional Characteristics and Sequence Attributes. *Genome Res.,* **13(8)**, 1863-1872.

Yao G, Chiang YC, Zhang C, Lee DJ, Laue TM, Denis CL. (2007) PAB1 self-association precludes its binding to poly(A), thereby accelerating CCR4 deadenylation in vivo. *Mol. Cell Biol* .; **27**:6243

Yin, Z.; Hatton, L.; Brown, A.J.P. (2000) Differential post-transcriptional regulation of yeast mRNAs in response to high and low glucose. *Mol. Microbiol.*, **35(3),** 553-565.

Yosef, N.; Regev, A. (2011) Impulse Control: Temporal Dynamics in Gene Transcription. *Cell*, **144 (18),** 886-896

Young, E. T., K. M. Dombek, C. Tachibana, and T. Ideker (2003) Multiple pathways are co-regulated by the protein kinase Snf1 and the transcription factors Adr1 and Cat8. *J. Biol. Chem*. **278**, 26146–26158.

Yuan, G.-C., Liu, Y.-J., Dion, M.F.; Slack, M.D.; Wu, L.F.; Altschuler, S.J.; Rando, O.J. (2005) Genome-Scale Identification of Nucleosome Positions in S. cerevisiae. *Science*, **309**, 626-630.

Zähringer, H., Thevelein, J. M., Nwaka, S. (2000) Induction of neutral trehalase Nth1 by heat and osmotic stress is

controlled by STRE elements and Msn2/Msn4 transcription factors: variations of PKA effect during stress and growth. *Mol. Microbiol.* **35(2)**, 397-406

Zapater, M., Sohrmann, M., Peter, M., Posas, F., de Nadal, E. (2007). Selective Reuquirement for SAGA in Hog1-Mediated Gene Expression Depending on the Severity of the External Osmostress Conditions. *Mol. Cell Biol.* **27**, 3900-3910.

Zhang, Y. (2008) *BMC Bioinformatics* **9:40**, http://www.biomedcentral.com/1471-2105/1479/1440

Zhang, Y. (2008) I-TASSER server for protein 3D sturcture prediction. *BMC Bioinformatics*, **9(40),** doi:10.1186/1471-2105-9-40.

Zhang, Z., Dietrich, F., S. (2005) Mapping of transcription start sites in Saccharomyces cerevisiae using 59 SAGE. *Nucleic Acids Res.*, **33**, 2838–2851.

Zhao, J., Herrera-Diaz, J., Gross, D.S. (2005) Domain-wide displacement of histones by activated heat shock factor occurs independently of Swi/Snf and is not correlated with RNA polymerase II density. *Mol. Cell. Biol.*, **25**, 8985-8999.

ABBREVIATIONS

Abbreviation	description
4-sU	4-thiouridine
5'cap	7-methylguanylate connected via triphosphate to the 5' position of mRNA
5'FOA	5-Fluoroorotic Acid
aa	Amino acid
ActD	actinomycin-D
ALS	Amyotrophic horizontal sclerosis
AR	androgen receptor
ARE	AU rich elements
ATP	adenosine triphosphate
AU-rich element	adenosine uracil rich elements
bp	Base pairs
BRE	TFIIB recognition element
BRE	5-bromo-2'deoxyuridine
BREd	TFIIB recognition element – downstream
BREu	TFIIB recognition element – upstream
CDK	cyclin dependent kinase
CDT	Pol II C-terminal domain
cDTA	comparative dynamic transcriptome analysis
CHD-type	chromodomain helicase DNA-binding family of enzymes
ChIP	Chromatin immunoprecipitation
CIAP	Calf Intestine Alkaline Phosphatase
CTD	Carboxy-terminal domain
C-terminus	Carboxy-terminus
CV	Column volumes
Da	Dalton
DAPI	4',6-diamidino-2-phenylindole
DDR	DNA demage response
DMSO	Dimethylsulfoxide

DNA	Desoxyribonucleic acid
DNA RE	DNA recognition element
dNTP	desoxy-nucleotide triphosphate
DPE	downstream promoter element
DTA	dynamic transcriptome analysis
DTT	1,4-dithio-D,L-threitol
EDTA	Ethylenediaminetetraacetic acid
eIF-4E	Eukaryotic translation initiation factor 4E
ESR	environmental stress response
et al.	et alii (*Latin:* "andothers")
g	earth´s gravity
GCRMA	Guanine Cytosine Robust Multi-Array Analysis
GFP	Green fluorescent protein
GO	gene ontology
GRO	genomic run on method
GTF	general transcription factor
HAT	histone acetyl transferase
HDACs	Histone deacetylase(s)
HEPES	N-2-hydroxyethylpiperazine-N'-2-ethane sulfonic acid
HOG	high osmolarity glycerol pathway
HPDP-biotine	*N*-[6-(biotinamido)hexyl]-3'-(2'-pyridyldithio)propionamide
HPLC	high performance liquid chromatography
HSP	heat shock protein
IgG	Immunglobulin *G*
IMAC	immobilized metal ion affinity chromatography
INR	initiator element
IPTG	isopropyl-*ß*-D-thiogalactopyranoside
ISWI	Imitation Switch protein
KH-domain	nuclear ribonucleoprotein K homologue domain
Km	Michaelis-Menten constant
KOAc	Potassium acetate
LB	Lauria-Bertani (medium)
LC MS/MS	liquid chromatography mass spectrometry
Lgr	labeled mRNA of gene "g" in sample "r"
LIMMA	Linear Models for Microarray data
Lys-C	Endoproteinase
M	molar
MALDI	Matrix-assisted Laser Desorption/Ionization

MAPK	mitogen activated kinase
MES	2-(N-Morpholino) ethanesulfonic Acid
MOPS	4-morpholinepropanesulonic acid
mRNA	messenger ribonucleic acid
Mrp	RNase multiprotein-complex
MS	mass spectrometry
MTE	motif ten 10 element
NFR	nucleosome free region
NLS	nuclear localization sequence/signal
NMD	nonsense mediated decay
NPC	nuclear pore complex
NTA	nitrilotriacetic acid
N-terminus	amino terminus
NUDIX-motif	Nucleoside Diphosphate Linked Moiety X
OD_{nm}	optical density at wavelength [nm]
ORF	open reading frame
p(STY)	localization probability of STY phosphorylation positions
pA	polyadenylation site
PAGE	polyacrylamide gel electrophoresis
P-bodies	processing bodies
PBS	phosphate buffered saline
PCR	polymerase chain reaction
PDB	protein data bank
PH-domain	Pleckstrin homology domain
Phen	1,10-phenantroine
PI	protease inhibitor
PIC	pre-initiation complex
Pol II	RNA polymerase II
poly(A)	polyadenylation
poly(U)	polyuracil
Puf	PUmilio-homology domain Family
PVDF	polyvinylidene fluoride
qRT-PCR	quantitative reverse transcriptase PCR
RiBi	ribosomal biogenesis genes
RNA	ribonucleic acid
RNPs	mRNA binding proteins
ROS	reactive oxygen species
RP	ribosomal protein genes

RP-HPLC	reverse phase high performance liquid chromatography
rpm	rounds per minute
rRNA	ribosomal ribonucleic acid
RSC	remodel the structure of chromatin – protein familiy
RT-PCR	reverse transcriptase PCR
S	Svedberg (sedimentation coefficient unit)
SAGA	Spt-Ada-Gcn5-acetyltransferase
SAPK	stress activated protein kinases
SC	synthetic complete medium
SD	synthetic defined medium
SDS	sodium dodecylsulfate
SILAC	stable isotope labeling of amino acids in cell culture
SOB	Super Optimal Broth
STE	stabilizer elements
SWI/SNF	SWItch/Sucrose NonFermentable nucleosome remodeling complex
SYBR-safe	fluorescent dye for DNA gel electrophoresis produced by Invitrogen
TAF	TBP associated factor
TAFs	TBP associated factors
TAP	tandem affinity purification
TATA	core DNA sequence 5'-TATAAA-3'
TCA	trichloroacetic acid
TCEP	tris(2-carboxyethyl)phosphine
TEV	tobacco edge virus protease
TFs	transcription factor(s)
Tgr	total mRNA of gene "g" in sample "r"
TOR	target of rapamycin pathway
TRIS	tris-(hydroxymethyl)-aminomethane
TSS	transcription start site
TTP	tristetraproline
U	units
UAS	upstream activation sequence
Ugr	unlabeled mRNA of gene "g" in sample "r"
URA	uracil
UTP	Uracil triphosphate
UTR	untranslated region
v/v	volume per volume
w/v	weight per volume
YPD	yeast extract peptone dextrose